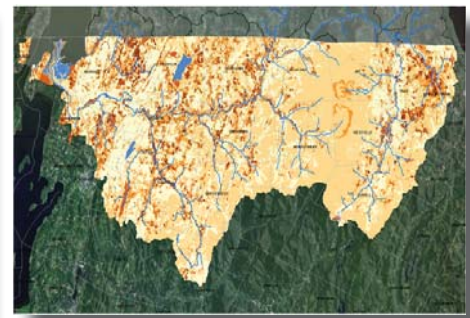Lake Champlain
Basin Program

Identification of Critical Source Areas of Phosphorus Within the Vermont Sector of the Missisquoi Bay Basin

STONE ENVIRONMENTAL INC

FINAL REPORT

December 15, 2011

Stone Project ID 092156-G

Prepared by:
Michael Winchell, Project Manager, Don Meals, Solomon Folle, Julie Moore, Dave Braun, Christine DeLeo, and Katie Budreski, Stone Environmental, Inc. and Roy Schiff, Milone and MacBroom, Inc..

for the
Lake Champlain Basin Program

IDENTIFICATION OF CRITICAL SOURCE AREAS OF PHOSPHORUS WITHIN THE VERMONT SECTOR OF THE MISSISQUOI BAY BASIN

FINAL REPORT

Stone Project ID 092156-G
December 15, 2011

Avg. Annual Total P (kg/ha)
<= 0.10
0.11 - 0.50
0.51 - 1.00
1.01 - 2.00
> 2.00
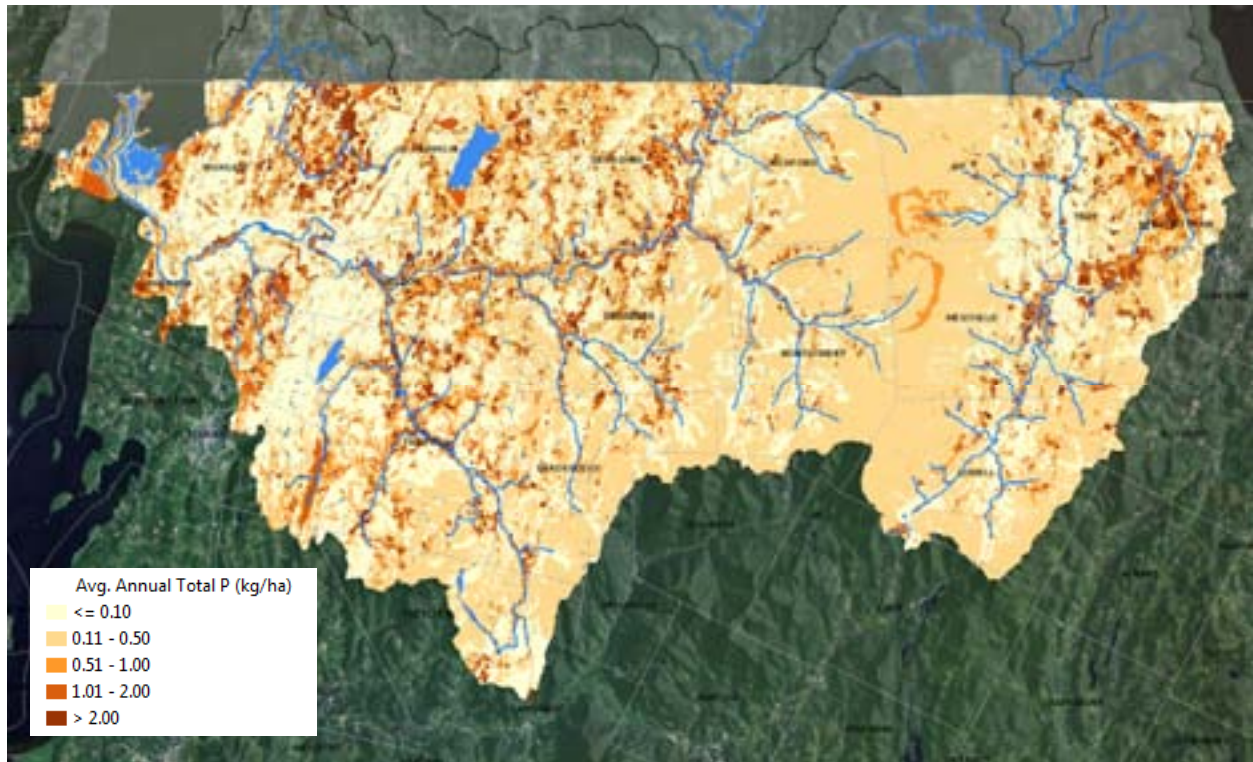
Prepared for:

Lake Champlain Basin Program
Eric Howe
54 West Shore Rd.
Grand Isle, VT 05458
Tel. / 802.372.3213
E-Mail / ehowe@lcbp.org

Prepared by:

Stone Environmental, Inc.

535 Stone Cutters Way
Montpelier, VT 05602
Tel. / 802.229.4541
E-Mail / sei@stone-env.com

STONE ENVIRONMENTAL INC

ACRONYMS

Acronym	Definition
APEX	Agricultural Policy Environmental Extender Model
ArcSWAT	ArcGIS SWAT Interface
AU	Animal Unit
BMP	Best Management Practice
BSTEM	Bank Stability and Toe Erosion Model
CCSM	Community Climate System Model
CDED1	Canadian Digital Elevation Data Level 1
CLU	Common Land Unit
CN	Curve Number
CREP	Conservation Reserve Enhancement Program
CRP	Conservation Reserve Program
CSA	Critical Source Area
CTI	Compound Topographic Index
DEM	Digital Elevation Model
EMC	Event Mean Concentration
GCM	Global Climate Model
GCRP	Global Change Research Program (US EPA)
GIS	Geographic Information System
HadCM3	Hadley Centre Coupled Model, Version 3
HEL	Highly Erodible Land
HRU	Hydrologic Response Unit
HUC	Hydrologic Unit Code
IRDA	Institut de recherche et de développement en agroenvironnement (Québec)
LCBP	Lake Champlain Basin Program
LFO	Large Farm Operation
LiDAR	Light Detection and Ranging
LOADEST	Load Estimation Model (USGS)
MBB	Missisquoi Bay Basin
MFO	Medium Farm Operation
MUSLE	Modified Universal Soil Loss Equation
NARCCAP	North American Regional Climate Change Assessment Program
NHD	National Hydrography Dataset
NLCD	National Land Cover Dataset

STONE ENVIRONMENTAL INC

Acronym	Definition
NRCS	Natural Resources Conservation Service (USDA)
NSE	Nash-Sutcliffe Error
NYSDEC	New York State Department of Environmental Conservation
PAC	Project Advisory Committee
PBIAS	Percent bias
PRISM	Parameter-elevation Regressions on Independent Slopes Model
RCM	Regional Climate Model
RMSE	Root Mean Square Error
RSR	Ratio of the root mean square error to the standard deviation of measured data
SFO	Small Farm Operation
SWAT	Soil and Water Assessment Tool
USDA	US Department of Agriculture
USGS	US Geological Survey
UVM	University of Vermont
VCGI	Vermont Center for Geographic Information
VHD	Vermont Hydrography Dataset
VSA	Variable Source Area
VSWI	Vermont Significant Wetland Inventory
VAAFM	Vermont Agency of Agriculture, Food & Markets
VTANR	Vermont Agency of Natural Resources
VTDEC	Vermont Department of Environmental Conservation
WRFP	Weather Research and Forecasting Model

STONE ENVIRONMENTAL INC

Table of Contents

STONE ENVIRONMENTAL INC

STONE ENVIRONMENTAL INC

STONE ENVIRONMENTAL INC

STONE ENVIRONMENTAL INC

List of Figures

STONE ENVIRONMENTAL INC

STONE ENVIRONMENTAL INC

STONE ENVIRONMENTAL INC

STONE ENVIRONMENTAL INC

List of Tables

STONE ENVIRONMENTAL INC

STONE ENVIRONMENTAL INC

STONE ENVIRONMENTAL INC

STONE ENVIRONMENTAL INC

STONE ENVIRONMENTAL INC

EXECUTIVE SUMMARY

The Missisquoi Bay Basin (MBB) straddles the Vermont-Québec border, and is dominated by forests (67%) and agricultural lands (17%). Urban and other built-up uses comprise less than 5% of the land cover in the watershed. Due to the extensive nature of agricultural land use in the watershed, an estimated 64% of the total upland phosphorus (P) load delivered by the MBB annually is attributable to agricultural sources.

Public concern over water quality in Missisquoi Bay remains high. Missisquoi Bay shows some of the most profound effects of P pollution, with recurrent blue-green algae blooms that are both unsightly and potentially toxic. Since 2002, Vermont has invested approximately $10 million annually, in combined state and federal resources, in programs designed to improve water quality in Lake Champlain. These efforts are subject to intense scrutiny, in part because to date they have failed to yield the desired improvements in Lake Champlain water quality. Further, in this era of shrinking government resources it is unlikely that increased annual funding will be provided to this effort. Tools are needed that can help program managers identify priorities for implementation and better target their efforts to those areas of the landscape that disproportionately contribute P pollution, often termed critical sources areas (CSAs).

The overall purpose of this project was to identify CSAs in order to improve the cost-effectiveness and efficiency of land treatment efforts to reduce P loads. This report presents the results of intensive watershed modeling of the MBB to identify critical source areas of phosphorus pollution at both a strategic and a tactical scale.

The strategic level assessment of critical source areas employed a Soil and Water Assessment Tool (SWAT) model that was capable of assessing broad watershed-scale trends, while also able to evaluate land use categories, sub-watershed characteristics, and field-level assessments of P source areas. In all cases, the SWAT model was applied over the entire watershed. The tactical level work combined data generated through the strategic assessment with other high-resolution datasets to define CSAs at a scale practical for specifying Best Management Practices (BMPs) at the farm and field scale.

Project Objectives

The principal goal of this project is to identify, locate, and rank the most important critical source areas of phosphorus loads in the Vermont sector of the Missisquoi Bay Basin. Key project objectives include:

- Identification and ranking of CSAs in the MBB at the watershed (i.e., strategic) scale using available basin-wide data sources and a calibrated/validated watershed model;

- Evaluation of the P load reduction potential for alternative BMP strategies following a traditional implementation approach versus implementation targeted to identified CSAs;

- Comparison of watershed model results with a simpler multivariate GIS-overlay technique that might be more easily applied to other regions of the Lake Champlain Basin;

- Evaluation of potential changes to P loading in the MBB and CSA ranking potentially resulting from climate change; and

STONE ENVIRONMENTAL INC

- Use of more precise, site-specific input data and better spatial resolution to improve identification, ranking, and prioritization of CSAs at a farm-scale (i.e., tactical) level.

Key Findings

Strategic Analysis

The SWAT model was used to evaluate sediment and P contributions at several scales as part of the strategic level analysis.

The watershed-scale SWAT simulations indicate that about 60% of the sediment and P loads from the assessment area (Vermont portion of the MBB) come from upland sources, whereas about 40% are attributable to erosion of streambanks. These values are within the same range of the 29% - 42% sediment contribution and ~50% total P contribution from bank sources suggested by a separate project (BSTEM modeling) recently conducted within the Missisquoi River watershed.

Some of the key findings, with respect to upland sources by land use type, are:

- Land in corn-hay rotation produced the greatest contribution (29%) of the total MBB P load from upland sources;

- Forest has the lowest total P areal loading rate at 0.14 kg/ha/yr, but because it is the predominant land use in the basin, is the second highest total contributor at 20% of the total;

- For cultivated cropland (soybean-corn, corn-hay, and permanent corn), the vast majority of total P load is in the form of sediment P (85 to 90%);

- For agricultural grassland (permanent hay and pasture), the majority of the total P load is in the form of soluble P (66% to 72%);

- The developed land use classes (medium and low density residential, dirt and paved roads) fall in the middle among the different land uses in terms of average P loading rates; however, because these areas comprise only a small fraction of the total area assessed (3.5%), their overall impact of total P load in the watershed is quite small; and

- Total P contribution as a percent of the total MBB load from upland sources can be summarized as follows for broad land uses classes:

    o Agricultural: 64%

    o Developed: 6%

    o Undeveloped: 30%

The SWAT model allowed identification of critical MBB subwatersheds based on P loading rate. Within the MBB, those watersheds with the highest fractions of agricultural land, such as the Rock, Mud, Pike, and Hungerford, have the higher total P loading rates, ranging from 0.55 – 0.81 kg P/ha/yr (subwatershed average). The modeling effort also calculated estimated sediment and P loading rate from HUC-12 sub-watersheds and

STONE ENVIRONMENTAL INC

from some 103,666 individual Hydrologic Response Unites (HRUs). Phosphorus loading rates have been mapped at each of these scales; maps are presented in the full report.

Three factors—hydrologic soil group, compound topographic index (CTI), and slope—were shown to be the most important factors driving the magnitude of P export and the incidence of CSAs. The CTI class was found to have the greatest influence on soluble P losses, while slope was most influential on particulate P export. Hydrologic soil group was highly influential for total P export, including both particulate and soluble forms of P. It should be noted, however, that interaction among different landscape and soils characteristics makes identification of one or two factors as direct predictors of the magnitude of total P export difficult. This complexity of interactions is what makes the SWAT model well suited to sorting out the subtleties in different characteristics that influence P export. This is accomplished through the independent parameterization of HRUs based on localized variability in soils, topographic, climate, and agronomic conditions. The HRU-level identification of P CSAs is presented and discussed in later sections of this report. CSAs identified at multiple scales are mapped in detail in the full report.

See Section 3.1 for additional detail on the strategic-level analysis

Traditional vs. Targeted BMP Implementation

To evaluate potential P load reduction when BMP strategies are targeted to priority problem areas (i.e., CSAs) as compared to implementation in a traditional manner (i.e., essentially random, based primarily on landowner voluntary participation), the model was used to test three BMPs. These were: manure P reduction, cover cropping, and changes in crop rotations. For each BMP tested, significant benefit resulted from implementing the BMP on a targeted area representing the eligible land in the highest CSA category. Phosphorus load reductions from targeted implementation were two to three times those achieved by random implementation for all three of the tested practices.

See Section 3.5 for a more detailed explanation.

Utility of GIS-based Techniques

The results of the GIS-based CSA analysis were generally as expected, and compare moderately well with the SWAT model assessment. Visually, the GIS-based results appear to be heavily influenced by land use classes. In general, agricultural, farmstead, and developed areas had higher risk values compared with areas of natural vegetation, such as forests and wetlands. Risk predicted by the GIS-based analysis increased as distance to stream decreased. The effect of the soil was less apparent in the GIS-based analysis then it was with the SWAT model, but in general, areas with clayey or silty soils tended to have higher risk than areas with sandy soil. Similarly, high slope seemed to have less influence over the result in the GIS-based approach than in SWAT; however, most areas with high slopes are forested and these areas are assumed to have extremely low risk under the GIS-based approach. The GIS-based method's prediction of wetlands as less significant potential CSAs compared to the SWAT model assessment results from the GIS method's lack of consideration of the phosphorus geochemical cycling simulated by SWAT.

See Section 3.4 for additional detail.

STONE ENVIRONMENTAL INC

Climate Change Scenarios

Two different climate change scenarios were evaluated using the MBB SWAT model, for the period 2041-2070. These scenarios represented the upper and lower bounds of projected changes in P loading, based on recent work in the LaPlatte River watershed in central Vermont (Perkins 2011). The SWAT model predicted an increase in the total sediment load of 21% and 57% over the baseline load for the lower and upper bound climate scenarios, respectively. This load increase did not occur uniformly over the different land uses with the study area. The farmstead and road land use classes saw the lowest increases in sediment; hay and pasture land uses saw the largest increases in sediment load both showing greater than 100% increases under the upper bound climate scenario. For total P, the load increased by 13% and 46% over the baseline for the lower and upper bound climate scenarios, respectively.

Although the magnitudes of the change in P loading rates varied across the land use classes, the land uses that ranked as highest P CSAs in the baseline scenario did not change under the future climate scenarios. The data suggest that designing BMPs and P reduction strategies based on an analysis of current climate conditions should target the same groups of P CSAs that will probably continue to be the most important under future climate conditions.

See Section 3.6 for additional detail on the predicted effects of climate change on P loading in the MBB.

Tactical Analysis

The SWAT model was built so that agricultural field boundaries were directly incorporated into the model structure. This strategy enabled the highly detailed field-level information to be developed as part of the strategic analysis. This was carried forward in the tactical analysis by combining the field-level results with additional information on the proximity of each field to the nearest receiving water.

Areas of intensive agriculture, such as the Rock, Hungerford, lower Black, and Mud sub-watersheds, still stand out as having high concentrations of CSAs; however, hydrologic proximity is an important determining factor in the total P load. This is most evident in considering undeveloped, higher elevation areas with shallow soils on steeper slopes that move up higher in the rankings when consideration of hydrologic proximity is included.

See Sections 3.2 and 3.3 for further information on the tactical analysis.

Limitations to the Analysis

Statistician George Box is generally credited with saying: "All models are wrong, some models are useful." The SWAT model required that certain agronomic management operations such as tillage, planting, and harvest dates, manure or fertilizer application rates, and crop rotations be specified for each unit of cropland, even though such data did not exist for specific fields in the MBB. Nevertheless, SWAT parameters had to be estimated. Thus, we developed reasonable descriptions of these agronomic operations, based on known conditions in the MBB and applied them basin-wide, because we were reluctant to create a bias by arbitrarily assuming different practices/conditions for different fields in the watershed. Although this approach may tend to over-estimate the contribution of fields that have already implemented management measures, the long-term simulation and uniform assumptions provide field-specific risk predictions that should hold great value for program managers in targeting the use of certain BMP interventions. Further, the model clearly demonstrates the value of implementing BMPs in the areas of highest risk.

STONE ENVIRONMENTAL INC

Conclusions

The results of this project show that that some land uses within the watershed produce a disproportionately high amount of P relative to the fraction of the total watershed area they represent. For example, while agricultural land uses represent 17% of the total land area in the MBB, they contribute nearly 65% of the total P load. Similarly, developed land uses (residential areas and roads) that account for less than 3% of the watershed area contribute approximately 6% of the total P load.

The MBB SWAT model was able to evaluate the P load associated with specific landscape units, from major sub-watersheds, through smaller subbasins, down to the highest resolution landscape representation—the unique combinations of land use, soils, and topographic characteristics that form a SWAT HRU. These areas have been mapped and described quantitatively. Identifying CSAs at multiple scales allows future management activities to be focused on major sub-watershed, subbasin, and field scale goals.

The model also clearly demonstrated the value of targeting BMPs to the areas of highest risk. For each BMP tested, significant benefit was realized by implementing the BMP on areas representing the most important CSAs. For the three BMP scenarios tested, targeted BMPs gave two to three times the P load reduction that resulted from traditional, more random, implementation.

As would be expected, model results also demonstrated that the proximity of a particular CSA to a surface water feature is quite important in estimating its relative impact. Specifically, giving consideration to surface water proximity allowed for important distinctions within an otherwise uniform ranking class that was largely driven by land use and soils.

A separate modeling analysis was also performed for a single farm operation in the MBB. This model was designed to identify CSAs at the level necessary to determine individual management measures that could be expected to have the greatest success in reducing P loads. In addition, the farmer was interested in using the farm-specific model to quantify the benefits of practices he has already installed. The ability to produce meaningful results at this scale was heavily influenced by the agronomic records the farmer made available for the project. Without detailed, farm-specific data the value of this modeling analysis would have been greatly reduced.

The methods used to identify CSAs in the MBB should have value to other efforts in other regions of the Champlain Basin. That said, the MBB represents a unique set of land use, soil, slope, and receiving water conditions and the modeling analysis relied on a suite of data (e.g., LiDAR, CLU boundaries) that is not currently available basin-wide. It would therefore be imprudent to simply extend the SWAT MBB model results directly to the rest of the Champlain Basin. Nevertheless, there are several key observations from this effort that should have broad application. These include:

- There is enormous value to long-term simulation. Wet weather events drive the annual P loads delivered to Missisquoi Bay, and are subject to a significant amount of year-to-year variability; coupled with ongoing crop rotations, it is virtually guaranteed that no two years will look the same. The value of a long-term simulation is that it can smooth the variability, and identify particular land units will contribute the greatest pollution load over the long term.

- The model also demonstrates the value of targeting BMPs to the areas of highest risk. For each BMP tested, significant benefit was realized by implementing the BMP in the areas identified as

STONE ENVIRONMENTAL INC

having the highest P loading rates in the baseline scenario. From both an environmental quality and an economic perspective, choosing a targeted BMP implementation strategy offers clear benefits.

- Although it can be tempting to use all available data, it is important to avoid introducing bias into the model by relying on incomplete datasets. For example, farmers who have invested heavily in conservation practices are understandably interested in having these investments reflected in the model. The challenge, however, is that complete, spatially-referenced datasets of all of the conservation practices that have been implemented in the MBB are simply not available. To incorporate data on a case-by-case into the model is neither practical, nor particularly useful for improving model results.

- Higher resolution data on the location of surface water features has important influence on identifying the most significant CSAs. Land use, soils, and slope tend to be the critical drivers in identifying CSAs. Introducing more detailed information on the location of surface water features created important distinctions within otherwise uniform ranking classes.

- Although a simpler, GIS-based analysis showed some promise for identifying CSAs in the MBB, results were only moderately well-correlated with the intensive SWAT analysis and application of the specific GIS approach to other parts of the Lake Champlain Basin cannot be fully recommended at this time as a substitute.

- The predicted effects of climate change do not appear to reorder implementation priorities. Although the magnitude of P loading rates are predicted to increase as a result of the changing climate, the land areas that ranked as the most significant P CSAs under current conditions did not change with future climate scenarios. The data suggest that designing BMPs and P reduction strategies based on an analysis of current climate conditions will target the same groups of P CSAs that will also be the most important under future climate conditions.

Finally, it must be emphasized that the process undertaken by this project cannot, nor is it intended to, be used as a wholesale substitute for site visits and one-to-one work between management agency staff and a landowner. Rather, the model results can help guide agency efforts at major sub-watershed, subbasin, and field scales in prioritizing and implementing land treatment measures. Such targeting will improve cost-effectiveness of conservation and restoration programs by helping deploy financial and technical resources to areas that will yield the maximum benefit to Lake Champlain.

STONE ENVIRONMENTAL INC

1. INTRODUCTION

1.1. Background on Phosphorus Critical Source Areas

It is widely believed that limited watershed areas generate surface runoff that may transport phosphorus (P) to a stream and that only a small proportion of a watershed is responsible for the majority of P exported in runoff (Sharpley et al. 1994, Daniel et al. 1994, Heathewaite et al. 2000, Walter et al. 2000, Srinivasan et al. 2002). These areas of disproportionate P contribution are typically defined by P levels that are also subject to hydrologic transport mechanisms that can mobilize and transport P. This intersection of P source areas and transport mechanisms is often described as a "critical source area" (CSA). Watershed management strategies to reduce P export could be more cost effective if treatments were targeted to these CSAs (Sharpley 1999, Pionke et al. 2000, Yang and Weersink 2004, Gburek et al. 2000a,b).

The existence of high P source areas on the landscape is predominantly a function of landscape features, land use, and management. Apart from the availability of fresh source materials (e.g., surface-applied manure on agricultural land), soil P levels play an important role in determining P losses via runoff (Sonneveld et al. 2006). Excessive soil P levels resulting from over-application of nutrients from fertilizers or manure have been linked to high P losses in runoff, especially in areas of animal-based agriculture (Pote et al.1996, Sims et al. 2000). Conditions that influence soil erosion such as soil erodibility, slope, tillage practices, and vegetative cover can also promote the availability of P for loss (Sivertun and Prange 2003).

P transport from the land surface in a watershed occurs mainly through surface runoff and erosion. In the Northeast, most surface runoff is believed to derive from saturation excess where precipitation cannot infiltrate because the soil is already saturated (Dunne and Black 1970, Ward 1984). These saturated runoff contributing areas vary spatially and temporally by geology, topography, soils, rainfall characteristics, and storm magnitude and are referred to as variable source areas (VSAs) (Dunne and Black 1970, Frankenberger et al.1999). One effective approach to identifying specific runoff contributing areas in a watershed is to identify probable saturated areas through a topographic index derived from analysis of a digital elevation model (DEM) (Beven and Kirkby 1979, Quinn et al. 1991).

In addition to upland P sources, streambanks and channels contribute to watershed sediment budgets via erosion and deposition. The sediment, and in particular the finer material that erodes from banks, typically enters the channel with associated nutrients that can be transported downstream, or become incorporated into a mobile bed for short or long-term storage. Research has documented a wide range of importance of streambank erosion as a source of P export relative to upland sources. Sekely et al. (2002) found that 10% of the P load in some Minnesota streams originated from mass bank failures; others have documented P originating from banks in agricultural watersheds to account for 50% of the total P load (e.g., McDowell and Wilcock 2007, Noll et al. 2009). Although the documented relative contribution of streambank and upland source of P has been quite variable, there is consensus that banks are important to consider when evaluating P sources, particularly in watersheds where agriculture has been taking place for a long time.

Past efforts to reduce nonpoint source P loads to impaired waters—in the Lake Champlain Basin and nationwide—through the implementation of conservation practices on the land have often not produced the desired measurable water quality outcomes. This shortcoming may in part result from applying the conservation practices to low-priority land areas, while failing to address CSAs. The goal of reducing P loads

STONE ENVIRONMENTAL INC

to Lake Champlain from nonpoint sources may be best achieved, therefore, by identifying CSAs and focusing treatment efforts on those areas that disproportionately contribute P.

1.2. Background on Issues Related to Missisquoi Bay Basin and Phosphorus Management

The Missisquoi Bay Basin includes the drainage areas of the Pike, Rock and Missisquoi Rivers, and the shoreline areas around Missisquoi Bay. The drainage area of 310,527 ha (767,312 ac) is split between the Province of Québec (42%) and the State of Vermont (58%). Some 154 km (96 mi) of the Missisquoi River and 67 km (42 mi) of the Pike River drain the basin to Missisquoi Bay.

Missisquoi Bay has one of the highest in-lake P concentrations of any segment of Lake Champlain; the Bay has long been impaired by eutrophication caused by excessive P loads from its watershed. Phosphorus loads to and concentrations in the Bay greatly exceed target levels designated by water quality criteria for P endorsed by the governments of New York, Québec, and Vermont (LCBP 2010). Loadings of sediment and nitrogen to the Bay are also a concern. The Missisquoi Basin was assessed in 2003 and nutrients and sediment from agricultural nonpoint sources were identified as the leading causes of impairment (VT DEC 2004); streambank erosion is also believed to be a significant source of sediment and nutrients to the Bay (VT DEC and NYS DEC 2002). Blue-green algae blooms have been a significant issue in Missisquoi Bay since the 1990s when severe blue-green algae blooms began to impair recreational uses in both Québec and Vermont (LCBP 2010).

While the governments and citizens of Vermont and Québec have made significant progress in reducing P loads to the Bay, more needs to be done in order to meet the target loads. The Province of Québec has undertaken several programs to reduce its share of P loads. Similarly, Vermont has initiated P reduction programs, but has found reducing P to be more problematic in its sector of the Basin.

1.3. Project Goals and Objectives

The principal goal of this project is to identify, locate, and rank the most important critical source areas of phosphorus loads in the Vermont Sector of the Missisquoi Bay Basin. The final product of the project is intended to provide resource agencies with a better understanding of the types and locations of areas they should target for better land stewardship in order to significantly and cost effectively reduce P loads to Missisquoi Bay.

Specific objectives of the project include:

- Conduct a strategic identification and ranking of CSAs in the Missisquoi Bay Basin at the watershed level using available basin-scale data sources and a calibrated/validated detailed watershed model (the SWAT model);

- Evaluate the P-load reduction potential for alternative Best Management Practice (BMP) strategies following a random implementation approach versus implementation targeted to identified CSAs;

- Assess the effects of predicted climate change on CSAs;

- Compare CSA identification from the strategic SWAT modeling analysis with simpler multivariate GIS-overlay techniques that may be more easily applied to other portions of the Lake Champlain Basin;

STONE ENVIRONMENTAL INC

- Refine the strategic approach by using more precise, site-specific input data and better spatial resolution to improve identification, ranking, and prioritization of CSAs at a tactical (farm-scale) level; and

- Communicate results to Lake Champlain Basin decision makers and other stakeholders to improve the P-reduction efforts in the Missisquoi Bay Basin and elsewhere.

1.4. Approach for Identification of Critical Source Areas with the Missisquoi Bay Basin

1.4.1. Strategic Analysis

Overall, the project identified and ranked CSAs in the Missisquoi Bay Basin (MBB) using available basin-level data on watershed characteristics and management activities and the SWAT model. Because of the need to calibrate and validate the model at points along the main stem Missisquoi River, the model encompassed the entire MBB, thereby including both the Vermont and Québec portions of the watershed. The analysis predicted a distribution of CSAs across the landscape based on climate, terrain, soils, and management analysis. CSAs were translated from the hydrologic response unit (HRU) of the SWAT model into field or land tract units for identification and prioritization. The SWAT model was used to simulate response of P load to implementation of BMPs, as well as to projected climate change.

This portion of the project involved this series of tasks:

- Construction and testing of the SWAT model;

- Collection of watershed data and parameterization of the model, including topography, climate, soils, land use, animal populations, crop management, urban/developed P sources, and stream channel characteristics;

- Development, calibration, and validation of a SWAT model;

- Application of the SWAT model to identify CSAs and aggregation of CSAs to field/tract scale ;

- Field verification of a sample of modeled CSA rankings;

- Evaluation of simulated changes in P loads, comparing random implementation of BMPs to implementation targeting highly-ranked CSAs;

- Assessment of P CSAs under projected conditions of climate change; and

- Application and testing of simpler approaches for identifying CSAs.

These results will enable watershed managers to focus on the most important regions of the MBB for P reduction.

1.4.2. Tactical Analysis

We performed a more detailed analysis on a smaller micro-watershed (single-farm) scale with highly site-specific data including enhanced hydrography and detailed agronomic records. In the tactical analysis, we were able to account for specific farm-level issues, including accounting for BMPs that have already been installed on the farm, which was not possible at the strategic level. The APEX model was used to evaluate P load under current and alternative conditions.

STONE ENVIRONMENTAL INC

1.4.3. Project Advisory Committee

The project was guided throughout its course by a Project Advisory Committee (PAC). The PAC included scientists and managers from state and federal agencies, the University of Vermont, and Texas A&M University, as well as a dairy farmer from the MBB. The individuals who served on the PAC represented expertise in spatial analysis, soils, hydrology, river geomorphology, agronomy, and modeling. The PAC met approximately quarterly to discuss project progress and assist in making important decisions. As noted further in the report, PAC members were instrumental in advising the project team on model parameterization, farm management, BMP options, and other key project inputs.

STONE ENVIRONMENTAL INC

2. METHODS

2.1. SWAT Model Development

2.1.1. SWAT Model Background

The Soil and Water Assessment Tool (SWAT) was developed at the United States Department of Agriculture Agricultural Research Service (USDA-ARS) Grassland, Soil, and Water Research Laboratory (Arnold et al., 1998; Neitsch et al., 2005). SWAT is a watershed-scale, continuous, physically-based, semi-distributed model designed for the simulation of flow, sediment, nutrient, and pesticide transport in ungaged watersheds. It has been designed for efficient simulation of the impacts of varying land management and climate conditions on water quantity and water quality in large, complex watersheds (Borah and Bera 2004, Arnold and Fohrer 2005). SWAT is the result of an evolution of Agricultural Research Service field and watershed-scale models, including CREAMS (Knisel, 1980), GLEAMS (Leonard et al., 1987), EPIC (Williams et al., 1984), and SWRBB (Arnold et al., 1990). SWAT is continually supported and developed by USDA-ARS and the international community, with major updates released every three to four years. The current version of SWAT, SWAT 2009 (Neitsch et al. 2011), is integrated with an ArcGIS interface called ArcSWAT (Winchell et al. 2010), that provides a set of tools for integrating the topographic, land use, soils, weather, and land management inputs required to parameterize the SWAT model

A watershed modeled with SWAT is divided into two levels of aggregation. The more general level is the subbasin. At the subbasin level, weather inputs are homogeneous and a single flowing water body (stream) can be defined for which model output can be generated. Routing of water, sediment, and nutrients occurs at the subbasin level. The more refined level of aggregation in a SWAT model is the hydrologic response unit, or HRU. The HRU represents a sub-area of a subbasin that has the same land use, soils, and optionally, topographic slope or characteristics. HRUs can further be distinguished based upon the agronomic practices of the sub-area. In this respect, individual fields (or even sections of fields) could be delineated and represented as HRUs in SWAT. The more common approach, however, is to allow HRUs to more represent multiple fields which have the same land use and soil characteristics. HRUs need not be spatially continuous areas within a subbasin, and more often than not, they are discontinuous areas.

SWAT simulates both upland and in-channel processes. Major upland components of the SWAT model include weather, hydrology, plant growth, erosion, nutrients and pesticide cycling, and land management. Detailed descriptions of the assumptions and algorithms associated with all the components of the SWAT model are provided in the model's theoretical documentation (Neitsch et al. 2011). Brief discussions of several of these model components are provided here.

The hydrology component of the model simulates the water balance for each HRU. This includes precipitation, snow accumulation and snowmelt, and irrigation on the input side and evapotranspiration, canopy interception, surface runoff, percolation, lateral flow, and ground water flow on the output side. The various components of the water yield at the HRU level (surface runoff, lateral flow, tile flow, baseflow) are aggregated to the subbasin level, where they are added to and routed through the channel system.

The plant growth sub-component of the SWAT model is designed to estimate crop yields and biomass and has a direct impact on the hydrologic, erosion, and nutrient cycling components. A wide range of vegetation types

STONE ENVIRONMENTAL INC

can be simulated, including dozens of crops, grassland/pasture systems, and tree crops. A broad collection of land management practices can be simulated for both agricultural and non-agricultural land covers. This includes crop planting and harvesting, crop rotations, tillage, burn-down, irrigation, fertilizer and manure applications, pesticide application, and animal grazing for agricultural lands. For developed lands, mowing, fertilizer applications, and street cleaning activities can be simulated. All these land management activities can be specified to occur at district points in time based on either calendar dates or growing degree days.

Soil erosion is a function of the land cover, soils, weather, and land management, with predictions made at the HRU level. The Modified Universal Soil Loss Equation (MUSLE) is used to calculate the upland sediment yield (Williams 1975, Williams 1995). The MUSLE approach is based upon the Universal Soil Loss Equation (USLE) but uses a runoff energy factor in place of the rainfall erosivity factor, eliminating the need for delivery ratios (Neitsch et al. 2011). This has implications for both sediment and sediment-bound nutrient transport, as the loading rates simulated at the HRU level are those that are predicted to enter the stream channel system as a result of the runoff energy available. The potential impact of land areas adjacent to HRUs (such as vegetated buffers) on upland sediment transport must be modeled through additional features in SWAT. As with the hydrologic components, erosion loads are aggregated to the subbasin level and then added to the channel system.

Upland phosphorus cycling and transport is another HRU level process in SWAT. The main components of the phosphorus (P) cycle modeled in SWAT include P added in the form of mineral fertilizer or manure, P present in the soil matrix, P in both live plant biomass and decomposing residue, and P buildup form sediment on impervious surfaces. Soil P has three mineral pools (solution, active, and stable) and three organic P pools (fresh organic, and active and stable humic substances). SWAT model algorithms simulate the mineralization, decomposition, and immobilization processes that control the transformations of soil P among these six pools. Other soil P processes simulated by SWAT include inorganic P sorption, leaching to groundwater, and surface runoff transport of soluble and sediment-bound P (both mineral and organic forms). The cycling and transport P in SWAT is heavily determined by the hydrology, plant growth, and erosion processes previously described. In this regard, SWAT is truly a physically processes-based simulation model. As with flow and soil erosion, P loads generated at the HRU level are aggregated to the subbasin level and then added into the channel associated with the subbasin.

The channel processes simulated in SWAT include routing of flow, sediment, and P. Flow routing is impacted by channel characteristics, including cross-section geometry, slope, and roughness. Flows can be lost through channel infiltration or surface evaporation. The sediment routing processes include sediment deposition and re-entrainment, and channel degradation. In SWAT 2009, new physically-based methods for sediment routing allow for tracking of sediment particle size distributions. The routing of nutrients through the channel system includes the contributions of P from eroding channel banks, the settling and resuspension of particulate P, and the transformations between organic and mineral P due to biological processes.

The SWAT model has proven to be an effective tool for assessing water resources and non-point source pollution for a wide range of scales and environmental conditions across the globe. This worldwide use and interest in the SWAT model has resulted in the continued development and customization of the model (Gassman et al. 2007, 2010). Among the customized versions of the model are: SWAT-G (Eckhardt et al. 2002) with improved flow estimates for German landscape conditions, ESWAT (van Griensven et al. 2005) with an enhanced hydrology and streamflow components, SWAT-DEG (Allen and Arnold 2005) which focused on more accurate channel degradation, SWAT-BF (Watson et al. 2009) focusing on forested

STONE ENVIRONMENTAL INC

watershed processes for the Canadian Boreal Plain, SWAT-K (Kim et al. 2008) with modified processes for Korean conditions, and SWAT-VSA (Easton et al. 2008) which conceptualized the SWAT model by including the topographic wetness index to redefine HRUs so that spatial runoff patterns would follow those observed in Variable Source Area (VSA) dominated landscapes. As an open source model, SWAT will likely continue to benefit from the research and contributions from scientists world-wide.

The application of SWAT in this study is intended to identify and rank P critical source areas within the Missisquoi Bay Basin. The SWAT model has a history of use in simulation of phosphorus transport and identification of CSAs (Srinivasan et al. 2005, Ouyang et al. 2007, Busteed et al. 2009). In addition, there have been several other SWAT modeling studies conducted within the Lake Champlain Basin. Michaud et al. (2007) studied the influence of different landscape and cropping system alterations on phosphorus mobility within the Pike River watershed of south-western Québec. Recent work by Ghebremichael et al. (2010) focused on modeling critical source areas of runoff and phosphorus losses in the Rock River watershed, a sub-watershed of the Missisquoi Bay. This current study's application of the SWAT model within the MBB will build upon the previous work in the Champlain Basin and other recent applications of SWAT to specifically address identification of P CSAs at a high resolution, capable of supporting both strategic and tactical level assessment of the problem.

2.1.2. Variable Source Areas and the Compound Topographic Index

It is widely believed that not all areas within a watershed generate surface runoff that may transport P from uplands to a stream channel. Furthermore, the areas that do contribute surface runoff and P transport are not constant in time and will vary annually, seasonally, or within inter-storm periods. This concept, referred to as variable source area hydrology, was pioneered by research conducted near Danville Vermont at the Sleepers River experimental watershed (Dunne and Black 1970). Dunne and Black found that saturated areas of their watershed varied spatially and temporally by geology, topography, soils, evapotranspiration rates, and precipitation form and amount. Furthermore, the areas that generated surface runoff within the watershed were found to be dominated by these saturated areas. This runoff process, from areas where the soil is saturated, came to be known as saturation excess runoff generation (Dunne 1978), and is in contrast to the infiltration excess (or Hortonian) runoff process in which the precipitation rate exceeds the soil's infiltration rate (Horton 1933). Since Dunne's work, considerable research has documented the variable source area concept (Beven and Kirkby 1979, O'Loughlin 1981, Ward 1984, Frankenberger et al. 1999), and it has been proposed that VSA hydrology and the saturation excess runoff process is a phenomenon that reflects the general hydrologic response of watersheds in the glaciated uplands of New England, including the Missisquoi Bay Basin (MBB). It is for this reason that the SWAT modeling approach for simulating P critical source areas of the MBB was designed to account for the VSA/saturation excess runoff principles.

One of the most common approaches for incorporating the VSA/saturation excess concept into hydrologic models has been the use of a topographic wetness index. The original use of this concept is often credited to Beven and Kirby (1976, 1979). Also referred to as the "topographic index" or "compound topographic index" (CTI), this index uses topographic information from a DEM to distinguish between areas with low potential for saturation from areas with high potential for saturation. The index is based on local upslope drainage area and slope and is represented as shown in equation 1.

STONE ENVIRONMENTAL INC

$$CTI = \ln(As/\tan B) \qquad\qquad \text{Eqn 1.}$$

Where As = the specific catchment area (m2/ unit width)
B = the slope angle (radians)

Based on equation 1, areas of the landscape with high upslope contributing areas and low slopes are more likely to generate saturation excess runoff, while areas of low upslope areas and high slopes are less likely to generate saturation excess runoff.

Since the work of Beven and Kirkby, numerous other authors have incorporated the CTI concept or similar concepts into the simulation of VSA hydrology, including the identification of critical source areas of non-point source pollutants (Moore et al. 1993, Gessler et al. 1995., Western et al. 1999). Additional applications have expanded the CTI concept to further incorporate the influence of soil transmissivity characteristics on prediction of saturated areas (Beven 1986), leading to the often used Soil Topographic Index (STI). Recently, the concept of incorporating a topographic wetness index into the SWAT model was introduced (Easton et al. 2008) which helped to guide the implementation of the VSA concept into the MBB SWAT model application.

2.2. Data Development for SWAT Parameterization

2.2.1. Topographic Data

Topographic data are instrumental when building a watershed model with SWAT. The topographic data determine watershed subbasin boundaries, identify locations of stream channels and overland flow path, provide the basis for slope calculations, define elevation variability that can influences climate, and allow for the determination of additional hydrologic characteristics, such as the compound topographic index. Topographic data in the form of digital elevation models (DEMs) provide a means for working with this data within a Geographic Information System (GIS). This section will discuss the compilation of the topographic data used in building the MBB SWAT model and describe the how the data were used in developing some of the primary inputs to the model.

2.2.1.1. Digital Elevation Model Compilation

The resolution of a DEM influences the accuracy and scale at which information that can be assessed from the data. Due to the large size of the MBB study area, the development of the MBB SWAT model required the compilation of DEMs from multiple sources and at multiple scales. Four datasets ranging from a minimum cell size of 1.6 m (2.56 m^2) to a maximum of 20 m (400 m^2) served as sources for the DEM that was built to develop the SWAT model. These four datasets are summarized in Table 2.1.

Table 2.1: DEM source datasets.

Dataset	DEM Resolution (m)
Western MBB LiDAR	1.6
Eastern MBB LiDAR	1.6
Vermont Hydro DEM	10
Canada Digital Elevation Level 1 (CDED1)	~20

STONE ENVIRONMENTAL INC

The DEM source data include two DEMs that were derived from recently acquired Light Detection and Ranging (LiDAR) data, from which the 1.6-m resolution DEMs were built. The first LiDAR-based dataset, covering the Rock River and western portion of the study area, was collected between 2008 and 2009, with the DEM released by the University of Vermont Spatial Analysis Laboratory in 2009 (UVM 2010). The second LiDAR-based dataset, covering most of the eastern portion of the study area, was collected in 2010, with the data and DEM released by the USGS in the fall of 2010 (USGS 2010). Combined, the two LiDAR datasets cover approximately 91% of the Vermont portion of the MBB area. The remainder of the Vermont sector is covered by the Vermont "hydrologically corrected" DEM (HYDRO-DEM), a 10-m resolution dataset developed by the Vermont Center for Geographic Information (VCGI) based on 1:5,000 scale orthophoto elevation points. A small portion of the two LiDAR datasets extends over the international border into Canada. The remainder of the Canadian portion of the study area was covered by a collection of DEM "tiles" from the Canadian Digital Elevation Data Level 1 (CDED1) dataset that have resolutions of 0.75 decimal seconds, which is equivalent to approximately 20 m.

A single, continuous DEM at a common resolution was required for the SWAT model. As such, the four source datasets were merged at a resolution that was a compromise between the high resolution LiDAR sources and the lower resolution HDYRO-DEM and CDED1 sources. Key considerations in arriving at the appropriate resolution of the merged DEM were the requirements and limitations of the SWAT model. One of the objectives of this study was to incorporate high resolution of topographic data in in the SWAT model to allow for more accurate and precise calculation of topographic attributes that influence phosphorus transport processes. At the same time, the resolution of the DEM dictates the resolution at which the building blocks of SWAT, the hydrologic response units (HRUs), are created. As the resolution of a DEM increases, the number of HRUs increased several fold. There is a practical (and computational) limit on the number of HRUs that a SWAT model can be built from. At the time of this study, a total of 100,000 HRUs was considered to be an upper limit of practicality and computational feasibility. Based on testing of hypothetical HRU delineations for the MBB SWAT model at a range of DEM resolutions, it was determined that a resolution of 10 m was the highest practical resolution. As will be discussed later in this report, this resulted in a MBB SWAT model that included approximately 109,000 HRUs.

Creation of a 10-m DEM from each of the source DEMs required several processing steps. For the LiDAR-based DEMs, the two LiDAR sections were merged into a seamless 1.6-m resolution DEM, then resampled up to a 10-m resolution, in two steps. First, the 1.6-meter DEM was resampled to a 5-m resolution using a bilinear interpolation algorithm that calculates the new cell value based on a weighted average of the neighboring cells closest to the center of the resampled cell. Next, the 5-mDEM was resampled up to a 10-m resolution DEM, also using bilinear interpolation. The area in Québec covered by the CDED1 20-m DEM required that it be resampled to a higher resolution. Taking a bilinear resampling approach on the coarser 20-m DEM down to a 10-m resolution DEM would result in significant flat areas in the DEM. These flat areas would be problematic in subbasin delineation and calculation of topographic parameters dependent upon slope. Because of this, elevation contours with a contour interval of 5-m was created from the CDED1 DEM. From these contours, a new 10-m resolution DEM was created using the ArcGIS "TopoToRaster" tool. Because the HYDRO-DEM datasets was already at a 10-m resolution, no additional processing was required for this dataset.

The final DEM used as the basis for the SWAT model was created by merging the 10-m DEMs derived from the four sources. Where overlap between the sources datasets existed, the priority was given first to the LiDAR-based DEMs, followed by the HYDRO-DEM, and lastly the CDED1-based dataset. This final DEM, along with the extent of each source DEM, is shown in Map 2.1. Although, the final resolution of this DEM

STONE ENVIRONMENTAL INC

provides less detail than the original LiDAR data, the elevation values are still superior to other lower resolution sources because of the high resolution and accuracy of the original LiDAR data from which it was derived. As will be discussed later in this report, a higher resolution DEM based on the LiDAR data was used in the development of an enhanced hydrologic network for the Vermont sector of the MBB.

2.2.1.2. Compound Topographic Index Development and Analysis

The concept of the compound topographic index (CTI) was introduced in Section 2.1.2. The CTI, as an indicator for areas of increased saturation excess surface runoff, was incorporated into the development of the MBB SWAT model as a way to both delineate HRUs and to parameterize the surface runoff response of those HRUs. This section describes the process for calculating the CTI for the MBB SWAT model area as well as the analysis of the resulting CTI dataset for use in HRU delineation and parameterization.

The calculation of the CTI dataset for the MBB was based on the 10-m SWAT model DEM, and required derivation of datasets representing upslope contributing area as well as slope. The processing of the DEM and the derivation of these datasets was conducted using TauDEM toolset (Tarboton 2010). These tools use an approach for calculating hydrologic flow paths and upslope contributing areas based on the assumption that flow from a single cell can flow to multiple adjacent cells. This approach for determining flow direction is referred to as the "d-infinity" approach (Tarboton 1997), indicating that the flow direction from one cell can go to any number of adjacent cells. This method has the advantage over more traditional single flow direction algorithms which assume that flow can only move from a given cell to a single adjacent cell. The d-infinity approach is particularly powerful in the case where divergent overland flow exists. The TauDEM tools "d-infinity specific catchment area" dataset was used to represent the upslope contributing area input to the CTI calculation. The TauDEM tools "d-infinity slope" dataset was used as the basis for representing the slope input for the CTI calculation. However, for areas where slopes were calculated as "0", a minimum threshold of 0.001% was applied. This is required because the calculation of CTI with value of zero for slope results in an undefined value.

The CTI was calculated based on Equation 1 shown in Section 2.1.1. A spatial filter was then applied to the raw CTI dataset in order to smooth out sharp discontinuities resulting from highly localized DEM variability. The resulting dataset covering the entire MBB study area is shown in Map 2.3. Areas with higher CTI values have a higher likelihood of saturation and therefore a greater amount of surface runoff generation, and are often found along relatively flat valley bottoms. Areas with lower CTI values are often steep hillsides or ridge-top areas; these areas will be less likely to saturate and are predicted to produce less surface runoff. In Map 2.2, the valley bottoms, flat areas, and wetlands are visible having high CTI, as are the high sloping and ridge-top areas with lower CTI. A zoomed area around Hungerford Brook is provided in Map 2.2 to show the detail in the CTI variability at a more local level.

In order to use the CTI in delineating HRUs, CTI values needed to be grouped into classes representing differing levels of saturation excess runoff potential. The number of different classes has a direct and significant impact the total number of resulting HRUs in the SWAT model. Originally, breaking up CTI into five quintiles was considered; however, based on testing of sample HRU delineations, it was determined that this would result in far too large a number of HRUs. Ultimately, it was determined that a maximum of three CTI classes could be used in the delineation of the SWAT model HRUs.

The approach for breaking the distribution of CTI values into classes was designed to capture the areas with considerably lower CTI values than the average (low saturation potential), as well as those areas with

STONE ENVIRONMENTAL INC

considerably higher CTI values than the average (high saturation potential). Classification of areas with low saturation potential (CTI class 1) was taken to be those areas with CTI values in the lowest 20% of the distribution of CTI values. Classification of areas with high saturation potential (CTI class 3) was taken to be those areas with CTI values in the top 20% of the distribution of CTI values. Areas with close the median CTI value, with average saturation potential were those with CTI values in the middle 60% of values in the distribution. In calculating the CTI percentile cutoffs values, the distribution of CTI values that was evaluated was limited to areas for which P CSA classification was being considered; namely, non-water land uses on in the Vermont sector of the study area.

The classification into of the MBB study area into three CTI classes resulted in the following class cutoffs:

- CTI Class 1: CTI < 5.51

- CTI Class 2: $5.51 \leq CTI \leq 8.15$

- CTU Class 3: CTI > 8.15

These classification cutoffs and the complete distribution of CTI values are shown in Figure 2.1. While there is a wide range in values (between 2 and 20) the vast majority of values fall between 3 and 14. A map of the MBB SWAT model area classified according to CTI class is shown in Map 2.3. Along, with land use and soils, this classification was used directly in the delineation of HRUs.

Figure 2.1: CTI distribution in the Vermont sector of the MBB.
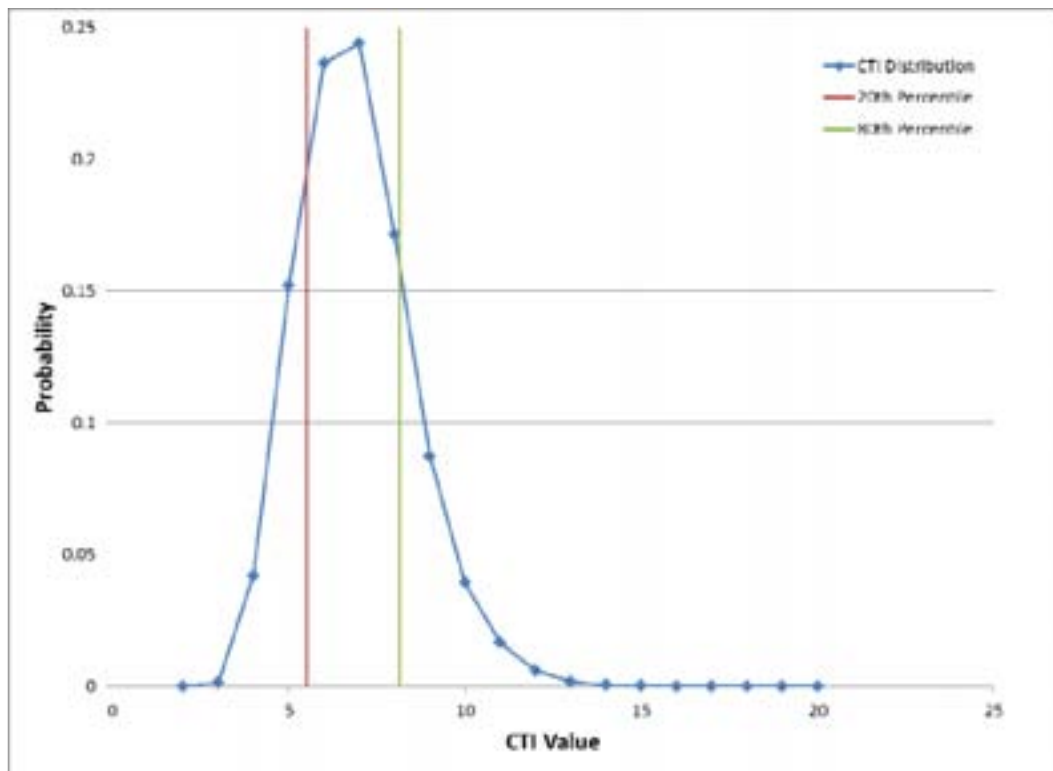
2.2.2. Weather and Climate

The SWAT model requires inputs of daily precipitation and daily maximum and minimum temperature. Because weather drives the hydrologic cycle and the processes that control P transport, constructing an accurate representation of the weather inputs is very important. Due to the topography within the MBB study area, the spatial variability of precipitation and temperature is significant. The average annual precipitation ranges from 36 in (91 cm) near the shores of Missisquoi Bay up to 74 in (188 cm) along the crest of the Green Mountains (PRISM 2006a). Similarly, the average annual temperature ranges from 45 ^{o}F to 36 ^{o}F (7 – 2 ^{o}C) for the same areas (PRISM 2006b,c). Because this variability is driven largely by topography, it is not entirely captured by the spatial distribution of weather observing stations located within and near the MBB study area. Development of precipitation and temperature time series that properly reflect the influence of topography required a procedure that includes both the daily weather observation stations and the annual variability as a function of topography.

2.2.2.1. Daily Weather Data

Daily weather station data were collected for the period 1980 through 2010 from three sources. Data for seven stations with long term records on the Vermont-side of the watershed were obtained from the National Climatic Data Center (NCDC 2010). While not all seven of these stations had complete records for the period of interest, they all had enough data to contribute to the development of SWAT inputs. Data for an additional four stations in Vermont were available for the period from late 2009 through 2010. Data at these four stations were collected by the USGS as part of a tributary monitoring program funded by the Lake Champlain Basin Program. Data for five additional stations in Québec were provided by the Institut de recherche et de développement en agroenvironnement (IRDA 2010a). Table 2.2 provides a summary of these stations and their periods of record. The locations of these weather stations are shown in Map 2.4. From the map, we see that the coverage of stations across the watershed is good; however, several of the stations shown on the map have limited periods of record.

Table 2.2: Weather stations used in the development of SWAT model precipitation and temperature inputs.

Station Name	COOP ID	Period of Record (MM/YYYY)	Source
Albany	430134	4/1993-4/1999	NCDC
Eden 2 S	432698	12/1997-9/2010	NCDC
Enosburg Falls	432769	1/1980-9/2010	NCDC
Jay Peak	434189	9/1988-9/2010	NCDC
Jeffersonville	434261	5/1999-9/2010	NCDC
Newport	435542	1/1980-9/2010	NCDC
St Albans Radio	437032	1/1980-9/2010	NCDC
Hungerford	N/A	10/2009-9/2010	USGS
Trout	N/A	11/2009-9/2010	USGS
Fairfield	N/A	10/2009-9/2010	USGS
Mud	N/A	9/2009-12/2010	USGS
Sutton	N/A	1/1980-9/2010	IRDA/Env. Canada
St. Bernard	N/A	1/1980-9/2010	IRDA/Env. Canada
Philipsburg	N/A	1/1980-9/2010	IRDA/Env. Canada
Brome	N/A	1/1980-9/2010	IRDA/Env. Canada
Bonsecours	N/A	1/1980-9/2010	IRDA/Env. Canada

STONE ENVIRONMENTAL INC

2.2.2.2. Annual Average Precipitation and Temperature Data

The influence that topography has on weather and climate variability is well known (Diodato 2005). The Parameter-elevation Regressions on Independent Slopes Model (PRISM) climate group at Oregon State University has developed a method for procuring national level climate datasets that accounts for topographic variability. The PRISM approach (Daly 1994) has been used to generate 1971 – 2000 climate normals for precipitation, temperature, and dew point on both a monthly and an annual basis at an 800-m resolution. In addition to more common relationships, such as the decrease in temperature with elevation, the PRISM approach is able to capture local climate characteristics such as rain shadow effects and temperature inversions.

The 800-m resolution PRISM raster datasets for 1971-2000 average annual precipitation, maximum temperature, and minimum temperature were obtained from the PRISM Climate Group. The spatial extent of these datasets is limited to within the borders of the United States. In order to incorporate the PRISM datasets into interpolation of the daily climate stations for the entire MBB study area, it was necessary to extrapolate the datasets to the Canadian portion of the study area. This extrapolation was performed by developing regression equations for each weather parameter as a function of elevation. The regression equations were developed by overlaying the climate data (from the PRISM rasters) and elevation (from the MBB DEM raster) within the MBB study area. Then a least squares regression equation based on the pairs of climate and elevation values at each grid cell was derived. These regression equations and their r^2 values are shown in Table 2.3. Based on the relatively high r^2 values, it was reasonable to use these equations to estimate the annual precipitation and temperature normal for the Canadian portion of the study area. The PRISM annual normals, extrapolated into the Canadian portion of the MBB study area, are shown for precipitation, maximum temperature, and minimum temperature in Maps 2.5, 2.6, and 2.7 respectively.

Table 2.3: Weather stations used in the development of SWAT model precipitation and temperature inputs.

Climate Parameter	Regression Equation (x = elevation in meters)	r^2
Precipitation (in)	$0.0376x + 34.35$	0.82
Max Temperature (degrees C)	$0.5432x + 1230.5$	0.96
Min Temperature (degrees C)	$0.0004x^2 - 0.8712x + 201.05$	0.91

2.2.2.3. Development of SWAT Model Climate Time Series

The SWAT model allows the daily climate time series to vary by subbasin. The "default" approach used in the SWAT model to assign weather time series to each subbasin is to identify the closest daily weather station and assign the time series from that weather station to the subbasin. In the current version of the ArcSWAT interface to the SWAT model, there are not any weather station interpolation options available. There are many different methods for interpolating precipitation (and temperature) from point locations to create a continuous surface of the parameter. Many of these methods were reviewed and tested in a paper by Zhang et al. (2009). In their paper, the authors reviewed eight different precipitation interpolation methods, ranging from simple Thiessen and inverse distance weighted (IDW) approaches, to a variety of kriging methods. One of the best performing methods was the approach referred to as "simple kriging with varying local means", or the "SKIm_EL_X method." The approach used both elevation and spatial coordinates as independent variables

STONE ENVIRONMENTAL INC

in the kriging interpolation. While Zhang's study used elevation directly as an additional independent variable, the same method could be applied with other spatially varying independent variables, such as other indicators of how precipitation or temperature vary across the region

One outcome of Zhang's study was a GIS toolset that performs all of the interpolation methods he tested, and generates daily SWAT subbasin climate inputs. This tool was obtained from the authors (Srinivasan 2010) and used to generate unique daily weather time series for each of the 223 subbasins within the MBB SWAT model. The interpolation method applied was the SKIm_EL_X algorithm. In the application of this method for the MBB SWAT model, the use of the elevation raster dataset as an independent variable was replaced by the PRISM-based average annual precipitation, minimum and maximum temperature datasets described in Section 2.2.2.2. Using the average annual precipitation (or temperature) dataset directly in the interpolation of daily values enforces the known annual spatial variability on the daily values.

2.2.3. Land Use Data

Land use data represent one of the primary inputs to the SWAT model and land use is one of the key factors in identifying P CSAs. There were several different existing land use datasets available that covered part or all of the MBB study area. Each of these land use datasets had strengths and weaknesses. In order to provide the SWAT model with the best possible representation of land uses across the study area, a "hybrid" land use layer was developed that took advantage of the strengths of the existing datasets, and incorporated some new enhancements.

2.2.3.1. Base Datasets

Two of the primary existing datasets used to develop the MBB hybrid land use layer were the 2001 Land Use Land Cover for the Lake Champlain Basin (UVM Spatial Analysis Lab 2007) and 2001 National Land Cover Dataset (NLCD). Both datasets have a 30-m cell size and are based upon classification of Landsat imagery. The 2001 Land Use Land Cover for the Lake Champlain Basin (LULC_LCBP) dataset was developed as an improved version of the 2001 NLCD by incorporating additional GIS data and supplementary Landsat imagery. In the development of the LULC_LCBP dataset, particular effort was made to achieve an accurate representation of agricultural areas and to differentiate them from developed open spaces. Additional improvements included "burning in" roads and manual correction procedures to improve classification accuracy. "Burning in" is equivalent to a GIS overlay process that imposes linear features from a vector dataset (such as streams or roads) onto a gridded raster dataset. The LULC_LCBP data aggregated the 19 NLCD 2001 classes found in the Lake Champlain Basin down to eight generalized classes. A listing of the LULC_LCBP classes and the NLCD 2001 classes that they represent is shown in Table 2.4. This shows that, for example, the three classes of urban land uses were lumped into a single urban class and three agricultural classes, grassland/herbaceous, pasture/hay, and cultivated crops were lumped into a single agricultural class.

STONE ENVIRONMENTAL INC

Table 2.4: Land use classes in the LCLU_LCBP and NLCD 2001 datasets.

LULC_LCBP Class	NLCD Class
	Developed, Low Intensity
	Developed, Medium Intensity
Urban	Developed, High Intensity
	Grassland/Herbaceous
	Pasture/Hay
Agriculture	Cultivated Crops
Brush/Scrub	Shrub/Scrub
	Deciduous Forest
	Evergreen Forest
	Mixed Forest
Forest	Palustrine Forested Wetland
	Palustrine Scrub/Shrub Wetland
	Estuarine Forested Wetland
	Estuarine Scrub/Shrub Wetland
Wetland	Estuarine Emergent Wetland
Barren	Barren Land
Urban-Open	Developed, Open Space
	Open Water
Water	Palustrine Aquatic Bed

While the processes used in the development of the LCLU_LCBP dataset resulted in several noted improvements over the NLCD 2001, the NCLD 2001 still offers some notable strengths. One of these advantages is the differentiation between the urban classes based upon the intensity of urban development. In the context of the SWAT model, this allows for differences in the parameterization of those areas, such as the fraction of impervious cover. For this reason, the original NLCD 2001 datasets was included as an input to the development of the MBB hybrid land use layer.

A third land use dataset that covers the Québec portion of the MBB study area was obtained from IRDA (IRDA 2010b). This 30-m resolution land use dataset includes 30 different classifications, including differentiation between agricultural crops for any of the insured crop land based on 2009 crops. While this dataset represents a more recent snapshot in time than do the 2001 LCLU_LCBP and the NLCD 2001 datasets, it was determined to be a better choice for representation of land use in Québec, largely because of the differentiation of agricultural land uses.

STONE ENVIRONMENTAL INC

2.2.3.2. Supplementary Datasets

The three "base" datasets described in the previous section all represented comprehensive land use datasets that, on their own, could have been used as the land use dataset input to the MBB SWAT model. To improve upon those base datasets, several supplementary datasets that contained valuable land use information were incorporated into the development of the hybrid land use dataset.

One of the most important supplementary datasets was a classification of agricultural fields by crop type. Delineation of agricultural field boundaries, known as "common land units" or CLUs, were developed by the USDA Farm Service Agency (FSA). The CLU spatial data that were available through USDA up until 2008 contained field boundaries and acreage, but did not contain any field crop information. Classification of many of the CLUs within the MBB into agricultural land use types was conducted as part of the Missisquoi Area Wide Plan developed by NRCS-Vermont (USDA-NRCS 2008) resulting in a datasets referred to as "MBB Crop and Hay". The MBB Crop and Hay dataset classified CLUs into corn, hay, pasture, idle land, or other crops based on manual interpretation of 2003 National Agricultural Imagery Program (NAIP) imagery. These data would prove invaluable in differentiating the generic agricultural land use classification in the LCLU_LCBP dataset into more specific land uses and crop types that were then assigned different agronomic management characteristics in the SWAT model.

A second CLU-based land cover layer, representing pasture and developed grassland, was also incorporated into the hybrid land use dataset. The dataset, referred to as "sSuburban Pasture" was developed by the UVM Spatial Analysis Laboratory specifically for differentiation of grassland land cover types (UVM SAL, 2006). The CLUs contained in this dataset were used to identify additional pasture areas not already contained in the "MBB Crop and Hay" dataset, as well as to serve as the primary basis for identifying open space within the developed land sector. This dataset was focused on the Champlain Valley counties, thus covered only Franklin County within the MBB study area.

The final land use layer used in classifying agricultural fields was the 2009 Cropland Data Layer (National Agricultural Statistics Service, 2010). This remote sensing dataset focused on the classification of agricultural land uses and differentiates between crop types. The 2009 version of this dataset was used as a means for classifying CLUs that were not already classified by the "MBB Crop and Hay" or the "Suburban_Pasture" datasets. The 2009 CDL was primarily used in Orleans County, which was outside the area covered by the "Suburban_Pasture," and principally identified additional pasture and hay areas.

The 2001 LCLU_LCBP data contained "burned-in" roads as part of the urban land use classification. One objective of the study to identify P critical source areas is to be able to differentiate the P loading potential between different developed land uses, including paved and dirt roads. The lumping of roads into the urban class in the LCLU_LCBP dataset would prevent this distinction from being made. In addition, the 30-m cell size of the LCLU_LCBP dataset significantly over-represents the width of most roads. In order to distinguish between different classes of roads (paved versus dirt) and to allow for a more accurate representation of their width, the Vermont e911 roads dataset (Vermont Center for Geographic Information 2010) was brought into the hybrid land use dataset. For the Québec portion of the study area, a roads dataset that had been clipped to the MBB study area was provided by IRDA and would serve the same purpose as the Vermont e911 roads dataset.

All three of the base land use datasets include a water classification. This classification represents the larger water bodies and wider sections of rivers well, but misses many of the smaller ponds and narrower sections of rivers and streams. The Vermont Hydrography Dataset (VHD), obtained from the Vermont Center for

STONE ENVIRONMENTAL INC

Geographic Information (VCGI 2010), was chosen to add additional information of the locations of lakes, ponds, and narrower river segments. For the Québec portion of the study area, a hydrography dataset that had been clipped to the MBB study area was provided by IRDA and would serve the same purpose as the Vermont VHD dataset to represent areas of water within the MBB study area.

Additional information regarding the location of wetlands was incorporated into the hybrid land use dataset from the Vermont Significant Wetlands Inventory dataset (VSWI) obtained from the Vermont Center for Geographic Information (VCGI 2010). In particular, the VSWI data was used to help distinguish forested wetland areas with more wetland characteristics from forested areas that should be classified as forest.

A final dataset that was used to supplement the development of the hybrid land use layer was a farmsteads footprint dataset. As part of the Missisquoi Area Wide Plan, a dataset representing point locations of farmsteads within the MBB was created (USDA-NRCS 2008). The farmstead locations in this dataset represent animal housing areas, milking parlors, outside livestock concentration areas, and manure and feed storage areas. The farmstead points in this datasets were identified through interpretation of aerial photography and a subset of the identified sites was subsequently ground-truthed. In total, there were 943 farmsteads identified in this dataset. Representation of these farmsteads in the land use layer in the SWAT model would require that the point locations be converted into "farmstead footprints" that represent the area that the farmstead covers on the landscape. To create farmstead footprints, each of the point locations was located with the 2009 NAIP true color imagery as a background. The region surrounding the point location that contained the farmstead, including heavy use areas, farmstead structures, and connecting areas was than manually digitized on screen. An example of a farmstead delineation is shown in Figure 2.2 below.

Figure 2.2: Farmstead footprint delineation in MBB.

STONE ENVIRONMENTAL INC

In addition to delineating farmstead footprints, each footprint was classified according to whether it was part of a small, medium or large farm operation. The addresses of the medium farm operations (MFOs) and large farm operations (LFOs) were obtained from the Vermont Agency of Agriculture, Food & Markets (AAFM) in 2007. This data was used as the basis for identifying which of the footprints digitized were associated with those farms. The classification of farmsteads as MFO and LFO was checked by Laura DiPietro from AAFM (DiPietro 2011a) and was determined to be accurate. The final farmsteads footprint dataset contained 905 individual footprints, of which five were classified as part of an LFO, 30 were classified as part of an MFO, and the remaining 870 were classified as part of an SFO. The 905 total footprints is less than the original 943 that were identified as part of the Missisquoi Area Wide Plan. The farmsteads that were not included in the footprint delineation were determined to no longer be active based on the latest imagery.

2.2.3.3. Enhancement of CLU Crop Classification

The CLU-based crop classification dataset described in the previous section identified the agricultural land use for individual fields based on a snapshot in time. This resulted in fields receiving a single crop or use type, predominantly corn, hay, or pasture. It is common agricultural practice in the Missisquoi Bay Basin to follow a crop rotation that involves both corn and hay on the same field. Recognizing that some fields are likely to follow a corn-hay rotation, rather than be copped in either permanent hay or permanent corn, will have a significant impact in the identification of critical source areas. While specific current or historical crop rotation information at the MBB watershed scale is not publicly available, estimation of the whether a given field is cropped as permanent corn, permanent hay, or a corn-hay rotation was made based on landscape and soils characteristics of the field.

A set of criteria for distinguishing crop rotations based on slope and soils characteristics were developed to classify each agricultural field within the Vermont sector of the MBB. The basis for these criteria was established through consultation with a sub-group of the Project Advisory Committee (PAC). These criteria are shown in Table 2.5 below.

Table 2.5: Topographic and soils criteria used for designating field-level corn-hay rotations.

Cropping Type	Slope	Drainage Class	HEL Class	Soil Phase	Soil Texture	Bedrock Depth
Permanent Corn	$\leq 3\%$	Well Drained	Not HEL	Not stony	Sandy, loamy	
Permanent Hay	$\geq 12\%$	Poorly Drained		Stony		Shallow

There are 7,571 CLUs within the MBB that have been classified as either corn or hay. To classify these CLUs as permanent corn, permanent hay, or corn-hay rotation, the characteristics described in Table 2.5 were determined for each of these CLUs. Each characteristic was identified as follows:

1. Slope: Slope was calculated for each CLU as the mean slope obtained from the 10-m DEM described in Section 2.2.1.

2. Drainage class: The NRCS SSURGO database drainage class attribute was used to characterize this characteristic. The drainage class covering the greatest percentage of each SSURGO mapping unit was assigned to that mapping unit. The mapping units classified as "well drained" or "moderately well drained" were designated as "well drained" for the purposes of identifying permanent corn. The mapping units classified as "somewhat poorly drained", "poorly drained",

STONE ENVIRONMENTAL INC

or "very poorly drained" were designated as "poorly drained" for the purposes of identifying permanent hay. The CLU boundaries were then overlaid with the SSURGO mapping units, and the predominant drainage class on a CLU was assigned to that CLU.

3. HEL (Highly Erodible Land) Class: The HEL class attribute for each SSURGO mapping unit was taken from the "VT Top 20" table. Map units classified as "highly erodible" were selected as "HEL" for the purposes of identifying are athat could NOT be permanent corn. The CLU boundaries were then overlaid with the SSURGO mapping units, and the predominant HEL class was assigned to each CLU.

4. Soil Phase: The designation of a soil phase being "stony" or "non-stony" was made based on the map unit name. If the name contained either "stony" or "rocky", then the soil was considered "stony" for the purposes of distinguishing areas a permanent hay, permanent corn, or corn-hay rotation . The CLU boundaries were then overlaid with the SSURGO mapping units, and the predominant soil phase designation was assigned to that CLU.

5. Soil Texture: While both "sandy" and "loamy" soils were initially identified as being likely areas for permanent corn, that designation was deemed too broad, because many fields had those two texture characteristics. Instead, only "sandy" soils would be considered when identifying permanent corn areas. If the soil mapping unit name contained "sand" or "sandy", then the soil was considered "sandy" for the purposes of identifying permanent corn. The CLU boundaries were then overlaid with the SSURGO mapping units, and the predominant soil texture designation was assigned to that CLU.

6. Bedrock Depth: The bedrock depth attribute "ROCKSHALLO" for each SSURGO mapping unit was taken from the "VT Top 20" table. Map units with "ROCKSHALLO" values of 20 inches or less were designated as having shallow depth to bedrock for the purposes of identifying permanent hay. The CLU boundaries were then overlaid with the SSURGO mapping units, and the predominant bedrock class was assigned to that CLU.

In addition to the six criteria listed above, for a CLU to be classified as "permanent corn" it had to have been identified as corn in the original CLU interpretation. Likewise, for a CLU to be classified as "permanent hay", it had to have been identified as hay in the original CLU interpretation.

There are many ways in which the criteria established for differentiating permanent corn or hay from corn-hay rotations could be combined to make this designation, resulting in a range of acreages assumed to be in each of the cropping classifications. In order to establish a combination of these criteria that resulted in the appropriate distribution between corn and hay land, estimations of the total corn and hay land in the watershed in any given year was made using two approaches. The first approach used the original crop classification of CLUs to calculate the acreage of corn and hay within the Vermont side of the MBB study area. The second approach used the 2002 and 2007 Census of Agriculture data to estimate the acreage of corn and hay. The process for calculating the corn and hay acreage from the Census of Agriculture dataset was a follows:

1. The average (2002 and 2007) total acres harvested of corn and hay crops were calculated or each county that falls within the MBB.

2. The fraction of total cropland in each county that falls within the MBB was calculated based on the fraction of NLCD 2001 "cultivated cropland" and "pasture hay" classes within each county.

STONE ENVIRONMENTAL INC

3. The county level Census of Agriculture acreages of corn and hay were multiplied by the fraction of total cropland in the county falling within the watershed, then summed for all the counties in the watershed.

The corn and hay acreages and the percent of the total cropland based on the two methods are shown in Table 2.6. Given the different time periods that the two approaches represent, the values are very close to one another, with the percent of corn versus hay within 6% of each other.

Table 2.6: Estimates of corn and hay acreage within the Vermont Sector of the MBB.

Crop	CLU Area Method		Census of Ag Method	
	Acreage	**% of Total**	**Acreage**	**% of Total**
Corn	16,779	25.0	21,352	30.9
Hay	50,231	75.0	47,852	69.1
Total	67,010	100	69,204	100

The crop acreage estimates shown in Table 2.6 were used to develop an appropriate combination of the crop rotation classification criteria that would result in a similar acreage distribution. Specific landscape criteria were developed in collaboration with a PAC sub-group. The resulting multi-attribute criteria used to designate each crop classification were as follows:

1. Permanent Hay: ((Slope $\geq$12%) Or (Slope $\geq$ 3% AND ((Shallow Bedrock = "Yes") Or (Stony Phase of Soil = "Yes") Or (Poorly Drained Soil = "Yes")))) AND (Original CLU Crop Class = Hay).

2. Permanent Corn: ((Slope $\leq$3) And (HEL = "No") And ((Well Drained Soil = "Yes") OR (Stony Phase of Soil = "No") Or (Sandy Soil ="Yes"))) AND (Original CLU Crop Class = Corn)

3. Corn-Hay Rotation: Not permanent hay and not permanent corn.

Based on the criteria above, the distribution of land into the three categories was derived as shown in Table 2.7. The acreages shown assume that for the corn-hay rotation classification, 50% of the land is corn and 50% is hay in any given year. The resulting acreage of total corn (30.3% of corn/hay land) and total hay percent (60.7% of corn/hay land) falls within the range of estimates from the CLU crop and the Census of Agriculture datasets (see Table 2.6), with the new estimates somewhat closer to the Census of Agriculture estimates. This suggests the multi-attribute criteria proposed does a reasonable job in achieving the correct proportion of the three different cropping classes.

Table 2.7: Estimated corn and hay crop rotation distribution within the Vermont sector of the MBB.

Crop	Acreage	Percent
Permanent Corn	6,522	9.7
Permanent Hay	27,628	49.0
Corn/Hay Rotation	32,860	41.3
Total Corn Acres	20,336	30.3
Total Hay Acres	46,674	69.7
Total Corn and Hay Acres	67,010	

STONE ENVIRONMENTAL INC

2.2.3.4. Development of a Hybrid Land Use Dataset

The datasets described in the previous sections were combined to create a hybrid land use dataset, taking the best aspects of each of the source datasets. The land use data were compiled independently for the Vermont and Québec sectors of the MBB study area, then the two sectors were merged together. The spatial resolution of both datasets was set at 10-m, corresponding to the resolution of the SWAT model DEM. For the Vermont sector, the 2001 LCLU_2001 was used as the primary "base" dataset. The processing steps in compiling the Vermont sector were as follows:

1. The VT e911 roads layer was re-burned into the 2001 LCLU_LCBP dataset. During this process, an effort was made to erase the original representation of roads from the 2001 LCLU_LCBP. The objective was to achieve a more accurate representation of road area allowed by using a 10-m cell size instead of the 30-m cell size of the original dataset.

2. The farmstead footprints were converted to a raster dataset and merged with results from step 1, above. The LFO and MFO farmsteads were given the same classification in this process, because they are both subject to the same non-point source runoff controls.

3. The CLU-based agricultural and suburban grassland data layer was converted to a raster dataset and merged in with the results from step 2.

4. From the results of step 3, the urban classification (based on the 2001 LCLU_LCBP class) was reclassified to the NLCD 2001 urban classification that stratifies the urban areas into low, medium and high intensity. This was only performed where both 2001 LCLU_LCBP and NLCD 2001 indicated and urban class.

5. The forested wetland class from NLCD 2001 was reclassified into forest or wetland. If the VSWI dataset indicated a Class 2 wetland, then the area was classified as wetland, otherwise, the area was classified as forest.

6. The VHD lakes and ponds and area river features were converted to a raster datasets and merged in with the results from step 5.

7. The results from step 6 were reclassified to create the final land use classes for the Vermont sector.

An example section of the final hybrid dataset compared with the original 2001 LCLU_LCBP dataset is shown in Figure 2.3.

STONE ENVIRONMENTAL INC

Figure 2.3: Example of hybrid land use dataset, near Highgate, Vermont.
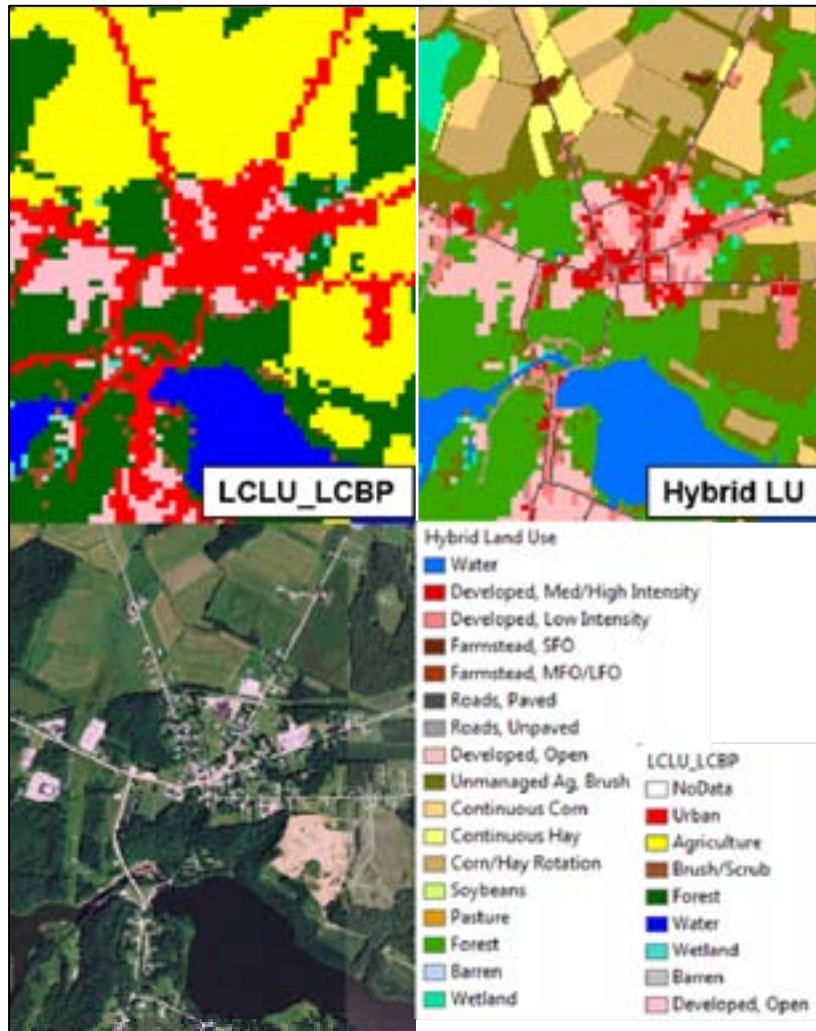
Several enhancements to the LCLU_LCBP dataset stand out in Figure 2.3. The area classified as "Agriculture" has been replaced by the CLU-based land classifications in the hybrid dataset, including continuous corn, continuous hay, corn/hay rotation, soybeans, and pasture. Also, the "Urban" class has been replaced by "Developed, Med/High Intensity", "Developed, Low Intensity", "Roads, Paved", and "Roads, Dirt". Regarding the new roads classification, the extent of the roads class in the hybrid dataset is now more representative of the actual width or roads, resulting in a more accurate estimation of their total area. Another important point is that the LCLU_LCBP areas that had been classified as "Agriculture", but were not part of a CLU have been now classified as "Unmanaged Ag, Brush". This is important, because these areas are not under active agricultural management, and are treated entirely differently within the context of the SWAT model.

The processing steps in compiling the Québec sector of the hybrid land use dataset were simpler than those for the Vermont sector of the MBB study area. These steps were as follows:

STONE ENVIRONMENTAL INC

1. The vector roads layer for Québec was classified into paved and unpaved roads and converted into a 10-m raster dataset. This road dataset was the then "burned into" the base land use layer for Québec.

2. The lakes, ponds, and river area hydrography features in Québec were converted to a raster dataset and merged with the resulting dataset from step 1.

3. The land uses form the base dataset were reclassified to match the land use classes developed for the hybrid dataset for the Vermont portion of the MBB study area.

The final land use dataset covering the entire MBB study area is shown in Map 2.8. The dataset consists of 18 different land use classes, including five developed classes, eight agricultural classes (including farmsteads), and five undeveloped classes (including water). One of the agricultural classes, "Cultivated Ag, General" is found only in Québec and primarily consists of uninsured cropland that is most likely hay (Beaudin 2010), as well as some minor crops that were too limited in extent to treat as a separate land cover class. A summary of land uses within the MBB study area, including both Vermont and Québec portions, is provided in Table 2.8. Substantial effort went into the development of the hybrid land use dataset, with a focus on incorporating higher resolution data into the foundation land use layers; however, it should be recognized that uncertainties exist in the land use interpretations. Many land use classifications represented in hybrid data layer have been interpreted from automated classifications of remote sensing imagery or manual interpretations of aerial imagery. Neither approach provides 100% accuracy, and some land cover classes are known to be particularly difficult to classify, such as pasture (Potter, 2011b). Nevertheless, the land cover dataset developed represents a compilation of the best available sources for land cover data key to the identification of phosphorus CSAs.

Table 2.8: Land use distribution over MBB study area.

Crop	Area (ha)	Percent of Area
Forest	170,017	66.95
Unmanaged Ag, Brush	18,491	7.28
Hay	15,050	5.93
Corn-Hay	11,144	4.39
Wetlands	7,190	2.83
Cultivated Ag, General	6,389	2.52
Pasture	5,388	2.12
Developed, Open	4,435	1.75
Water	4,264	1.70
Corn	3,633	1.43
Developed, Low Intensity	3,566	1.40
Roads, Dirt	1,820	0.72
Roads, Paved	953	0.40
Farmstead, SFO	489	0.19
Developed, Med/High Intensity	380	0.20
Barren	358	0.14
Soybean	283	0.11
Farmstead, MFO/LFO	113	0.04
Total	253,963	100%

STONE ENVIRONMENTAL INC

2.2.4. Soils Data

Soils data, along with land use, are among the primary determinants for HRUs in the SWAT model. Different combinations of land use and soil will exhibit different responses to hydrologic inputs and will therefore show variability in their potential to transport P. Two datasets, one for the Vermont sector of the MBB study area and one for the Québec portion served as primary sources for soils inputs to the SWAT model. A second supplementary dataset provided additional information of soil-test P levels.

2.2.4.1. Base Soils Data Compilation

2.2.4.1.1. Vermont Soils

The SSURGO dataset (USDA-NRCS, 2009) served as the base soils layer for the Vermont sector of the MBB study area. This dataset is a 1:20,000 scale vector dataset that includes soil mapping units with a minimum area of about 3 ac (1.2 ha). Each mapping unit in SSURGO represents from one to three soil series (occasionally up to five). These soils series within a SSURGO mapping unit are referred to as components, and with each component, there are associated soil horizons. The number of soil horizons varies depending on the soil, and can range from a single horizon, up to five or more horizons. The soils information required by the SWAT model includes both physical and chemical attributes, including bulk density, available water capacity, saturated hydraulic conductivity, organic carbon content, and P content. All of the required parameters for SWAT are generally available in the SSURGO database.

The preparation of soils data for use in SWAT requires that each soil mapping unit be assigned a single set of soil attributes. However, SSURGO mapping units, however, contain multiple soil components – each representative of a different fraction of the total mapping unit area, and each with different characteristics. In order to assign a single set of soil characteristics to each mapping unit, the soils component covering the greatest fraction of the mapping unit (the dominant component) was selected to represent the unit.

During the discussion of DEM resolution and the CTI classification in Section 2.2.1, the issue of input data resolution and its impact of HRU delineation and model complexity was introduced. The concept was that when higher resolution inputs (such as a higher resolution DEM) and datasets with greater variability (such as a CTI datasets with a large number of classifications) are used as criteria for HRU delineation, we can quickly build a model where the number of HRUs is impractical, if not impossible, to manage. A number of 100,000 HRUs was proposed a practical upper limit for a single SWAT model. This concept has relevance to the development of the soils input dataset as well, because opportunities for simplification in the complexity of the soils inputs is necessary to keep the total number of HRUs, and complexity of the model, to a manageable level.

There are a total of 303 unique SSURGO mapping units within the MBB study area. The dominant component for each of these was selected to represent the mapping unit. In many cases, the dominant component for multiple mapping units was exactly the same, meaning that component key was the same, indicating that all of the soils attributes were the same. In these cases, it was clear that those mapping units need not be distinct soils in the SWAT model. There were additional situations where mapping units may have a different component keys (meaning not all attributes are exactly the same), however the soil series component name, and many of the other primary attributes were the same. These situations offered an opportunity to further reduce the number of different soils in the SWAT model input dataset. To handle these situations where nearly identical soils occurred on different mapping units, the following rules were applied:

STONE ENVIRONMENTAL INC

1. To be considered as the same soil, the soil components must have the same:

   a. Component name (e.g., "Adams")

   b. Hydrologic soil group

   c. Number of soil layers

   d. Soil layer thickness for each layer

2. For soils meeting the criteria to be classified as the "same" soil, the required SWAT attributes (e.g., bulk density) would be calculated as the area weighted average of the values for each of the soils being aggregated into the same soil (based on each soils relative area within the MBB study area).

As a result of the soil aggregation steps described, the total number unique soils within the MBB study area dropped from 303 to 119, of which 112 ultimately fell within the MBB watershed boundary. This aggregation process provided a great benefit in terms of keeping the complexity of the model inputs in check, while still providing the detail to capture the spatial variability in soil characteristics.

2.2.4.1.2. Québec Soils

The soils geospatial and attribute data for the Québec portion of the MBB study area were provided by IRDA (IRDA 2011a). This datasets had been developed by IRDA based on the best available public information, and an evaluation of the relevant soils databases. In some cases, soil polygons did not have any attribute information available, and in those cases, the attributes for the nearest neighboring polygon were assigned. For some additional polygons, multiple soil descriptions were available (similar to multiple components with each SSURGO mapping unit). In these situations, it was most common to choose the description associated with the agricultural use of the soil to assign to the soil polygon. In total, there were 26 unique soil types in the Québec portion of the MBB study area.

2.2.4.1.3. Combined MBB Soils Dataset

The Vermont and Québec soils data layers were combined into a single dataset for use as input to the SWAT model. This resulted in a total of 138 different soils present within the study area. Map 2.9 shows the spatial variability in soil types over the full study area. Because there are 145 different soil names, a legend has not been provided to describe each soil present in the map; the variability in symbols shown on the map, however, provides a means for understanding the differences in the spatial variability in soils between the Vermont and Québec portions of the watershed. The 1:20,000 scale SSURGO data source for Vermont resulted in considerably greater spatial variability in soils, even with the aggregations that were performed.

2.2.4.2. Soil Phosphorus Data Analysis

Soil P is a critical parameter for defining CSAs. Excessive soil P levels have been linked to high P losses in runoff, especially in areas of animal-based agriculture (Pote et al. 1996, Sims et al. 2000). P export in runoff has been observed to be proportional to soil-test P levels (Sharpley 1995). The SWAT model requires soil-test P as a key input parameter.

STONE ENVIRONMENT INC

Unfortunately, extensive soil P data for agricultural fields in the MBB do not exist, and what data exist are not spatially referenced. Therefore, default soil-test P concentrations were assigned by land use classification. The UVM Agricultural Testing Laboratory conducts soil analysis for Vermont farmers, although the results are located only by town and contain limited additional data on crop and soil type. A database of some 3,400 soil test reports from 2005 – 2010 for the towns (or portions of towns) in the MBB was obtained from UVM. Using these data, the distribution of soil-test P results for identified land uses in the MBB towns was assessed. The records also included data on some other site and soil characteristics (e.g., drainage, tillage, and soil organic matter), which allowed for exploration of correlations that could help adjust default soil-test P values to more site specific conditions.

Unfortunately, no useful correlations were found. While there were some differences among mean soil-test P by town, these differences did not support application of any particular geographic pattern to soil P. No useful association between soil organic matter and soil P was observed. There was a weak relationship between soil-test P and tillage (i.e., soil-test P tended to be lower on reduced tillage compared to conventional tillage fields); this relationship was confounded, however, by land use because tillage was reported not only for cornland but also for hayland. In the end, only significant differences of mean soil-test P among major agricultural land uses allowed us to assign generic values of soil-test P to land in corn, hay, soybeans, and pasture.

The specific chemical analysis used to generate the soil-test P data was an additional complicating factor. Several different extraction/analytical procedures can be employed to determine soil-test P levels; these procedures differ among states in order to account for regional differences in soil chemistry and agronomic recommendations. Results from different analytical procedures are not directly comparable. Vermont uses the Modified Morgan (MM) test, an extraction that helps account for the effects of soil aluminum (Al) on bioavailable P. The SWAT model, however, requires soil-test P data generated from the Mehlich-3 (M3) extraction. Therefore it was necessary to convert UVM soil-test P data from the Modified Morgan to the Mehlich-3 scale.

We evaluated a number of options for making this conversion (e.g., Ketterings 2005), but were unable to use existing tools either because a direct MM to M3 conversion tool did not exist or because additional data needed for conversion (e.g., soil calcium levels) did not exist in our MM dataset. We were able to obtain a data set of 200 soil-test P analyses conducted by the UVM Agricultural Testing Laboratory using both the MM and M3 methods (Tilley 2011). Using this dataset, we derived a satisfactory multiple linear regression model that was used to convert MM to M3. This model incorporated MM soil-test P, soil pH, and soil reactive Al concentration, all of which were available for the larger MBB soil test database, to estimate M3 soil-test P from the reported MM values. This model is shown in Figure 2.4. The regression model shown in resulted in an $R^2 = 0.73$, with $P \leq 0.001$. The regression equation was:

Mehlich-3 P = 6.718(MM P) – 11.83(pH) – 32.757(MM P/Al) + 90.73

STONE ENVIRONMENTAL INC

Figure 2.4: Plot of relationship between soil-test P analyzed by MM and by M3 procedures.
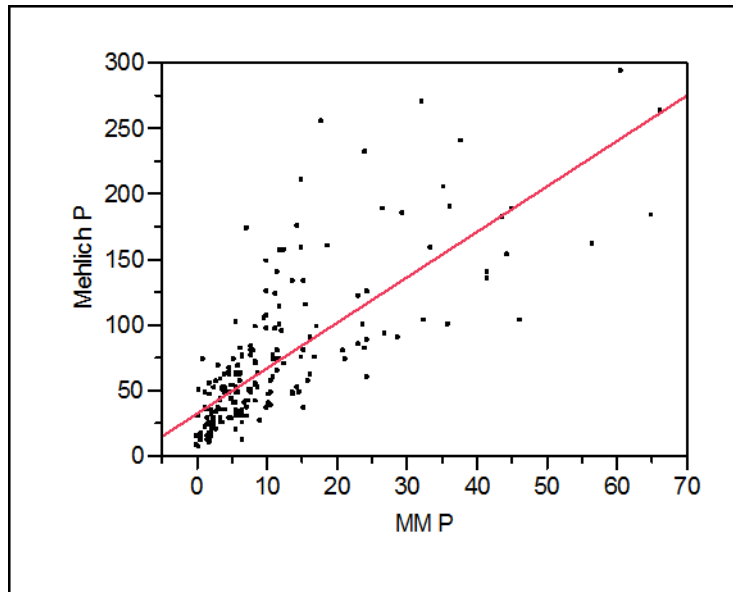
We then applied the estimation equation to all records in the large soil sample dataset from the UVM Agricultural Testing Laboratory. The median values for each crop type were selected to initialize SWAT (Table 2.4).

Table 2.9: Descriptive statistics for Mehlich-3 soil test-P (mg/kg) from 3,400 soil samples in the MBB.

	All samples	Corn	Grass	Alfalfa	Beans	Pasture
Mean (mg/kg)	55.5	68.1	45.9	51.8	31.4	51.5
Median (mg/kg)	43.1	55.8	38.7	43.9	31.1	36
Interquartile range (mg/kg)	31.3 – 62.3	35.7 – 82.8	30.1 – 52.2	32.0 – 62.2	27.2 – 36.6	27.3 – 50.6
Overall range (mg/kg)	2.2 – 544.0	6.2 – 375.2	2.2 – 352.4	14.0 – 168.6	21.5 – 39.1	2.2 – 352.4

2.2.5. Animal Density and Manure Production in the MBB

One of the primary P inputs in the MBB is animal manure. Manure is both a waste product and a valuable resource in the management of soil fertility and crop production. In Vermont, dairy farmers typically apply all their manure to the land, often with priority given to corn land; any additional nutrient needs are met using purchased inorganic fertilizers. It is believed that most dairy farms in the MBB have an adequate land base on which to apply their on-farm manure nutrients at agronomic rates, although there are no systematic data to support this belief.

For farms under a rigorous nutrient management plan, manure is usually analyzed for N and P content and quantities of manure are applied based on nutrient content, crop need, and soil test. In many cases, however, "textbook" values for these parameters are used. UVM Extension, for example, cites a typical P_2O_5 concentration in liquid dairy manure of 8 lb/1000 gal ($1kg/m^3$) and provides recommendations for N and P

STONE ENVIRONMENTAL INC

application rates for a variety of Vermont field crops (Jokela et al. 2004). Other statistics are available that estimate the per animal daily manure production and nutrient excretion, e.g., a milking dairy cow is estimated to produce 115 lb (52 kg) or 13.9 gal (52.6 L) of manure each day, excreting 0.57 lb (0.26 kg) of N and 0.24 lb (0.11 kg) of P each day (e.g., MN Dept. of Ag. 1995).

An important aspect to manure nutrients is the N:P ratio of animal manure. The N:P ratio in manure is generally less than 5:1, while uptake ratios of plants are usually considerably higher, on the order of 8 or 9:1, in part due to over-supplementation of P in livestock diets. The imbalance between the N:P ratio in manure and that in crops often leads to excessive P application soil if application rates of manure are based on N requirement.

These general values of manure production and nutrient content can be used to check the general order of magnitude of our estimates of manure P generation and land application in the MBB.

2.2.5.1. Calculation and Allocation of Farm Phosphorus Production to Sub-watersheds, Vermont Sector

The approach taken for estimating the amount of phosphorus from farm waste within the Vermont sector of the MBB was to directly calculate phosphorus generated based on the number and types of animal units within located within the study area. The approach required the following steps:

1. Determine the total number of animal units within each county intersecting the MBB study area, and calculate the total P generated based on the number and type of animal units, typical animal unit weights, and standard P excretion rates for the different animal types.

2. Estimation of the fraction of manure P generated that occurs on pasture, that was assumed to not end up in the farm manure storage.

3. Allocation of county-level total farm P to crop and pasture areas within sub-watersheds of the MBB study area.

These steps are described in more detail in the sections that follow.

2.2.5.1.1. County Level Farm Total P Generation

The total count of animals units at the county level was obtained from the 2007 Census of Agriculture (USDA-NASS 2009). No attempt was made to independently verify the number from the Census of Agriculture. These animal counts are provided in Table 2.10.

Table 2.10: Animal counts for counties intersecting the MBB watershed. Numbers represent the entire county.

Animal Type	Animal Count			
	Franklin	**Lamoille**	**Orleans**	**Grand Isle**
Beef Cows	986	288	1,109	160
Milk Cows	37,770	3,589	20,733	3,041
Calves	23,880	2,488	16,076	2,656
Hogs and Pigs	531	56	89	
Sheep and Lambs	526	431	895	

STONE ENVIRONMENTAL INC

	Animal Count			
Animal Type	Franklin	Lamoille	Orleans	Grand Isle
Layers	3,149	1,727	1,199	
Broilers	620	1,426	315	
Horses and Ponies	708	614	702	
Goats	738		778	

1. The hogs and pigs count for Lamoille county was estimated based on the number of farms

2. The layers count for Franklin County was estimated based on the number of farms.

It does not include the Vermont Egg Farm, which transports its waste outside of the MBB watershed.

For each animal type reported in the 2007 Census of Agriculture, the average animal weight and the typical phosphorus excretion rate in the animal's manure was estimated. The P excretion rates are based on a per animal unit (AU) basis, where one animal unit is equivalent to 1,000 lb (454 kg). These values and their sources are provided in Table 2.11.

Table 2.11: Average animal weights and P excretion rates used in the calculation of total animal P generation.

	Average Animal Weight		Average Animal P Excretion Rate	
Animal Type	Weight (kg)	Source	P Excretion (kg/d-AU)	Source
Beef Cows	589.7	1	0.050	7
Milk Cows	589.7	1	0.032	7
Heifers/Calves	317.5	1,2	0.018	7
Hogs and Pigs	90.7	3	0.073	7
Sheep and Lambs	81.6	4	0.023	7
Poultry	1.4	5	0.141	7
Horses and Ponies	498.9	5	0.032	7
Goats	81.6	6	0.032	7

1. Cassell et al., 1998

2. Heinrichs et al., 1998

3. National Pork Producers Council, 1998

4. American Sheep Industry Association, 2011

5. Vermont Methane Pilot Project, 2011

6. American Dairy Goat Association, 2011

7. USDA, 1992

Based on the animal counts in each county (Table 2.10) and the animal weights and P excretion rates in Table 2.11, the total P generated from animal manure was calculated for each county. In addition, the P from excreted manure, P contributions from animal bedding and milkhouse waste were also quantified based on the

STONE ENVIRONMENTAL INC

number of animal units. The amount of bedding material was assumed to be 1.4 kg/d-AU and the P content of bedding material was assume to be 0.001 kg/kg (Casell et al. 1998). The amount of milkhouse wastewater was assumed to be 0.22 ft3/d-AU, with a P content of 0.58 lb P/d-AU (USDA, 1992). Based on these farm P sources, the total amount of P generated per year was calculated for each county. These data are summarized in Table 2.12.

Table 2.12: Total farm P generated by county.

	Annual Total Farm P (kg/yr) by County			
P Source	**Franklin**	**Lamoille**	**Orleans**	**Grand Isle**
Manure	715,188	79,684	423,388	61,906
Bedding	34,997	3,877	20,896	3,089
Milkhouse Waste	7,758	737	4,259	625
Total	757,944	84,298	448,543	65,620

The total farm P generated by county was used as the basis for estimating the total P applied to cropland and pasture for the different sub-watersheds within the Vermont sector of the MBB.

2.2.5.1.2. Estimation of Total P Applied to Pasture from Grazing Animals

A portion of the amount of P calculated for each county (Table 2.11) is applied to directly to pasture land as manure from grazing animals. In order to develop an estimate, the fraction of time in a year that different types of animals spend in pasture was estimated using several assumptions that were developed in consultation with Laura DiPietro of AAFM (DiPietro 2011b). A summary of these assumptions are provided in Table 2.13.

Table 2.13: Animal grazing assumptions used in calculating amount of farm P applied as animal manure to pasture.

Animal Type	**Fraction Grazed**	**Grazing Start Date**	**Grazing End Date**	**Hours Grazing (per day)**	**Fraction Grazing Full Day (24 hours)**
Beef Cows	0.90	5/1; 5/15	11/1; 11/15	14	0.8
Milk Cows	0.28	5/1; 5/15	11/1; 11/15	14	0
Calves/Heifers	0.65	5/1; 5/15	11/1; 11/15	14	0.4
Sheep/Goats	1.00	5/1; 5/15	11/1; 11/15	14	0.8
Horses/Ponies	1.00	5/1; 5/15	11/1; 11/15	14	0.2

1. Grazing start and end dates dependent upon growing season length

Based on the data in Table 2.13, the fraction of the total P from animal manure that gets applied directly to pasture was calculated for each county. The fraction of manure P that is not applied directly to pasture ("Pasture Manure P") ends up in the farm waste storage, referred ("Pit Manure P"). The partitioning of the total manure P between pit and pasture is summarized in Table 2.14. These values, combined with the non-manure farm P sources shown in Table 2.12 were then allocated to distinct sub-watersheds within the Vermont

STONE ENVIRONMENTAL INC

sector of the MBB and annual application rates on cropland and pasture were determined. This allocation process is described in the next section.

Table 2.14: Animal grazing assumptions used in calculating amount of farm P applied as animal manure to pasture.

| P Source | Annual Manure P Distribution (kg/yr) by County | | | |
	Franklin	Lamoille	Orleans	Grand Isle
Total Manure P	715,188	79,684	423,388	61,906
Pit Manure P	630,902	67,755	369,390	52,932
Pasture Manure P	84,286	11,929	53,999	8,974
Fraction Pasture Manure P	0.12	0.15	0.13	0.14

The data in Table 2.14 shows that the annual application rate of P on cropland and pasture does not vary significantly among the different HUC12 sub-watersheds. This is because the amount of P available for application in a given sub-watershed was allocated based upon the cropland or pasture area. One reason for the variability that does exist is the different amounts of total P produced in each county and how the various watershed fall within of between those counties. The other reason for variability is the differences in the types of animals in each county and their grazing characteristics.

2.2.5.1.3. Allocation of Total Farm P Applied to Crop and Pasture Areas within the MBB

The allocation of total farm P generated at the county level was allocated to each HUC12 sub-watershed within the Vermont sector of the MBB study area. The allocation was based on the fraction of agricultural land (pasture and cropland) within each county that fell within each HUC12. The dataset used to calculate area of agricultural land within each county and within each HUC12 watershed was the NLCD 2001 dataset. The NLCD land use classes that were used to represent agriculture were the "Pasture/Hay" class and the "Cultivated Cropland" class. The total farm P spread as manure to cropland (representing corn, hay, and soybean) and that applied directly by grazing animals is summarized by HUC12 sub-watershed in Table 2.15. The application rates, in kg/ha-yr, were calculated by dividing the total P by the land area available for application for use in the SWAT model.

The P application rates in Table 2.15 can be converted to an approximate application rate of gallons/acre to provide a means for comparison with common agronomic practices. This requires several assumptions regarding the nutrient content and density of pit manure, which can vary by farm and by time of year. A manure pit analysis for liquid dairy manure in Vermont suggests that a typical P content is 8 pounds P_2O_5 / 1000 gallons liquid manure (Jokela et al. 2004). Assuming a manure density 8.5 pounds/gallon (as was also reported in Jokela et al. (2004)), this is equivalent to 0.00041 pounds of mineral P per pound of liquid manure. Based on these assumptions, and after several additional calculations, the manure P cropland application rate most common in Table 2.15 (21.9 kg P/ha) is found to be roughly equivalent to 5,607 gallons liquid manure/acre. This represents the average annual manure application rate applied to all corn, hay, and soybean land, assuming those three crops receive equal amount of manure each year. The P inputs from farm waste sources listed in Table 2.15 were converted to equivalent manure fertilizer applications rates and pasture daily manure inputs for use in the SWAT model.

STONE ENVIRONMENTAL INC

Table 2.15: Allocation of farm P to cropland and pasture, Vermont HUC-12 sub-watersheds.

HUC12 Sub-Watershed	Total P Applied to Cropland (kg/yr)	Total P Applied to Pasture (kg/yr)	Cropland P Application Rate (kg/ha-yr)	Pasture P Application Rate (kg/ha-yr)
020100070101	4,464	300	21.1	12.7
020100070102	9,464	353	20.4	12.7
020100070103	14,958	309	20.0	12.7
020100070104	49,001	3,526	21.2	12.7
020100070105	29,389	2,206	21.3	12.7
020100070302	89	-	19.6	-
020100070303	4,296	98	21.9	11.6
020100070304	33,314	4,647	21.8	11.6
020100070401	7,752	1,059	21.9	11.6
020100070402	7,503	2,220	21.9	11.6
020100070501	32,462	6,078	21.9	11.6
020100070502	81,009	12,616	21.9	11.6
020100070601	29,071	5,310	21.2	11.6
020100070602	12,312	2,057	21.9	13.7
020100070603	47,849	10,662	21.9	11.6
020100070701	22,223	861	21.9	13.7
020100070702	40,814	2,254	21.9	13.7
020100070703	20,346	516	21.9	13.7
020100081001	39,793	6,544	21.9	11.6
020100081004	10,319	697	21.9	11.6
020100081101	74,094	3,450	21.9	13.7
020100081102	17,291	1,138	18.7	12.2
Total	**587,813**	**66,899**		

2.2.5.2. Calculation and Allocation of Farm Phosphorus Production to Sub-watersheds, Québec Sector

An approach similar to the one just described for the Vermont sector of the MBB was followed in estimating amount of P from farm sources applied to cropland in Québec; however, there were several differences. These were due to differences in the source data for animal units, and the fact that pasture areas were not represented as a distinct land use classification in the Québec portion of the MBB study area. Also, because of the higher resolution animal unit data, animal units were first allocated to HUC12 watersheds, then the total P generated was calculated for the HUC12. This order of steps is in reverse of what was followed for the Vermont side, where the total P generated was first calculated at the county level, and then allocated to the HUC12 level. The steps followed for the Québec farm P allocation were as follows:

1. Estimate the total number of animal units within the different sub-watersheds (HUC12s) of the MBB in Québec.

STONE ENVIRONMENTAL INC

2. Calculate the total P generated in each sub-watershed based on the number and type of animal units, typical animal unit weights, and standard P excretion rates for the different animal types.

These steps are described in more detail in the sections that follow.

2.2.5.2.1. Estimation of Animals within Missisquoi Bay Basin Sub-Watersheds

The spatial resolution of animal unit data in Québec was much higher that the resolution of animal unit data available for Vermont. While Vermont's data was on a county level, the data from Québec was on a 5 km. by 5 km. grid (IRDA 2011b). In addition, the animal categories for the Québec data were slightly different than the categories for the Vermont data, primarily due to a higher level of differentiation of cattle classifications in the Québec data.

To estimate the numbers of each animal type within the HUC12 watersheds within the Québec portion of the MBB watershed, a two-step land area based allocation process was followed. The first step was to estimate the fraction of animals in a 5 km grid cell that falls within MBB watershed. This fraction was based only on the fraction of the grid cell that falls within the watershed boundary. The next step was then to allocate the fraction of animals within each grid cell that fall within the MBB watershed to the different HUC12 sub-watersheds that intersect that grid cell. This second step used the hybrid land use dataset agricultural land use classes to allocate the animals to different HUC12s based in the fraction of agricultural area. Figure 2.5 shows a map of the of the animal density grid overlaid with the HUC12 sub-watersheds and hybrid land use dataset to provide a visual aide in how animal aggregation from grid cells to sub-watersheds was conducted.

Figure 2.5: Datasets used in the allocation of animal units from grid cells to HUV12 sub-watersheds.

STONE ENVIRONMENTAL INC

2.2.5.2.2. Calculation of Total Farm P Generated by Sub-Watershed

Using the same process as was followed for calculating total farm P at the county level for the Vermont-side of the study area, the total farm P generated within each HUC12 watershed was calculated for the Québec-side. The assumptions regarding animal weights, P excretion rates, bedding and milkhouse waste were the same, although the somewhat different animal classifications required that weight and P excretion rate values be assigned to these additional animal classes. The animal classes from the Québec dataset and their associated average weights and P excretion rates are shown in Table 2.16.

Table 2.16: Average animal weights and P excretion rates used in the calculation of total animal P generation, Québec.

Animal Type	Average Animal Weight		Average Animal P Excretion Rate	
	Weight (kg)	Source	P Excretion (kg/d-AU)	Source
Beef Cattle - Cattle Finishing	589.7	1	0.050	7
Beef Cattle - Cattle semi-finishing	589.7	1	0.050	7
Beef Cattle - Heifers	317.5	1,2	0.050	7
Beef cattle - breeding bulls	589.7	1	0.050	7
Beef Cattle - Heifers replacement	317.5	1,2	0.050	7
Beef Cattle - Cows (a calving or more)	589.7	1	0.054	7
Beef - Feeder Calves	181.4	1,2	0.045	7
Dairy Cattle - Heifers	317.5	1,2	0.018	7
Dairy Cattle - Bulls	589.7	1	0.023	7
Dairy Cattle - Heifers	317.5	1,2	0.018	7
Dairy Cattle - Cows	589.7	1	0.032	7
Horse	498.9	5	0.023	7
Sheep	81.6	4	0.032	7
Pigs	90.7	3	0.073	7
Calves	181.4	1,2	0.018	7
Poultry, other	1.4	5	0.141	7
Poultry, chickens	1.4	5	0.141	7

1. Cassell et al., 1998

2. Heinrichs et al., 1998

3. National Pork Producers Council, 1998

4. American Sheep Industry Association, 2011

5. Vermont Methane Pilot Project, 2011

6. American Dairy Goat Association, 2011

7. USDA, 1992

STONE ENVIRONMENTAL INC

Using the assumptions in Table 2.16 and the same animal bedding and milkhouse waste assumptions used in the Vermont sector calculation (see Section 2.2.5.1.1), the total farm P produced within each HUC12 sub-watershed was calculated. The P application rate from farm waste was then calculated based on the assumption that all agricultural cropped areas receive an equal amount of P application from manure. The total P generated and the associated P application rate on cropland is summarized by HUC12 in Table 2.17. In addition, a map showing the P application rates of cropland for HUC12 sub-watersheds in both Vermont and Québec is shown in Map 2.10. Comparing these P application rates with those for the Vermont side of the watershed, there are two items to note. First, the application rates for the sub-watersheds with more significant amounts of agriculture (e.g., the Rock River) are similar. Second, there is greater variability in the P application across the Québec sub-watersheds than is seen in across the Vermont sub-watersheds. This is in part a function of the higher resolution of the animal units data in Québec, that leads to greater variability in P available for application.

Table 2.17: Allocation of farm P to cropland by HUC-12 watershed, Québec HUC-12 sub-watersheds.

HUC12 Sub-Watershed	Total P Applied to Cropland (kg/yr)	Cropland P Application Rate (kg/ha-yr)
020100070104	5,558	6.4
020100070105	1,099	4.6
020100070301	40,986	20.6
020100070302	1,673	2.5
020100070303	32,500	13.2
020100070304	3,104	26.3
020100081001	2,495	9.3
020100081004	5,641	22.5
020100081101	50,940	21.3
Total	**143,995**	

2.2.6. Agronomic Management Operations and Crop Rotations in the MBB

The SWAT model requires that certain agronomic management operations such as tillage, planting, and harvest dates, manure or fertilizer application rates, and crop rotations be specified for each unit of cropland. Clearly, such data did not exist for each field in the MBB and we were reluctant to create a bias by assuming different practices/conditions for different fields in the watershed. Nevertheless, SWAT parameters had to be estimated. We met on several occasions with farmers from the MBB, through the Farmers' Watershed Alliance, to establish representative values for the required agronomic management parameters. Although it was made clear to us that all of these management operations varied depending on weather, soil type, location, and the individual, we nevertheless had to come up with representative values. We further discussed these values with members of the PAC, particularly representatives from VTAAFM, UVM Extension, and NRCS, all of whom had direct experience working with farmers in the basin. In addition, we received guidance regarding agronomic management practices through correspondence with scientists at IRDA (Michaud 2011a). In many cases, the Québec practices were very similar to practices in the Vermont sector of the MBB.

The dates for the occurrence of agronomic practices represent average dates that were arrived at through the consultations with the PAC and farmers. While these dates may vary from year to year, they represent a

STONE ENVIRONMENTAL INC

reasonable set of dates that is representative of all areas within the watershed. The option of varying the agronomic practices dates for different fields was considered, but not chosen. Using a constant set of dates for all fields was chosen to minimize the introduction of bias into the ranking of fields as P critical source areas. If, for example, planting dates for corn were allowed to vary over a 1 month planting window, then the timing of fertilizer and manure applications could vary significantly over those same fields. This could lead to the situation where one field would appear as a more significant critical source area simply due to the date on which manure application was specified relative to significant runoff events. As such, the approach of using uniform agronomic operations and operation dates was determined to the best approach for SWAT modeling application aimed at identifying critical sources areas.

The agronomic practices incorporated into the SWAT model for each crop or crop rotation will be described in the following sections. A few points regarding the management operation schedules that apply to several of the crop rotations should be noted. First, for some crop rotations, practices differed depending upon whether the crop was grown on clay or non-clay soils. Second, the P that is applied as manure is applied at the same total rate per year to all the crops that receive manure (corn, hay, soybean in Vermont; corn and hay in Québec); however, the number applications that occur in each year may vary from crop to crop. Finally, P application rates from manure vary spatially (by HUC12) based on the analysis presented in Section 2.2.5. The manure P application rates shown in the operations schedule tables that follow are examples of common application rates.

2.2.6.1. Permanent Corn, Vermont

The 2007 US Census of Agriculture (USDA 2009) showed that 95% of the corn grown in Franklin, Orleans, Lamoille, and Grand Isle counties was corn for silage, with only 5% corn for grain. Therefore, all corn crops in Vermont were assumed to be silage corn in the MBB SWAT model. Agronomic practices for permanent corn were determined to vary depending upon whether the crop was on clay or non-clay soils. For clay soils, primary tillage (and manure application) occurs in the fall following harvest, while on non-clay soils, primary tillage (and manure application) occurs before planting in the spring. For corn, there is one manure application per year, that is followed by tillage to incorporate the manure into the soils. In Tables 2.18 and 2.19, the agronomic operations for non-clay and clay soils are shown, with a typical manure P application rate taken from Table 2.15.

Table 2.18: Permanent corn in Vermont, non-clay soils, agronomic management operations schedule.

Management Operation	Date	Fertilizer Application Rate
Manure Fertilizer	5/1	21.9 kg-P/ha (varies by HUC12)
Tillage, Chisel Plow	5/5	
Tillage Disk	5/10	
Starter N Fertilizer, as Urea	5/15	44.8 kg-N/ha
Starter P Fertilizer, as P2O5	5/15	14.8 kg P/ha
Plant Corn	5/15	
Side-dress N Fertilizer, as Urea	7/10	89.7 kg-N/ha
Harvest Corn	10/1	

STONE ENVIRONMENTAL INC

Table 2.19: Permanent corn in Vermont, clay soils, agronomic management operations schedule.

Management Operation	Date	Fertilizer Application Rate
Tillage Disk	5/10	
Starter N Fertilizer, as Urea	5/15	44.8 kg-N/ha
Starter P Fertilizer, as P2O5	5/15	14.8 kg P/ha
Plant Corn	5/15	
Side-dress N Fertilizer, as Urea	7/10	89.7 kg-N/ha
Harvest Corn	10/1	
Manure Fertilizer	10/10	21.9 kg-P/ha (varies by HUC12)
Tillage, Chisel Plow	10/15	

2.2.6.2. Permanent Corn, Québec

Data form the 2006 Canadian Census of Agriculture (Statistics Canada 2006) shows that for the Census Consolidated Subdivisions that intersect the MBB study area in Québec, 92% of the corn is grown for grain. Therefore, all crops grown in Québec were corn for grain in the MBB SWAT model. In addition, the typical agronomic practices for permanent corn in Québec were found to have a few differences form the Vermont practices. In the case of non-clay soils, corn in Québec is fall chisel plowed as opposed to spring chisel plowed. In the case of clay soils, corn in Québec is fall conservation plowed, and then manure is applied in the spring. Otherwise, the operations were the same. As with permanent corn in Vermont, the P application rate from manure varies geographically, and a representative rate from Table 2.17 is shown as an example. The complete operation schedules for non-clay and clay soils are shown in Tables 2.20 and 2.21, respectively.

Table 2.20: Permanent corn in Québec, non-clay soils, agronomic management operations schedule.

Management Operation	Date	Fertilizer Application Rate
Manure Fertilizer	5/5	21.3 kg-P/ha (varies by HUC12)
Tillage Disk	5/10	
Starter N Fertilizer, as Urea	5/15	44.8 kg-N/ha
Starter P Fertilizer, as P2O5	5/15	14.8 kg P/ha
Plant Corn	5/15	
Sidedress N Fertilizer, as Urea	7/10	89.7 kg-N/ha
Harvest Corn	10/1	
Tillage, Chisel Plow	10/15	

STONE ENVIRONMENTAL INC

Table 2.21: Permanent corn in Québec, clay soils, agronomic management operations schedule.

Management Operation	Date	Fertilizer Application Rate
Manure Fertilizer	5/5	21.3 kg-P/ha (varies by HUC12)
Tillage Disk	5/10	
Starter N Fertilizer, as Urea	5/15	44.8 kg-N/ha
Starter P Fertilizer, as P2O5	5/15	14.8 kg P/ha
Plant Corn	5/15	
Sidedress N Fertilizer, as Urea	7/10	89.7 kg-N/ha
Harvest Corn	10/1	
Tillage, Conservation Tillage	10/15	

2.2.6.3. Permanent Hay, Vermont and Québec

The agronomic practices for permanent hay were the same for all soil types. In addition, the agronomic practices for permanent hay land in Québec were determined to be similar to those in Vermont. Therefore, a single set of management operations was used to simulate permanent hay in both Vermont and Québec. During consultation with the PAC and local farmers, it was indicated that the frequency of hay harvests could vary between three and four cuttings per year. Similarly, the number of manure application could vary between two and three per year. For the purposes of this study, it was assumed that there would be three cuttings and two manure applications per year for all hay land. As has been mentioned already, keeping practices uniform for different cropping types limited the amount of bias that could be introduced during the ranking of P critical source areas. Orchard grass was identified as one of the more common species grown for hay (Darby, 2011a) and was thus chosen as the grass for all hay fields. The complete operations schedule for one year of permanent hay is shown in Table 2.22. In the SWAT model management operations, permanent hay was plowed and re-seeded every six years. In the first year of re-establishment, the first cutting and first manure application is skipped.

Table 2.22: Permanent hay in Vermont and Québec, agronomic management operations schedule.

Management Operation	Date	Fertilizer Application Rate
Harvest Hay	6/15	
Manure Fertilizer	6/16	10.9 kg-P/ha (varies by HUC12)
Harvest Hay	7/30	
Manure Fertilizer	7/31	10.9 kg-P/ha (varies by HUC12)
N Fertilizer, as Urea	7/31	44.8 kg-N/ha
Harvest Hay	9/15	

STONE ENVIRONMENTAL INC

2.2.6.4. Corn-Hay Rotation, Vermont and Québec

In Vermont, fields were explicitly identified as being in a corn-hay rotation based on their soils and slope characteristics (see Section 2.2.3.3). In Québec, the areas that were classified as either corn or hay in the hybrid land use dataset were assumed to be in permanent corn or permanent hay respectively. For the areas in Québec classified as "Cultivated Ag, General", a portion of these areas were assigned to a corn-hay rotation management schedule and a portion was set to be permanent hay. Based on an evaluation of the 2006 Canadian Census of Agriculture (Statistics Canada 2006), it was determined that assigning a corn-hay rotation to these areas in the Rock River watershed would result in the proper ratio of cropland in corn and versus hay. In regions further to the east, in the Sutton and Missisquoi Nord watersheds, it was determined that minimal corn was grown, so the "Cultivated Ag, General" class was given a permanent hay rotation in these areas.

The most common corn-hay rotation was determined to be four years of hay followed by four years of corn. The management operations during corn years were set the same as those for a permanent corn rotation, while the management operations during hay years were the same as those for a permanent hay rotation. The same variations for clay versus non-clay soils were applied. In years with hay plantings, a tillage operation was performed on April 20 followed by hay planting on May 1.

The corn-hay rotation of four years corn followed by four years hay was applied to all land simulated as having a corn-hay rotation in SWAT. To achieve a nearly constant distribution between total land in hay and total land in corn from year to year, half of the fields within the MBB SWAT model were set to start off their rotation in hay and the other half was set to start off their rotation in corn. Because the splitting of corn-hay rotation fields into half beginning with hay and half beginning with corn was conducted for the entire MBB study area, the fraction of fields starting in hay and those starting in corn was not necessary equal at the local sub-watershed level. Nevertheless, this approach did provide a nearly equivalent distribution of the full watershed, and prevented the possibility of some years having too much corn and some years having too much hay.

2.2.6.5. Soybean-Corn Rotation, Vermont

Compared to corn and hay, soybean represents a much less significant crop in terms of cropped area within the MBB in Vermont, accounting for only 0.4% of the total cropland (corn, hay, and soybean) in the MBB SWAT model. Despite being a relatively minor crop, evaluating soybeans crops as a potential P critical source area was of interest, so management operation schedules were developed for soybean. Based on correspondence with the UVM Extension (Darby 2011b), it was suggested soybean be rotated every other year with corn. As discussed, agronomic practices differ between corn on clay soils and corn on non-clay soils. Therefore, separate operations schedules were developed for a soybean-corn rotation on clay versus non-clay soils. As was the case for corn, primary tillage occurs in the spring on non-clay soils and in the fall on clay soils. Unlike corn, soybeans do not receive nitrogen fertilizer or phosphate P fertilizer. The full 2-year soybean-corn rotations for non-clay and clay soils are shown in Tables 2.23 and 2.24 respectively.

STONE ENVIRONMENTAL INC

Table 2.23: Soybean-corn rotation in Vermont, non-clay soils, agronomic management operations schedule.

Management Operation	Year	Date	Fertilizer Application Rate
Manure Fertilizer	1	5/15	21.9 kg-P/ha (varies by HUC12)
Tillage, Chisel Plow	1	5/21	
Tillage Disk	1	5/26	
Plant Soybean	1	6/1	
Harvest Soybean	1	10/15	
Manure Fertilizer	2	5/1	21.9 kg-P/ha (varies by HUC12)
Tillage, Chisel Plow	2	5/5	
Tillage Disk	2	5/10	
Starter N Fertilizer, as Urea	2	5/15	44.8 kg-N/ha
Starter P Fertilizer, as P2O5	2	5/15	14.8 kg P/ha
Plant Corn	2	5/15	
Side-dress N Fertilizer, as Urea	2	7/10	89.7 kg-N/ha
Harvest Corn	2	10/1	

Table 2.24: Soybean-corn rotation in Vermont, clay soils, agronomic management operations schedule.

Management Operation	Year	Date	Fertilizer Application Rate
Tillage Disk	1	5/26	
Plant Soybean	1	6/1	
Harvest Soybean	1	10/15	
Manure Fertilizer	1	10/25	21.9 kg-P/ha (varies by HUC12)
Tillage, Chisel Plow	1	10/31	
Tillage Disk	2	5/10	
Starter N Fertilizer, as Urea	2	5/15	44.8 kg-N/ha
Starter P Fertilizer, as P2O5	2	5/15	14.8 kg P/ha
Plant Corn	2	5/15	
Side-dress N Fertilizer, as Urea	2	7/10	89.7 kg-N/ha
Harvest Corn	2	10/1	
Manure Fertilizer	2	10/10	21.9 kg-P/ha (varies by HUC12)
Tillage, Chisel Plow	2	10/15	

STONE ENVIRONMENTAL INC

2.2.7. Urban and Developed Phosphorus Sources

2.2.7.1. Build-up and Washoff of P from Impervious Surfaces

2.2.7.1.1. Buildup and Washoff Simulation

The default accumulation rates of pollutants on impervious surfaces used in SWAT are taken from Manning et al. (1977), who cite Sartor and Boyd (1972) as a primary source. More recently, researchers have found that solids accumulation rates calculated in the study by Sartor and Boyd were too high. Because SWAT simulates washoff processes in a manner consistent with this earlier research, the default washoff rate in SWAT is also too high.

Pitt et al. (2004) suggest that because default street dirt accumulation and washoff rates used in continuous models such as SWAT were generally unrealistically high, calibration of sediment transport to observed event mean concentrations has typically resulted in overestimation of sediment loading from paved surfaces and underestimation of sediment loading from pervious areas of the watershed.

Modeling buildup and washoff using current generation watershed-scale models requires gross simplification of complex, interacting processes. According to James et al. (2008), simulating urban runoff water quality entails "very large uncertainties…both in the representation of the physical, chemical, and biological processes and in the acquisition of data and parameters for model algorithms"; however, alternative approaches, such as assuming a constant pollutant concentration in runoff or applying a statistical method based on a distribution of empirical concentration data, appear even less satisfactory, especially with limited empirical data. Therefore, it is necessary to select realistic starting values for buildup and washoff parameters in SWAT, recognizing that these may be refined during calibration.

2.2.7.1.2. Buildup and Washoff Formulation in SWAT

SWAT offers two options for simulation of solids and associated phosphorus loading from developed land. One is a set of linear regression equations developed by USGS for estimating storm runoff volumes and constituent loads. The other option is to simulate buildup and washoff. The buildup and washoff option was chosen because it considers solids availability for transport, which the regression equation approach does not.

Buildup of solids is simulated on dry days with a Michaelis-Menton equation:

$$SED = (SED_{mx} * td) / (T_{half} + t_d)$$

Where:

SED is the solid buildup (kg/curb km) td days after the last occurrence of SED = 0 kg/curb km;
SEDmx is the maximum accumulation of solids possible for the urban land type (kg/curb km);
t_d = time (days); and
thalf is the length of time needed for solid buildup to increase from 0 kg/curb km to ½ SEDmx (days)

The buildup function is clearly an idealized simplification of many complex mechanisms. The shape of the buildup curve is determined by the maximum amount of solids on the street (SEDmx) and the time required for half this amount of solids to accumulate (T_{half}). The Michaelis-Menton equation represents rapid initial accumulation (where deposition>> loss to air as fugitive dust). As air losses increase due to the increased

STONE ENVIRONMENTAL INC

supply of street solids, the accumulation rate declines, until the loss rate is nearly equal to the deposition rate. Buildup has also been represented as a linear function to a maximum amount.

There is a paucity of appropriate data to use in parameterizing the urban component of the SWAT model. Most sources on buildup and washoff present dirt and dust accumulation rates, either as sediment mass per unit area per unit time or sediment mass per length of street curb per unit time. These rates presume linear buildup, so while these data are instructive, they are not directly applicable to our case. There are some sources (see below) to aid in selecting values for SEDmx, but, outside the model documentation no data were found for T_{half}. If it were appropriate to use EMCs from monitoring of small urban watersheds to derive SEDmx and T_{half}, the body of data would be far greater; however, Pitt et al. (2004) present a convincing argument that this is not appropriate. We are left with few sources of accurate buildup data and we found no buildup data in New England.

SWAT uses an exponential relationship is used to simulate washoff of accumulated solids:

$$Y_{sed} = SED_0 \cdot \left(1 - e^{-kk \cdot t}\right)$$

where:

Ysed is the cumulative amount of solids washed off at time t (kg/curb km);
SED_0 is the amount of solids built up on the impervious area at the start of the event (kg/curb km); and
kk is a coefficient, which may be estimated by assuming it is proportional to the peak runoff rate:

$$kk = urb_{coef} \cdot q_{peak}$$

where: urbcoef is the washoff coefficient (mm-1) and qpeak is the peak runoff rate (mm/hr).

Because the washoff function does not include a mechanism to constrain the efficiency of the washoff process once the readily available street dirt has been removed, in large events washoff will proceed until there is a negligible solids load on the street surface. The urbcoef variable is typically used to calibrate to observed data.

The exponential washoff relationship used in SWAT means that the washoff rate at any time is proportional to the remaining (or the remaining available) solids load. In other words, washoff is limited by supply. In SWAT, the rate of solids washoff becomes asymptotic when the amount of solids built up at the beginning of the event is nearly gone. Note that in the alternate formulation by Pitt et al. (2004), the washoff rate would become asymptotic when the available street dirt is nearly gone, leaving the non-available residual. This recognition of sediment supply seems preferable to regression approaches that show ever increasing washoff with increasing runoff. The sediments are assumed to have a constant concentration of phosphorus, based on the land use type.

2.2.7.1.3. SWAT Parameter Adjustments

We selected an appropriate set of buildup and washoff values for each surface type. Ultimately we only identified values for solids accumulation on paved surfaces. To our knowledge there is no local buildup and washoff data to use in the simulation. SWAT default values were used in some cases, where more refined estimates were not found in the literature. Because the texture of paved surfaces was not differentiated across the SWAT land use classes, the mean value of the smooth textured and rough textures surfaces was applied to all SWAT impervious surfaces. This data is summarized in Table 2.25, followed by the sources of each parameter.

STONE ENVIRONMENTAL INC

Table 2.25. TSS and P buildup and washoff parameter used in SWAT model

Land Type	SED_{mx} (kg/curb km)	T_{half} (days)	urb_{coef} (mm^{-1})	TP_{conc} (mg/kg)
Smooth and intermediate textured roads	140[A]	11.7[b]	0.055[D]	2,567[E]
Rough and very rough textured streets	370[A]	18.5[c]	0.055[D]	2,567[E]
SWAT model values[F]	255	15.1	0.055[D]	2,567[E]

Notes on sources:

A. 140 kg/curb-km is the maximum observed street dirt loading value given in Pitt et al. (2004) for "US nationwide—residential streets in good condition". More local or recent data were not found. 370 kg/curb-km is the maximum observed street dirt loading value given in Pitt et al. (2004) for "US nationwide—industrial streets (poor condition)". To derive this value, Pitt et al. (2004) corrected data originally presented in Sartor and Boyd (1972).

B. SWAT defaults for T_{half} range from 0.75 days for low and medium/high density residential land to 3.90 for transportation. The values are from studies in 10 US cities by Sartor and Boyd (1972). Pitt et al. (2004) corrected the accumulation rates of Sartor and Boyd (1972) to account for the initial loadings. The deposition rate presented by Pitt et al. (2004) corresponding with the maximum observed loading (140 kg curb-km^{-1}) for "US nationwide—residential streets, good condition" is 6 kg curb-km^{-1} d^{-1}. From this rate, T_{half} was calculated for smooth textured roads as:

$$T_{half}=0.5 \times 140 \text{ kg curb-km}^{-1} / 6 \text{ kg curb-km}^{-1} \text{ d}^{-1} = 11.7 \text{ d}$$

This calculation implies linear buildup, which is counter to the Michaelis-Menton formulation.

C. T_{half} for rough textured roads was calculated in the same manner as for smooth textured roads (above). The deposition rate presented by Pitt et al. (2004) corresponding with the maximum observed loading (370 kg curb-km^{-1}) for "US nationwide—industrial streets (poor condition)" is 10 kg curb-km^{-1} d^{-1}. From this rate, T_{half} was calculated for rough textured roads as:

$$T_{half}=0.5 \times 370 \text{ kg curb-km}^{-1} / 10 \text{ kg curb-km}^{-1} \text{ d}^{-1} = 18.5 \text{ d}$$

D. The default value for the washoff coefficient in SWAT is 0.18 mm^{-1} (4.6 in.$^{-1}$). This value was proposed during the original SWMM development. As described by James et al. (2008), Sonnen (1980) used sediment transport theory to estimate values for the washoff coefficient ranging from 0.052 in.$^{-1}$ to 6.6 in.$^{-1}$ (0.002 – 0.26 mm^{-1}) and indicated that 4.6 in.$^{-1}$ (the SWAT default) was relatively high. However, James et al. (2008) concluded that washoff coefficient values in the range of 1.0 in.$^{-1}$ to 10 in.$^{-1}$ appear to give concentrations in the range of most observed values in urban runoff.

STONE ENVIRONMENTAL INC

Given that 1) much of the historic buildup and washoff data is erroneous (Pitt et al. 2004), 2) the form of the washoff coefficient as incorporated in SWAT is not common in the literature, 3) the washoff coefficient has been found to vary by more than two orders of magnitude (Sonnen 1980), and 4) it is typically adjusted in model calibration, a more extensive search for appropriate literature values was not performed. The value used by CADMUS (2010) as part of a TMDL study for Lower Fox River Basin and Lower Green Bay, Wisconsin (e.g., 0.055 for residential areas and 0.039 for high density areas) is likely a more appropriate starting point than the SWAT default value given that the default value was almost certainly based on an overestimation of street dust and dirt accumulation.

E. SWAT's default values for TP_{conc} appear to have been derived from values for "PO_4-P" reported by Sartor and Boyd (1972), as summarized by Manning et al. (1977). The PO_4-P values are exactly one quarter of the corresponding SWAT default TP_{conc} values, because PO_4-P was assumed to represent a fixed 25% of the total phosphorus concentration in solids. Multiplication of the PO_4-P values by a factor of four to derive TP_{conc} in solids appears to be a crude and unsupported extrapolation of these data.

Limited, more recent P data is available from studies in Wisconsin and Vermont. Waschbusch et al. (2000) measured the total phosphorus content values in two urban basins near Madison, Wisconsin and found median concentrations that ranged from 569 mg/kg for streets to 2,649 for driveways and sidewalks to 3,777 mg/kg for roofs. In the St. Albans (Vermont) Green Streets project (conducted by VTDEC and Stone Environmental in 2010-2011) the total event mean P concentration in runoff samples from two streets ranged from 76.1 to 1,380 µg/L. TSS concentrations in corresponding samples ranged from 16.4 mg/L to 876 mg/L. If 100% of the total P is assumed to be particulate P, then the TP concentration of the transported solids ranged from 937 to 4,640 mg/kg and averaged 2,567 mg/kg.

F. SWAT is not able to distinguish between smooth and rough textured streets, therefore SED_{mx} and T_{half} were parameterized with a value obtained by averaging these coefficients.

2.2.7.2. Residential Fertilizer Use

No information was available on residential/non-agricultural fertilizer use in the MBB. Because very high soil test P levels had been measured on residential lawns in nearby St. Albans City (Gaddis 2007), we believed that it was important to estimate fertilizer P applications to land in the non-agricultural, developed category.

Limited survey data from elsewhere in Vermont provided some useful information. A 2003 survey of residents of the Englesby Brook watershed in Burlington (Lake Champlain Sea Grant et al. 2003) indicated that about one-third of residents regularly applied lawn fertilizer and that the majority of these relied on lawn service or bag label recommendations to determine application rates. A similar survey around Malletts Bay in Colchester showed that 30% of respondents applied lawn fertilizers and again the majority relied on bag or lawn service information for application rate (Center for Rural Studies 2004). A second survey of the Englesby Brook watershed showed that about 40% of residents regularly apply lawn fertilizers (Lake

STONE ENVIRONMENTAL INC

Champlain Committee 2004). Two 2007-2008 stormwater opinion and behavior surveys in Chittenden County (Regional Stormwater Education Program et al. 2007, 2008) revealed that 33 – 50% of residents use lawn fertilizers and most respondents did not base application rates on soil tests. In a report to the 2009 Vermont legislature, AAFM reported that although sales of non-agricultural phosphate fertilizers in the state have declined since 2003, some 161 tons of P were sold in Vermont in 2007 in the form of non-agricultural fertilizers (VTAAFM 2008).

Thus, it seemed reasonable to assume that some residential turf in the MBB receives P fertilizer. However, because the data described above come entirely from Chittenden County, the most urban/developed county in the state, we believed that frequency of lawn fertilizer application was likely to be somewhat lower in the more rural/agricultural MBB. Thus, we estimated that 20 – 25% of residential lawn area in the MBB receive P fertilizer applications each year, with the specific areas more concentrated around more densely populated village centers.

The parameterization of residential fertilizer applications into the SWAT model was based on the survey information just described, and the nutrient content of typical lawn fertilizer. A common formulation for a bag of Scott's lawn fertilizer contains a nutrient content of 29-3-3. Based on the size of the bag and the recommended fertilizer application rate, the mineral P application rate is equivalent to 2.06 kg P/ha. To handle the fact that only a fraction (20% - 25%) of residential grass receives fertilizer applications, it was decided that all residential grass areas would receive a reduced application rate (20% - 25% of bag rate) rather than have a randomly selected group of residential HRUs receive the full application rate. This approach was designed to minimize the introduction of bias into the CSA assessment by treating all residential HRUs of a given class equally. The final assumption employed was that the medium density residential areas had a higher likelihood of applying fertilizer than the more rural low density residential areas and developed open grass areas. This resulted in the following annual P application rates applied to developed land areas:

1. Low Density Residential (20% applying fertilizer): 0.41 kg P/ha

2. Medium Density Residential (25% applying fertilizer): 0.52 kg P/ha

3. Developed Open Areas (20% applying fertilizer): 0.41 kg P/ha

These annual application rates of P were applied uniformly to the pervious areas of the residential land uses in the MBB SWAT model.

2.2.7.3. Septic Systems

The current version of the SWAT 2009 model includes processes for simulating nutrient inputs to the subsurface due to septic system effluent contributions. The way in which these processes have been designed in the model requires that each septic system simulated be delineated as a distinct HRU. While this structure is appropriate for localized simulations of septic system impacts on subsurface water quality, it is not compatible with the conceptual framework of the MBB SWAT model, which focused on a detailed delineation of HRUs based on land use, field management, and topographic characteristics. For this reason, it was not possible to represent septic system inputs in the model simulation. As justification for the exclusion of septic systems from the analysis, we point to previous work by Budd and Meals (1994) which concluded that P contributions from septic systems were not an important source of P at the basin scale.

STONE ENVIRONMENTAL INC

2.2.8. Channel Characteristics

Bank and channel data were obtained from field data (e.g., Vermont ANR Stream Geomorphic Phase 1 and Phase 2 Assessments (VTANR 2009), the ANR-LCBP-USDA Missisquoi River Bank Erosion Study being conducted by Dr. Andrew Simon, soils information collected by NRCS as part of the Missisquoi River Bank Erosion Study, and UVM soil analyses performed as part of this project); existing and newly generated empirical relationships; information from the scientific literature; and guidance from the SWAT manual and developers. This section provides an overview of the data sources and approaches to estimating channel parameters, with additional details provided in Appendix A

A GIS database of mainstem reaches for each subbasin was used to spatially organize data from various sources. When multiple data points existed over a SWAT subbasin reach, an average of the most accurate data source was used. Mainstem and tributary data were parameterized separately because the data inputs differ. Approximations and extrapolation were required as the available data do not cover the entire Missisquoi Bay Basin study area. For example, headwater tributary subbasins lack data across much of the basin.

Channel width and depth were taken from existing geomorphic data, or from the Vermont Hydraulic Geometry Curves (VTANR 2009) where no data existed.

Manning's n-value of the lower mainstem Missisquoi River was estimated to be 0.041 based on existing FEMA Flood Insurance Studies and field observations. Geomorphic data of dominant bed particle appear to stratify by elevation (Figure A.1). This follows the general trend of decreasing particle size and channel roughness moving towards the outlet of a watershed (i.e., with decreasing elevation) (FISRWG 1998). N-values were assigned based on this spatial distribution of bed particles in conjunction with typical values in the FEMA and other hydraulic studies. Subbasins with elevation $\leq$ 100 m were assigned an n of 0.040, elevation between 100 and 200 m were assigned an n of 0.045, and higher subbasins were assigned n-values of 0.050.

The channel bank vegetation coefficient was set using field data or GIS riparian land cover. The range in SWAT was compressed to more accurately represent the influence of vegetation on erosion. The channel vegetation coefficient was set to a value of 1, assuming most channels in the basin are not vegetated.

Fifteen NRCS bank soil samples were analyzed by UVM for average total P to parameterize the nutrient load from the banks (Table 2.26). Where no data existed, soil P levels were set based on known values for soil series or soil texture.

Table 2.26: Bank soil P analysis results.

SWAT Subbasin	Year	Pedon	ID	Name	Site	TP (mg/kg)	Mehlich-3 P (mg/kg)
91	2010	Pedon 3	MC2	Mud Creek	MC-2	422.0	23.6
87	2010	Pedon 2	MC1	Mud Creek	MC-1	511.0	19.6
86	2010	Pedon 6	MSII2	Troy slaughterhouse	MSII-2	520.8	15.0
158	2009	Pedon 1	TY1	Tyler Branch	Welch	526.6	12.1
88	2009	Pedon 8	M7	Mississquoi	Stockman	572.3	16.0
112	2009	Pedon 4	TR2	Trout River	Rico	599.5	37.5
99	2010	Pedon 1	J1	Jay Branch	JB-1	613.2	15.2

STONE ENVIRONMENTAL INC

SWAT Subbasin	Year	Pedon	ID	Name	Site	TP (mg/kg)	Mehlich-3 P (mg/kg)
129	2009	Pedon 5	M2	Mississquoi	Montane	619.7	12.2
185	2010	Pedon 4	MSII5	Mississquoi River	MSII-5	626.1	15.4
86	2010	Pedon 5	MSII1	North Troy	MSII-1	669.0	15.2
108	2009	Pedon 9	M1	Mississquoi	Louie's Landing	672.9	12.4
119	2009	Pedon 6	M6	Mississquoi	Gervais	742.3	44.0
136	2009	Pedon 3	TR1	Trout River	Archambault	813.0	30.6
124	2009	Pedon 7	M4	Mississquoi	Kane	842.4	103.0
218	2009	Pedon 2	BL2	Black	Cahill	973.8	24.8

Bank side slope was either taken from field measurements or set to the most frequently measured value in the basin of 1.1 horizontal to 1 vertical (moderate to steep).

The dry bulk density of the banks was taken from the twenty-eight ANR-LCBP-USDA Missisquoi River Bank Erosion Study sites. The mean of 1.30 g/cm^3 was applied where no data exist as this value represents the central tendency. Bulk density of the bed was not measured, and so typical values were selected based on measured or estimated bed particle type (Bunte and Abt 2001).

Median bank particle size was assigned from data or extrapolated based on soil texture was (M.Tomer et al. 2005). Median bed particle size was taken from field data or extrapolated based on a relationship between particle size and subbasin elevation. Subbasins with elevation $\leq$ 100 m were assigned a value of sand, elevation between 100 and 200 m were assigned gravel, and higher subbasins were assigned cobble.

Critical shear stress of the bank was measured at twenty-nine sites during the Bank Erosion Study. Where no data existed, estimates were generated by an empirical equation in SWAT based on silt-clay percentage (that is a function of median particle size) and the vegetation cover factor for beds and banks with finer-grained (sand, silt, clay) material. Shear stress for coarser beds (particles larger than sand) was determined from documentation of characteristics for a given particle size (Fischenich 2001).

The general procedure used in SWAT is to evaluate the hydraulic shear stress based on the above parameters and remove material where the force exceeds the critical shear stress of the banks or beds. The critical shear stress was adjusted during calibration to improve agreement between the field-based estimates of bank erosion generated in the ANR-LCBP-USDA Bank Erosion Study. This will be discussed further in Section 2.5.4.

2.3. Development of an Enhanced Hydrologic Network

The acquisition of LiDAR data for approximately 91% of the Vermont side of the MBB enabled the development of an enhanced hydrologic flow network. The objective of the dataset development was to delineate the minor stream tributaries, ditches, gullies, and concentrated overland flow paths that connect to the primary stream systems in the watershed. The ultimate use of the dataset would be in determining hydrologic proximity of P CSAs to the hydrologic network. The approach to delineating this network was an automated GIS-based approach that used the best available topographic analysis tools, combined with some manual interpretations. The tools chosen for this analysis were the TauDEM tools (Tarboton 2010).

STONE ENVIRONMENTAL INC

The source datasets used in the development of the enhanced hydrologic network included the two LiDAR DEMs and the VT HYDRO DEM, all of which were described in section 2.2.1. As was discussed in the development of the SWAT model DEM, the extent of the LiDAR data does not cover all of the Missisquoi River Basin. For the portion of the MBB missing LiDAR coverage (the eastern-most portion of the study area covering largely the Mud Brook sub-watershed), the coarser VT Hydro DEM was used. From these source DEMs, a seamless DEM covering the entire Vermont sector if the MBB would be required in order to apply the TauDEM tools. After texting the TauDEM tools with the full 1.6 m resolution LiDAR data, it was determined that a reduce resolution DEM would be require in order to run the analysis over entire study area. Aggregating the native 1.6 m DEM to a 3 meter cell size, resulted a dataset that the TauDEM tools were capable of working with, while still maintaining the high resolution require to delineate the hydrologic features of interest.

A seamless 3 meter DEM was created from the 1.6 m. LiDAR DEMs and the 10 m. SWAT model DEM. The SWAT model DEM (described in Section 2.2.1) incorporated the VT HYDRO DEM directly, and included a merged in Québec DEM. Five foot contours were created from the 10 meter SWAT DEM to generate a 1.6 meter DEM. The eastern and western 1.6 meter LiDAR blocks were then merged with the 1.6 meter SWAT DEM, with the SWAT DEM only used for the portion of the study area that exceeded the LiDAR extent. The seamless 1.6 meter DEM was then resample to 3 meters using bilinear interpolation for use in the TauDEM analysis tools.

A wall defining the perimeter of the MBB watershed was added to the seamless 3 meter DEM to prevent hydrologic features from extending beyond the established watershed boundary. In order to force the enhanced hydrologic network delineation to follow the existing VHD network, the VHD streams were burned into the 3 meter seamless DEM. The streams burned into the DEM include the Québec hydrograph connected into the VHD. This is the same dataset described in Section 2.2.1 that was used in the processing of the SWAT model DEM.

The TauDEM tools offer several different approaches to delineating streams from a DEM. These include methods based purely on upstream contributing area, methods based on a combination of slope and area thresholds, and those that consider connectivity and curvature of cells. The method chosen as the primary approach for delineation of the enhanced hydrologic network was the Peuker Douglas with Drop Analysis approach (Peuker and Douglas 1975, Band 1986).

This approach identifies hydrologic channels based on connectivity of upwardly curving cells along the hydrologic flow path grid based on a threshold range specified by the user, or based on an optimal threshold identified by the tool. Due to the size of the study area, the watershed was broken into twelve sub-watersheds and the hydrologic network analysis was run separately on each. The goal was to run the Pueker Douglas method using the automated identification of the optimal threshold of connected upwardly curving cells for each sub-watershed. In some sub-watersheds, the tool was unable to identify a threshold automatically. In these cases, a user defined threshold was defined based on the optimally identified thresholds from neighboring sub-watersheds and through manual testing of a range of threshold values. Furthermore, the Peuker Douglas with Drop Analysis did not run successfully for two of the 14 sub-watersheds, including the Mud Brook sub-watershed and small, mostly unnamed tributaries long the main stem of the Missisquoi River . We were unable to resolve why the Peuker Douglas method failed for these areas, and in its place used the Stream Definition by Threshold TauDEM tool in its place.

STONE ENVIRONMENTAL INC

The Missisquoi main stem and Lake Champlain were run together using the same input grids. The sub-watershed for the Mud was run separately. The Stream Definition by Threshold tool requires the user to specify the "threshold" to define a stream network based on the D8 Contributing Area grid. The thresholds used for the Mud and the main stem are based on thresholds used for topographically similar watersheds that produced similar results as the Peuker Douglas with Drop Analysis.

The stream network grids from the Peauker Douglas Drop Analysis and the Stream Definition by Threshold were merged together to create one stream network grid for the Missisquoi Basin watershed. The stream grid was then converted to vector format. The TauDEM tool, Stream Reach and Watershed, converts the stream network grid to a linear shapefile. Once again, the Missisquoi Basin Watershed was broken down into 13 sub-watersheds and the remaining main stem of the Missisquoi River due to the size of the watershed. The Stream Reach and Watershed tool was run for each of the 12 sub-watersheds (listed above), however, did not run successfully for the Mud or the main stem. The ESRI tool, raster to feature, was used to convert the stream network grid for the Mud and the main stem of the Missisquoi. The individual vector formats were then merged creating one stream network feature class of hydrologically significant channels that preserve Vermont's Hydrologic Dataset because it was burned into the input DEMs. A smooth tolerance of 50 meters was run on the merged stream network grid to eliminate the blocky flow of the lines.

2.4. SWAT Model Initial Model Setup and Parameterization

The MBB SWAT model was setup using ArcSWAT version 2009.93.6 (Winchell et al., 2010). There was customization to the interface that was required in order to accommodate some of the approaches taken with this model. The primary model development steps and input assumptions are described in the sections that follow.

2.4.1. Subbasin Delineation

Subbasin delineation is the process of dividing up a large watershed into smaller subwatersheds or basins. In a SWAT model, a subbasin is required for every stream reach that is delineated and at locations on the stream network where the streamflow, sediment, or phosphorus is to be predicted. Subbasins also have a single set of weather inputs, but can have a significant number of different landscape units, referred to as "Hydrologic Response Units" (HRUs) within each subbasin. Choosing the number of subbasins to divide a watershed into depends upon the objectives of the study and the amount of data available to parameterize both the subbasin upland parameters and the reach channel parameters.

Subbasin delineation for the MBB SWAT model was performed using the automated DEM-based option in ArcSWAT. The source DEM was the 10-m DEM that was constructed based on multiple source datasets in order to cover the entire study area (see Section 2.2.1). Prior to its use for subbasin delineation in ArcSWAT, the 10-m DEM was "conditioned" in order to provide some controls on the delineation process. The first process applied to the DEM was to build "walls" representing the outer boundary of the MBB study area that conformed to established watershed boundaries. For the Vermont-side of the watershed, the HUC12 watershed boundaries from NRCS were determined to be the most accurate established boundaries to use to enforce the perimeter of the study area. For the Québec-side of the watershed, watershed boundaries provided by IRDA (Beaudin, 2010) were recommended as being most accurate for the Québec portion of the MBB watershed. These second DEM conditioning step was to "burn-in" the vector stream network into the DEM. The burning in process forces the hydrologic network in SWAT to follow the paths defined by an established stream network. The Vermont Hydrography Dataset (VHD) stream network was chosen to represent the Vermont-side

STONE ENVIRONMENTAL INC

of the watershed. For the Québec portion of the watershed, the USGS 1:24,000 scale NHD data for the 8-digit HUCs "02010007" and "02010008" provided the best connectivity to the VHD network on the Vermont-side. Stream segments form the NHD data on the Québec side were then manually linked to the stream segments in the VHD network in order to create a continuous network. Once the network was complete, the ESRI ArcHYDRO toolset (ESRI, 2010) was used to burn the stream network.

The conditioned 10-m DEM was used as input to ArcSWAT for subbasin delineation. The number and size of subbasins is determined in ArcSWAT by a threshold minimum drainage area for a stream segment. The primary considerations in determining the appropriate threshold were the number of resulting subbasins and the implications regarding model complexity, and the detail with which we were interested in modeling the channel system. The stream drainage area threshold that was found to result in a suitable subbasin delineation was a drainage are of 750 ha. Based on our review of VHD and aerial imagery, however, we felt that the stream segment lengths for headwater subbasins were not long enough with this threshold value. Therefore, the subbasin reaches were re-delineated using a 500 ha, minimum drainage threshold, that extended the length of headwater streams. The final subbasin delineation resulted in 223 subbasins. The delineated subbasins are shown in Map 2.11.

2.4.2. HRU Delineation

Hydrologic Response Units (HRUs) are smallest building blocks in SWAT. An HRU is a homogeneous area that represents the smallest at which inputs (e.g., manure applications) and outputs (total P load) can be tracked. In most traditional SWAT applications, HRUs represent a unique combination of a land use and soil type. In some SWAT applications, slope is added in as a third criterion when delineating HRUs. A HRU must be contained entirely within a single subbasin; however, an HRU may not be a contiguous area. This is because if the same combination of land use, soils, and slope are found in different parts of a watershed, they are conceptualized to respond hydrologically in the same way. An example of this concept is shown in Figure 2.6, where the cyan highlighted area is single HRU.

The primary drawback with the approach to HRU delineation shown in Figure 2.6 is that it is not possible to associate these HRUs with individual agricultural fields. This is because the same soil and land use characteristics could exist on multiple fields. This shortcoming has implications for the utility of the resulting SWAT model for evaluating management activities on specific fields. If an objective for the SWAT modeling is to be able to both specify model inputs (such as management practices) and evaluate model outputs (such as sediment yield or phosphorus load) at the field scale, then special accommodations for this must be made when constructing HRUs. Because evaluation of model inputs and outputs at the field level was on an objective of this study, these special accommodations were made during the delineation of HRUs for the MBB SWAT model.

There were four landscape characteristics used in delineating HRUS for the MBB SWAT model: land cover from the hybrid land use dataset, soils, the compound topographic index class (CTI), and the common land unit (CLU) ID for the Vermont sector of the study area. Slope was not explicitly included as a criterion for HRU delineations. While slope is an important characteristic in determining phosphorus export, it is already largely captured in the CTI class identifier. In addition, by including the CLU ID as an added component in the HRU delineation, we are ending with very small, sub-field level HRUs, each of which will have its slope calculated independently using the DEM. Because ArcSWAT allows only three landscape characteristics to be used in HRU delineation, it was necessary to combine two of our four characteristics into a single unique value. We therefore combined the soil class identifier with the CTI class identifier to create a unique classification. These

STONE ENVIRONMENTAL INC

combined soil-CTI classes were treated as separate soils within the context of the ArcSWAT model database structure. The field CLU ID was relevant only to the agricultural areas within the Vermont sector of the study area. For the purposes of HRU delineation, the CLU ID was treated as unique SLOPE code in the ArcSWAT database structure, which resulted in 9285 unique slope (CLU) codes in the model.

Figure 2.6: Example HRU delineation.
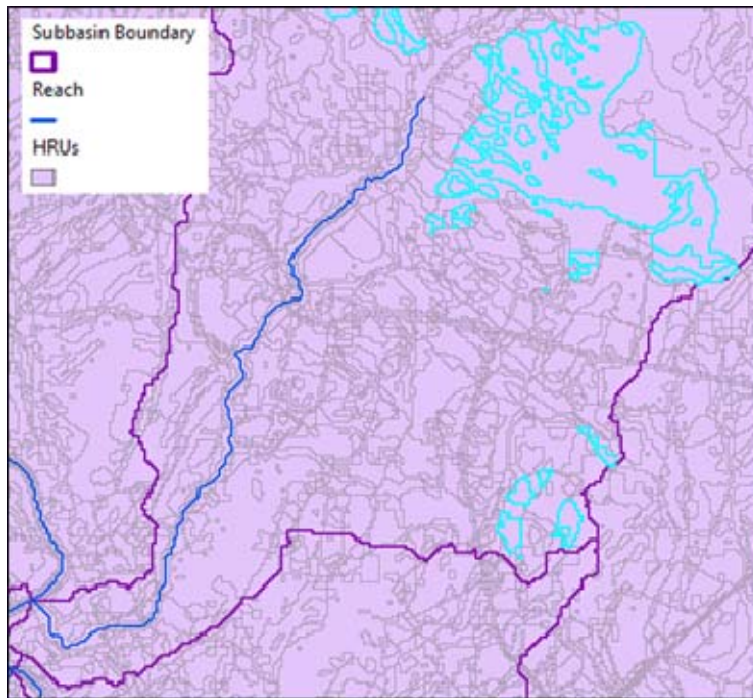
The delineation of HRUs in ArcSWAT provides the option for aggregating the minor land uses or soils (those that cover a small fraction of the area) into the more predominant ones. This option is excellent for improving model efficiency, but it results in a model structure that does not allow for the location of all HRUs to be resolved spatially, and some portions of the landscape will not have any model results associated with them. This is fine when the model output of interest is at watershed or subbasin outlets, but does not work as well when the objective is to identify critical source areas on the landscape. For landscape level critical source area identification, all delineated HRUs should be maintained and no aggregation should be performed. This was the strategy followed for the MBB SWAT model HRU delineation.

In developing an approach for HRU delineation, tests were conducted with different resolutions of the input datasets to assess whether a certain approach would result a final model with an practical number or HRUs. This approach was used when deciding on subbasin size, the number of CTI classes, and the complexity of the land use and soils inputs. The final HRU delineation for the MBB SWAT model resulted in 109,811 HRUs. As was mentioned in earlier discussions, this represents a very large number of HRUs and required the SWAT model code be modified in order to accept this large number of inputs. Map 2.12 shows the HRUs over the Mud Brook area of the watershed, indicating the level of landscape discretization that resulted from this approach. While this HRU delineation strategy resulted in challenges with respect to data management and

STONE ENVIRONMENTAL INC

model calibration, it offered the benefits of predictions at a resolution more typical of a tactical level analysis than a strategic level one.

2.4.3. Estimation of Tile Drained Areas

The presence (or absence) of subsurface (or "tile") drainage on agricultural fields has an important impact on how the field will behave hydrologically. In the parts of the Missisquoi Bay watershed it has been shown that for fields with subsurface tile drainage, a significant amount of that field's total water yield is transported through the tile drainage system (Michaud et al. 2007). Datasets depicting the specific locations or fields with tile drainage do not exist for either the Vermont or Québec sectors of the MBB study area. In the absence of field-specific data, estimations of tile drained areas was made based on landscape characteristics and through consultation with local Vermont NRCS scientists familiar with tile drainage in the region (Potter, 2011). The Vermont NRCS scientists also provided their best estimates of the percentage of cropland in different regions of the MBB that are tile drained.

The two criteria were used to identify fields with tile drainage were the hydrologic soil group and slope. These criteria varied geographically across the watershed; for example, it was indicated that areas in the eastern portion the watershed in Vermont (in Orleans County) tile drainage is much less common. It should be noted that in applying these criteria to the SWAT model HRUs, it was assumed that an entire fields was tiled or not tiled. Table 2.27 summarizes the landscape criteria and estimated percent of cropland tile drained based on both the original NRCS estimate and applying the specific criteria to the SWAT HRUs within the MBB model. The data shows that the criteria used to estimate the fields with tile drainage in the SWAT model agree very well with the estimates provided by NRCS.

Table 2.27: Criteria for and estimations of tile-drained cropland in the MBB.

Sub-Watershed / Region	Hydrologic Soil Group	Average Slope (%)	MBB SWAT Model	NRCS Estimated
Black Creek	C or D	≤ 6%	37.0	-
Hungerford	C or D	≤ 6%	76.9	~ 60
Lower Mainstem Miss. (VT)	C or D	≤ 6%	55.7	-
Missisquoi Nord (QC)	C or D	≤ 6%	48.6	-
Mud Creek	C or D	≤ 3%	6.7	~10
Upper Miss. (North Troy)	C or D	≤ 3%	14.1	~10
Pike	C or D	≤ 6%	45.8	-
Rock (VT)	C or D	≤ 6%	72.8	~ 60
Rock (QC)	C or D	≤ 6%	82.3	-
Sutton	C or D	≤ 6%	36.3	-
Trout	C or D	≤ 6%	13.6	10 - 20
Tyler	C or D	≤ 6%	11.9	10 - 20
Upper Mainstem Miss. (VT)	C or D	≤ 6%	31.8	-
Full VT Side of MBB			40.5	~40

STONE ENVIRONMENTAL INC

2.4.4. Assignment of SCS Runoff Curve Numbers

The selection of SCS runoff curve numbers is one of the primary ways in which the runoff potential for different portions of the landscape is controlled in SWAT. NRCS has generated standard tables of runoff curve numbers for different combinations of land use, cropping practice, and soil hydrologic group (Soil Conservation Service Engineering Division 1986). These values are referred to as "CN2" values, and represent the curve number for antecedent soil moisture condition II (average soil moisture). The SWAT model updates the CN value daily based on the current soil moisture levels, and whether the ground is frozen (Neitsch et al., 2005). The maximum value that a curve number can reach occurs when the soil is at field capacity (very wet), which is referred to as "CN3". The minimum value that a curve number can reach occurs when the soil is at wilting point (very dry), which is referred to as "CN1". The CN3 and CN1 values are function of the CN2 value for the land use and soil, so that areas with higher CN2 values (more prone to surface runoff) would also have higher CN1 and CN3 values.

The typical approach to estimating CN2 values for use in SWAT is based on the standard NRCS tables. An alternative is to adjust the CN2 values based on the slope of the HRU following the method developed by Williams (1995). Other methods for assigning CN2 values to SWAT HRUs have been proposed that account for the variable source area hydrology concept, where parts of the landscape with low slopes and high upslope contributing areas are more likely to produce surface runoff (Easton et al., 2008). In the work by Easton et al. (2008) the CN2 value assigned to HRUs in SWAT was based entirely upon the value of the Soil Topographic Index (an index similar to the CTI that also includes a soil transmissivity component). In building the MBB SWAT model, the CTI was explicitly built into the HRU delineation because of the importance that variable source area hydrology and saturation excess runoff has in the study area. Therefore, an approach to assigning CN2 values to HRUs was developed that combined the standard method for assigning CN2 values (based on land use and hydrologic group) with that proposed by Easton et al. (2008) which uses a topographic wetness index to specify curve numbers was employed in the MBB SWAT model.

The approach taken to assigning initial CN2 values to each HRU in the MBB SWAT model included the following steps:

> CN2 values based on the HRUs land use, cropping practice, condition, and soil hydrologic group were assigned based on the table of standard values in the SWAT manual (Neitsch et al. 2009).

> The CTI raster dataset for the MBB study area (described in Section 2.2.1.2) was overlaid with the delineated HRU boundaries so that average CTI values for each HRU could be calculated.

> All HRUs within the MBB SWAT model were ranked from highest to lowest CTI value. The CTI percentile (of the population of HRU CTI values) was calculated for each HRU. Those HRUs with percentiles greater than 0.5 (the median) have a greater than average potential for saturation excess surface runoff relative to the other HRUs in the watershed. Those HRUs with a CTI percentile less than 0.5 have a less than average potential for saturation excess runoff.

> Based on an HRU's CTI percentile, adjust its CN2 value from the "standard" value to an CTI-adjusted value. The CN2 adjustment is made so that HRUs with a CTI much higher than the median have a higher potential for surface runoff, and HRUs with a CTI much lower than the median a lower potential for surface runoff. An equation was developed to perform this adjustment that constrains the minimum and maximum for the adjusted value based on the standard CN1 and CN3 values. This equation was as follows:

STONE ENVIRONMENTAL INC

if CTI% <= 0.5, then:

CN2_Adj = CN2 – 0.67 *((0.5 – CTI%)/0.5) * (CN2 – CN1)

if CTU% > 0.5, then:

CN2_Adj = CN2 + 0.67 *((CTI% - 0.5)/0.5) * (CN3 – CN2)

where,

CN2_Adj = CTI adjusted CN2 value

CN2 = standard CN2 value

CN1 = standard CN1 value

CN3 = standard CN3 value

CTI% = percentile (0 – 1) of CTI for the HRU

The method shown in the steps above results in a CN2 value being adjusted upwards a maximum of 2/3 of the way between the standard CN2 value and the CN3 value for the "wettest" HRU in the watershed. Likewise, the method results in a CN2 value being adjusted downward a maximum of 2/3 the way between the standard CN2 value and the CN1 value for the "driest" HRU in the watershed. The CN2 adjustments for all other HRUs in the model would fall somewhere in between those two extremes. An example of the distribution of the CTI-adjusted of CN2 values for pasture on hydrologic group C soils is shown in Figure 2.7. The median value is equal to 74 which is the standard CN2 value for pasture on a hydrologic group C soil. The minimum value is 62, which would occur for a hydrologic group C soil with a very low CTI value; this value of 62 happens to be close to the standard CN2 for a hydrologic group B soil (61). The maximum value is 83, which would occur for a hydrologic group C soil with a very high CTI value; this value happens to be close to the standard CN2 value for a hydrologic group D soil (80). The approach developed acknowledges that topographic factors can have an important impact on surface runoff potential that is not captured by soil characteristics and land use class alone, and provides a consistent means for adjusting the SWAT model parameterization to reflect this.

Figure 2.7: Distribution of CTI-Adjusted CN2 values for pasture hydrologic group C, within the MBB study area.

STONE ENVIRONMENTAL INC
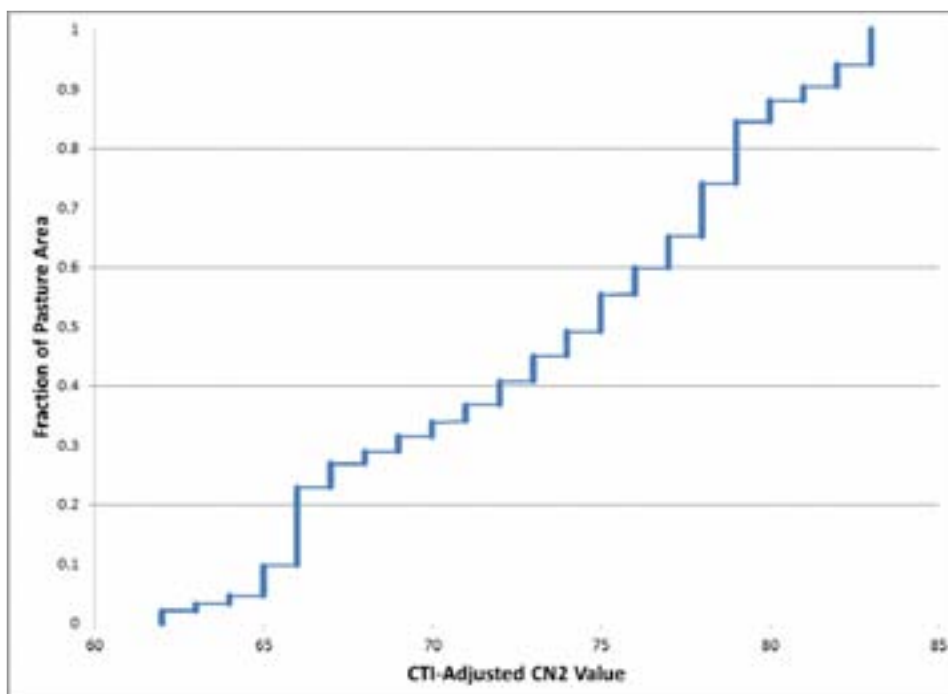
2.4.5. Baseflow Parameters

An analysis of historical streamflow can be used to provide context for the contributions of shallow groundwater flow (baseflow), lateral sub-surface flow, and surface runoff to total streamflow in a watershed. In addition, some of the same techniques can be used to estimate parameters that describe the baseflow characteristics, namely the baseflow recession constant. The approach used in the development of the MBB SWAT model is that described in Arnold et al. (1995) and Arnold and Allen (1999). The method described in their paper has been built to a software program called "BFLOW" that was obtained from the SWAT model web site (Texas A&M University 2011).

The technique was applied to four streamflow gages with long historical records within the MBB study area. Three were USGS gages located in Vermont and a fourth was a MDDEP maintained gage located in Québec. The BLFOW program was run for each of these gages to generate estimates of the baseflow recession constant (ALPHA_BF) and an estimation of the baseflow fraction of total streamflow. The results from the BFLOW program are summarized for the four gages in Table 2.28.

Table 2.28: Historical baseflow analysis for streamflow gages within the MBB.

Flow Gage	Period of Record	ALPHA_BF	BF1	BF2	BF-Mean
Missisquoi at North Troy	2001 - 2010	0.0414	0.56	0.42	0.490
Missisquoi at East Berkshire	2001 - 2010	0.0493	0.60	0.45	0.525
Missisquoi at Swanton	2001 - 2010	0.0483	0.55	0.39	0.470
Rock River at Saint Armand	2001 - 2009	0.0607	0.50	0.34	0.420

In Table 2.28, the BF1 and BF2 values represent the estimated streamflow fraction that is baseflow from the first second pass of the baseflow filter. The BFLOW program user guide suggests that, in general, the fraction of streamflow that is baseflow should fall between the BF1 and BF2 values, which is why the midpoint (BF-Mean) has been provided in the table. The ALPHA_BF values that were calculated in the historical baseflow analysis were used as the basis to set the SWAT model ALPHA_BF values for different segments of the watershed. The baseflow fractions of streamflow calculated served as a guide during model calibration.

2.4.6. Adjustment of Initial Parameterization

The ArcSWAT interface to the SWAT model contains databases built in logic that selects appropriate initial values for many of the model parameters. This includes initial values for groundwater flow parameters, surface runoff routing characteristics, plant growth characteristics, and numerous others. In short, the ArcSWAT interface allows users to build a SWAT model, run the model, and obtain results with minimal additional effort beyond the initial collection of the topographic, land use, and soils information. These initial parameter values provided by the interface perform adequately in many environments. However, even prior to calibration, better estimates can often times be made. A summary initial parameter values used in development of the MBB SWAT model can be found in Appendix A.

2.4.7. SWAT Model Version and Modifications

The SWAT model is an open source model, allowing scientists and researchers to make customizations to the code that may be required to better represent their particular geography or application. The basis for the MBB

STONE ENVIRONMENTAL INC

SWAT model was the SWAT 2009 Revision 477 (Sammons 2010). During the development of the MBB SWAT model, several modifications were made to the model code. These changes can be grouped into those that updated process algorithms, those that allowed for greater spatial heterogeneity of input parameters, and those that updated potential bugs. Several of these updates were based on code used by the SWAT development team in Temple Texas and abroad. Section A.3 of Appendix A describes these modifications that were incorporated into the MBB SWAT model.

2.5. SWAT Model Calibration and Validation

The MBB SWAT model was built, calibrated, and validated using the datasets and processes described in Sections 2.2 and 2.3. There are several approaches that can be taken when calibrating a complex hydrologic and water quality watershed model. Many papers have described both manual and automatic approaches to calibrating the SWAT model (Bekele and Nicklow 2007, Boyle et al. 2000, Di Luzio and Arnold, 2004, Feyereisen et al. 2007, Muleta, and Nicklow 2005). Manual approaches rely upon the experience and knowledge of the modeler to choose appropriate adjustments to parameter values that are both justifiable conceptually and result in an improvement in the simulation when compared to an "observed" measurement. In manual calibration, many different aspects of the model simulation can be considered by the modeler when evaluating the merit of an adjustment that is made (Boyle et al. 2000, Feyereisen et al. 2007). This may include not only comparisons with multiple types of observed data, but also evaluations of model output describing the distribution of runoff components, sources of sediment, and plant growth and crop yield. Automatic approaches typically focus on identifying a set of parameter adjustments that minimize the difference between a quantity simulated by the model and a set of observations, often times through the use of an optimization algorithm (Duan et al. 1992). In automatic calibration, the modeler must provide ranges for parameter values which constrain the possible parameter values selected as the optimum. One of the challenges in automatic calibration is defining meaningful and realistic ranges for parameters that are appropriate for a given environment. Often times, these ranges are not well understood without taking time, through manual calibration, to carefully evaluate different aspects of the model simulation results. Automatic calibration methods, if not applied with great care, can result in parameterizations that provide good fit to the data but have unrealistic parameter values.

The approach that was taken in the calibration of the MBB SWAT model was primarily a manual one, along with some "ad hoc" automatic calibration aimed at testing particular parameterization concepts or evaluating the sensitivity of certain parameters or combinations of parameters. This primarily manual approach was chosen because of the advantage in being able to consider many different aspects of the model calibration concurrently that could not be captured through comparisons of streamflow, sediment, or phosphorus load data alone.

Another important aspect of the calibration approach was that adjustments to parameters were made either uniformly or based on quantifiable landscape characteristics whenever possible. By uniform adjustment, we are saying that, for example, if the SCS curve number gets lower by 10% in part of the watershed, then it should be lowered by that same amount in other parts of the watershed. Following this type of approach is important in a modeling application where the objective is identifying critical source areas at the HRU or field level. If adjustments to parameters were made variably over many different portions of the watershed, this could easily introduce bias into the ranking of critical source areas, due to the lack of data available to support these types of adjustments. The remainder of this section will discuss the calibration, and validation of the MBB SWAT model.

STONE ENVIRONMENTAL INC

2.5.1. Monitoring Data

The calibration and validation periods were selected based on the periods of record corresponding to the long term water quality monitoring sites. While streamflow data was available going back as far as 1915 (Missisquoi at East Berkshire), and water quality data going back as far as 1992 (Missisquoi at Swanton), most of the long term water quality monitoring sites began collecting data in 2001. An additional five sites in Vermont began collecting flow and water quality data in the late summer and early fall of 2009. Based on the availability of monitoring data, the period chosen for streamflow, sediment, and hydrologic calibration and validation was set to run from 2001 through 2010. The more recent portion of that record was selected for calibration and the earlier portion of the record for validation. Specifically, these periods were:

- Calibration: 10/1/2005 - 9/30/2010

- Validation: 10/1/2001 - 9/30/2005

Water quality data at the long term monitoring sites was available through the end of the 2009 water year (9/30/09). Monitoring data for the short-term sites began in late summer and fall of 2009, so generally a year or less of data was available at those sites.

The emphasis during the MBB calibration was on simulations at the long term monitoring sites. In the case of streamflow calibration, a long term record is important so that a sampling of wet, dry, and average years can be used to evaluate the model. A single year or two of data may not be enough to sufficiently determine if the model is able to adequately simulate the full range of environmental conditions (Refsgaard, and Storm 1996, Refsgaard, et al. 2001). In the case of water quality data (sediment and phosphorus), the same limitations associated with a short period of record hold. In addition, a relationship between sampled pollutant concentrations (e.g., TSS, P) and flow must be established for comparisons with model predicted loads. The uncertainty in the flow/concentration relationship increases as the amount of data or period of record used in establishing that relationship decreases (Smith and Croke 2005). While the calibration procedure focused on the long term monitoring sites, the short term sites located on several of the major tributaries to the Missisquoi provided valuable additional data for comparison with the SWAT model.

2.5.2. Evaluation of Model Performance

Evaluation of model simulations included several components, which varied somewhat depending on whether streamflow, sediment, or phosphorus was under consideration. These components included visual comparisons of the simulated and observed data, evaluation of model output describing different model processes, as well as the calculation of statistical measures of model performance. The statistical measures of model performance were those recommended by Moriasi et al. (2007), who recommend consideration of three statistics:

1. The Nash Sutcliffe Efficiency (NSE): The NSE (Nash and Sutcliffe, 1970) is an indicator of how well the simulated versus observed data fall on the 1:1 line. NSE can vary from a value of negative infinity to 1. Values above 0 are considered acceptable, with a value of 1 indicating a perfect match between the model and the observed data.

2. The Percent Bias (PBIAS): PBIAS measures the tendency for simulated values to be larger or smaller than the observed values (Gupta, 1999). Values of PBIAS < 0 indicate that the model tends to over–predict the observations, while values > 0 indicate that the model tends to under-predict the observations. The optimal value for PBIAS is a value of 0.

STONE ENVIRONMENTAL INC

3. The ratio of the root mean square error to the standard deviation of measured data (RSR): The RSR provides a way of normalizing the often measured root mean squared error (RMSE) based on the standard deviation of the observations (Moriasi et al., 2007). RSR varies from a minimum value of 0, (indicating an RMSE of 0) up to a large number greater than 1. The optimal value for RSR is 0.

Moriasi et al. (2007) also provide guidance for acceptable levels of mode performance based on these statistical values. These values have been replicated here in Table 2.29.

Table 2.29: Model performance ratings for statistics on a monthly time step (from Moriasi et al., 2007)

Performance Rating	RSR	NSE	PBIAS (%) Streamflow	Sediment	N,P
Very Good	0.00 < RSR < 0.50	0.75 < NSE < 1.00	PBIAS < ±10	PBIAS < ±15	PBIAS< ±25
Good	0.50 < RSR < 0.60	0.65 < NSE < 0.75	±10 < PBIAS < ±15	±15 < PBIAS < ±30	±25 < PBIAS < ±40
Satisfactory	0.60 < RSR < 0.70	0.50 < NSE < 0.65	±15 < PBIAS < ±25	±30 < PBIAS < ±55	±40 < PBIAS < ±70
Unsatisfactory	RSR > 0.70	NSE < 0.50	PBIAS > ±25	PBIAS > ±55	PBIAS > ±70

Although the statistical performance rating guidance in Table 2.29 was developed for statistics on a monthly time step, it can be applied to data on a daily time step as well (particularly for streamflow); however, calibration statistics will typically not be as high when comparing daily data.

2.5.3. Hydrology

Calibration of the hydrologic parameters to the SWAT model were focused on the long term flow gages at the Missisquoi at North Troy, the Missisquoi at East Berkshire, the Missisquoi at Swanton, and the Rock River at Saint Armand. The calibration included both the daily flows and the monthly flows at these sites. Including daily flows better enabled evaluation of the model's timing and the simulation of peak flows. Evaluation of model simulations included visual comparisons of the simulated and observed hydrographs as well as calculation of statistical measures of model performance.

During calibration, an effort was made to make adjustment to parameter values uniformly over all areas of the watershed, over all areas of a given land use, or base the adjustments on a metric with known variability across the watershed. Two metrics that were used during hydrologic calibration as the basis for parameter adjustments at the subbasin level were mean elevation and forest cover. These metrics were used to adjust some parameters, including: snowmelt, ET, and groundwater flow. Subbasins were classified based no their mean elevation into three classes:

1. Elevation Class 1: < 150 m

2. Elevation Class 2: 150 m. – 300 m.

3. Elevation Class 3: > 300m.

The distribution of these elevation classes is shown in Figure 2.8.

STONE ENVIRONMENTAL INC

Figure 2.8: Classification of subbasins by mean elevation.
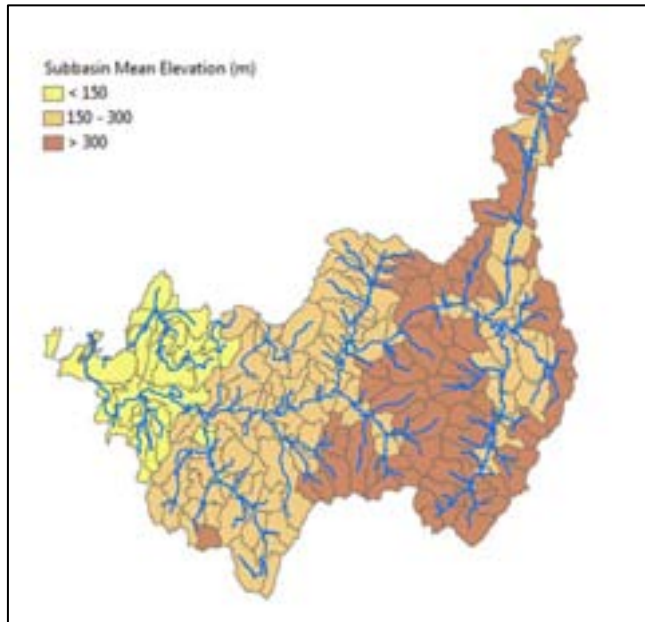
A second metric used in the adjustment of snowmelt parameters was the fraction of forest cover. The forest cover fraction of each subbasin was calculated and subbasins were classified into three groups:

1. Forest Cover Class 1: < 50%

2. Forest Cover Class 2: 50% - 75%

3. Forest Cover Class 3: > 75%

The distribution of these forest cover classes is shown in Figure 2.9.

Figure 2.9: Classification of subbasins by fraction of forest cover.

STONE ENVIRONMENTAL INC
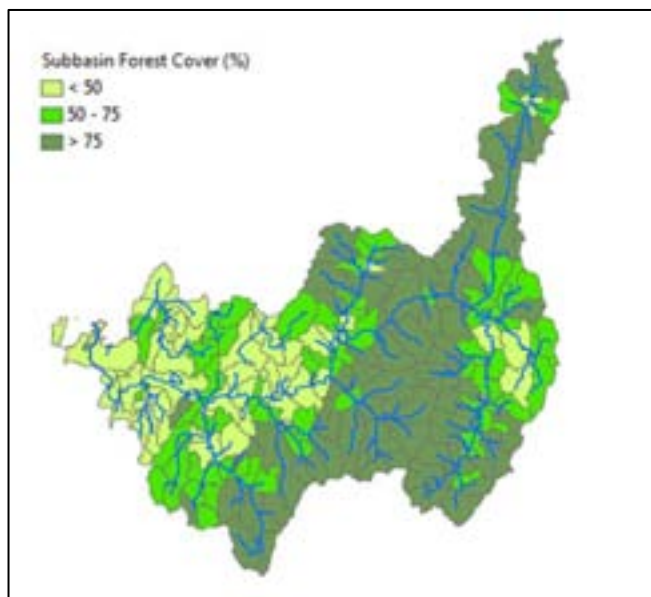
During hydrologic calibration, one focus was achieving an appropriate balance between surface runoff and baseflow contributions to streamflow. Achieving a proper balance between runoff processes has important implications for both sediment and phosphorus transport. Recall from the baseflow analysis that was conducted on the historical streamflow records that the baseflow fraction of total streamflow varied between 42% and 53% of total streamflow (Table 2.28). For the watershed outlet for the mainstem Missisquoi, the target baseflow fraction was in the middle of the range, at 47% of total streamflow.

The parameter adjustments made during calibration were made concurrently over the entire study area with an effort to balance the model simulation performance at multiple locations. The following represent the primary adjustments that were made:

- Adjustment of snowmelt parameter based on elevation and forest cover;

- Adjustment of ET coefficients based on elevation;

- Uniform adjustments to surface and subsurface slope lengths;

- Uniform reduction in curve numbers;

- Baseflow response based on elevation;

- Adjustments to tile drain and impermeable layer depth characteristics based on soils; and.

- Sub-watershed level adjustments to surface runoff and channel routing parameters.

Note that no adjustments were made directly to the SWAT soil physical properties during hydrologic calibration. The resulting simulated daily and monthly streamflow results for the calibration period are shown for the Missisquoi at Swanton in Figures 2.10 and 2.11.

Figure 2.10: Missisquoi at Swanton, daily flow calibration, 10/2005 – 9/2010.

STONE ENVIRONMENTAL INC
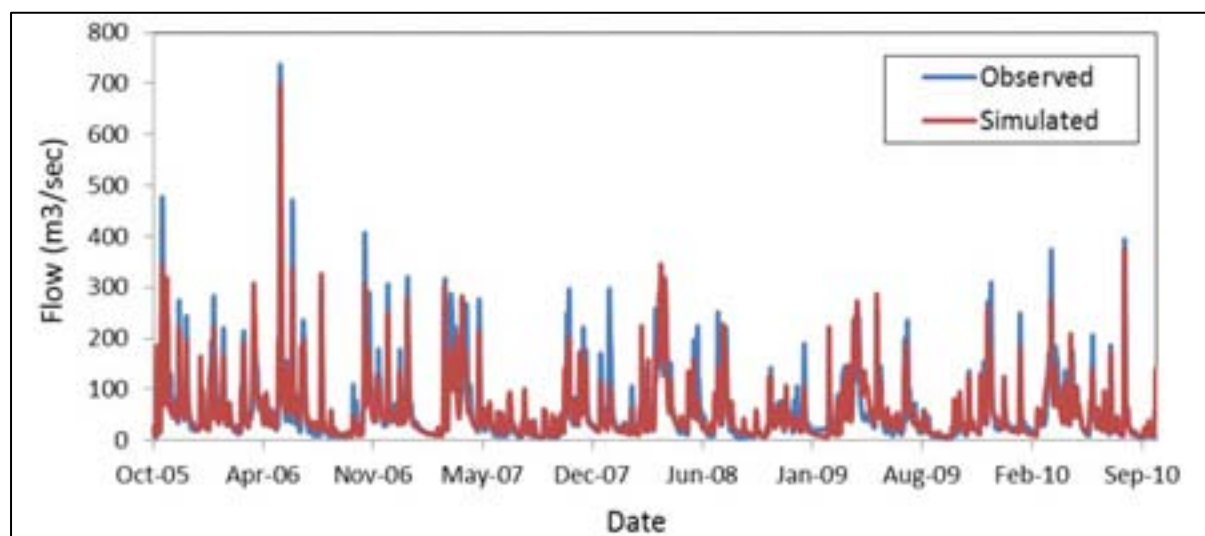
Figure 2.11: Missisquoi at Swanton, monthly flow calibration, 10/2006 – 9/2010.
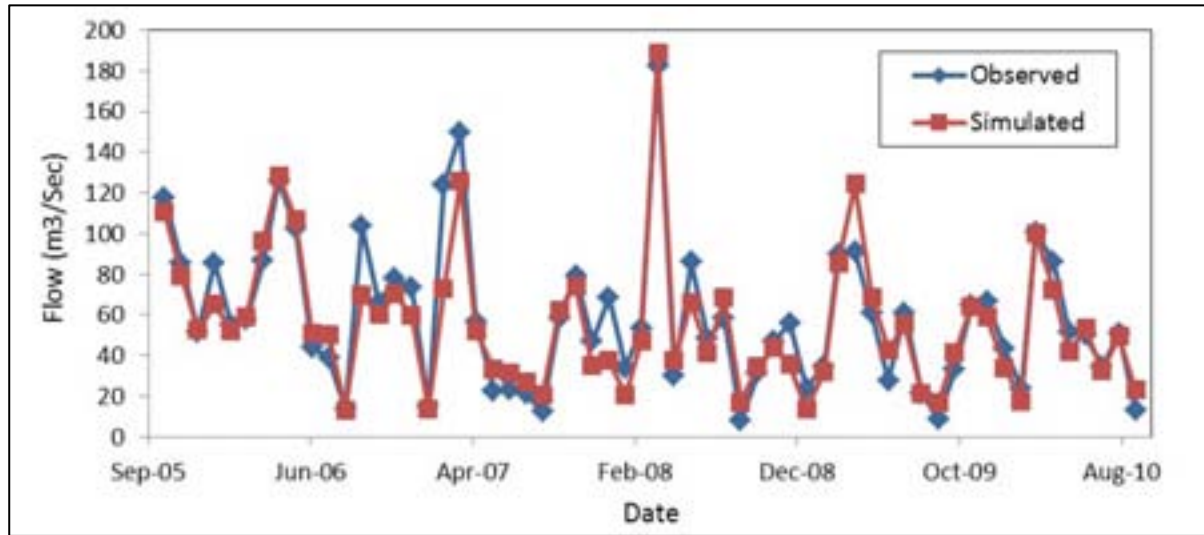
The flow calibration results at the Missisquoi at Swanton were very good. The NSE and PBIAS for the monthly flows were 0.86 and 5.0% respectively. These both place this flow calibration in "very good" category based on Moriasi's criteria (see Table 2.29). Graphs for monthly and daily flow simulations during the model calibration period can be found for the remaining long term and short term flow monitoring sites evaluated in Appendix C. A summary of the calibration period statistics for all the sites evaluated is provided in Table 2.30. Both the long term flow records and flows from the short term monitoring sites was evaluated using the statistical measures suggested by Moriasi (2007). All of the monthly and daily statistics fall within the "satisfactory" category or better. For the monthly NSE and RSR statistics fall in the "good" or "very good" category, and all of the monthly PBIAS statistics fall within the "very good" category.

Table 2.30: Hydrology simulation, calibration statistic summary.

	NSE		PBIAS (%)		RSR	
Location	Daily	Monthly	Daily	Monthly	Daily	Monthly
Miss. N Troy	0.75	0.84	3.69	3.64	0.50	0.40
Miss. E. Berkshire	0.71	0.79	-0.62	-1.09	0.54	0.46
Miss. Swanton	0.77	0.86	5.08	5.03	0.48	0.37
Rock at S. Armand	0.68	0.82	6.58	6.68	0.57	0.42
Mud	0.71	0.81	-5.67	-5.30	0.54	0.44
Trout	0.67	0.74	-5.79	-5.79	0.57	0.51
Tyler	0.74	0.70	0.26	0.57	0.51	0.54
Black	0.54	0.73	7.77	7.72	0.68	0.52
Hungerford	0.59	0.68	8.54	8.76	0.64	0.57

STONE ENVIRONMENTAL INC

As has already been discussed, one advantage to the manual calibration approach was that evaluation of intermediate model process output in addition to comparison of output with gage data could be considered concurrently. One of these was the distribution of the components of streamflow. The total distribution of average total water yield (streamflow) by runoff components was calculated for the outlet of the Missisquoi River for the period form 1/2005 – 9/2010 (the first nine months of 2005 are not part of the calibration period but were included in this summary). SWAT tracks four contributions to streamflow; surface runoff, lateral flow (shallow subsurface flow), tile flow, and groundwater flow. There is not a clear definition in SWAT as to whether lateral flow is considered to be a component of baseflow or "quick flow" (quick flow being that flow associated with the majority of the rise in a hydrography during and immediately following a storm event). We have considered shallow subsurface flow contributions to streamflow, from both lateral flow and tile flow, to be portioned equally into what would appear as a baseflow response and what would appear as a quick flow response on a hydrograph. Using this assumption, the 43% of water yield composed of lateral and tile flow can be split equally into 21.5% quick flow and 21.5% baseflow. The baseflow fraction of streamflow is then equal to the groundwater contribution (26%) plus half the shallow subsurface flow (21.5%), for a total of 47.5%. This is almost identical to the fraction of baseflow estimated based on historical hydrography analysis for the Missisquoi at Swanton (Table 2.28). It should be noted that this distribution of streamflow into runoff components is representative of the entire Missisquoi watershed and that this distribution will vary over different sections of the watershed and for different land uses. For example, the tile flow fraction for tile drained HRUs will be much higher than 2% of the annual water yield.

Figure 2.12: SWAT simulated distribution of average annual water yield at the Missisquoi outlet, 2001 - 2009.
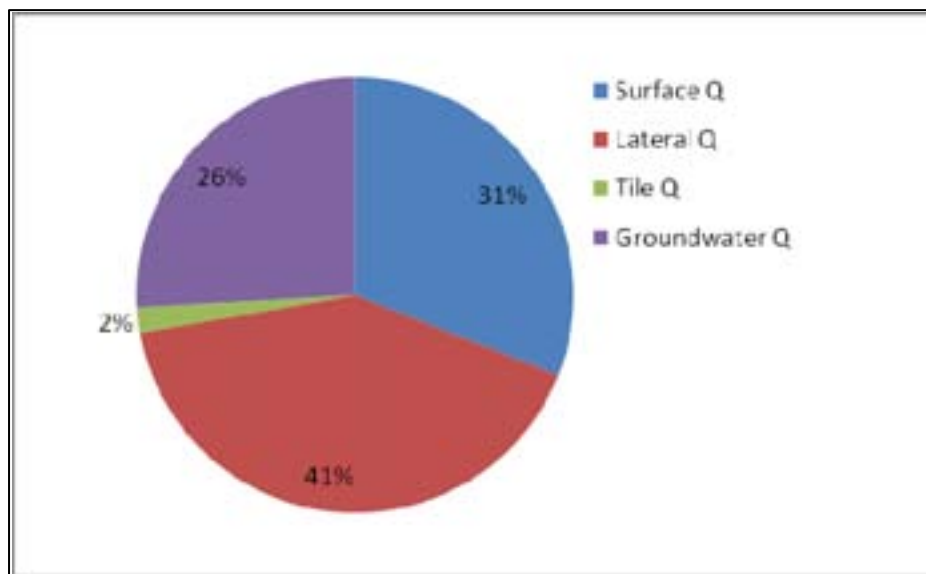
The MBB SWAT model was run to evaluate the model for the validation period from 10/1/2001 – 9/30/2005.The model simulation began on 1/1/1999, allowing for 2 year and 9 month warm up period. The simulated daily and monthly hydrographs for the Missisquoi at Swanton are shown in Figures 2.13 and 2.14 respectively.

STONE ENVIRONMENTAL INC

Figure 2.13: Missisquoi at Swanton, daily flow validation, 10/2001 – 9/2005.
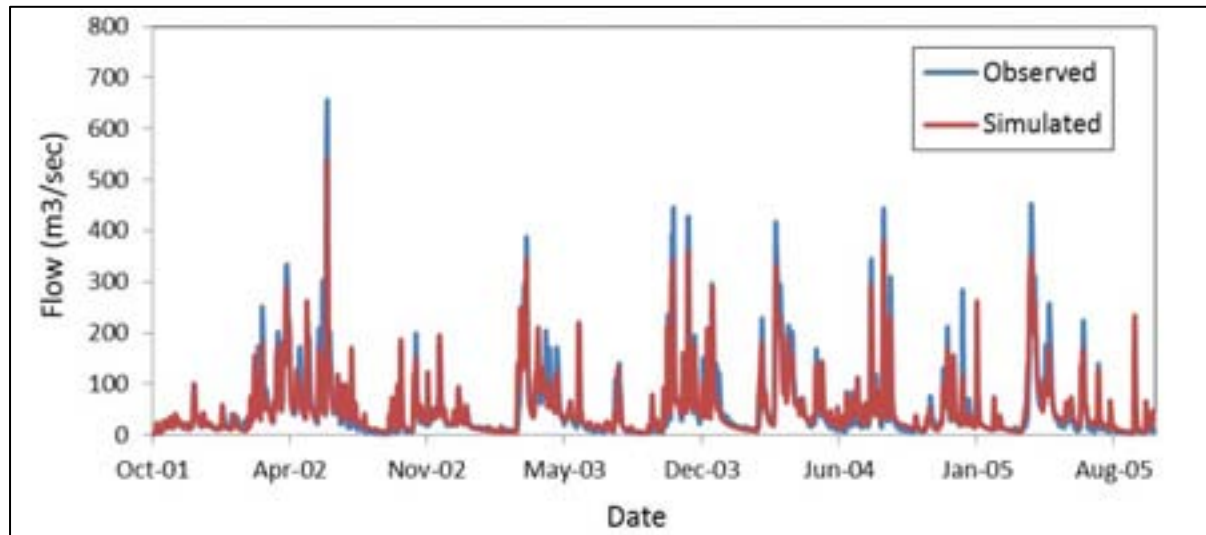
Figure 2.14: Missisquoi at Swanton, monthly flow validation, 10/2001 – 9/2005.
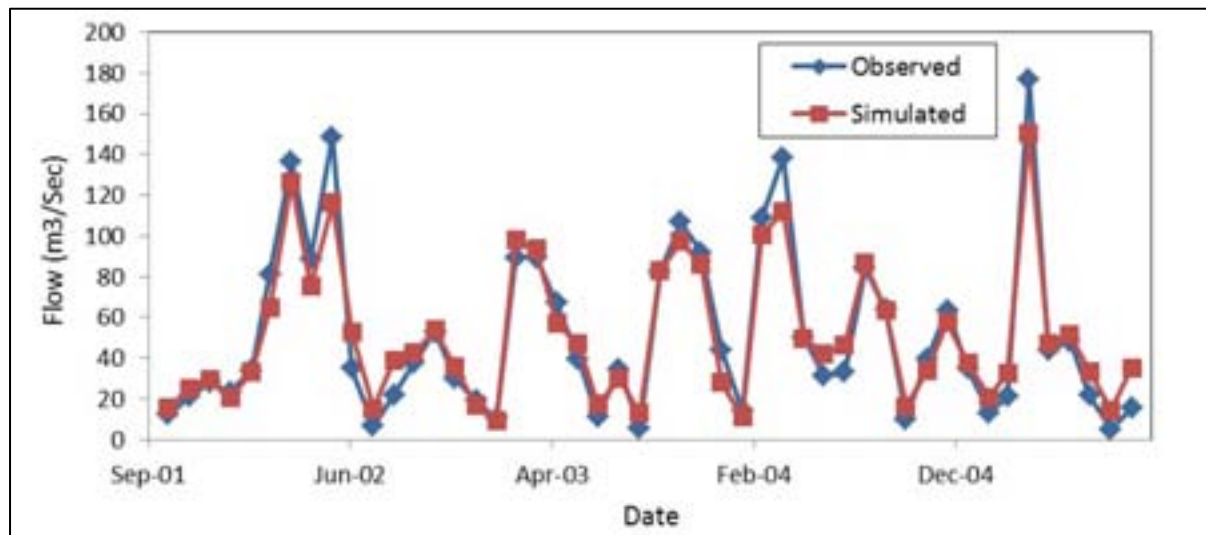
As was true for the validation period, model simulation performance at during validation periods was very good for the Missisquoi at Swanton with monthly NSE and PBIAS values of 0.93 and 0.1% respectively. This was actually somewhat better than for the calibration period. Daily and monthly plots of the observed versus simulated hydrographs for the additional monitoring points evaluated can be found in Appendix C.

Table 2.31 provides a summary of the validation periods statistics for flow. For the four sites evaluated the monthly statistics are all in the "good" to "very good" categories. The simulation for the Rock River at Saint Armand has slightly a lower NSE and a larger PBIAS than the other monitoring points on the Missisquoi. A challenge on the Rock River watershed is that being a heavily agricultural watershed, there is a significant

STONE ENVIRONMENTAL INC

amount of land use rotation from year to year. In the MBB SWAT model, we used landscape characteristics to make our best estimates regarding locations following a crop rotation, and then used local knowledge to define the most common rotation schedule. There is some uncertainty in these assumptions in any given year, that could lead to periods where the extent of particular crop is over or underrepresented. This could have an impact on the bias in simulated flows during certain periods of time.

Table 2.31: Hydrology simulation, validation statistics summary.

Location	NSE		PBIAS (%)		RSR	
	Daily	Monthly	Daily	Monthly	Daily	Monthly
Miss. N Troy	0.75	0.87	-1.87	-1.79	0.50	0.36
Miss. E. Berkshire	0.78	0.94	-1.83	-1.81	0.47	0.24
Miss. Swanton	0.80	0.93	0.11	0.14	0.45	0.27
Rock at S. Armand	0.58	0.73	-17.68	-17.68	0.65	0.52

2.5.4. Sediment Calibration and Validation

The SWAT model is capable of simulating sediment load coming from both upland areas (e.g., agricultural fields, residential areas, and undeveloped areas) as well as from stream and river banks and channels. The capabilities of SWAT in modeling channel erosion and sediment transport processes have expanded in recent years, with new methods that allow for more physically based approaches for both the bank erosion process and the transport of sediments of different particle sizes (Neitsch et al. 2011).

One of the objectives of the sediment calibration was to achieve an appropriate balance between sediment contributions from the upland and the channel bank sources. The documented balance between upland and channel sources varies widely ranging between 10% and 75% contribution from channels (Sekely et al. 2002, Simon et al. 2002, McDowell and Wilcock 2007, Noll et al. 2009). In some SWAT modeling applications, the channel erosion processes are parameterized to not allow any bank erosion and then the contribution of the channel to TSS is assumed to be equal to the difference between the observed TSS load and the simulated load from the uplands (Solomon 2010); however,

TSS load measurements exist at the long term and short term water quality monitoring stations within the MBB study area. Bank erosion data are available from the ANR-LCBP-USDA Bank Erosion study, that focused on predictions of bank erosion from the main stem Missisquoi and its major tributaries. The Bank Erosion study used the Bank Stability and Toe Erosion Model (BSTEM) to predict long term bank failures and resulting contributions of sediment and phosphorus to the total load leaving the Missisquoi River watershed (Simon 2011). This study provided several sources of input data used to define the initial parameterization of the SWAT channel characteristics described in Section 2.2.8. During the calibration of the MBB SWAT model, the Bank Erosion study had completed analysis and was able to provide results that were used to guide parameterization and calibration of the SWAT model channel processes. In addition to what was described in Section 2.2.8, three primary pieces of data from the Bank Erosion study were considered in the SWAT calibration:

STONE ENVIRONMENTAL INC

- Estimates of the percent of the banks failing were made from field surveys for 56 sections of the main stem Missisquoi and several tributaries. These percent failing value ranged from between 10% and 55%.

- BSTEM model output for seven main stem and six tributary sites was provided. This data included predicted bank erosion rates for the reaches associated with the model results.

- Preliminary estimates of the total contribution of channel banks to sediment and phosphorus load at the outlet of the Missisquoi River were made by the Bank Erosion modeling group. This was estimated to be 40% or more contribution of TSS and approximately 50% of total P.

In order to incorporate the percent of bank failing data into the SWAT model calibration, the SWAT 2009 source code was modified to include a new parameter at the subbasin reach level representing the estimated percent of the banks failing. The version of SWAT 2009 that served as the basis for the modeling in the MBB was version 477, that contains a built-in assumption that 100% of one on the two banks is eroding (this would be equivalent to 50% of the both banks, which is how the VTANR study reported the average bank failing rate). This assumption could potentially lead to excessive erosion rates in the more stable sections of the channel system. Many of the 223 reaches in the SWAT model did not have any percent bank failing data from the Bank Erosion study. In order to assign failing rates to the reaches without data, typical average failing rates for larger main stem reaches and smaller tributary reaches were calculated from the VTANR-LCBP-USDA data and extrapolated to the SWAT model reaches. The percent of reach failing values used as input to the SWAT model is shown in Map 2.13.

During initial evaluation of the SWAT model bank erosion simulation, it was observed that bank erosion was occurring on only a very limited number of reaches within the model. Furthermore, the rates of erosion could not be increased by following the standard approach of reducing bank critical shear stress and increasing erodibility. After examination of the model code, it was determined that bank erosion was being limited by the sediment transport capacity of the channel reach on a given day, regardless whether the shear stress on the bank exceeded its critical shear stress. Through communication with SWAT model development team (Narasimhan 2011), it was decided that a change should be made to address this issue, and a modified version of the SWAT 2009 sediment routing and bank erosion code was produced. This modified version did not constrain bank erosion based on the sediment transport capacity, and resulted in the expected relationship between critical shear stress and erodibility.

The sediment transport option chosen for all reaches within the MBB SWAT model was the Bagnold method (Bagnold 1977) with the addition of the particle size tracking option. The Bagnold method uses a stream power equation to predict the sediment transport capacity of a reach on any given day. The parameters to this stream power equation are only definable in SWAT at the watershed level, requiring that all reaches have the same transport capacity function. Recognizing that the parameters of Bagnold stream power equation may vary for different portions of the watershed, an additional modification to the SWAT model code was made to allow the Bagnold stream, power equation parameters to vary by reach. This modification was made in consultation with the SWAT development team (Narasimhan 2011).

The calibration of the in-stream sediment load focused initially on comparing the model simulated TSS with TSS load estimates at the long-term monitoring sites within the watershed, while at the same time evaluating the simulated channel bank erosion rates, the extent of bank erosion (i.e., the number of banks eroding), and the contributions of bank erosion and upland erosion to the total sediment load entering the stream channel

STONE ENVIRONMENTAL INC

system. While Bank Erosion study BSTEM modeling results provided estimates of bank erosion rates associated with specific reaches, the SWAT model calibration approach did not attempt to match erosion rates at the individual reach level. The objective of the SWAT model calibration was to achieve bank erosion rates that generally fell within the range of rates estimated by BSTEM and previously observed in the scientific literature. Following this approach, adjustments to the primary channel parameters controlling the occurrence and rate of bank erosion (critical shear stress and erodibility) were made uniformly to all reaches (during final calibration adjustments some additional adjustments were made for groups of reaches). In general, it was found the original critical shear stress values and erodibility parameters resulted in far too high rates of bank erosion in the SWAT model. Bringing these erosion rates into the range being predicted by BSTEM required that a threshold for the minimum allowable shear stress was set. In addition, the erodibility that was calculated as a function of critical shear stress was scaled down to produce a more reasonable amount of erosion. The goal of this approach was to try and maintain variability in bank erosion based on the observed and estimated characteristics of the individual reaches, while at the same time making the necessary adjustments to achieve an appropriate simulation at the watershed scale.

The parameters adjusted during sediment calibration included both upland and channel process parameters; however, the majority of adjustments occurred to parameters related to the channel processes which were guided heavily by the BSTEM modeling data. The primary adjustments were as follows:

- Adjustment of USLE C-factors for a limited number of land use classes for upland erosion control.

- Adjustment to in-channel sediment transport parameters, with some variability at the sub-watershed level.

- Watershed-wide uniform adjustments to channel bank erosion parameters, with limited local adjustments.

The SWAT model simulation results for the calibration period are shown for two of the long term tributary monitoring sites; the Missisquoi at Swanton in Figure 2.13 and the Rock River at Saint Armand in Figure 2.14.

Figure 2.15: Missisquoi at Swanton, monthly sediment calibration, 10/2005 – 9/2009.

STONE ENVIRONMENTAL INC
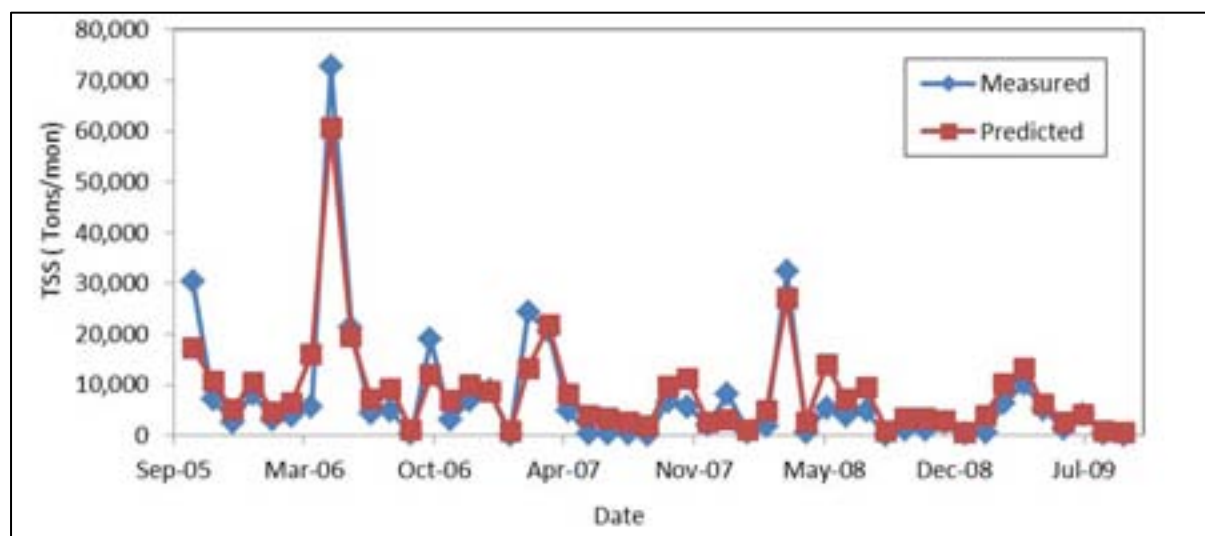
Figure 2.16: Rock River at Saint Armand, monthly sediment calibration, 10/2005 – 9/2009.
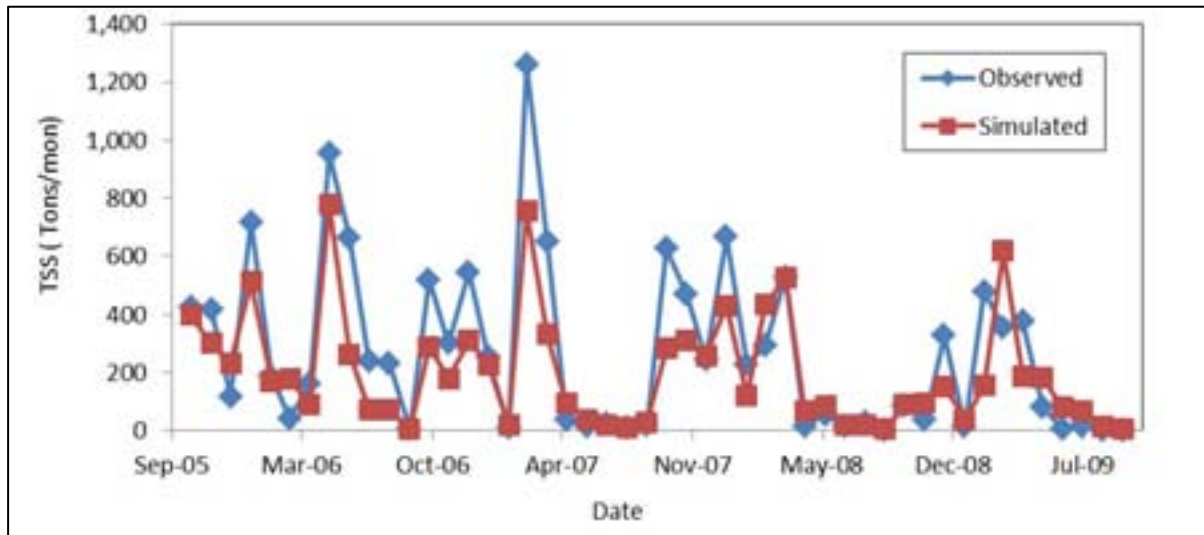
The sediment calibrations at the two sites shown indicate good agreement with the load estimates from the monitoring data. Graphs of the monthly observed versus predicted sediment loads for the other three long term monitoring sites evaluated can be found in Appendix C. A summary of the calibration period statistics is provided in Table 2.32. As is typical in hydrologic mode calibration, the statistics for the sediment calibration are not quite as strong as for the flow calibration. Still, with the exception of the Upper Missisquoi, all the statistics for the remaining sites fall within the good to very good range (the Upper Missisquoi is right on the boundary between satisfactory and good).

Table 2.32: Sediment simulation, calibration period statistics summary.

Location	NSE	PBIAS (%)	RSR
Upper Missisquoi upstream of Mud Brook	0.65	13.89	0.59
Missisquoi Nord near East Richford	0.71	11.69	0.54
Missisquoi at Swanton	0.86	-13.56	0.37
Upper Rock at S. Armand	0.66	24.51	0.58
Lower Rock (north of boarder)	0.70	21.01	0.55

Average annual bank erosion rates from the BSTEM model results were calculated for the 4-year time period corresponding to the SWAT calibration period. There were 13 BSTEM reaches with data available for this calculation. The average annual bank erosion rates based on the SWAT model output were similarly calculated (for 200 reaches in the main stem Missisquoi watershed) and the distributions of the two sets of values were compared. This comparison is shown in Figure 2.17.

STONE ENVIRONMENTAL INC

Figure 2.17: BSTEM and SWAT bank erosion rate frequency, sediment calibration period, 10/2005 – 9/2009.
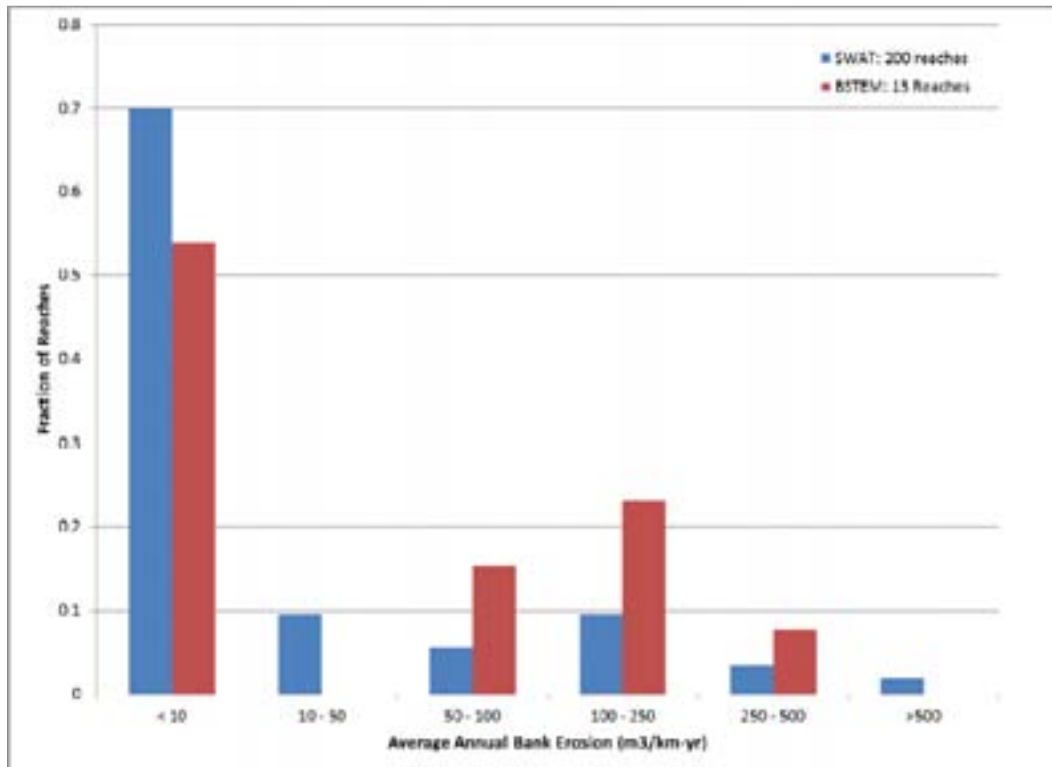
In both models, the majority of reaches generated less than 10 m^3/km-yr of bank erosion. Both models also predicted reaches with bank erosion rates in the 50 – 500 (m^3/km-yr) range. The objective of adjusting SWAT simulated channel erosion rates to fall within the same range as the BSTEM model predictions was accomplished. It is important to note that SWAT channel parameters were calibrated to approximate the BSTEM predicted rates because the BSTEM simulation of the bank erosion processes is more rigorous – accounting for both hydraulic and geotechnical processes. While there is uncertainty associated with the BSTEM predictions, the model was considered to be a sound basis for informing the calibration of SWAT's channel erosion components.

Collection of TSS and P concentration data at the short term tributary monitoring sites began in December 2009. Between December 2009 and the end of the SWAT model calibration period (September 2010) there were 13 samples taken at the Mud, Trout, Tyler, and Black sites and 19 samples taken Hungerford site. For each of five sites, TSS and total P load estimates were made using the Loadrunner interface to the LOADEST program (Runkel et al. 2004). LOADEST was set up to select the optimal model (regression equations of different forms are tested) for estimating the loads of TSS and total P based on the observed flows and the water quality data.

LOADEST generates its best estimate of load and the 95% confidence bounds of load estimates for the period over which flow data is provided. The 95% confidence bounds are generated based on the uncertainty in the estimates. From the beginning of flow data collection up until the end of the SWAT model calibration period, the total TSS load estimated by LOADEST was calculated and compared with the SWAT model prediction of total TSS load over same period. These results for the five sites are shown collectively in Figure 2.18. The simulated TSS loads from SWAT follow the same trends between tributary sites as the LOADEST estimates.

STONE ENVIRONMENTAL INC

In addition, the SWAT predictions are very close to the LOADEST estimates and are all within the 95% confidence interval (shown as error bar above and below the LOADEST values.

Figure 2.18: Annual TSS load at short term tributary monitoring sites, 10/2009 – 9/2010.
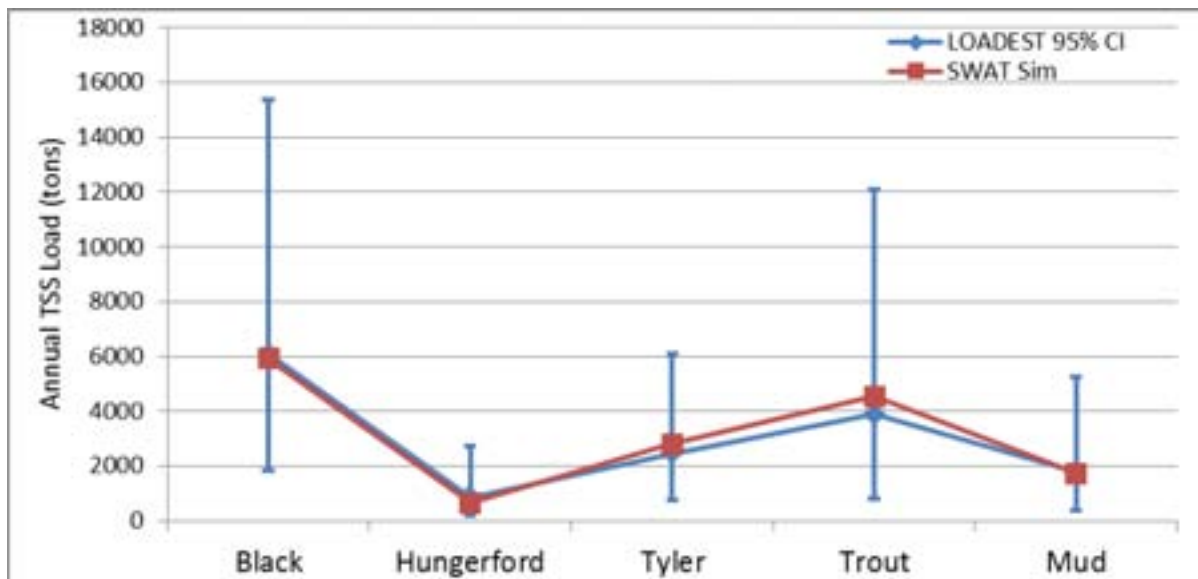
Based on review of sediment simulations at the long term monitoring sites, the comparison with the BSTEM predicted bank erosion rates, and the comparison with the sediment loads at the short term tributary sites, the SWAT models simulations of sediment loading during the calibration period were judged to be very good.

The MBB SWAT model was run to evaluate sediment predictions for the validation period from 10/1/2001 – 9/30/2005. The results for the same two sites presented during the calibration period, the Missisquoi River at Swanton and the Rock River at Saint Armand, are shown in Figures 2.19 and 2.20.

Figure 2.19: Missisquoi River at Swanton, monthly sediment validation, 10/2001 – 9/2005.

STONE ENVIRONMENTAL INC
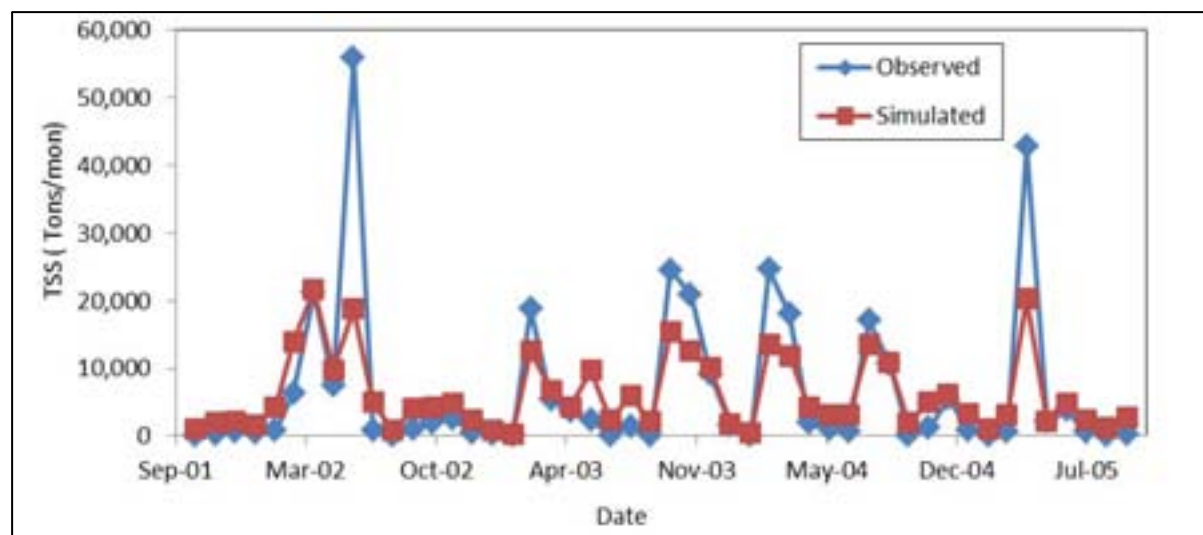
Figure 2.20: Rock River at Saint Armand, monthly sediment validation, 10/2001 – 9/2005.
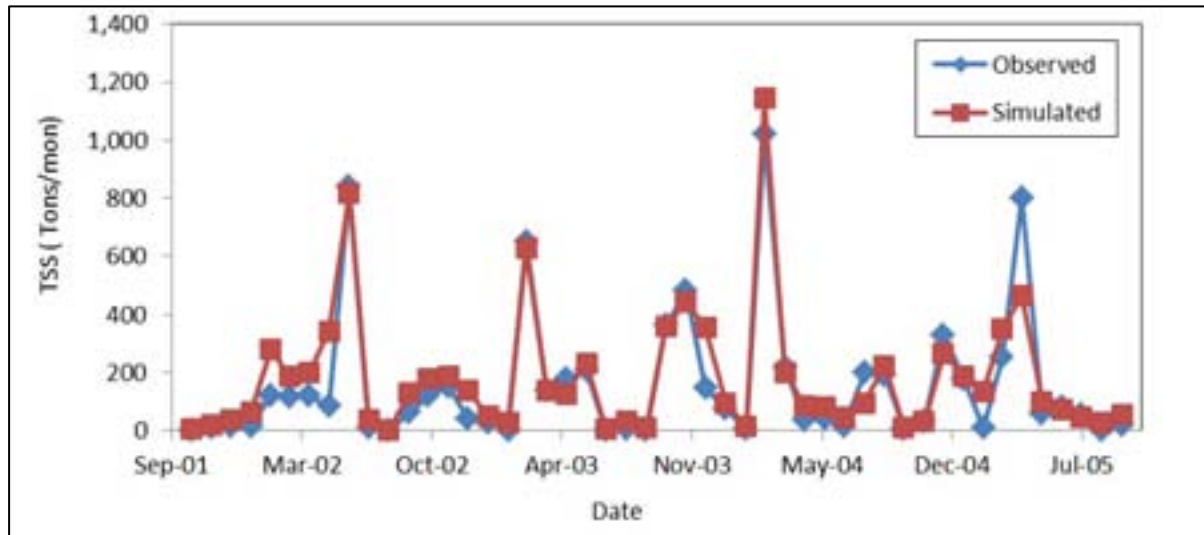
During the calibration period, the model simulation performance was better for the Missisquoi River at Swanton, while for the validation period, the simulation performance was better for the Rock River. Graphs of the observed and simulated sediment loads for the other three long term monitoring sites are located in Appendix C. The summary of validation period statistics for the long term monitoring sites is provided in Table 2.33. The Missisquoi River at Swanton had two statistics (NSE and RSR) fall in the satisfactory range, while the PBIAS was in the very good range. For the other four sites, all three statistics were in the good to very good range.

Table 2.33: Sediment simulation, validation period statistics summary.

Location	NSE	PBIAS (%)	RSR
Upper Missisquoi upstream of Mud Brook	0.81	-7.43	0.43
Missisquoi Nord near East Richford	0.69	19.25	0.56
Missisquoi at Swanton	0.60	7.77	0.63
Upper Rock at S. Armand	0.86	-15.95	0.37
Lower Rock (north of boarder)	0.82	-22.31	0.42

The BSTEM bank erosion rates were calculated for the period corresponding to the SWAT validation simulation. A comparison of the relative frequency of bank erosion rates generated by the two models is shown in Figure 2.21. Similar to the calibration period, the SWAT predicted bank erosion rates during the validation periods fall within the same range predicted by the BSTEM model.

STONE ENVIRONMENTAL INC

Figure 2.21: BSTEM and SWAT bank erosion rate frequency, sediment validation period, 10/2001 – 9/2005.
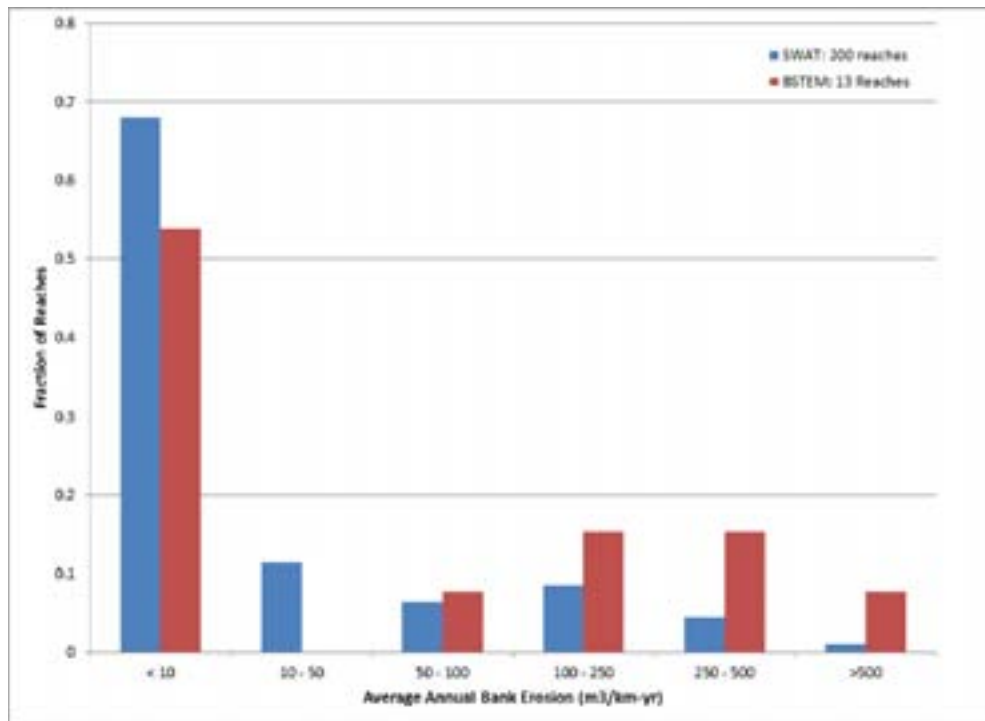
2.5.5. Phosphorus Calibration and Validation

Phosphorus in the MBB SWAT model has both upland and channel sources. Calibration of the hydrology, with particular attention to the runoff source contributions to streamflow, was an important step in achieving an appropriate simulation of upland phosphorus transport. The sediment calibration discussed in the previous section focused on both achieving a simulation of TSS in agreement with several in stream monitoring locations, as well as obtaining a distribution of sediment from upland and channel bank sources that was supported by sophisticated channel modeling recently conducted using the BSTEM model. The steps followed in hydrology and sediment calibration went a long way towards achieving a satisfactory P simulation. Additional calibration focused primarily on the transport of sediment organic P as well as the partitioning of P between soluble and sediment bound forms.

As was the philosophy followed through hydrology and sediment calibration, an effort was made to apply uniform adjustments to parameters affecting P transport. The reason this approach was followed was to minimize the introduction of bias into the model through local adjustments to parameters that could affect an area's critical source area ranking. In addition, the agronomic management practices defined for cropland, as well as non-cropland areas, have a significant influence on the P transport potential. Because the descriptions of these management practices was based on the best local knowledge and data available, characteristics of the management practices were kept as originally designed. The primary adjustments to SWAT model parameters that were made during P calibration were changes that affected:

- Organic and particulate P transport
- Soluble P uptake and sorption
- In-channel P transport

STONE ENVIRONMENTAL INC

The results of monthly P simulations for the calibration period are shown for the Missisquoi River at Swanton and the Rock River at Saint Armand in Figures 2.22 and 2.23 respectively.

Figure 2.22: Missisquoi River at Swanton, monthly phosphorus calibration, 10/2005 – 9/2009.
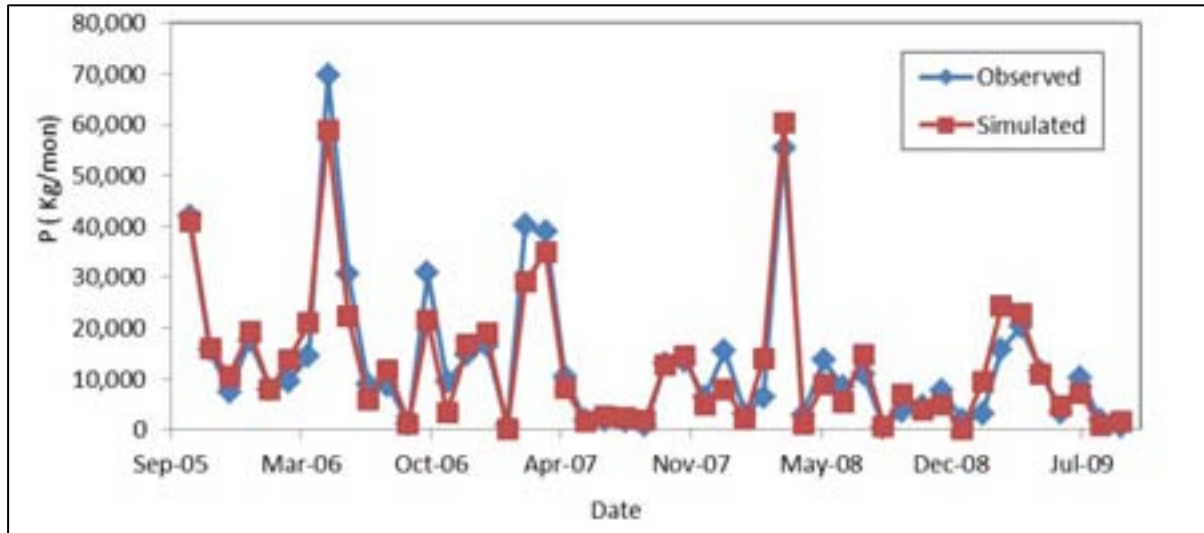
*Figure 2.23: Rock River at Saint Armand, monthly phosphorus calibration, 10/2005 – 9/2009.*
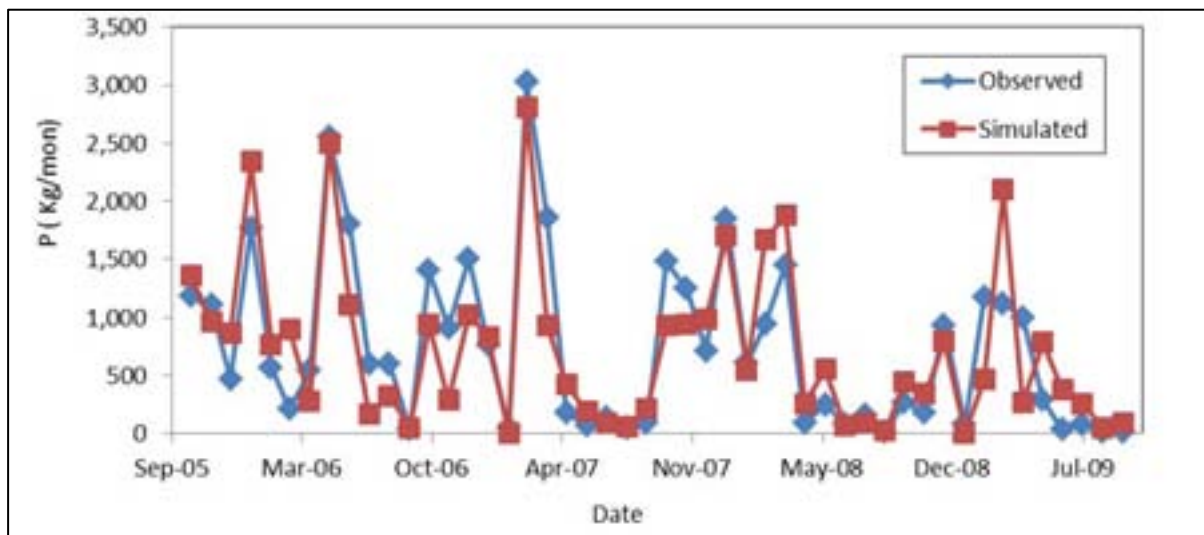
The Missisquoi River at Swanton simulation shows a somewhat closer agreement to the load estimates based on the measured data than does the Rock River simulation, although the PBIAS for both sites is very low (3 % and 1% respectively). A summary of the validation period statistics provided in Table 2.34 show that all three statistics at all five sites fall in the good to very good rankings. In some cases, the calibration statistics for the P simulation are better than those that were calculated for the sediment calibration (this is true at four of the five monitoring locations).

STONE ENVIRONMENTAL INC

Table 2.34: Phosphorus simulation, calibration period statistics summary.

Location	NSE	PBIAS (%)	RSR
Upper Missisquoi upstream of Mud Brook	0.78	2.01	0.47
Missisquoi Nord near East Richford	0.81	11.33	0.44
Missisquoi at Swanton	0.91	3.18	0.30
Upper Rock at S. Armand	0.70	1.38	0.55
Lower Rock (north of boarder)	0.67	18.50	0.57

The P monitoring data at the short term tributary monitoring sites was used to estimate P loading at each of the five sites using the Loadrunner interface to the LOADEST program, in manner consistent with that described for sediment load in Section 2.4.4. Specifically, the P load estimated by LOADEST at each monitoring site was calculated for the 1-year period ending on 9/30/10 (the end of the model calibration period). This was then compared with the loads for the same period predicted by SWAT. This comparison is shown in Figure 2.24. The 95% confidence interval for the LOADEST values are shown as error bars around the LOADEST estimated values. The SWAT-predicted loads at the tributary monitoring points show a similar trend to the LOADEST estimates. However, there is variability in that SWAT under-predicts relative to LOADEST at some sites (Black and Trout) and over-predicts at other sites (i.e., Tyler). Overall, the annual SWAT predictions show close agreement with LOADEST, and fall within the 95% confidence intervals at all sites.

Figure 2.24: Annual P load at short term tributary monitoring sites, 10/2009 – 9/2010.
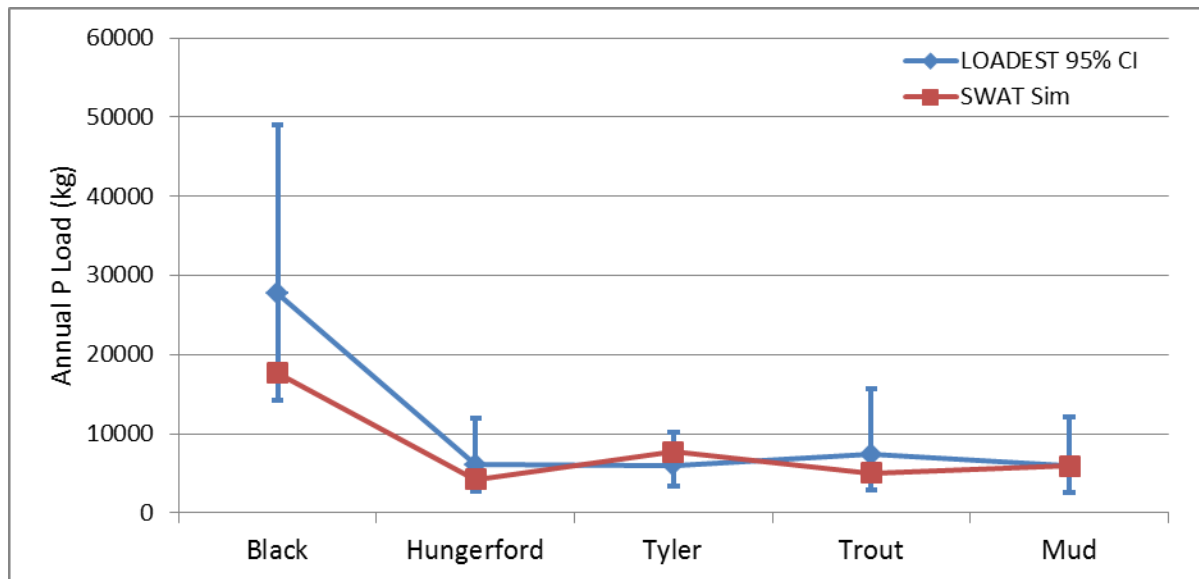
The MBB SWAT model was run to evaluate P load predictions for the validation period from 10/1/2001 – 9/30/2005 at the long term monitoring points. The results for, the Missisquoi River at Swanton and the Rock River at Saint Armand, are shown in Figures 2.25 and 2.26. For Missisquoi River, the model simulation performance for the validation period is nearly as good as for the calibration period. For the Rock River, there

STONE ENVIRONMENTAL INC

is a tendency for over-prediction, particularly in the first few months of the period, resulting in a PBIAS of -35%. Despite the higher PBIAS value, the graph in Figure 2.26 looks quite reasonable for the majority of the validation period. The validation period graphs for the additional long term monitoring sites are available in Appendix C. Table 2.35 provides a summary of all validation period model performance statistics. As was seen at the upper Rock River location site at Saint Armand, the lower Rock site has a PBIAS nearly 40% lower than the calibration period. Recall that for the Rock River hydrology calibration that the simulated flows had a relatively high negative PBIAS as well. This provides evidence for the interconnectedness of many component so the SWAT model.

Figure 2.25: Missisquoi River at Swanton, monthly phosphorus validation, 10/2001 – 9/2005
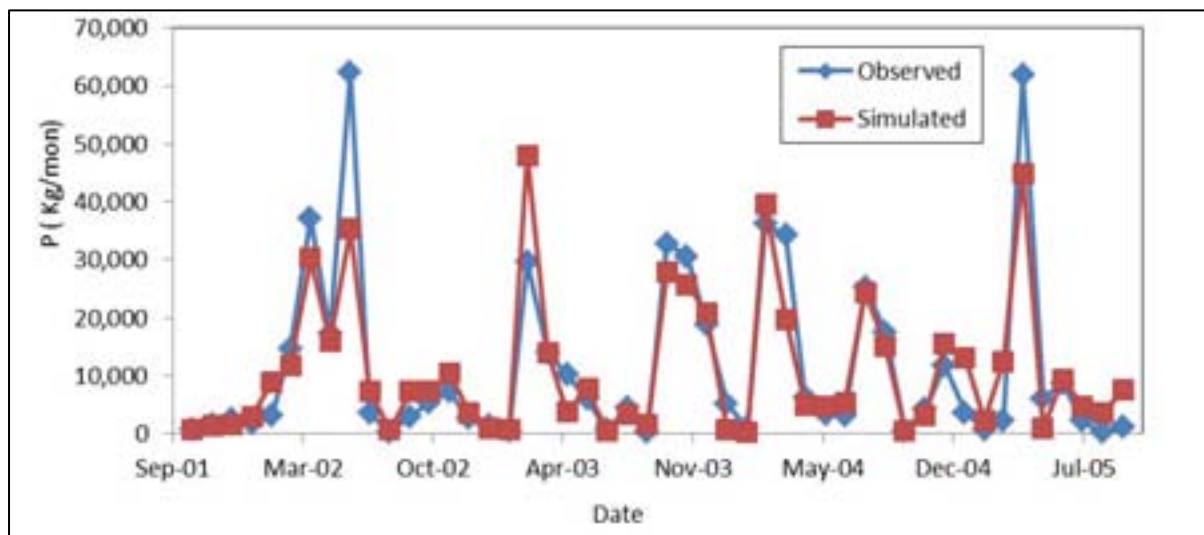
Figure 2.26: Rock River at Saint Armand, monthly phosphorus validation, 10/2001 – 9/2005.


STONE ENVIRONMENTAL INC
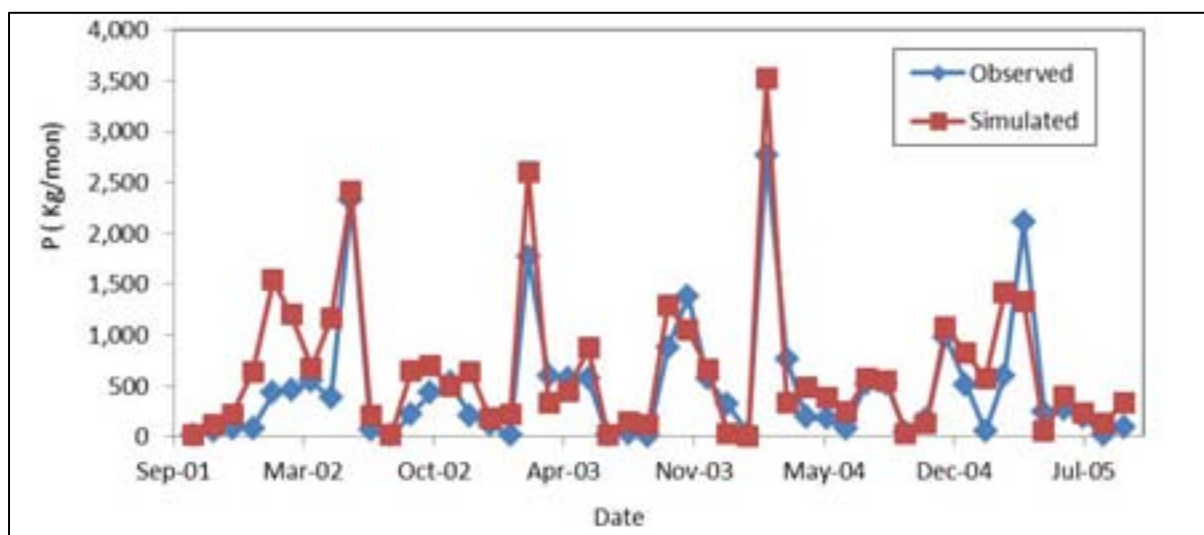
Table 2.35: Phosphorus simulation, validation period statistics summary.

Location	NSE	PBIAS (%)	RSR
Upper Missisquoi upstream of Mud Brook	0.75	-9.51	0.50
Missisquoi Nord near East Richford	0.90	8.41	0.31
Missisquoi at Swanton	0.80	2.63	0.44
Upper Rock River at S. Armand	0.61	-35.63	0.63
Lower Rock River (north of border)	0.72	-17.55	0.53

2.6. Sources of Model Uncertainty

Any SWAT model application, aAs with all environmental modeling applications, any SWAT model application has uncertainties associated with the simulation results. Model uncertainty comes from several different sources including, model inputs (weather, manure application rates, soil P), model calibration adjustments (changing parameters for the right or the wrong reasons), and model structure uncertainty (are the algorithms written into the model accurately representing the physical processes?). An additional source of model uncertainty comes fromis the measured data used to calibrate the model. Recent publications have reported that these measurement uncertainties can be significant, and should be considered what evaluating model goodness-of-fit criteria (Harmel et al. 2006, Harmel and Smith 2007).

The evaluation and quantification of model uncertainty has been studied in the context of the SWAT model, and water quality models in general, by a number of researchers (Beven and Binley 1992, van Griensven and Meixner 2006, Abbaspour 2009). These approaches require running large numbers of model simulations (generally thousands of simulations) to evaluate the model response to changes in inputs or parameter values. This assessment of uncertainty is almost always based upon model output at the watershed or sub-watershed level. Applying a traditional uncertainty analysis was not practical for the MBB SWAT model for several reasons. First, the model, with over 100,000 HRUs requires significant computational resources, and would require months to execute the number of simulations necessary to conduct a meaningful uncertainty assessment. Second, even if such an uncertainty assessment were completed, it would be impossible to assess the uncertainty at the HRU level; the scale at which we are interested in identifying critical source areas.

The sources of uncertainty specified in the beginning of this section also apply to the MBB SWAT model simulations. It should be re-emphasized that the approaches taken in the model development and parameterization were designed to minimize the introduction of bias and uncertainty that might influence the identification of CSAs. Based upon our work with the model and evaluation of the data, the most significant areas of uncertainty (in no particular order) would include: crop rotations on specific fields, field-level variability in manure application rates, locations of existing BMPs, variability of grazing intensity and manure inputs on pasture areas, P loading rates from farmsteads, build-up and wash-off of P from impervious surfaces, the significance of high organic P levels on P loads from high elevation forested and wetland soils. While we are unable to quantify these uncertainties, it is important to recognize them when interpreting the results of the CSA assessment presented in the subsequent sections.

2.7. Methods and Model Development Summary

The MBB SWAT model was developed for the explicit purpose of enabling the identification of critical source areas of phosphorus on the landscape. Great care was taken as P inputs were specified and the modeled

STONE ENVIRONMENTAL INC

calibrated to minimize the introduction of unnecessary bias in to the model. In some cases, this required that a set of common assumptions be applied to broad areas, such as the choice to simulate all land in corn and hay rotation as consisting of four years of corn followed by four years of hay. While this may not be exactly the rotation everywhere in the study area, introducing additional rotation option without knowledge on where that various options are practiced would have introduced additional uncertainty into modeling process, making the differentiation of critical source areas more difficult. It is also well known that there had been a number of conservation practices implemented on farms throughout the MBB that are not reflected in the "baseline" MBB SWAT model. For the same reason that crop rotations were given minimal variability, it was necessary to presume that all agricultural fields of a given rotation are subject to the same suite of conservation practices. Without explicit knowledge regarding where specific BMPs have been implemented, there would have been no justification in assuming a BMP was applicable to one field and not another. The components to this study that examine the effectiveness of random versus targeted BMP implementation offers some insight into how a potential critical source area's significance might change if extra conservation practices are followed.

The high resolution of the SWAT model developed for this study offers opportunities for evaluating P critical source areas at the strategic and tactical levels concurrently. This concept will be presented in the next section, beginning at the full watershed scale and working down to the sub-field scale, all based on evaluation of the MBB SWAT model simulations.

STONE ENVIRONMENTAL INC

3. RESULTS

3.1. Strategic Level Identification of Phosphorus Critical Source Areas

The identification of P CSAs at the strategic level was completed using a SWAT model simulation that used 30 years of historical climate data applied to the entire study area, including both the Vermont and Québec sectors of the basin. The 30-year simulation ran from January 1, 1980 until December 31, 2009, the 30 most recent calendar years for which complete climate data were available. Using a long climate record ensures that the modeling results reflect a broad range of weather conditions that have been historically experienced within the watershed. This is particularly important when simulating an area as large as the Missisquoi Bay Basin (MBB) where year-to-year spatial variability in weather conditions could result in wetter than normal conditions in some parts of the watershed and dryer than normal conditions in other parts of the watershed. The results summarized in this section are based on the 3rd through 30th year of the simulation, allowing the first two years of the simulation to serve as a model warm-up period. A model warm-up period is necessary to bring the model states (e.g., soil moisture, vegetation) up to a level consistent with recent environmental conditions.

The discussion of strategic level identification of CSAs will focus on the portion of the study are within the Vermont sector of the MBB (henceforth referred to as the "CSA assessment area"). It will begin with a watershed scale view that will assess the total contributions of P from various sources. The discussion will proceed by moving into more discrete landscape units, beginning with major sub-watersheds, through smaller subbasins that were represented in the SWAT model, continuing down to the highest resolution landscape representation – the unique combinations of land use, soils, topographic characteristic known in SWAT as the hydrologic response units (HRUs). Identifying CSAs at multiple scales will allow future management activities to be defined in terms of the major sub-watershed, subbasin, and field scale goals.

3.1.1. Watershed Scale Results

The contributions of P from both upland sources and channel sources were predicted based on the 28-year SWAT model simulation. The total average annual upland sediment and P quantities generated were computed by totaling the contributions from 103,666 non-water HRUs within the CSA assessment area. The total from channel sources was estimated by totaling the individual channel loads for all the subbasins within Vermont. For those subbasins that cross the Vermont/Québec boarder, the fraction of the channel sediment and P loads in Vermont was based on the fraction of the reach length within Vermont. These total loads and the percent of the total they represent are summarized in Table 3.1. While the SWAT model routes sediment and keeps track of particle size distribution, this approach for reporting the sources of sediment and P load sources was chosen for several reasons. First, once upland and channel based sediments are combined within the SWAT channel network, there is no way of tracking their source of origin. Also, while the particle size distribution is reported for sediment load as it leaves the outlet of each SWAT subbasin, SWAT does not provide output to report on the particle size distribution of sediments received from the two sources (channel and upland). Finally, the BSTEM model does not route sediment through a channel system, so by reporting the SWAT-predicted sediment contribution to the channel system, these results can be more easily compared with BSTEM estimations. As a result of this, the loads summarized in Table 3.1 cannot be directly compared to TSS measurements at water quality monitoring stations. Also, the total loads of sediment and P reported in Table 3.1 represent the amount entering the channel system and are not directly analogous to the load reaching the watershed outlet. The difference exists due to floodplain and channel deposition and nutrient chemical

STONE ENVIRONMENTAL INC

transformations. As was the rationale for reporting total sediment contribution and not TSS contribution, the reason for choosing this approach is that once sediment and P are combined in the channel system, SWAT does not keep track of the original sources. Therefore, basing the sources of origin assessment for sediment and P on the loads entering the channel system is the best approach.[1]

The data in Table 3.1 show that upland sources account for approximately 59% of total sediment load, with channel banks accounting for the other 41%. The distribution of total P is similar, with a slightly higher 61% coming from upland sources and the other 39% attributable to channel sources. These rates are within the same range of the 29% - 42% sediment contribution and ~50% total P contribution from bank sources suggested by the BSTEM modeling work recently conducted within the Missisquoi watershed.

Table 3.1: Sources of sediment and phosphorus load within CSA assessment area.

Source	Average Annual Sediment Contribution (kg)	Average Annual P Contribution (kg)	Average Annual Sediment Contribution (%)	Average Annual P Contribution (%)
Uplands	107,992	75,626	59.3	61.3
Channel Bank	74,213	47,786	40.7	38.7
Total	182,205	123,413	100	100

The total P losses generated from all upland areas within the watershed are shown as a function of the fraction of contributing land area contributing in Figure 3.1. The data represent the average annual total P load over the full simulation period for all HRUs within the CSA assessment area. The average annual total P load generated from this area was 75,626 kg; this is equivalent to a total P loading rate of 0.43 kg/ha over the 177,307 hectare area. The data in Figure 3.1 show that a relatively small fraction of the watershed contributes a disproportionately high amount of the total P; these fractions are summarized in Table 3.2. More than half of the total P is generated from only 10% of the watershed area, with the top 20% of the area accounting for nearly 74% of the total P. From a management perspective, this may be considered advantageous, as the areas to target for P reduction represent a relatively small fraction of the total watershed.

The data in Figure 3.1 indicate that the upland sources within the MBB generate total P over a broad range of areal loading rates. This range of loading rates is shown in Figure 3.2 and summarized in Table 3.3. The data are shown on a log scale to better display P loading rates that vary over several orders of magnitude. Note that the cumulative distribution shown in Figure 3.2 does not extend below 0.001 kg/ha on the x-axis, indicating that roughly 5% of the area contributes P at less than 0.001 kg/ha. The median P loading rate simulated was 0.145 kg/ha, while the maximum was 19.1 kg/ha. This variability in P loading is attributable largely to differences in land use and land management, with local characteristics of soils, topography, and climate also playing an important role. How these factors impact the identification of P critical source areas will be addressed in the following sections of this report.

---

[1] During calibration the MBB SWAT model, direct comparisons between TSS and total P predictions from the SWAT model and estimates made from monitoring station data were made. This was suitable for the calibration process because differentiating the sources of the TSS and total P was not necessary.

STONE ENVIRONMENTAL INC

Figure 3.1: Total P loss as function of area within CSA assessment area.
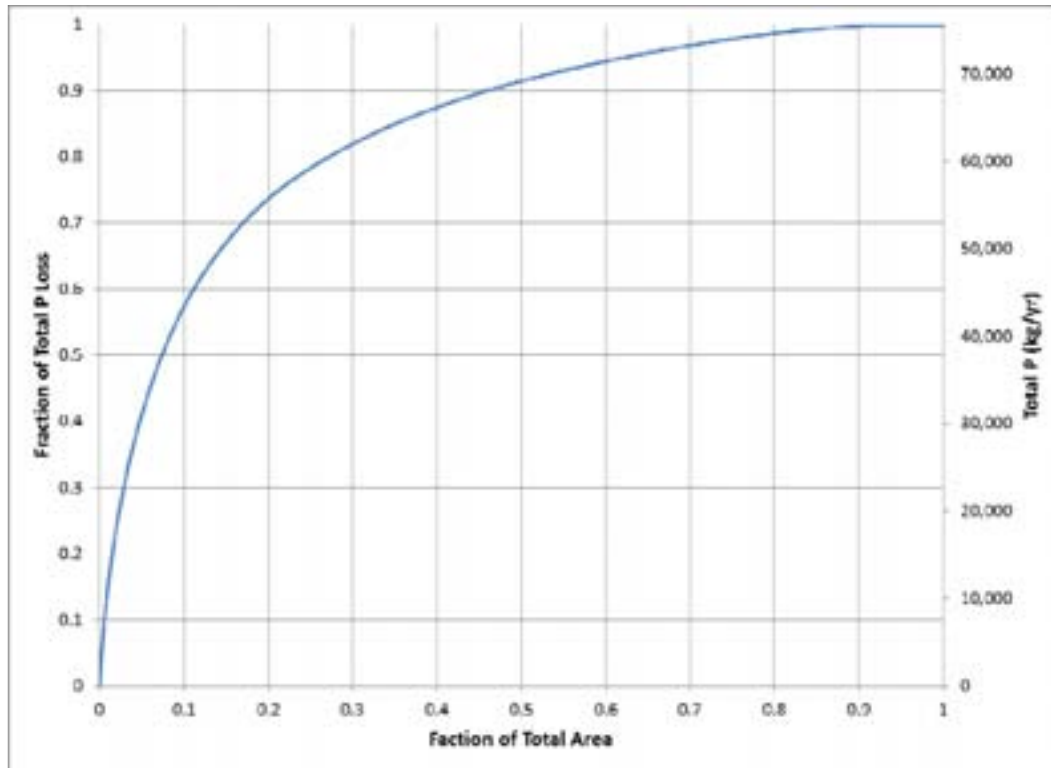
Table 3.2: Summary of total P generated a function of the fraction of area within the CSA assessment area.

Percent of Watershed Area	Percent of Total P
10	57.3
20	73.7
30	82
40	87.5
50	91.5
60	94.5
70	96.9
80	98.7
90	99.8
100	100

STONE ENVIRONMENTAL INC

Figure 3.2: Total P loading rate as function of area within the CSA assessment area.
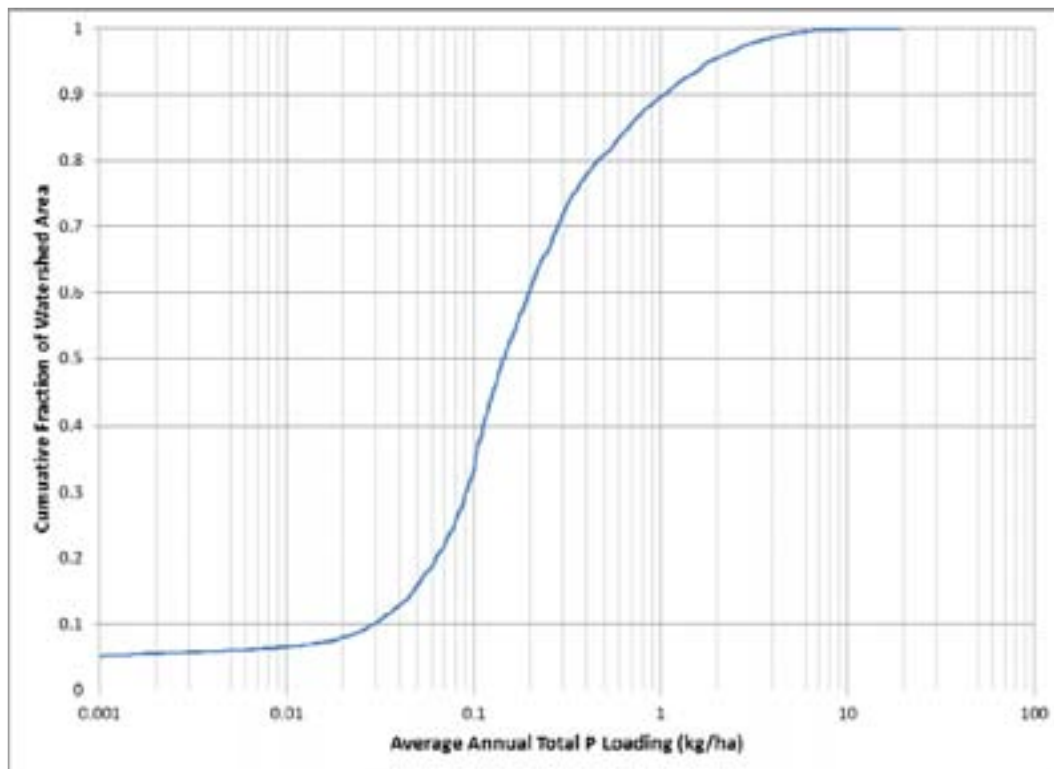
Table 3.3: Summary of total P loading rate a function of the fraction of area within the CSA assessment area.

Percentile	Total P Loading Rate (kg/ha)
10	0.029
20	0.063
30	0.091
40	0.113
50	0.145
60	0.198
70	0.281
80	0.46
90	1.05
100	19.1

3.1.1.1. Land Use Level Characteristics

The HRU-level results for the 30-year SWAT model simulation were summarized at the land use level for all of the HRUs occurring within the CSA assessment area. These results, shown in Table 3.4, have the sources sorted from highest to lowest average annual total P load. Note that if this table had been sorted according to average annual loading rate, the ordering would be significantly different.

STONE ENVIRONMENTAL INC

Table 3.4: Summary of sediment and P loads by land use for areas within the CSA assessment area.

Land Use Classification	Area (%)	Area (ha)	Sediment Loading Rate(ton/ha)	Total Sediment Load (ton)	Sediment P Loading Rate (kg/ha)	Percent Sediment P (%)	Soluble P Loading Rate (kg/ha)	Percent Soluble P (%)	Total P Loading Rate (kg/ha)	Total P Load (kg)	Percent of Total Upland P (%)
Corn-Hay	6.28	11,142	4.18	46,585	1.68	84.4	0.31	15.6	1.99	22,214	29.4
Forest	64.55	114,449	0.19	21,816	0.07	51.7	0.07	48.3	0.14	15,458	20.4
Hay	7.47	13,249	0.37	4,860	0.25	28.2	0.63	71.8	0.88	11,711	15.5
Pasture	3.04	5,387	0.82	4,425	0.44	33.6	0.86	66.4	1.30	7,000	9.3
Corn	1.49	2,637	4.71	12,412	1.81	86.5	0.28	13.5	2.10	5,533	7.3
Wetland	3.30	5,843	0.10	556	0.15	20.4	0.58	79.6	0.72	4,232	5.6
Brush	8.89	15,762	0.18	2,894	0.08	45.3	0.10	54.7	0.18	2,833	3.7
Developed, Open	2.50	4,431	0.70	3,094	0.27	75.0	0.09	25.0	0.37	1,622	2.1
Farmstead, SFO	0.28	489	0.37	181	0.87	28.6	2.18	71.4	3.05	1,494	2.0
Road, Paved	0.40	709	0.48	339	0.87	74.6	0.30	25.4	1.17	830	1.1
Residential, Low	0.74	1,310	0.64	832	0.45	74.3	0.16	25.7	0.61	799	1.1
Road, Dirt	0.57	1,007	8.42	8,476	0.66	84.3	0.12	15.7	0.78	788	1.0
Soybean-Corn	0.07	118	7.95	938	3.38	89.5	0.40	10.5	3.78	446	0.6
Farmstead, MFO	0.06	113	0.44	49	0.94	30.3	2.17	69.7	3.12	352	0.5
Residential, Med	0.17	308	0.50	154	0.52	72.2	0.20	27.8	0.72	222	0.3
Barren	0.20	354	1.08	381	0.21	80.1	0.05	19.9	0.26	93	0.1
Total	100.0	177,307	0.61	107,992	0.25	51.4	0.18	48.6	0.43	75,626	100.0

STONE ENVIRONMENTAL INC

Table 3.4 contains a great deal of information regarding sediment and P contributions from the major land uses considered in the strategic level CSA identification. Some of the more significant findings are as follows:

- Soybean-corn rotation has the highest total P loading rate at 3.78 kg/ha

- Corn-hay rotation produced the greatest contribution of total P at 29.4% of the total

- Forest, has the lowest total P loading rate at 0.14 kg/ha, but because it is the predominant land use in the basin it is the second highest total contributor, at 20.4% of the total

- All 7 of the 16 land uses that are classified as agricultural fall within the top 50% of total P loading rates

- For cultivated cropland (soybean-corn, corn-hay, and permanent corn), the vast majority of total P load is in the form of sediment P (85%-90%)

- For permanent hay and pasture, the majority of the total P load is in the form of soluble P (66%-72%)

- The developed land use classes (medium and low density residential, dirt and paved roads) fall in the middle among the different land uses in terms of average P loading rates; however, because these areas make up such a small fraction of the total area assessed (3.5%) their overall impact of total P load in the watershed is quite small

- Total P contribution as a percent of the total can be summarized as follows for broad land uses classes:

  o Agricultural: 64.5%

  o Developed: 5.6%

  o Undeveloped: 29.9%

The information in Table 3.4, above, shows that some land uses within the watershed produce a disproportionately high amount of total P relative to the fraction of the total watershed area they represent. One approach to quantifying this disparity is to calculate the ratio of the fraction of total P produced by a land use to the fraction of the total watershed area it covers. Land use classes where the ratio exceeds1 produce a disproportionately high amount of P and those where the ratio is less than 1 produce a disproportionately low amount of P. These ratios, along with the total P loading rates for each land use, are plotted in Figure 3.3. Forest has the lowest ratio (0.32), while soybean-corn rotation has the highest ratio of 8.86. The cultivated cropland classes of corn-hay, permanent corn, and soybean-corn all have P-load to area ratios of greater than 4. The only land uses with P-load to area ratios of less than 1.0 are forest, brush, barren, and urban open space. The data presented in both Table 3.4 and Figure 3.3 suggest that although agricultural areas represent about 20% of the total land area in the MBB, they represent the largest contributors to P load within the watershed.

STONE ENVIRONMENTAL INC

Figure 3.3: Total P loading rate and load to area ratio for major land uses (CSA assessment area).
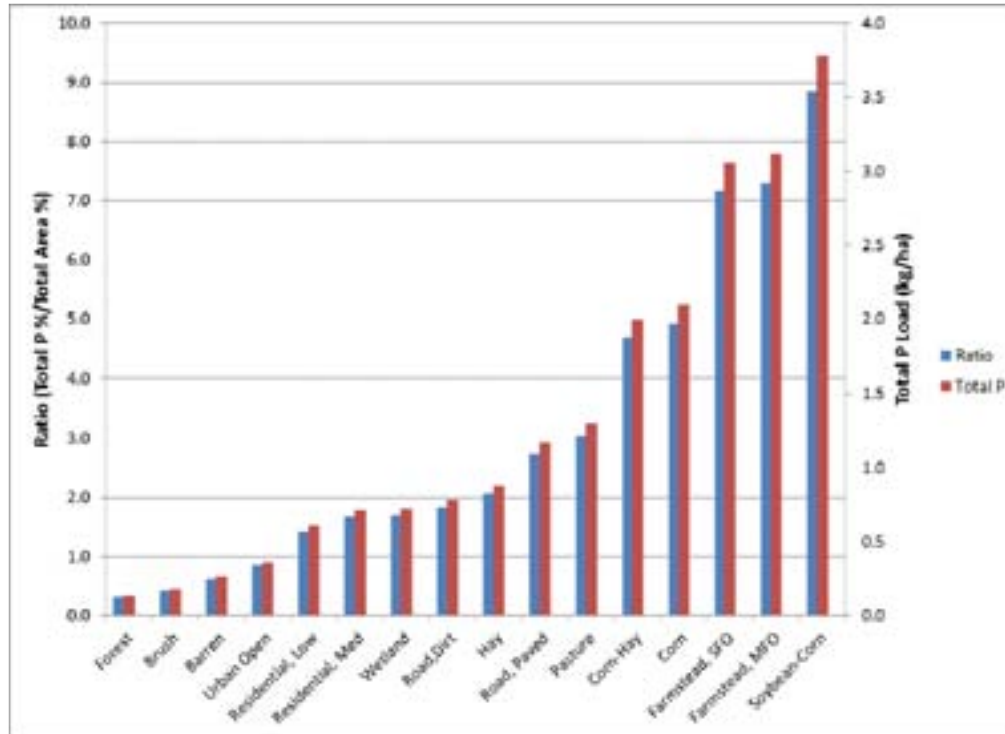
While the average annual P loads attributable to a land use class are broadly indicative of the characteristics of that land use, P loads vary significantly within a given land use class. This variability can be attributed to local soil, topographic, climate, and management characteristics of a given field, neighborhood, or land tract. Figure 3.4a presents the cumulative distribution of average annual total P load for all of the permanent corn, permanent hay, corn-hay rotation, and pasture HRUs within the Vermont sector of the study area. The figure shows that the P load can range widely within a given land use, with the 10th percentile of corn loading rate at approximately 0.44 kg/ha and the 90th percentile loading rate at approximately 4.1 kg/ha. Corn-hay rotation has an even wider range, varying from 0.25 kg/ha for the 10th percentile to a rate or 4.69 kg/ha for the 90th percentile. Figure 3.4b is analogous to Figure 3.4a, but presents the cumulative distributions for developed land uses. Here we see that variability in loading rate is lowest for paved roads, followed by the residential medium intensity and residential low intensity. These land uses have the lowest variability because they have the highest impervious fractions and runoff rates are nearly constant for all impervious areas. Dirt roads have fairly high variability in P loading rates, because the transport of P from these areas is driven by erosion that is highly dependent on slope. Finally, the urban open class has both the lowest P loading rates and the greatest variability in rates among the developed classes.

Figure 3.5 shows the variability in total P loading rates for all major land use classifications, showing the median, 25th and 75th percentiles, and the maximum and minimum loading rates for each land classification. The data regarding total P loading rates by land use show that significant variability exists within individual categories of land use. Several of the factors contributing to this variability will be explored in section 3.1.1.2.The total P load from developed areas is shown to be significantly less than that from agricultural land uses (5.6% of upland total versus 64.5% for developed and agricultural area respectively). This is in part

STONE ENVIRONMENTAL INC

attributable to the relative land use areas of the two broad classifications (4.4% for developed and 18.7% for agricultural). Also, if you remove the "Developed, Open" class from the develop grouping, then you have 3.5% of the total P from 1.9% of the total area. Still, even when removing the "Developed, Open" area, average annual P loading rates for developed areas is 0.8 kg/ha compared to nearly 1.5 kg/ha for agriculture. This assessment indicates that on average, agricultural areas generate nearly two times the P loading rate than developed areas. This appears to be inconsistent with previous assessments in the Lake Champlain Basin (Budd and Meals 1994) which indicated that representative P loading rates are three times higher for urban areas than for agricultural areas (1.5 kg/ha versus 0.5 kg/ha).

It should first be noted that given the prevalence of agricultural land uses in the MBB, the development of the SWAT model was much more influenced by the proper representation of agricultural areas than it was to developed land areas. Thus, a slight misrepresentation of P load from developed areas would be almost unnoticeable at the watershed scale. Therefore, extending results from the MBB SWAT assessment for land uses that account for less than 4% would not be appropriate. That said, there are several possible factors contributing to the differences in the two assessments First, the dominant developed land use class in the MBB is the Low Intensity Residential, which is estimated to be approximately 33% impervious area. The remaining pervious areas generate limited runoff and P export. The urban coefficients developed by Budd and Meals may be more reflective of higher density developed areas. Second, the agricultural areas from which the P loading rates are reported in the current CSA study are reflective of the intensely managed agricultural lands, and excludes adjacent fallow or unmanaged grass and brush areas. These adjacent unmanaged areas are often lumped in with agricultural areas in land use assessments and in the calculation of watershed scale loading rates. While it is not clear how these areas were handled in the previous work, had these areas been included in the calculation of average agricultural P loading rates in the current study, the average P loading rate would have dropped to near 1.0 kg/ha. Another consideration is that the Missisquoi sub-watershed has been consistently found to be an outlier in terms of the total P load from agricultural areas compared to other sub-watersheds in the Champlain Basin (Troy, Wang, and Capen 2007). It should also be noted that the average P loading rate for both agricultural and developed land uses based on the MBB SWAT assessment fall well within the full range of load coefficients reported by Budd and Meals (1994) and just outside of the most commonly reported values. Finally, P CSAs require both a source and a transport mechanism. The sources available in the agricultural lands in the MBB far exceed the sources in developed areas. Given the high runoff potential of some agricultural soils within the MBB, it certainly seems reasonable the P loading rates from managed agricultural lands would exceed that from residential areas.

The discussion above points out that the differences between results from the current MBB assessment and past studies within the Lake Champlain Basin may be justified from several perspectives. Regardless of any inconsistencies between the MBB SWAT assessment and past studies, one conclusion that is clear from the current assessment is agricultural areas generate significant amounts of P, and that strategies aimed at reducing P loads form these areas have the greatest potential for reducing the total P contributions to the Bay.

STONE ENVIRONMENTAL INC

Figure 3.4a: Total P loading rate for selected agricultural land uses as function of area (CSA assessment area).
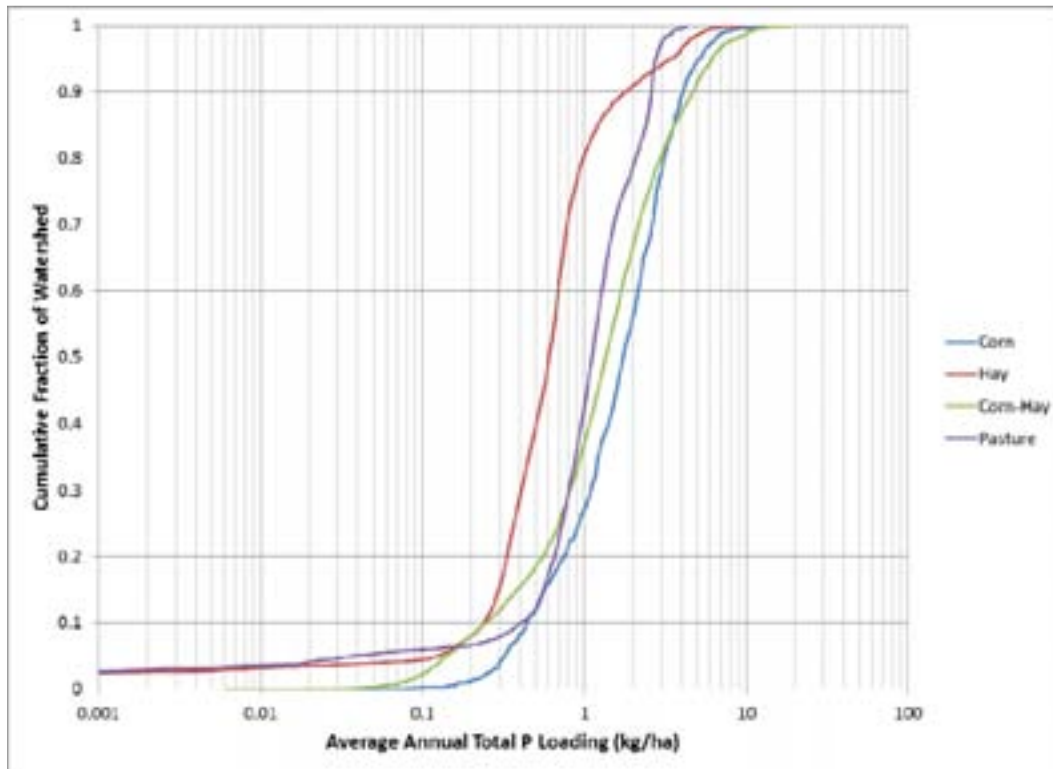
Figure 3.4b: Total P loading rate for developed land uses as function of area (CSA assessment area).

STONE ENVIRONMENTAL INC
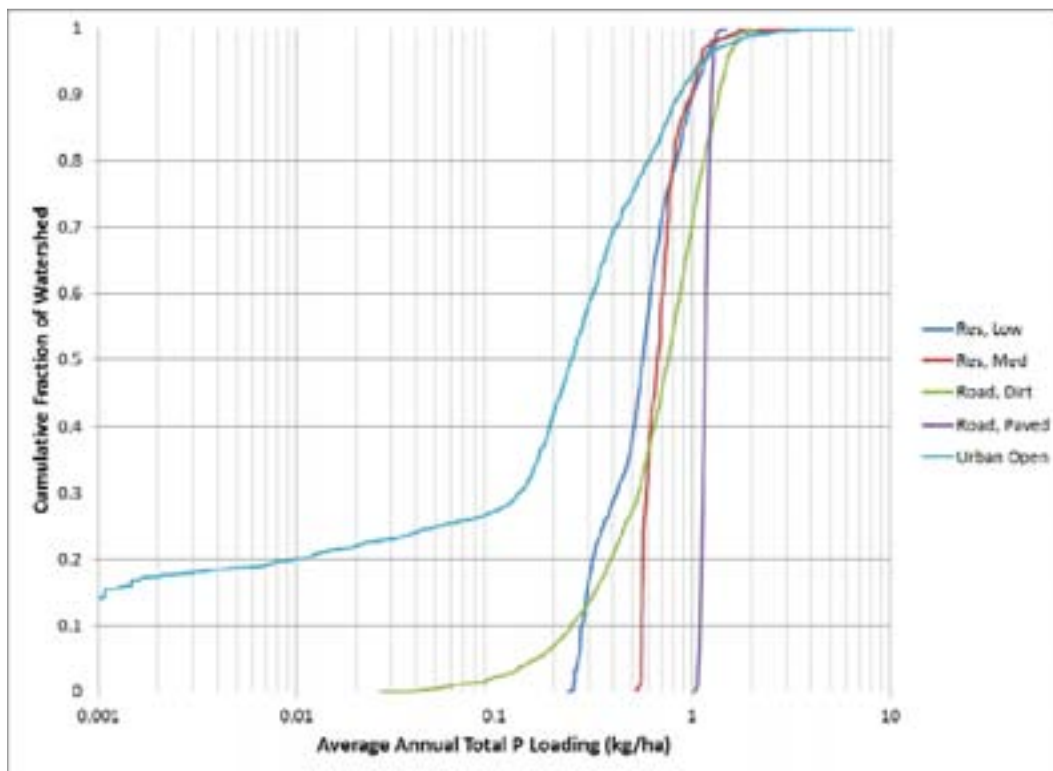
Figure 3.5: Box-plot of total P loading rate for all land uses within the MBB (Vermont sector).
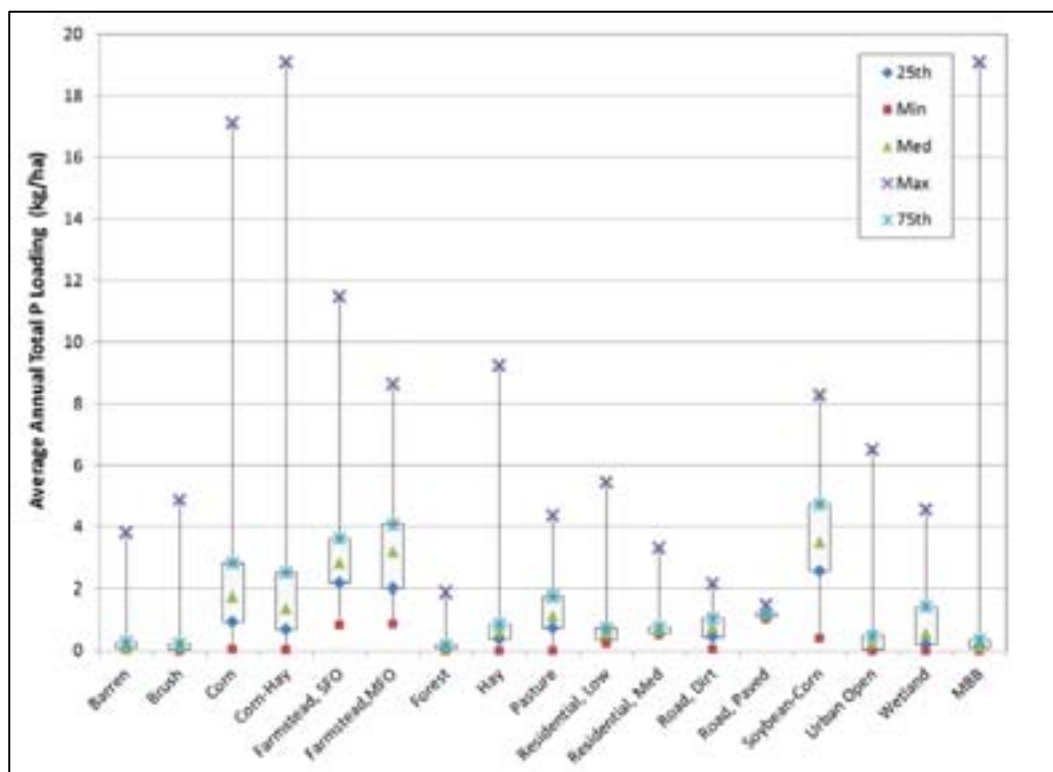
3.1.1.2. Factors Contributing to Phosphorus Loading Rate Variability

The SWAT model is a complex, process-based simulation tool that accounts for the interactions of dozens of environmental processes, as well as the physical and chemical characteristics of the landscape when predicting P loss from an HRU. The broad range in total P loading rates that have been predicted within a single land use classification in the MBB SWAT model is testament to the effects of local landscape, climate, and cropping systems on total P export rates. This section of the report will examine three landscape characteristics that are readily quantifiable for a given field or land tract, and that seem to have a strong influence on total P loading rates. These characteristics; soil hydrologic group, compound topographic index (CTI), and slope, will be discussed in the following sections.

3.1.1.2.1. Effects of Hydrologic Soil Group on Phosphorus Loading Rates

The hydrologic soil group describes the soil's drainage and infiltration characteristics and generally describes a soil's potential to generate surface runoff. There are four hydrologic group designations that have been defined by the Natural Resource Conservation Service as follows (NRCS 2007):

> ■ Group A: Soils in this group have low runoff potential when thoroughly wet. Water is transmitted freely through the soil. Group A soils typically have less than 10 percent clay and more than 90 percent sand or gravel and have gravel or sand textures. Some soils having loamy sand, sandy loam, loam or silt loam textures may be placed in this group if they are well aggregated, of low bulk density, or contain greater than 35 percent rock fragments.

STONE ENVIRONMENTAL INC

- Group B: Soils in this group have moderately low runoff potential when thoroughly wet. Water transmission through the soil is unimpeded. Group B soils typically have between 10% and 20% clay and 50% to 90% sand and have loamy sand or sandy loam textures. Some soils having loam, silt loam, silt, or sandy clay loam textures may be placed in this group if they are well aggregated, of low bulk density, or contain greater than 35% rock fragments.

- Group C: Soils in this group have moderately high runoff potential when thoroughly wet. Water transmission through the soil is somewhat restricted. Group C soils typically have between 20% and 40% clay and less than 50% sand and have loam, silt loam, sandy clay loam, clay loam, and silty clay loam textures. Some soils having clay, silty clay, or sandy clay textures may be placed in this group if they are well aggregated, of low bulk density, or contain greater than 35% rock fragments.

- Group D: Soils in this group have high runoff potential when thoroughly wet. Water movement through the soil is restricted or very restricted. Group D soils typically have greater than 40% clay, less than 50% sand, and have clayey textures. In some areas, they also have high shrink-swell potential. All soils with a depth to a water impermeable layer less than 50 cm (20 in) and all soils with a water table within 60 cm (24 in) of the surface are in this group, although some may have a dual classification, as described in the next section, if they can be adequately drained.

The soil hydrologic group is used directly in the determination of the runoff curve number for a field or land tract, that directly affects the simulation of surface runoff that can be expected from the area. Soils classified as hydrologic group A will have very little surface runoff, while soils classified as hydrologic group D will have a much higher amounts of surface runoff. Because P moves primarily with sediment through soil erosion or in its soluble form with surface runoff, hydrologic group has a significant effect on the amount of P loss form a given area.

The average annual total P loading rates by land use classification, categorized by soil hydrologic group, are summarized in Figure 3.6. For all of the land use classifications, the total P export rate increases at the hydrologic group moves from A to D; however, the magnitude of the increase is not uniform across different land use classifications. The increases are somewhat less pronounced for the developed classes of low and medium intensity residential and paved roads, because the impervious fractions in those land use classes are not sensitive to hydrologic group, and only the pervious fractions are influenced. For the permanent hay land use class, total P export ranges from 0.08 kg/ha for group B soils to 1.69 kg/ha for group D soils (a 20-fold increase). Likewise, the permanent corn land use P export increases from 1.17 kg/ha for group B sols to 4.32 kg/ha for group D soils (a 3.7 fold increase). Table 3.5 summarizes the total P loading rates for each land use and hydrologic group classification and includes the total area that each classification represents. The more runoff prone hydrologic group C and D soils represent nearly 90% of the soils in the CSA assessment area.

STONE ENVIRONMENTAL INC

Figure 3.6: Total P loading rate by land use and soil hydrologic group.
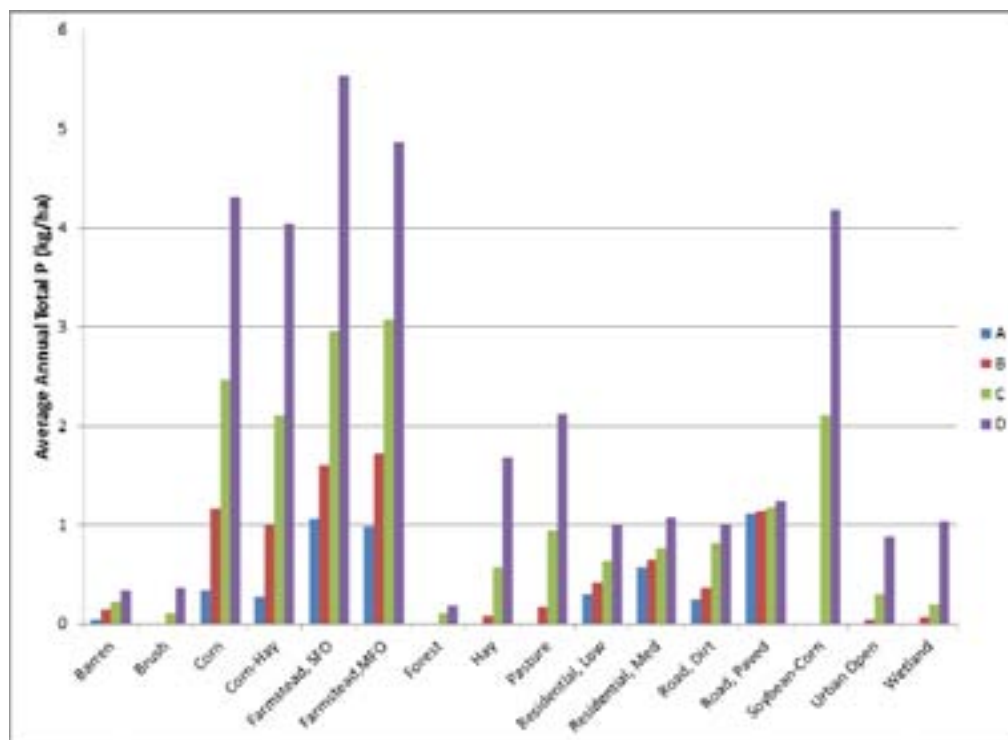
Table 3.5: Total P loading rate summary by land use and soil hydrologic group.

Land Use	Hydro Grp. A		Hydro Grp. B		Hydro Grp. C		Hydro Grp. D	
	P (kg/ha)	Area (ha)	P (kg/ha)	Area (ha)	P (kg/ha)	Area (ha)	P (kg/ha)	Area (ha)
Barren	0.04	60	0.15	22	0.22	51	0.34	221
Brush	0.00	1,400	0.01	1,079	0.11	7,907	0.37	5,376
Corn	0.35	301	1.17	788	2.47	1,175	4.32	372
Corn-Hay	0.28	1,660	1.00	1,911	2.11	5,568	4.05	2,003
Farmstead, SFO	1.06	54	1.61	49	2.96	302	5.54	84
Farmstead, MFO	0.99	18	1.72	8	3.07	56	4.87	30
Forest	0.00	4,953	0.01	2,865	0.10	50,593	0.18	56,038
Hay	0.00	338	0.08	353	0.57	8,475	1.69	4,083
Pasture	0.00	215	0.17	229	0.94	2,980	2.12	1,963
Residential, Low	0.30	313	0.42	149	0.64	567	1.00	282
Residential, Med	0.58	117	0.65	42	0.77	106	1.07	43
Road, Dirt	0.25	98	0.36	60	0.81	569	1.01	279
Road, Paved	1.12	137	1.13	88	1.17	325	1.24	159
Soybean-Corn[1]					2.11	23	4.18	95
Urban Open	0.00	863	0.04	335	0.29	2,122	0.88	1,112
Wetland	0.01	135	0.07	258	0.20	1,689	1.03	3,761
Total		10,663		8,236		82,509		75,900

1.None of the soybean-corn rotation areas simulated were on hydrologic group A or B soils.

STONE ENVIRONMENTAL INC

The fraction of total P generated for each hydrologic group for a given land use classification is shown in Figure 3.7. The data in this figure reflect both the relative area of each hydrologic group and the magnitude of the total P load from that area (both relative to the total P generated over the land use). For example, greater than 90% of the total P load from wetlands comes from group D soils. This is not surprising, as most areas classified as wetlands will have group D soils, and the runoff rate from those areas will be high. The significance on hydrologic group C soils is also evident in Figure 3.7, where for land uses such as corn and corn-hay, the majority of total P losses come from these soils.

Figure 3.7: Total P loading rate by land use and soil hydrologic group.
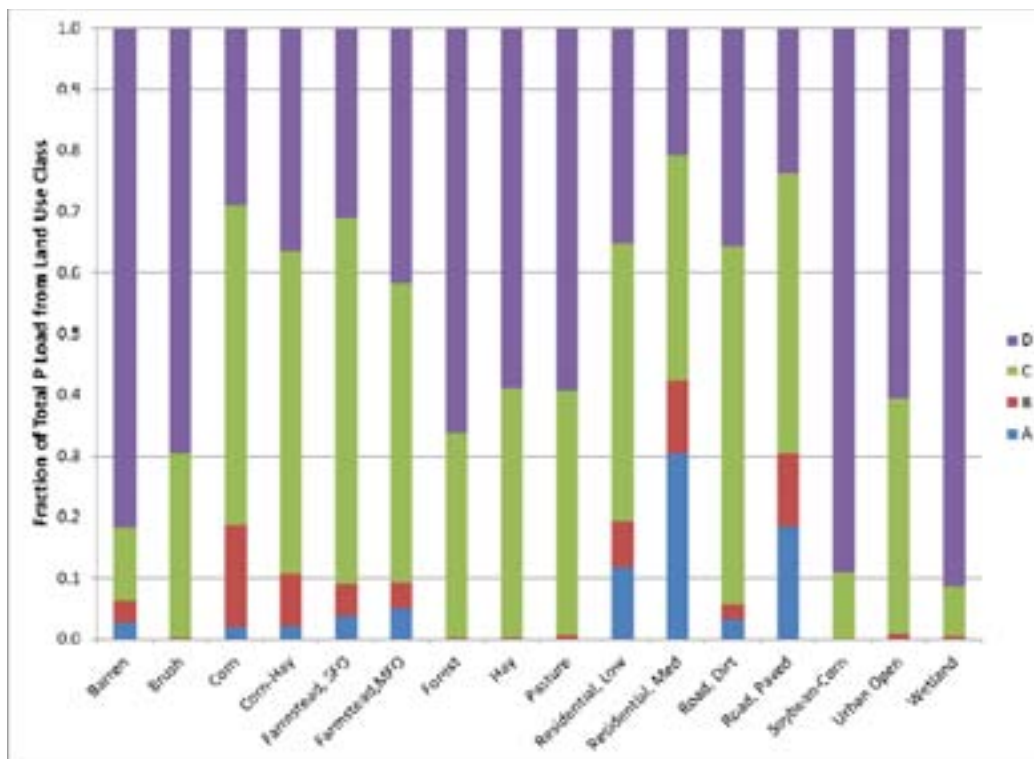
The runoff potential of a soil, i.e., the hydrologic group, clearly has a significant impact on total P loss and is an important factor in the identification of P CSAs. Identification of P CSAs based purely on the land use and soil hydrologic group would capture a significant fraction of the most critical areas. There are, however, additional factors that bear important consideration in the identification of CSAs.

3.1.1.2.2. Effects of Compound Topographic Index on Phosphorus Loading Rates

The compound topographic index (CTI) considers the upslope contributing area and the local landscape slope to estimate the likelihood of soil saturation (and therefore saturation-excess runoff) at a given location. Areas with high upslope contributing areas and low slopes will have high CTI values and have a greater likelihood of saturation, while areas with low upslope contributing areas and high slopes will have low CTI values and a lesser likelihood of saturation. The CTI concept was presented in detail in Section 2.2.1.2 of this report. In the MBB SWAT model, runoff curve numbers were adjusted independently for each HRU to reflect the local CTI value; this approach avoided biasing the assignment of the highest CTI values entirely to the low slope river

STONE ENVIRONMENTAL INC

valley parts of the MBB and the lowest CTI values entirely to the steeper eastern upland region Using this approach, landscape areas with the same land use and soil hydrologic group could have different levels of runoff potential based on their local topographic characteristics (i.e., CTI). Figure 3.8 shows the average annual total P loading rates by land use classification and CTI class. The CTI classes shown in Figure 3.8 represent the following:

- CTI Class 1: Areas with CTI values below the 20th percentile of all CTI values within the watershed. These areas have the lowest probability of saturation.

- CTI Class 2: Areas with CTI values between the 20th and 80th percentile of all CTI values within the watershed. These areas have close to the average likelihood of saturation.

- CTI Class 3: Areas with CTI values greater than the 80th percentile of all CTI values within the watershed. These areas have the highest probability of saturation.

Figure 3.8: Total P loading rate by land use and CTI group.
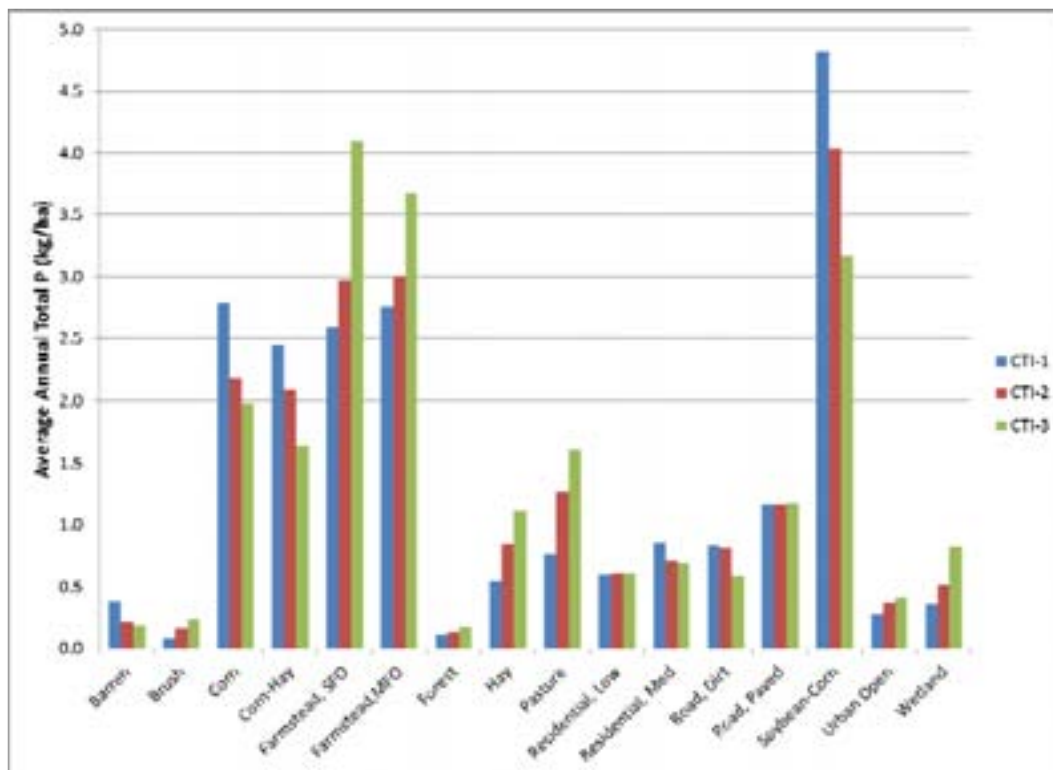
At first, some of the results in Figure 3.8 seem to contradict the notion that area with high CTI values (likely to saturate) produce greater surface runoff rates, because the corn, soybean, and corn-hay results that show that high total P loading rates occur with lower CTI values. At the same time, review of land uses such as the farmsteads, hay, pasture, and wetlands supports the theory that areas with high CTI values produce greater surface runoff and higher total P loading. These apparent contradictions can be explained by further considering the primary drivers influencing P export; surface runoff and sediment yield.

STONE ENVIRONMENTAL INC

Figure 3.9 shows the average annual percent of water yield that occurs as surface runoff for the different CTI classes associated with each land use. The results in Figure 3.9 clearly support the theory that areas with higher CTI values generate greater amounts of surface runoff. If this is the case, why do corn areas with low CTI values have higher total P loading rates than areas with high CTI values? The answer is sediment yield. Figure 3.10 shows the average annual sediment yields based on land use and CTI group classification. For the majority of land uses, sediment yield is higher for lower CTI values than for higher CTI values. This is particularly true for the land uses with generally high sediment yields, namely the heavily cultivated agricultural classes (corn, corn-hay, and corn-soy) and the dirt roads. The next question to arise might be why the sediment yields are higher when surface runoff is lower (for CTI class 1 for example). One of the primary causes for this is the land surface slope. Recall that high slope values are associated with low CTI values. Therefore, the corn areas in CTI class 1 are also those which likely have high slopes, while the corn areas on CTI class 3 are areas which likely have much lower slopes. The data in Figures 3.8, 3.9, and 3.10 suggest that, slope is a more significant driver in determining sediment yield than is total surface runoff (although a certain amount of surface runoff MUST occur for sediment erosion to take place). For those land uses where sediment P is the dominant form being lost from the landscape, the sediment yield, not the surface runoff will ultimately be a better indicator of the total P loss. Conversely, where soluble P is the dominant form exported, surface runoff will be a better indicator of the amount of total P loss. This hypothesis is supported by Figure 3.11 that shows the soluble P loading rates for each land as a function of the CTI class. Here we see that almost uniformly, higher soluble P loads are associated with higher CTI values. This is further supported by Figure 3.8 that shows that total P loss for land uses where soluble P dominates transport (i.e., hay and pasture) have higher rates of P loading with increasing CTI class.

Figure 3.9: Average surface runoff fraction of annual water yield by land use and CTI group.

STONE ENVIRONMENTAL INC
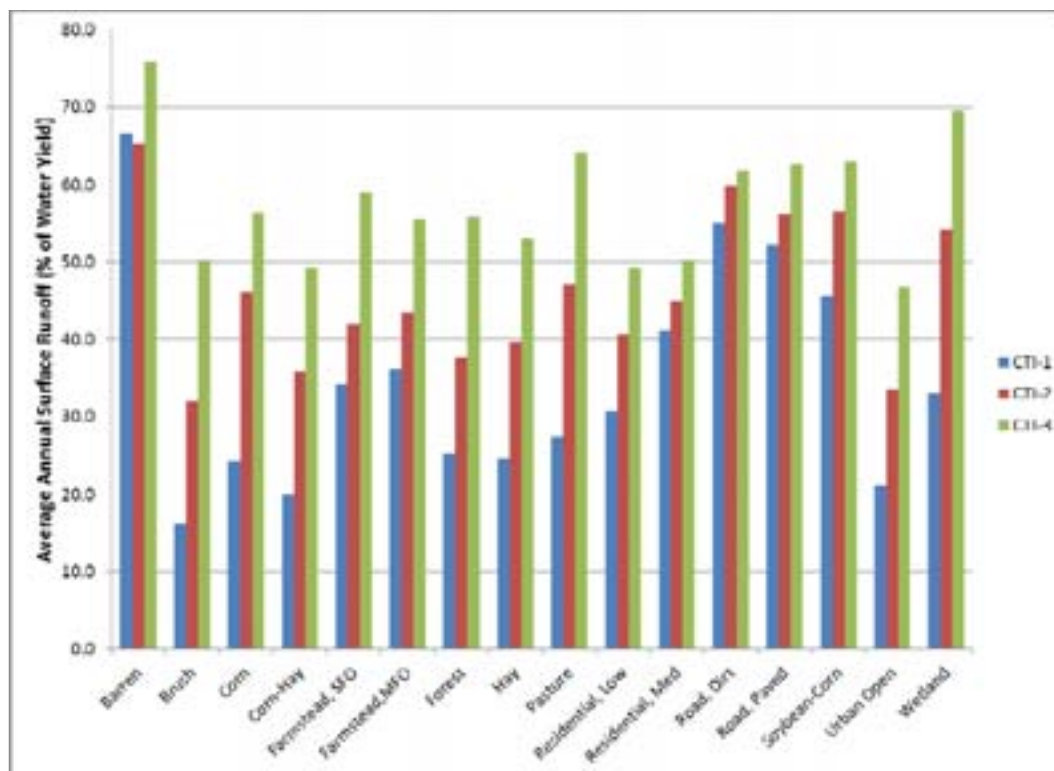
Figure 3.10: Average annual sediment yield by land use and CTI group.
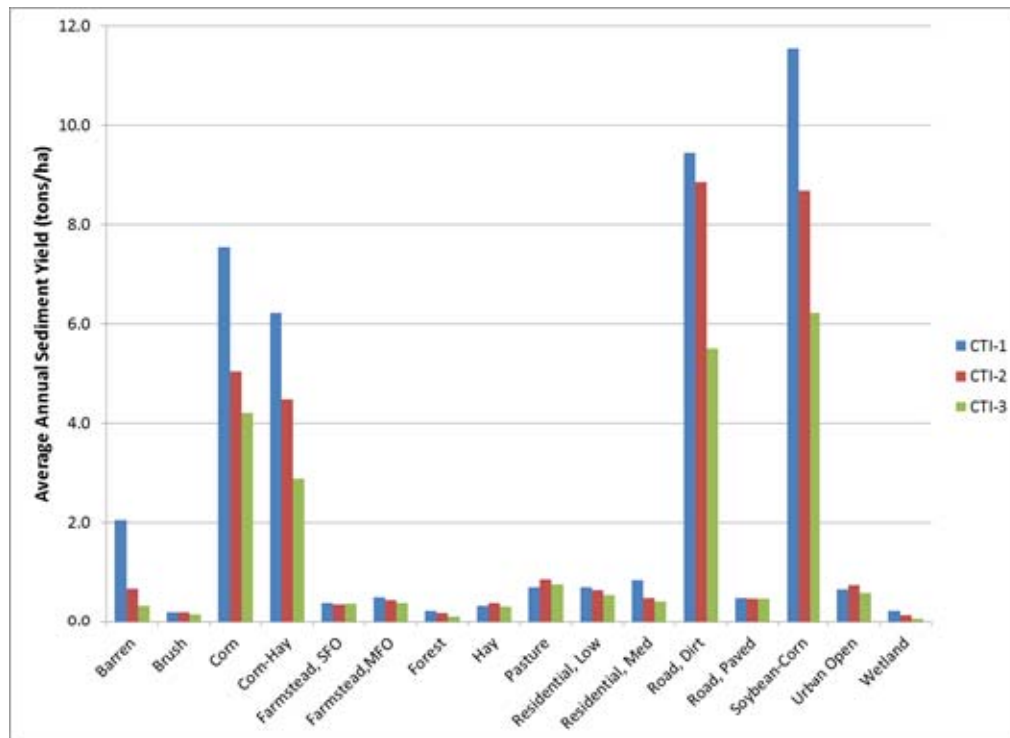
Figure 3.11: Average annual soluble P loading by land use and CTI group.

STONE ENVIRONMENTAL INC
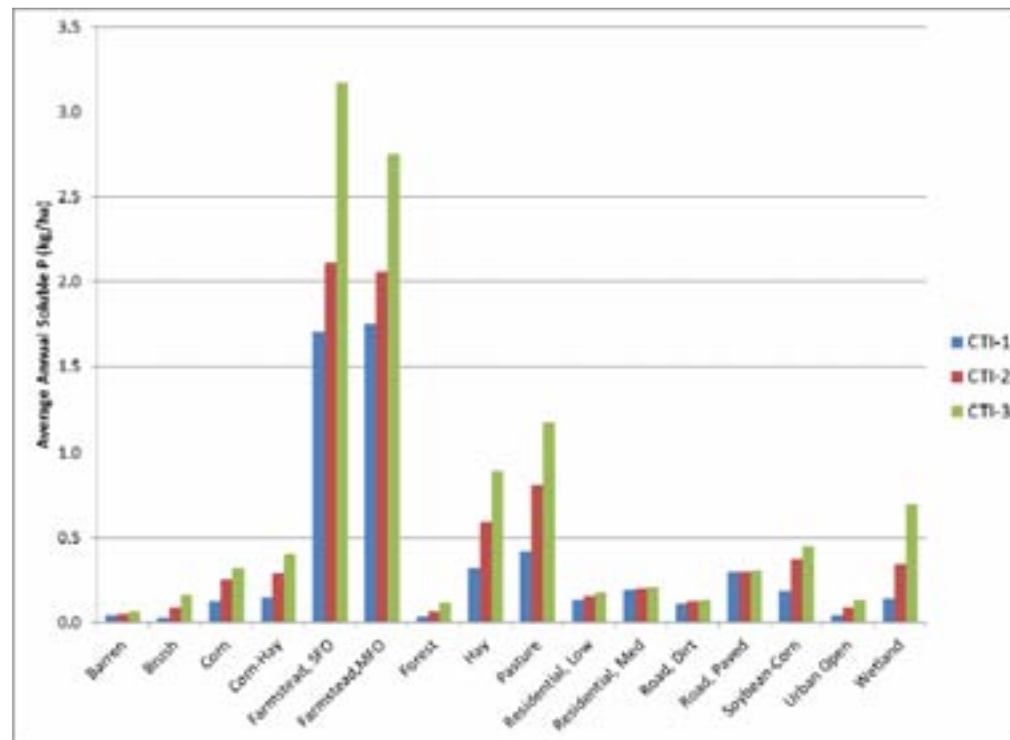
Because slope has been suggested to be a key factor in determining total P export rates, and suggested to be more influential than total surface runoff in predicting sediment yield, the next landscape characteristic to be examined will be slope.

3.1.1.2.3. Effects of Slope on Phosphorus Loading Rates

Land surface slope has a significant influence on sediment yield and thus, total P export. For land uses where the soil is exposed or has limited vegetative cover for a portion of the year, the effects of higher slopes to increase sediment yield and total P loss will become significant. For land uses where more established vegetative cover exists and erosion rates are lower, slope will be less of a factor driving total P loss. Figure 3.12 shows the total P loading rates for different land uses and slopes classes. As was the case when total P export was examined as a function of CTI, different trends are apparent depending on land use. For those land uses where total P loading is largely in the form of particulate P (e.g., corn, corn-hay, corn-soybean), increasing slope shows a direct correlation with increasing total P. For many other land uses, the correlation is less clear, or even shows the opposite trend (see wetlands). This disparity can again be explained by the form of P export (soluble versus particulate). Figure 3.13 shows only the particulate P export as a function of land use and slope class. Now, the trend of higher P loss with increasing slopes isseen almost uniformly across the different land uses, supporting the notion that higher slopes contribute to higher particulate P loss through erosion.

Figure 3.12: Average annual total P loading by land use and slope.

.

STONE ENVIRONMENTAL INC
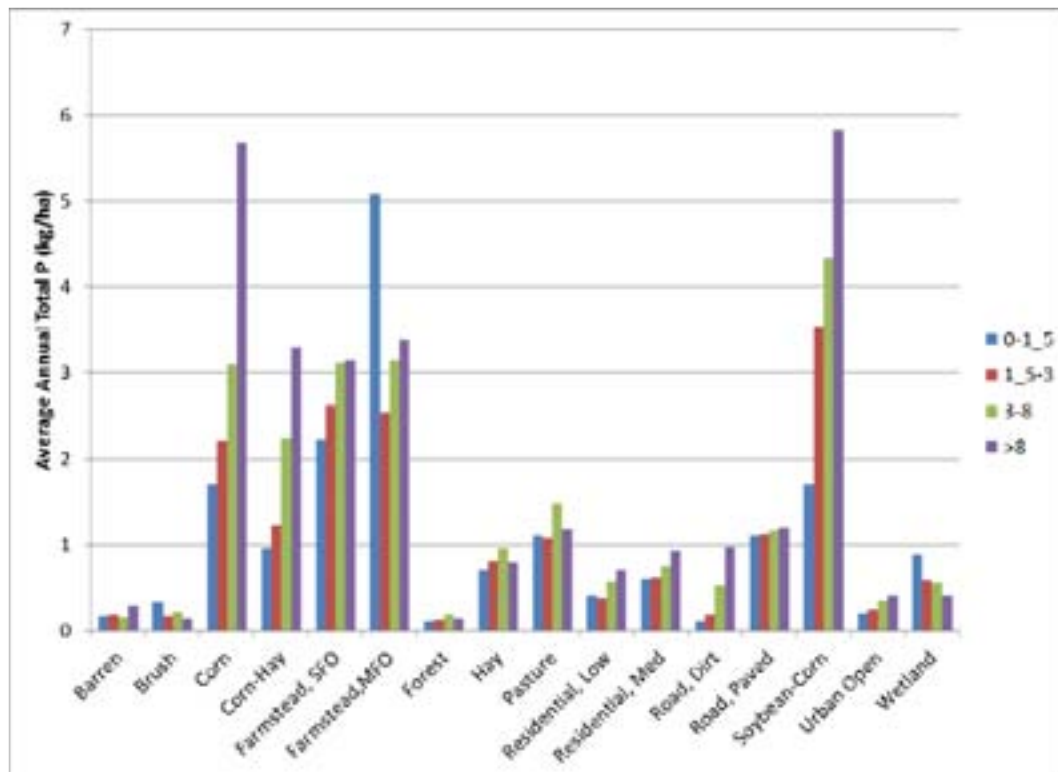
Figure 3.13: Average annual particulate P loading by land use and slope.
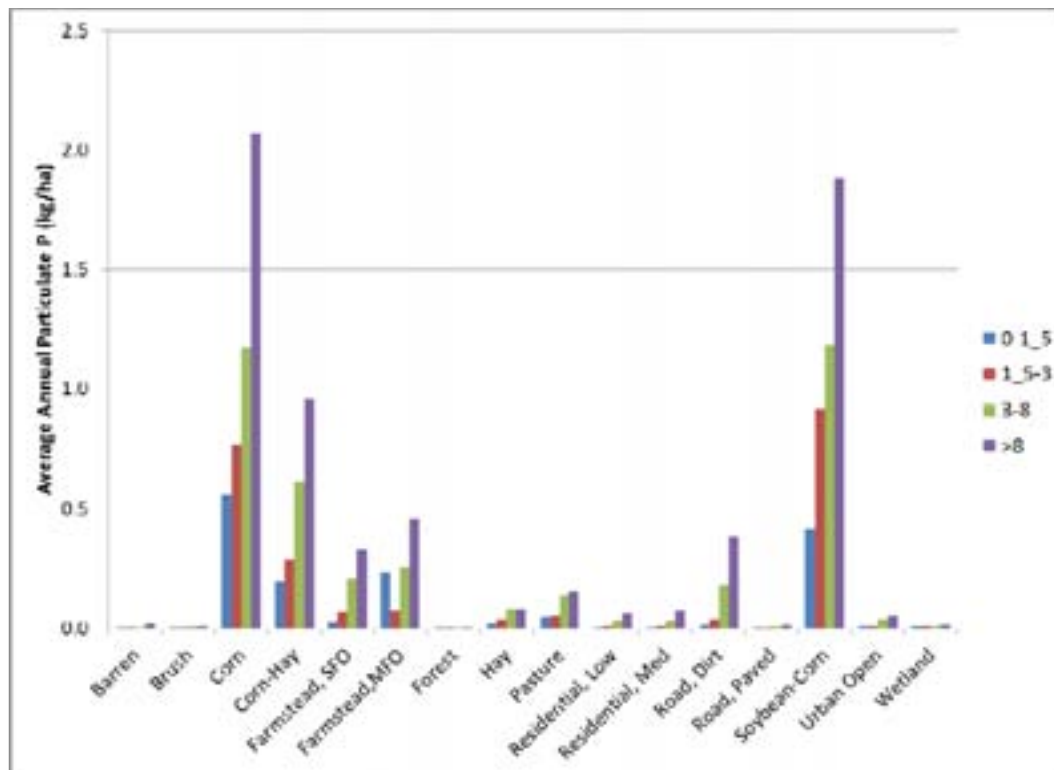
3.1.1.2.4. Summary of Landscape Factors Contributing to Phosphorus Loading Rates

The three factors evaluated in the previous sections - soil hydrologic group, CTI, and slope - were all shown to influence the magnitude of P export. The CTI class was found to have the greatest influence on soluble P losses while slope was most influential on particulate P export. Soil hydrologic group was highly influential for total P export, including both particulate and soluble forms of P. As was shown through the previous discussion, interaction among different landscape and soils characteristics can make identification of a single factor or even a collection of factors difficult as direct predictors of the magnitude of total P export. This complexity of interactions, that includes numerous additional factors, is what makes the SWAT model well suited to sorting out the subtleties in different characteristics that influence P export. This is accomplished through the independent parameterization of HRUs based on localized variability in soils, topographic, climate, and agronomic conditions. The HRU-level identification of P CSAs will be presented in later sections this report.

3.1.1.3. Distribution of Phosphorus Critical Source Area at the Watershed Scale

One method by which P critical source areas can be defined is based on their total P loading rates relative to all of the other source areas within the watershed. This is equivalent to assessing where a particular land area's loading rate falls along the cumulative distribution of loading rates across the watershed. For example, land areas whose loading rates are at or above the 90th percentile P loading rate (10% of the area) could be classified as critical. Or, instead of the 90th percentile, the 80th percentile could be used as a cutoff, which would result in

STONE ENVIRONMENTAL INC

classification of 20% of the area as critical source areas. Figures 3.14 and 3.15 show how the top 20% and top 10% of P CSAs are distributed by area across the different land uses classes within the watershed. The highest ranking CSAs are dominated by agricultural lands, with corn, corn-hay, hay, and pasture making up more than two-thirds of the total land area whose loading rates are above the 80th percentile. Wetlands are the next highest, with almost 9% of the area. While farmsteads and some developed classes were shown to have relatively high loading rates (see Figure 3.3), they cover such a small fraction of the total land area in the Missisquoi Bay Basin that they do not represent a significant portion of the CSAs by this metric. Figure 3.15 shows that the land use distribution of the top 10% of CSAs has some similarities and some differences compared to the top 20%. For the top 10%, the agricultural field areas are even more predominant, with corn, corn-hay, hay, and pasture making up 79% of the top 10%. Recall from Table 3.2 that 57% of the total P generated goes from the top 10% of CSAs. Focusing mitigation efforts that address these land uses specifically has the potential to result in significant reductions in the total P load in the watershed. As with the top 20%, undeveloped land uses (e.g., forest, brush) and farmsteads make up a small fraction of the land area in the top 10%.

Another way to consider critical source areas at the land use level is to evaluate the fraction of the area for each land uses that falls within the top ranked CSAs. This approach does not diminish the significance of land uses that cover a small amount of area, but have high P loading rates. Figure 3.16 and 3.17 show these distributions for the top 20% and top 10% of CSAs respectively. For the top 20% of CSAs (Figure 3.16) there are four land uses for which 100% of the area falls within the top 20% (residential, medium, both farmsteads, paved roads, and soybean-corn). At the opposite end of the spectrum, there are four land use classes where less than 30% of the area falls within the top 20% of CSAs (forest, brush, urban open, and barren). Looking at the 10% CSA threshold (Figure 3.17), the trends are similar, with a few notable differences. First, none of the land uses have 100% of their area within the top 10% of CSAs. Second, there is a more distinct cut-off between those land uses where a significant fraction of the area is within the top 10% and those where a much smaller fraction falls within the top 10%. As shown in Figure 3.17, there is a visible break between the pasture and the unpaved road classes - all the classes from dirt roads and to the left have 26% or less of their area in the top 10%, while all the classes from pasture and to the right have 54% or greater of their area within the top 10%. This may serve as a guide to focusing mitigation strategies on those land uses that are most consistently high ranking CSAs.

STONE ENVIRONMENTAL INC

Figure 3.14: Land us distribution of the top 20% of CSAs based on average annual total P load.
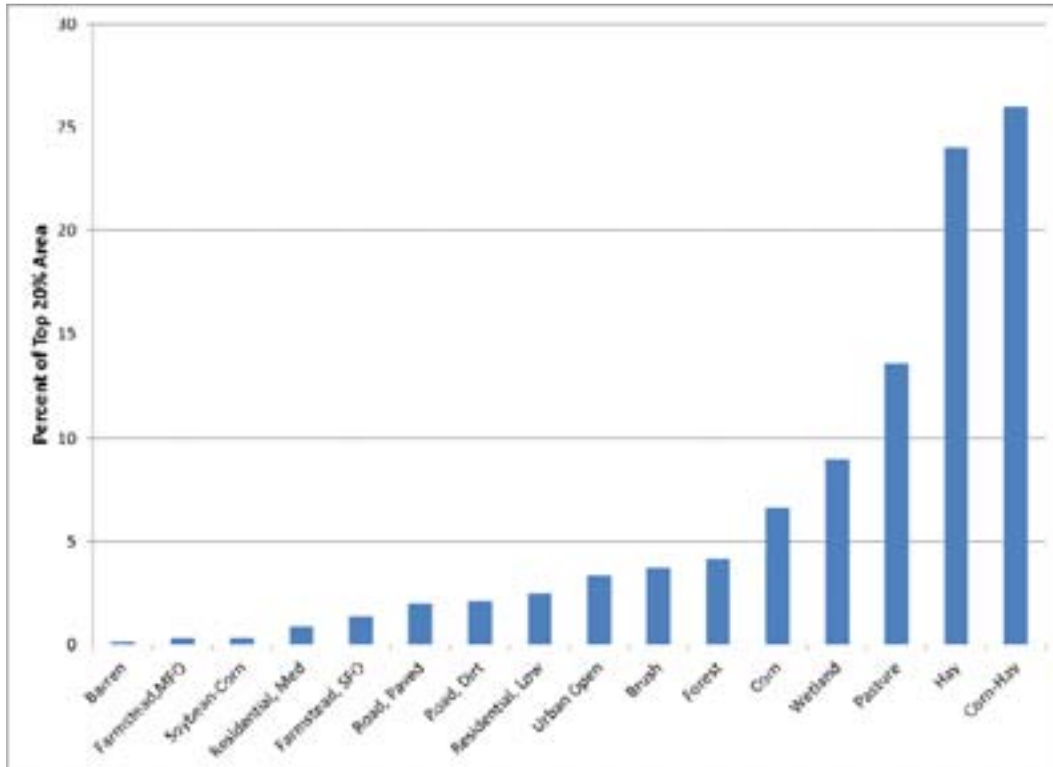
Figure 3.15: Land use distribution of the top 10% of CSAs based on average annual total P load.

STONE ENVIRONMENTAL INC
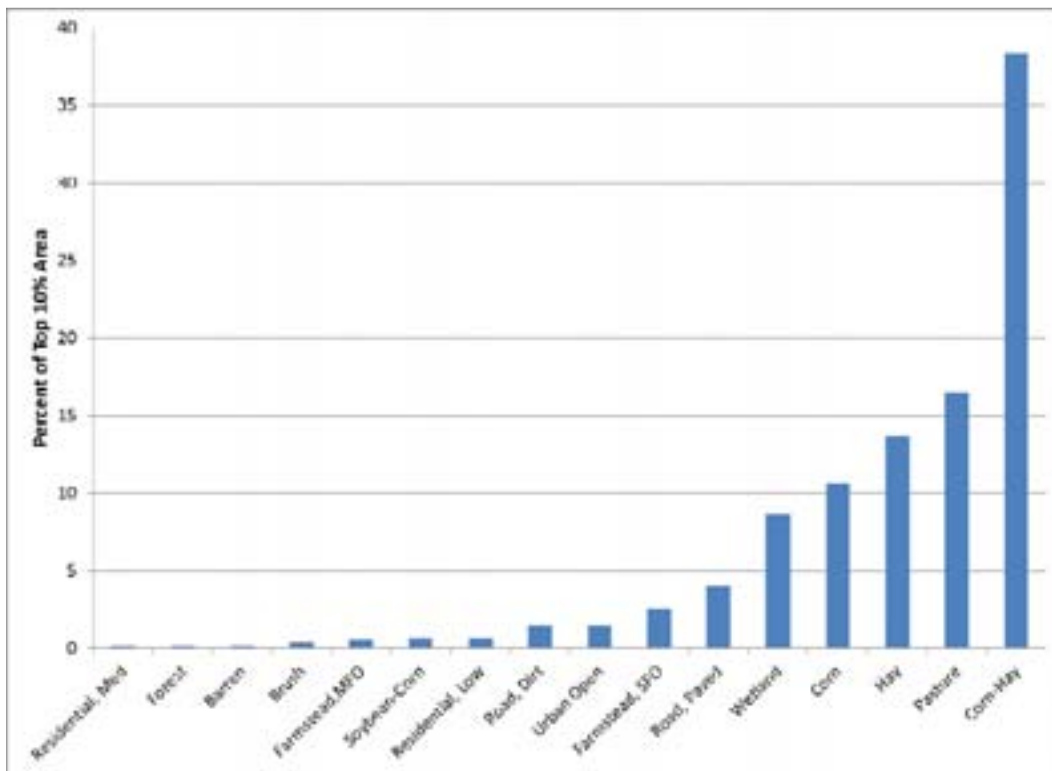
Figure 3.16: Percent of each land use within top 20% of CSAs based on average annual total P load.
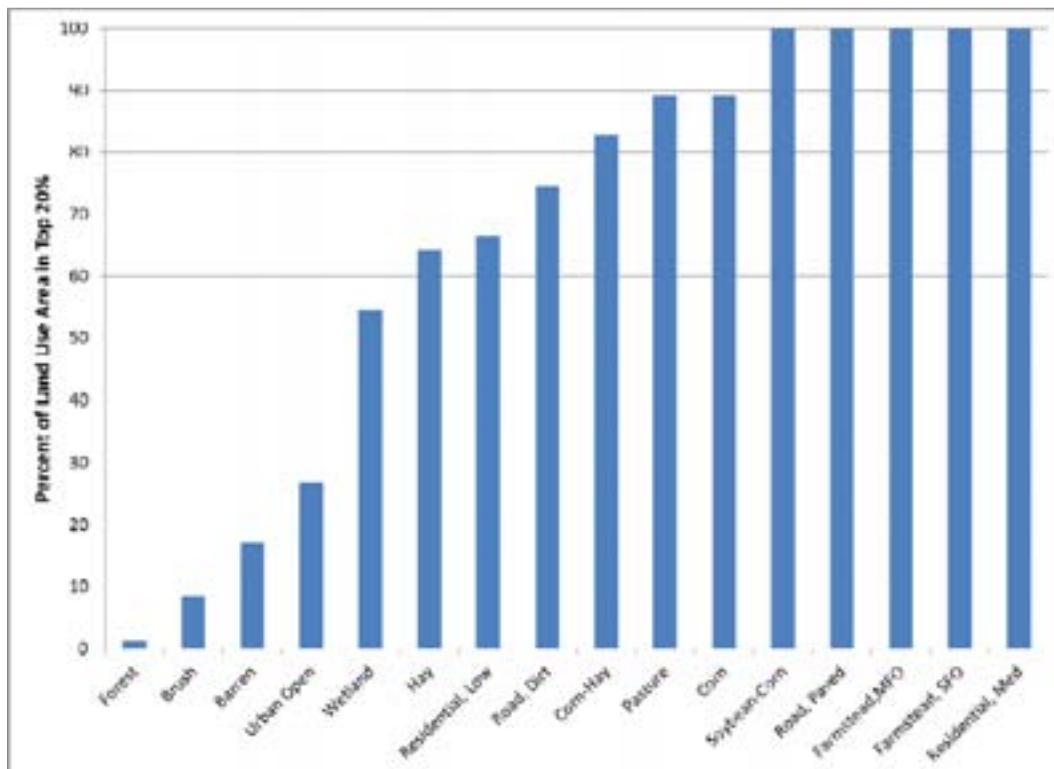
Figure 3.17: Percent of each land use within top 10% of CSAs based on average annual total P load.

STONE ENVIRONMENTAL INC
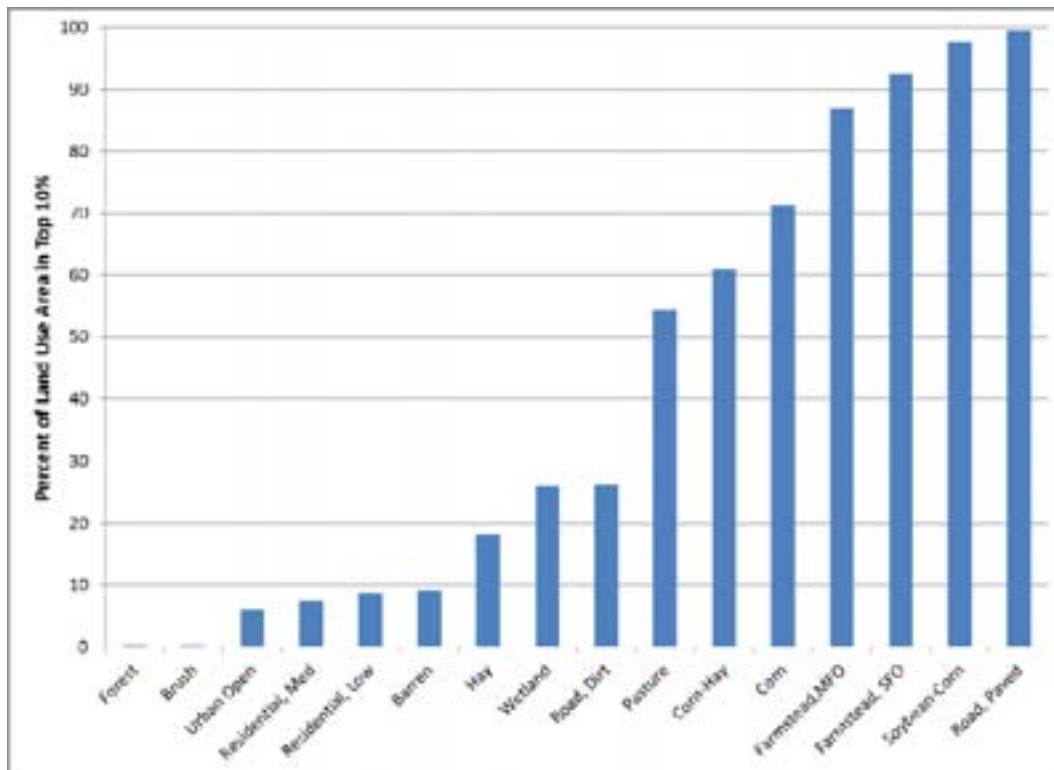
3.1.2. Sub-Watershed and Subbasin Level Results

Section 3.1.1 of this report focused on an assessment of the P loads and loading rates at the full watershed scale. The variability in P load as a function of land use and differences in soil and topographic characteristics was discussed. It is useful to consider how this variability, both between and within land use categories, can be aggregated into logical management units such as major sub-watersheds and smaller subbasins. This section will present results of the SWAT modeling at three different watershed scales: major sub-watershed, HUC-12 sub-watershed, and SWAT subbasin scales. As was done for the analysis of the full watershed level results presented in Section 3.1.1, the sub-watershed and subbasin level results were based on HRUs that fall within the Vermont sector of the MBB (the CSA assessment area).

3.1.2.1. Phosphorus Loading by Major Sub-Watershed

The Vermont sector of the study area was sub-divided into nine major sub-watersheds, defined by the outlets of the primary tributaries to the mainstem Missisquoi River and different segments of the mainstem Missisquoi River itself. The delineation of these sub-watersheds is shown in Map 3.1. Each sub-watershed has been symbolized based on its average annual total P loading rate (aggregated across all land uses within the sub-watershed). Table 3.6 summarizes the total P and sediment load and loading rates for the nine sub-watersheds.

Map 3.1 and the data in Table 3.6 show that the average annual total P loading rate across the major sub-watersheds can vary by over a factor of three, ranging from 0.25 kg/ha for the Trout River sub-watershed, up to 0.81 kg/ha in the Rock River sub-watershed. As might be expected, those watersheds with the highest fractions of agricultural land, such as the Rock, Mud, Pike, and Hungerford, have the higher total P loading rates. The more heavily forested sub-watersheds, such as the Trout, Tyler Branch, and Upper Missisquoi, have lower total P loading rates.

Table 3.6: Model-estimated average annual total P loading rate by major sub-watershed.

Sub-Watershed	Area (%)	Area (ha)	Sediment Loading Rate (ton/ha)	Total Sediment Load (ton)	Total P Loading Rate (kg/ha)	Total P Load (kg)
Rock	5.2	9,278	1.33	12,383	0.81	7,522
Mud	5.2	9,262	0.48	4,481	0.64	5,962
Pike	5.4	9,545	0.57	5,435	0.58	5,511
Hungerford	2.9	5,070	0.94	4,782	0.55	2,776
Miss Mainstem	23.5	41,641	0.69	28,760	0.48	20,087
Black	17.2	30,514	0.59	17,905	0.39	11,988
Upper Miss	20.1	35,623	0.43	15,465	0.33	11,608
Tyler	8.4	14,876	0.52	7,722	0.32	4,799
Trout	12.1	21,499	0.51	11,059	0.25	5,373
Total	100	177,307	0.61	107,992	0.43	75,626

STONE ENVIRONMENTAL INC

3.1.2.2. Phosphorus Loading by HUC-12 Sub-Watershed

The USGS 12-digit hydrologic unit code (HUC) watershed boundaries represent a standard watershed delineation that is recognized across multiple environmental agencies, making them useful management and accounting units. There are 22 HUC-12 watersheds that cover the Vermont sector of the MBB. These HUC-12 watersheds and their average annual total P loading rates are shown in Map 3.2. The total sediment and P loads and loading rates are summarized in Table 3.7. The average P loading rates vary from a minimum of 0.2 kg/ha for the Leavit Brook sub-watershed up to 0.81 kg/ha for the Rock sub-watershed. In Table 3.7, the Riviere Sutton is shown as having a higher P loading rate than the Rock; however, this is only representative of the small portion of the Sutton that is on the Vermont side of the boarder. Consideration of the entire Sutton sub-watershed (including the Québec portion) would show a considerably lower P loading rate.

Table 3.7: Model-estimated average annual total P loading rate by HUC-12 sub-watershed.

HUC12-ID	HUC12 NAME	Area (%)	Area (ha)	Sediment Loading Rate (ton/ha)	Total Sediment Load (ton)	Total P Loading Rate (kg/ha)	Total P Load (kg)
020100070101	Headwater Missisquoi River	4.7	8,384	0.37	3,126	0.24	1,974
020100070102	Snider Brook-Missisquoi River	3.3	5,835	0.42	2,459	0.31	1,794
020100070103	Mineral Spring Brook-Missisquoi River	4.9	8,754	0.39	3,420	0.31	2,733
020100070104	Mud Creek	5.2	9,262	0.48	4,481	0.64	5,962
020100070105	Jay Branch-Missisquoi River	7.2	12,770	0.51	6,480	0.40	5,144
020100070302	Leavit Brook-Riviere Missisquoi	0.9	1,559	0.24	371	0.20	305
020100070303	Riviere Sutton	0.3	448	1.71	766	0.89	400
020100070304	Lucas Brook-Missisquoi River	7.1	12,537	0.52	6,521	0.36	4,531
020100070401	Headwaters Trout River	8.3	14,794	0.53	7,909	0.25	3,687
020100070402	Trout River	3.8	6,705	0.47	3,150	0.25	1,686
020100070501	Tyler Branch	8.4	14,876	0.52	7,722	0.32	4,799
020100070502	Goodsell Brook-Missisquoi River	7.2	12,696	1.05	13,347	0.70	8,942
020100070601	Headwaters Black Creek	8.0	14,261	0.60	8,553	0.31	4,463
020100070602	Dead Creek	3.3	5,917	0.25	1,483	0.35	2,050
020100070603	Black Creek	5.8	10,339	0.76	7,881	0.53	5,481
020100070701	McGowan Brook-Missisquoi River	3.4	6,068	0.47	2,838	0.28	1,721
020100070702	Hungerford Brook	2.9	5,070	0.94	4,782	0.55	2,776
020100070703	Outlet Missisquoi River	2.3	4,045	0.62	2,492	0.42	1,700
020100081001	Pike River	4.1	7,272	0.60	4,398	0.62	4,502
020100081004	Ruiss Coslett-Riviere Aux Brochets	1.3	2,272	0.46	1,037	0.44	1,009
020100081101	Rock River	5.2	9,278	1.33	12,383	0.81	7,522
020100081102	Carman Brook-Missisquoi Bay	2.3	4,163	0.58	2,394	0.59	2,446
Total		**100.0**	**177,307**	**0.61**	**107,992**	**0.43**	**75,626**

STONE ENVIRONMENTAL INC

3.1.2.3. Phosphorus Loading by SWAT Subbasin

The MBB SWAT model includes 223 subbasins, 171 of which fall partially or completely within the Vermont sector of the watershed. The SWAT subbasins vary in size from 1 ha to 5,000 ha, with a median size of 980 ha. Evaluation of total P loading at the SWAT subbasin scale is useful for identifying concentrated regions of high P loading that may share common characteristics (such as slope or soils). The SWAT subbasins and their total P loading rates are shown in Map 3.3. Total P average annual loading rates vary from a minimum of 0.06 kg/ha to 1.67 kg/ha.

3.1.3. Phosphorus Loading by Hydrologic Response Unit

The SWAT model for the MBB was constructed in a way that maintained all of the heterogeneity in land use, soils, CTI class, and agricultural fields delineated from common land unit boundaries (CLUs). This resulted in a model with 109,811 individual HRUs, 103,666 of which represent non-water HRUs within the CSA assessment area and provides an enormous level of detail and spatial variability in landscape and P loading characteristics. Map 3.4 presents estimated average annual total P loading for each HRU in the entire CSA assessment area. The areas with the highest P loading rates, exceeding 2.0 kg/ha, are most often associated with agricultural fields and farmsteads. Areas with second highest total P loading rates between 1 and 2 kg/ha are also heavily weighted towards agricultural fields and farmsteads, but also commonly include wetlands and some developed lands. The areas with loading rates between 0.1 and 1 are associated with a wide range of land uses, including less vulnerable agricultural fields as well as more vulnerable undeveloped forest and brush areas. The areas classified as with the lowest loading rates of <0.1 kg/ha are generally low runoff producing low sloped undeveloped areas. Maps 3.5- 3.17 provide HRU-level total P loading results by major sub-watershed.

The detailed accounting of the spatial variability in P loading rates at the HRU levels allows for the identification of P critical source areas at the sub-field scale. Because agronomic management practices are uniform over an agricultural field, within-field variability in P loading tends to result from differences in soils, slope, and CTI (that influences runoff potential). Figure 3.18 shows an example of the within-field variability in total P loading rates. This field, a corn-hay rotation field, includes nine HRUs, with average annual total P loading rates varying from 0.79 kg/ha to 4.88 kg/ha. All of the soils in the field are hydrologic group C soils, however they represent three different soils series. The topographic characteristics of the different sections of the field are driving the variability in total P loads. The highest P loads of 4.88 kg/ha originate from an area with high slopes (>8%) and high CTI (class 3). An area with similarly high slopes but a much lower CTI value (class 1) is producing 3.45 kg/ha. The largest section of the field is producing 1.39 kg/ha of P, and has more moderate 4.4% slope and a class 2 CTI value.

STONE ENVIRONMENTAL INC

Figure 3.18: Example of within-field variability in total P loading rate.
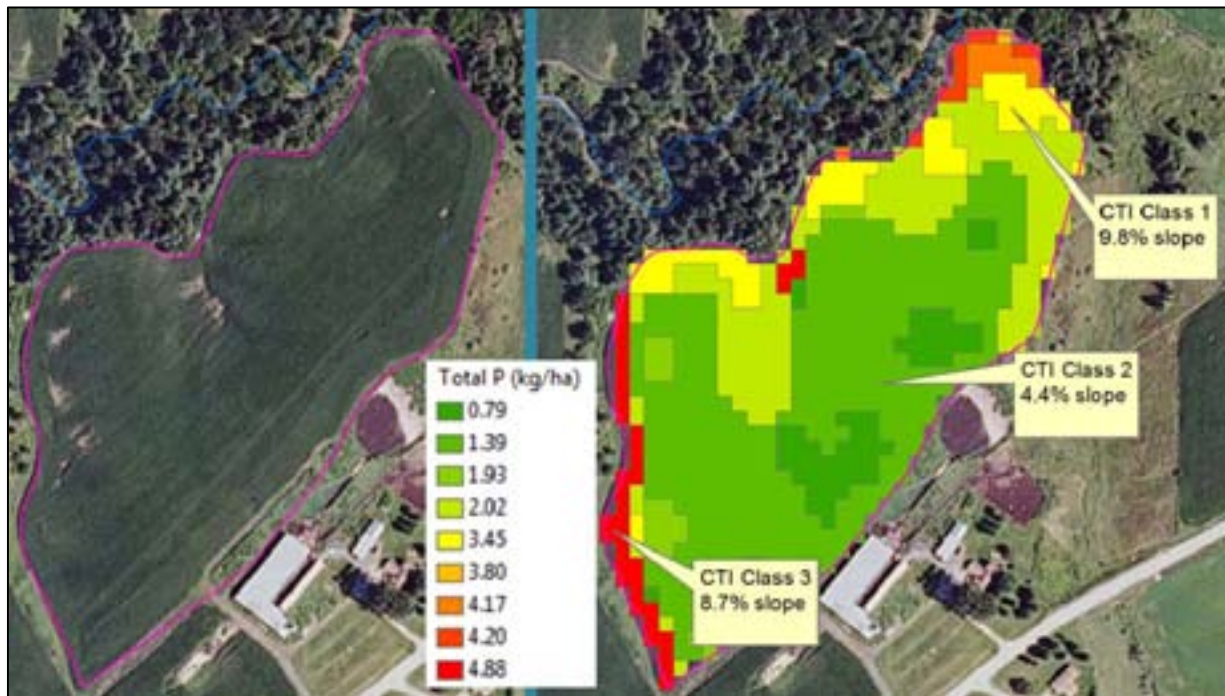
The sub-field level information such as that provided in Figure 3.18 has potential for guiding management activities needed to mitigate P losses from vulnerable sections of fields. This could include pulling specific areas of fields out of annual crop production or targeting BMPs such as vegetated waterways and buffers in specific locations. It should be noted, however, that the scale of the data inputs that went into the development of the strategic-level MBB SWAT model did not capture all the details of field characteristics that can be gathered from on the ground observations. Management decisions concerning specific fields or sections of fields will still need to be made in conjunction with on-site assessments.

3.2. Tactical Level Identification of Phosphorus Critical Source Areas

The strategic level assessment of critical source areas began by addressing broad watershed scale trends, moving into land use categories, sub-watershed characteristics, and finally HRU-level assessments of P source areas. This strategic level assessment spanned a broad range in scales, but was in all cases applied over the entire watershed (CSA assessment area). The approach chosen for strategic level assessment was designed to be able to inform the tactical level assessment. In essence, the results from the strategic level modeling could be applied in a tactical framework.

In the tactical level identification of CSAs, we will start from the highest resolution data generated during the strategic level SWAT modeling (HRU level total P loading rates) and combine that data with other high resolution datasets to define at critical source areas at a scale practical for tactical level mitigation prioritization. For agricultural areas (representative of the largest fraction of critical source areas), this practical scale will be the field level.

STONE ENVIRONMENTAL INC

3.2.1. Field Level Assessments

The SWAT model was built such that agricultural field boundaries were directly incorporated into the HRU structure. This strategy enabled the highly detailed HRU-level information (discussed in Section 3.1.3) to be aggregated to a scale more practical for targeting and prioritizing management practices. Furthermore, individual field units can be assessed by other characteristics that impact their potential as a P CSA, such as their connectivity to the channel network (this characteristic will be discussed later).

The concept of field-level assessment is applicable only to the agricultural land use classes of corn, corn-hay, hay, pasture, and soybean-corn. For these land use classes, Table 3.8 presents a comparison of the selected percentiles of total P loading rates for the population of HRUs versus the population of CLUs (fields) within each land use class. Similar systems for grouping tracts of developed areas (e.g., parcel boundaries for low and medium intensity residential land classes) and undeveloped areas (e.g., forest and brush) do not exist or would have been impractical to implement for a watershed scale SWAT assessment.

Considering the distribution of total P loading at the field level results in a general reduction in the variability in the magnitude of total P export, because it requires averaging of a range in total P export rates occurring within a field, acting to smooth out the extremes. Figure 3.19 provides a visual example of the area weighted averaging of sub-field (HRU-level) P loading over the extent of an entire field. Both the sub-field level and the field-level P export characteristics can be useful in the identification of CSAs and the design of BMPs to address those CSAs. The field level results are practical for identifying the basic agricultural management units that are generating excess P loads. The field-level results can also be used to evaluate the impacts of some field-level agronomic management alternatives, such as modified tillage and crop rotations. The sub-field level results can help to identify those sections of fields that may require special treatment (such as buffer strips or grassed waterways) in order to reduce the P export to a tolerable level. In summary, both scales of results and analysis have important functions in identifying P CSAs and determining the most appropriate mitigation strategies to address them.

The next section of this report will consider additional landscape characteristics that may be used to further classify and rank potential CSAs. The approach will focus on proximity to the channel network and will use the field-level aggregation that has been introduced in this section.

Table 3.8: Comparison of HRU versus field-level total P load distributions.

| Land Use | 10th %-ile | | 25th %-ile | | Median | | 75th %-ile | | 90th %-ile | |
	HRU-Level	CLU-Level	HRU-Level	CLU-Level	HRU-Level	CLU-Level	HRU-Level	CLU-Level	HRU-Level	CLU-Level
Corn	0.44	0.62	0.94	1.36	1.74	1.85	2.80	2.76	4.09	3.72
Corn-Hay	0.25	0.51	0.70	0.93	1.36	1.56	2.50	2.49	4.69	4.27
Hay	0.24	0.32	0.37	0.44	0.61	0.65	0.86	0.96	1.78	1.81
Pasture	0.41	0.60	0.73	0.88	1.12	1.20	1.76	1.68	2.60	2.22
Soybean-Corn	1.78	1.79	2.69	2.14	3.49	3.88	4.72	4.41	5.33	4.59

STONE ENVIRONMENTAL INC

Figure 3.19: Aggregation of HRU-level P loadings to field level.
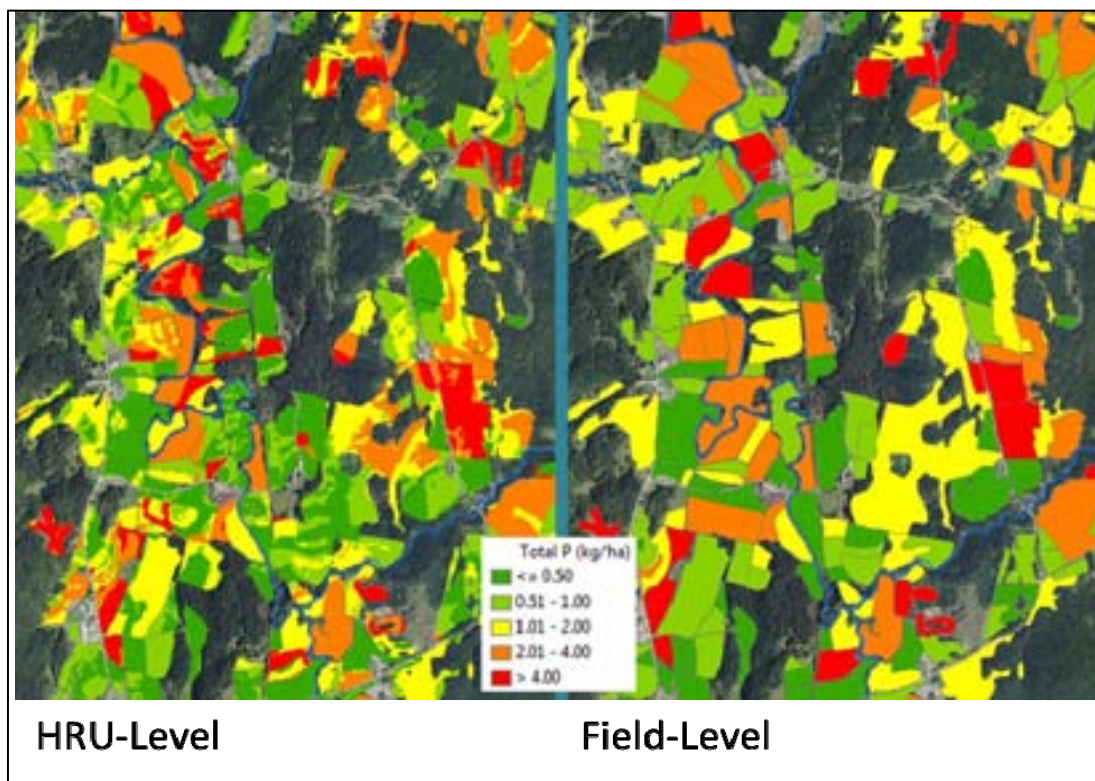
3.2.2. Prioritization of Critical Source Areas Based on Hydrologic Proximity

The SWAT model assessment provided predictions of total P loading rates for individual landscape units throughout the Vermont portion of the Missisquoi Bay watershed. The SWAT model does not explicitly recognize the proximity of each HRU to a waterbody, stream channel, or concentrated overland flow path and bases the amount of P delivered to the channel system from an HRU on the amount of runoff and sediment that the HRU produces. It is recognized that P source areas that are directly connected to the channel network will have a more significant contribution to the ultimate P load at the watershed outlet. Those sources that are further removed are likely to see P losses actually reaching the channel network mitigated by sediment deposition, overland flow infiltration, and other attenuation processes. In order to account for the importance of hydrologic connectivity in prioritizing P CSAs, we conducted an assessment of hydrologic proximity of P source areas to the hydrologic network to obtain a second metric for ranking P CSAs. This proximity metric was then combined with the total P loading rate metric to arrive at a more refined CSA prioritization.

3.2.2.1. The Enhanced Hydrologic Network

The development of an enhanced hydrologic network dataset developed from 2009-2010 high resolution LiDAR for approximately 91% of the Vermont side of the Missisquoi Bay was described in Section 2.3. The high resolution DEMs derived from these datasets (1.6 m cell size) enabled the development of an enhanced hydrologic network representative of the minor stream tributaries, ditches, gullies, and concentrated overland flow paths that connect to the primary stream systems in the watershed. These new hydrologic features connect directly to the existing Vermont Hydrography Dataset stream network. The resulting channel density is very

STONE ENVIRONMENTAL INC

high, and in some cases, the features would be better characterized as concentrated flow paths. A concentrated flow path may not have a well-defined channel, however, the high resolution topography indicates that surface runoff will focus in these areas, resulting in concentrated overland flow during significant storm events.

The enhanced hydrologic network is shown at three different scales in Maps 3.18 – 3.20. Map 3.18 shows the entire extent of the Vermont sector of the MBB. The enhanced hydrologic network has a combined length of all features of approximately 8,640 km. This compares to a combined length of 664 km for the VHD stream network. Map 3.19 shows a focused view of the Hungerford Brook sub-watershed, with the VHD stream network in the background for comparison. Map 3.20 shows a much more localized area within the Rock River sub-watershed. With the aerial imagery in the background, it is evident how the enhanced hydrologic network features have captured some of the ditches and low paths along roads and through the agricultural fields shown in the image. These areas represent the more critical sections of the fields that have greater potential for sediment and P transport. The quantification of proximity to the hydrologic network and its use in prioritizing P CSAs will be discussed in the sections that follow.

3.2.2.2. Development of a Spatially Distributed Hydrologic Proximity Ranking

Based on the flow paths identified in the enhanced hydrologic network, the overland hydrologic travel distance from any point in the watershed to the nearest location on the hydrologic flow network can be calculated. This distance was calculated for the entire extent of the hydrologic network (covering the CSA assessment area). This dataset is equivalent to the shortest overland flow distance to the nearest water body, stream, channel, or concentrated flow path. This hydrologic proximity dataset is shown in Map 3.21.

The approach taken to ranking locations on the landscape based on their proximity to the hydrologic network was to assign the ranking based on the proximity relative to the distribution of proximities within the watershed. This was accomplished by calculating the cumulative distribution of proximities and determining the associated percentiles those proximities represent. The resulting datasets has values ranging from 0 to 1, where a value of 0 indicates the most distant points from the network, a value of 1 indicates the closest points to the network, and a value of 0.5 indicates points with the median distance to the network. The hydrologic proximity percentile dataset is shown in Map 3.22. This map looks very similar to the flow path distance dataset shown in Map 3.21, only the values have been constrained to fall between 0 and 1. The hydrologic proximity percentile dataset will be used to characterize individual HRUs and CLUs, and will serve as an input to a CSA ranking based on a combination of hydrologic proximity and total P loading rate.

3.2.2.3. Development of a Spatially Distributed Total P Loading Ranking

The average annual total P loading rate has already been presented as the primary indicator for identifying critical source areas. The SWAT model predictions of total P loading rates at the HRU level were presented in Section 3.1.3 and Maps 3.4 – 3.17. We have also presented the cumulative distribution of total P loading rates across the entire Vermont sector of the MBB (Section 3.1.1). From this cumulative distribution, we calculated the percentile that each loading represents as a means for ranking each P source area on a scale from 0 to 1; this dataset is shown in Map 3.23.

The dataset of total P loading percentile is analogous to the hydrologic proximity percentile dataset described in the previous section. Both datasets are scaled from 0 to 1 with a uniform distribution of values between the two extremes. In addition, for both datasets, a value of 0 corresponds to the least critical areas and a value of 1

STONE ENVIRONMENTAL INC

corresponds to the most critical areas. This scaling similarity will allow these two metrics to be combined into a single index form with which to rank CSAs.

3.2.2.4. Combined Total P Loading and Hydrologic Proximity Ranking

A ranking based on weighting the relative importance of model-estimated total P loading rate and the proximity of landscape locations to the hydrologic network was applied to all areas within the CSA assessment area using the total P loading and hydrologic proximity percentile datasets.

The relative importance of total P loading rate versus proximity to the hydrologic network was determined through an interactive process of testing the outcomes of assigning different weights to the two metrics. The weightings tested were as follows: 1.) equal weighting, 2.) total P loading rate weighted 2 * proximity, 3.) total P loading rate weighted 3* proximity. Although equal weighting was considered, it was quickly dismissed as we believed that P loading rate is a more important factor in CSA determination. The second two weighting options considered were applied over the entire watershed area and compared with the original total P and hydrologic proximity ranking datasets. Figure 3.20 shows an example of this comparison for a small area of the watershed. Agricultural field boundaries are shown in orange on the maps. The differences in the percentile rankings are obvious when comparing the purely total P and the proximity rankings. In reviewing both of the weighted ranking approaches, the influence that the proximity component has on the overall ranking is also very evident. The generally uniform ranking class that is common over broad areas in the total P ranking (which is largely driven by land use and soils) now shows greater variability due to the differences in hydrologic proximity. Although the differences between the two weighted ranking approaches is subtle, based on our own experience and professional judgment, the ranking approach selected was the one that weights total P loading at 3* the importance of proximity to the hydrologic network.

Map 3.24 shows the final weighted ranking of P CSAs over the entire Vermont sector of the MBB using the 3* weighting scheme. A few characteristics of this map should be noted. First, the hydrologic proximity component is clearly apparent in the rankings, even though it was not weighted as heavily as the total P component. In addition, some undeveloped areas (forest and brush) show up rather high in the rankings. These are typically higher elevation, high precipitation areas with shallow soils on steeper slopes that have a high organic matter content. The hydrologic proximity ranking component is partly a function of the local density of the hydrologic network. As was discussed earlier in Section 2.3, lower resolution elevation datasets were used in some portions of the study area; namely the eastern portion of the study area near Mud Creek. This had some level of impact on the final network density that could be reasonably developed in these areas. Finally, areas with a heavy predominance of agriculture, such as the Rock, Hungerford, lower Black, and Mud sub-watersheds, still stand out as having high concentrations of critical source areas.

STONE ENVIRONMENTAL INC

Figure 3.20: Comparison of CSA rankings approaches.

STONE ENVIRONMENTAL INC

Lake Champlain Basin Program / Identification of Critical Source Areas of Phosphorus Within the Vermont Sector of the Missisquoi Bay Basin / December 15, 2011   106
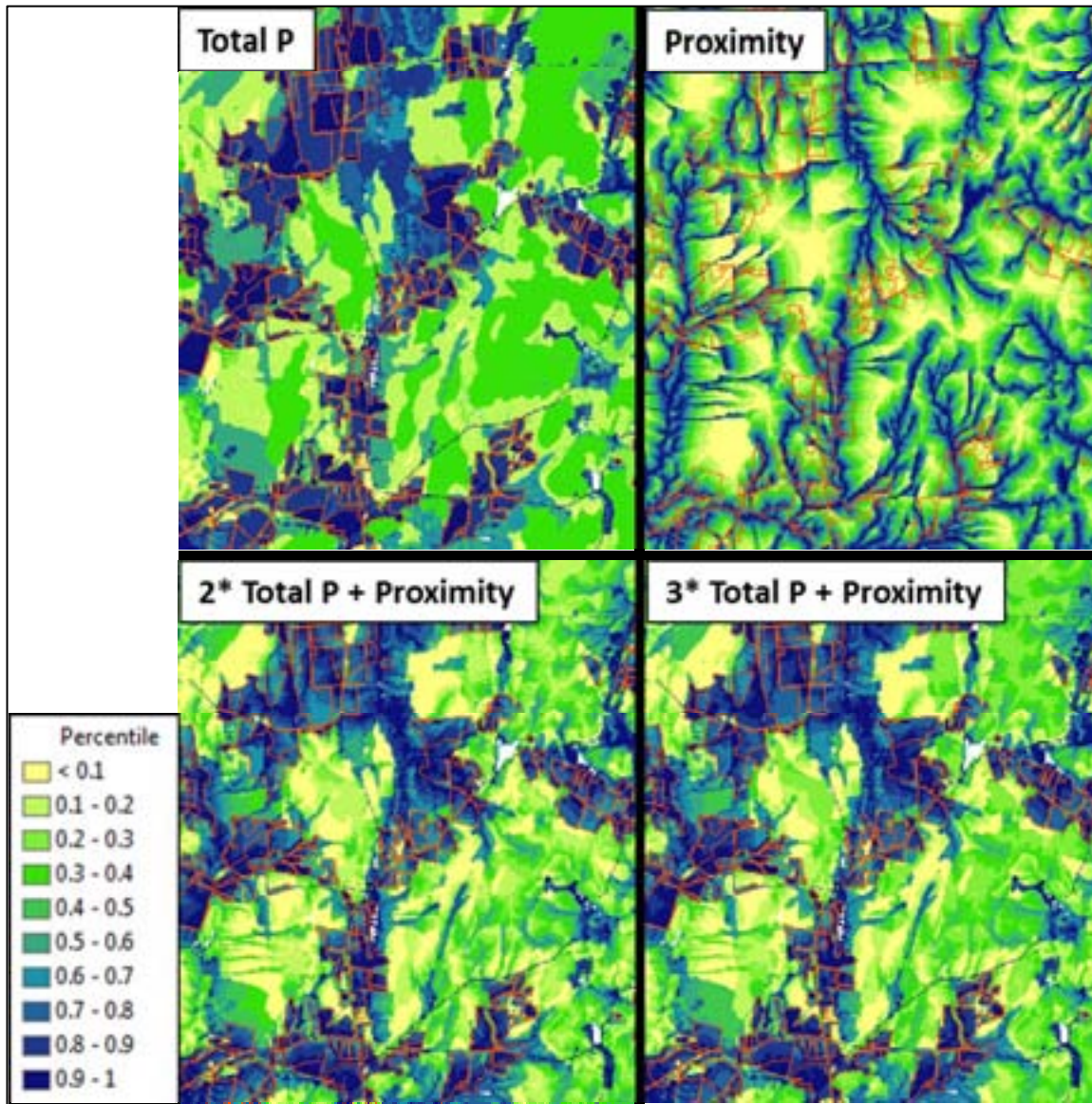
3.2.2.5. Use of the Weighted Ranking Dataset in Prioritizing CSAs

The CSA ranking datasets that have been developed (including both the purely total P and the weighted ranking) have been created as a 10-m raster dataset. This results in every pixel having a slightly different ranking. This level of information is useful for narrowing focus on specific areas that warrant treatment or additional field level assessment. Another use of this datasets is as the foundation for evaluating and prioritizing CSAs within individual or groups of land use classes.

As an example, if developed land uses are of interest, the land cover dataset used in the development of the SWAT model can be used to extract the weighted CSA ranking for only the developed land use classes. Once extracted, the weighted CSA ranking values for these developed areas can be isolated, readily allowing identification of the highest priority areas. This is shown for the area surrounding Swanton and Highgate in Figure 3.21. The values of the weighted ranking metric have been classified into five quantiles, providing a means for identifying the areas falling within the top 20% of critical developed land use areas based on the model-estimated P export and proximity to the hydrologic network. This approach can be applied to additional land use classes or groups of classes with a few standard ArcGIS operations.

Figure 3.21: Identification of highest ranking CSAs for developed land uses.
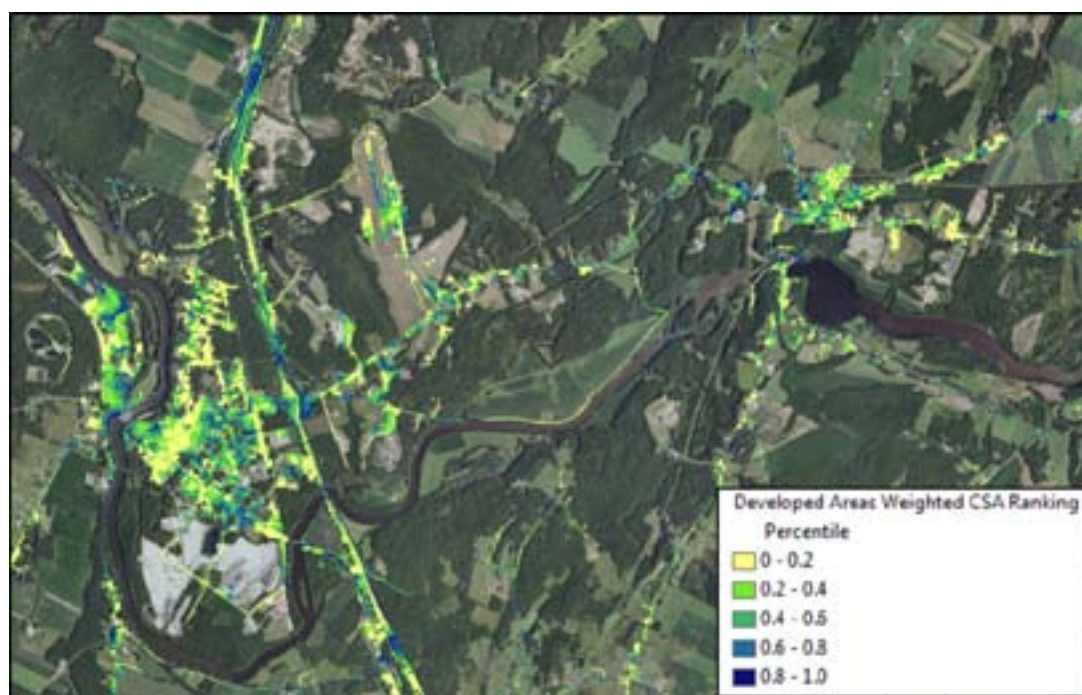
For agricultural land uses, we have the benefit of delineated field boundaries (CLUs) that can be used to aggregate CSA rankings to the field level. This concept was already discussed in the context of estimating total P export at the field level. The aggregation of the weighted CSA ranking to fields was conducted by first calculating the mean total P export and mean proximity to the hydrologic network for each field. Then, each field was independently assigned a percentile representative of its total P ranking and hydrologic proximity ranking. Finally, the weighted ranking was calculated for each CLU (total P with three times the weight of hydrologic proximity), and the final result converted back into percentiles. As result, each field has been

STONE ENVIRONMENTAL INC

assigned a ranking (percentile) according to its total P loading, according to its hydrologic proximity, and according to the weighted total P and proximity ranking. The ranking for each field has been normalized so that the ranking is relative to the agricultural fields only (comprised of corn, corn-hay, hay, pasture, and soybean-corn).

A comparison of the total P percentile ranking versus the weighted total P/hydrologic proximity percentile ranking is shown for a section of the Black Creek watershed in Map 3.25. Clearly, there is some correlation between the two approaches; however, some fields have moved up or down in their ranking on the basis of their hydrologic proximity. The weighted ranking metric maintains much of the information that the SWAT model predictions produced, while providing an added level of refinement not captured by the model. The dataset of field level rankings that has been developed allows future users of this dataset to prioritize CSAs based on the metric that is most suited the intended mitigation strategies (total P, hydrologic proximity, or the weighted ranking). It is our recommendation that metric based on combining model-estimated total P export and proximity to the hydrologic network be considered first for most applications.

3.2.3. Field Verification of Critical Source Areas

3.2.3.1. Objectives and Approach

To help verify model results, we made site visits to specific fields in the MBB that the model analysis had identified as among the highest and lowest ranked CSAs. These visits were made with a highly experienced Resource Conservationist (RC) from the Vermont State Office of USDA-NRCS. At each site, the RC visually evaluated the site based on current land use, land use used in the modeling analysis, soil type and hydrologic soil group, topography, proximity to surface water or drainage, up-gradient contributing area, and other factors he typically used in evaluating the conservation needs of a site. The RC was not informed of model results (e.g., CSA ranking) until after he had rendered his evaluation.

3.2.3.2. Selection of Sites

Sites were randomly selected from among the highest 10% and lowest 10% of CSA-ranked fields based on total P loading rate and proximity to the hydrologic network. Additional criteria included location within Franklin County and proximity to a public road so that the field could be viewed without entering the property. A location map with land use and soils data was produced for each of 36 potential sites. The spatial distribution of these sites is shown in Map 3.26.

3.2.3.3. Field Results

A total of 19 of these sites were visited and rated on October 4, 2011. Due to the late spring planting date, none of the corn on the selected fields had been harvested at the time of the visit. Results of the field verification are summarized in Table 3.9. In general, there was excellent agreement between our CSA ratings and the risk ratings of the RC. Field and model assessments agreed for all of the ten high-ranked CSA sites. Of the nine low ranked sites, the RC rated one (#1680) field as moderate risk, compared to the model ranking of low, primarily focusing on the portion of the field that was made up of hydrologic group C soils and therefore prone to runoff. On one additional field (#4501), the RC rated the site as high, while the model had ranked it low. This discrepancy was undoubtedly due to the fact that the field had been modeled as permanent hay land, while the field was actually in corn at the time of the visit.

In general, the field evaluations conducted by an experienced NRCS professional agreed very well with the model ratings, giving an additional level of confidence in the model analysis.

STONE ENVIRONMENTAL INC

Table 3.9. Results of field verification site visits with NRCS Resource Conservationist.

Field #	Location	Model LU	Actual LU	HSG	R.S. Evaluation	RC rating	Our rating
2283	Fairfield	C-H	Hay	C/D	5-20% slopes, surface water on both sides. Confirms rotational status from past observation. C and D soils suggest high runoff potential, especially if fall spreading and tillage	High	High
2952	Fairfield	C-H	Hay	C/D	Top of field near road is ~flat; back side slopes to streams. When in corn, some parts of field would be in up & down slope rows. Some sections of field are low, others very high runoff potential, especially if in corn	High	High
1724	Fairfield	C-H	Hay	C/D	Steep slopes, surface water on two sides at bottom of slopes. Field topography funnels water directly to stream. Field is not suitable for cross-slope farming	High	High
1195	Fairfield	C-H	Corn	D/C	~6% slopes, some drainage area contributing from above. Everything would flow to ditch; no buffer	High	High
1478	Fairfield	C-H	Hay	D/C	8-10% slopes; watercourse at bottom. Significant runoff especially if in corn.	High	High
1028	Fairfield	C-H	Corn	D	Substantial runoff expected from area to the North; stream/ditch at South edge of field	High	High
4860	Highgate	C-H	Corn	C/B/D	Steeply sloped in places; some areas have rows planted up & down on >10% slopes. Drains to brook.	High	High
1947	Highgate	C-H	Hay	C	>12% slopes, down to ditch/stream	High	High
621	Highgate	C-H	Hay	C	Very steep slopes toward stream	High	High
5695	Highgate	Soy-C	Soy?	D/C	Currently in poor/failed soybean crop or fallow. ~3% slope, drainage from above may be diverted. Surface water at bottom of slope.	Med. High	High
7194	Highgate	C-H	Corn	D/B/C	8-10% slope, drainage at bottom. Some corn planted up & down. All runoff to stream	High	High
2205	St. Albans	Hay	Hay	B/A	No surface runoff nearby; diversion berm to the West reduces slope length and contributing area. Predominantly B soils. Little potential for runoff, sediment, P	Low	Low
2374	St. Albans	Hay	Hay	C	~3-4% slopes and moderate ditching. Mostly C soils, higher runoff potential. Intermittent streams nearby; water can move to ditches on either side of field	Low	Low
1680	Fairfield	Hay	Hay	C/A	High slopes and close to water, but short slope-lengths. Assume stone wall/hedgerow at edge of up-gradient forest land diverts flow from above. Has no doubt that there could be manure runoff, at least from C soils portion of field	Moderate	Low
647	Bakersfield	Hay	Hay	A	Small drainage area contributing; no obvious streams or watercourses.	Low	Low
1905	Highgate	CHNC	Hay/Res	A	Flat, essentially no contributing watershed	Low	Low

STONE ENVIRONMENTAL INC

Field #	Location	Model LU	Actual LU	HSG	R.S. Evaluation	RC rating	Our rating
4501	Highgate	Hay	Corn	C/D	~4-5% slopes, lots of ditches/channels. Close to Missisquoi River	High	Low
3422	Fairfield	Hay	Hay	C/A	Flat, <2% slopes, no up-gradient watershed, no watercourses nearby	Low	Low
1424	Fairfax	Hay	Idle	C	Currently idle/old field succession. 3-4% slopes, no nearby water, drains to corn field	Low	Low
1024	Fairfax	Hay	Hay	C/D	Rolling topography, 8-10% slopes in places. No water in close proximity. Most drainage would be toward road, no obvious outlet	Low	Low

3.2.4. Farmsteads as Potential Critical Source Areas

The farmsteads identified by NRCS (Sims 2007) and delineated by Stone for this study comprise 0.34% of the non-water area on the Vermont side of the MBB and account for 0.23% of the total MBB study area. There are no data available at the basin-scale regarding the composition of farmsteads; however, the farmstead polygons delineated by Stone typically include farm houses, barns and milking parlors, barnyards, feed bunks, manure pits, and driveways.

Figure 3.22. Heavy use area in Fairfield.

3.2.4.1. Limitations to Farmstead Assessment at the Watershed Scale

Lacking specific data about each farmstead in the MBB, several assumptions were necessary to parameterize the model, as discussed in the Section 2.4 of this report. These assumptions included the fraction of a typical farmstead that is impervious and the rate of P additions to pervious areas in the form of manure. These assumptions were applied uniformly to farmstead areas across the MBB.

STONE ENVIRONMENTAL INC

To summarize the modeling approach, farmstead impervious areas, including roofs, driveways, and feed bunks, were treated in the same manner as impervious commercial land. Runoff production from pervious areas, consisting of barnyards, cow paths, lawns, and other vegetated areas, was modeled using the curve number method. A constant rate of phosphorus addition on pervious areas was assumed to account for manure deposition. Because the total farmstead area represents at most a small fraction of the total watershed area at any stream gage and sampling station in the MBB, no specific calibration of farmstead P loadings was possible as part of the strategic level analysis.

The assumptions regarding runoff production by farmstead pervious areas and significant P accumulation in soils due to manure deposition are supported by the available literature. Unfortunately, P export rates from farmstead areas have not been extensively characterized, as noted by Hively et al. (2005) in one of the few recent publications on the subject:

> *"Although controls on P losses in overland flow from agricultural fields are now generally understood, some important challenges remain. In particular, the relative importance of P contributions from non-field areas such as barnyards, stream crossings, and cow paths is poorly understood, especially with respect to seasonal differences in the hydrological cycle."*

The available literature offers a great range in P export rates among the farmsteads studied. Although they may comprise a small fraction of a watershed, farmsteads have been estimated to contribute a substantial percentage of total P export in certain watersheds. A review of recent research on P runoff from barnyards or other heavy use areas suggests that barnyards represent significant potential critical source areas, and that to understand the significance of individual farmsteads requires site specific assessments of highly localized P source areas. Although this was simply not practical at the strategic level, a site-specific assessment was completed as part of the tactical modeling work described in Section 3.3 below.

3.2.4.2. Magnitude of Phosphorus Losses in Farmstead Runoff

The Cannonsville Reservoir in the Catskill Mountain region of New York has been a focus of agricultural runoff research for many years. Brown et al. (1989) measured P concentrations in runoff from two barnyards in the watershed over a three-year period, finding total P concentrations ranging from 7 – 30 mg/L and dissolved P ranging from 2 – 15 mg/L. While the monitored flow was referred to as barnyard runoff, the authors note that "the total watershed of a barnyard typically includes the barn roof, paved surfaces, and wastewater disposal systems, in addition to upland drainage." Therefore, the monitored drainage areas may be more or less comparable in use intensity to the farmsteads defined in the present study and the P data provides a useful reference.

Hively et al. (2005) used a rainfall simulator (rainfall rate = 3.8 mm in 30 minutes) to generate runoff from several types of non-field areas on a dairy farm in the Cannnonsville Reservoir watershed. In 30-minute flow composites of runoff from a heifer barnyard, the authors found average concentrations of total P of 13.16 mg/L, total dissolved P of 11.60 mg/L, and total suspended solids of 375 mg/L. Morgan's soil test P was exceedingly high in both runoff plots tested, 1344 mg/kg and 2020 mg/kg. A monitored cow path with Morgan's soil test P of 8.8 mg/kg and 4.6 mg/kg in replicate plots generated runoff quickly, within 8 minutes, and had moderately high concentrations of total P (0.99 mg/L), total dissolved P (0.18 mg/L), and total suspended solids (540 mg/L). The authors developed a predictive equation relating total dissolved P runoff to soil test P by extraction in Morgan's solution: TDP (mg/L) = 0.0056 + 0.0180 x Morgan's STP (mg/kg) (R2 =

STONE ENVIRONMENT INC

84%). For manured areas with excessively high soil test P, Hively et al. (2006) derived a second relationship: TDP (mg/L) = 0.4735+0.0065 x Morgan's STP (mg/kg) (R2 = 84%).

Hively et al. (2006) concluded that "overland-flow from heavily-manured impervious source areas, including barnyards, roadways, and cowpaths, can play a significant role in delivering water and TDP to the stream, particularly during dry summer periods when the extent of saturated soils is small." Using the earlier work in this watershed by Brown et al. (1989), Gitau et al. (2008) used SWAT to simulate average dissolved P and total P concentrations in barnyard runoff of 4.1 mg/L and 16.1 mg/L, respectively.

Hill and others (2000) measured average total dissolved P concentrations in barnyard runoff of 14.2 mg/L. This very high average concentration is comparable to concentrations reported in Hively et al. (2005).

In Vermont, Schellinger and Clausen (1992) measured P concentrations and loads in barnyard runoff entering a filter strip on a 110-animal dairy farm in Charlotte from December 1984 to May 1986. Roof runoff was diverted away from barnyard and filter strip. The authors found exceedingly high total P concentrations in runoff, averaging 20.01 mg/L over 87 events. The majority of the total P was dissolved; the average total dissolved P concentration was 17.64 mg/L over 31 events and the average orthophosphate concentration was 16.17 mg/L over 52 events. Based on the defined area of the barnyard, the total P export measured by Schellinger and Clausen was correspondingly high: 0.174 kg/m^2/yr or 1,740 kg/ha/yr. The authors found that the filter strip was overloaded and was not particularly effective as a P treatment practice, with only 12 percent of the total P mass retained.

In the 1990s, USGS performed a long-term study in the Otter Creek and Halfway Prairie Creek watersheds in southeast Wisconsin (Stuntebeck 1995). Monitoring was conducted upstream and downstream of farmsteads in both watersheds, bracketing runoff inputs from two farmsteads that had been identified as potentially critical nonpoint sources based on herd size, lot size, and proximity to the stream. Because these farmsteads had been selected because of their presumed high pollution potential, the data may not be representative of typical conditions in Wisconsin (or Vermont). Upstream and downstream monitoring showed large, significant increases at the downstream station in event mean concentrations of total P, ammonia, and BOD, despite imperceptible changes in flow. The authors found that a 0.7 acre farmstead in the Otter Creek watershed exported 2.4-115.6 kg/ha of total P per event over 12 storms (Stuntebeck, personal communication August 12, 2011). Total P export from the 1.8 acre farmstead in the Halfway Prairie Creek watershed ranged from 2.08-19.73 kg/ha per event over 11 storms.

Using data from the Otter Creek watershed monitoring program in calibration, USGS (1998) compared sediment and P runoff predictions generated by two barnyard runoff models, BARNY and WINHUSLE . USGS calculated that the proportion of the watershed total P load attributable to farmsteads in three study areas was between 24 and 76 percent. In these small study areas, farmsteads are clearly a dominant source of total P.

3.3. Tactical Level CSA Identification, Farm Scale

3.3.1. Objectives and Approach

In additional to the strategic-level assessment, a farm-specific model was developed that was capable of identifying CSAs at the level necessary to determine individual management measures that could be expected to have the greatest success in reducing P loads. The data needed to populate such a model include actual soil-

STONE ENVIRONMENTAL INC

test P, manure/fertilizer application rates, nutrient management plans, cropping patterns, design and management of barnyard areas.

The Agricultural Policy Environmental Extender Model (APEX) model was used to identify farm-scale CSAs and to evaluate BMPs specifically targeted to the characteristics of the farm operation. Farm-scale modeling was able to emphasize proximity to surface waters with a level of detail permitted only by a small-scale approach, and includes explicit representation of the barnyard, manure storage area, micro-channels and ditches, tile drains, vegetated filter strips and riparian buffers that was not possible at the strategic level due to lack of site-specific information.

3.3.2. Site Selection

Although the results of the farm-scale modeling are site-specific, an effort was made to select a farm with characteristics representative of other farms in the basin. Particular emphasis was placed on finding a willing farmer that cultivated a mix of silage corn and hay. It was also important that several years of accurate agronomic records that could be used to support model development would be available. A conventional dairy operation in Franklin County with approximately 100 mature animals was selected. A map showing the farm configuration along with several of the BMPs that have already been established is shown in Figure 3.23.

Figure 3.23. Farm site selected for tactical analysis modeling.

STONE ENVIRONMENTAL INC
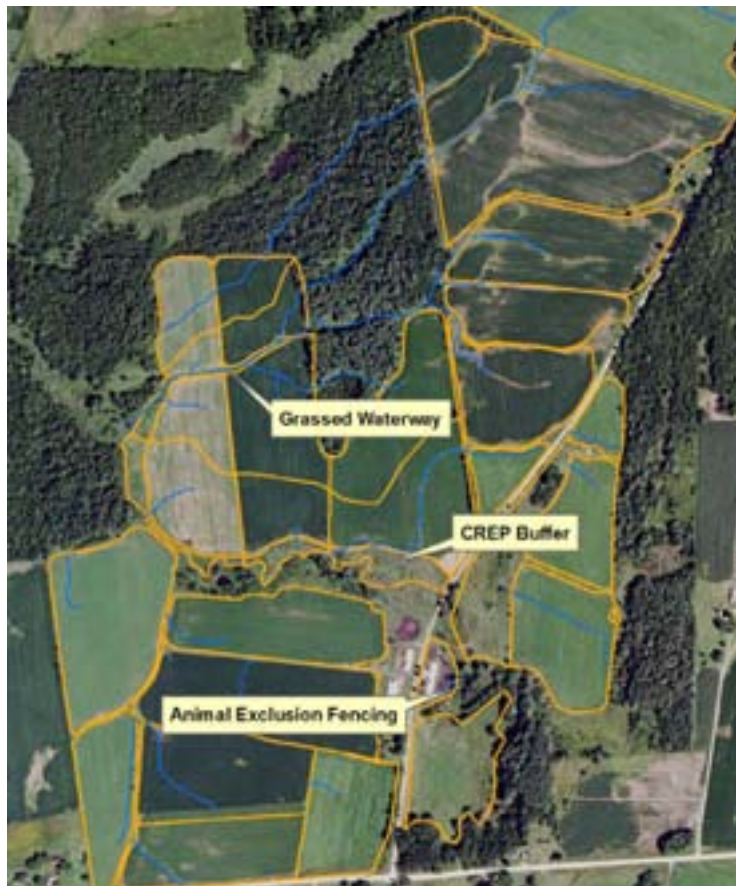
3.3.3. Data Collection

Five years of actual crop data were collected, including planting and harvest dates, manure and fertilizer application rates and timing, as well as estimated crop yields. This data, a summary of which is shown in Table 3.10, was compiled from informal farm records, and then reviewed and verified by the farmer. In addition, the farm had worked with a consultant in 2009 to prepare a nutrient management plan consistent with NRCS' 590 standard. A copy of the plan was obtained from the farmer, which included information on soil-test P levels and manure quality that was used to inform the farm-scale model.

In addition to the cropping system, information was collected related to management practices currently employed on the farm. These include: cover cropping, grassed waterways, reinforced animal walkways, animal exclusion fencing, and riparian buffers.

Table 3.10. Historical crop rotations of tactical analysis farm, 2005 - 2009.

Field	Area (acres)	2006	2007	2008	2009	2010
B1	21.4	hay	hay	hay	hay	hay
B2	29.5	corn-silage	corn-silage	corn-silage	corn-silage	corn-silage
B3	14.3	corn-silage	corn-silage	corn-silage	corn-silage	corn-silage
B6	10.7	corn-silage	corn-silage	corn-silage	corn-silage	corn-silage
B12	15.4	hay	hay	hay	hay	hay
H1	12.6	corn-silage	hay	hay	hay	hay
H2	5.7	corn-silage	hay	hay	hay	hay
H3	8.8	hay	corn-silage	corn-grain	corn-grain	soy
H4	8.5	hay	hay	soy	corn-grain	soy
H5	6.7	hay	hay	hay	hay	hay
H6A	9.5	hay	hay	corn-grain	soy	corn-grain
H6B	12.1	hay	corn-grain	soy	corn-grain	soy
H7AN	5.4	hay	hay	hay	corn-silage	corn-grain
H7AS	11.9	hay	hay	hay	corn-silage	corn-grain
H7BN	4.5	corn-grain	corn-grain	corn-silage	hay	hay
H7BS	9.8	corn-grain	corn-grain	corn-silage	hay	hay
H8	16.2	hay	hay	corn-silage	soy	corn-silage
	total hay	115.9	113.3	79.1	76.1	76.1
	total soy	0.0	0.0	20.6	25.7	29.4
	total corn-silage	72.8	63.3	85.0	71.8	70.7
	total corn-grain	14.3	26.4	18.3	29.4	26.8

STONE ENVIRONMENTAL INC

3.3.4. Management Scenarios and Practices Simulated

The farmer installed a range of management practices over the past 20 years, although the majority of them were implemented within the past five years. In discussing the value of farm-scale modeling with the farmer, it became apparent the value in not only looking forward to estimate the effectiveness of a suite of potential practices, but also in looking back and estimating the pollutant reductions achieved through past practice implementation. Specifically, the farmer enrolled a considerable amount of riparian land in the CREP (conservation reserve enhancement program) in 2009, and was very interested in understanding the value of that action in terms of P abatement.

3.3.4.1. Past and Current Practices

The farmer employs field-specific cropping systems on the approximately 200 acres he owns or operates. These include: 50 acres in hay-corn rotation (five years of each); 44 acres in permanent hay; 55 acres in permanent corn. Approximately 25% of the corn acres planted each year is grain corn, with the balance planted in corn silage. Since 2008, the farmer has transitioned the remaining 51 acres from a hay-corn rotation to one that also includes soy. Prior to introducing soy into the rotation, the farmer was harvesting 110-120 acres of hay and 80-90 acres of corn annually. Currently, the farmer harvests 75-80 acres of hay, 20-30 acres of soy, and, 90-100 acres of corn annually. In addition to utilizing a crop rotation system, for the past five years the farmer has planted a cover crop of winter rye on all of the corn silage acres each year. The farm-specific APEX model assumed a crop rotation fashioned after that which the farmer has employed since 2008, including a mix of hay, silage and grain corn, and soy.

The barnyard and cropland is situated adjacent to a second-order stream. Several minor tributaries (both intermittent and perennial) to this stream flow through the cropland and join this stream, many of which have been actively managed via ditching and straightening. Many years ago the farmer installed a grassed waterway on a key intermittent flow path. APEX was used to simulate the water quality benefits of the grassed waterway.

Cropping activities, including manure and fertilizer application, historically extended to top of bank. In addition, animals in the barnyard historically had unfettered access to the stream. In 2009, the farmer enrolled several acres in the Conservation Reserve Enhancement Program (CREP), creating naturally vegetated buffers of at least 35 feet along the entire length of the second-order stream as it passes through his property. In addition to the vegetated buffer, animal exclusion fencing and reinforced animal walkways were installed in the barnyard. APEX was used to simulate phosphorus and sediment loads from the farm both before and after the vegetative buffer and fencing were installed.

3.3.4.2. Future Conditions

The APEX model was also used to predict the anticipated water quality benefits associated with three changes to the farm operation. These are:

- Altering the cropping system for the fields in permanent corn to a corn-hay rotation (three years of corn followed by two years of hay);

- Employing contour farming on select fields; and,

- Relocating the barnyard away from the second-order to stream to a location more than 500 feet from the nearest surface water.

STONE ENVIRONMENTAL INC

3.3.5. APEX Model Development

The APEX Model (Williams et al. 2008) is a farm/small watershed scale model designed to simulate a wide range of farm management and conservation practices. APEX has similarities to SWAT in that both models split up a study area into areas with homogeneous land use, soils, and slope characteristics; both are designed for the evaluation of the long term effects of agricultural activities on the environment; and both can be used to evaluate environmental quality metrics at the field or HRU area or at the aggregation of many fields or HRUs, such as a watershed outlet. From a practical perspective, SWAT is better suited for simulating large watersheds because of the efficiencies offered by the HRU concept, allowing similar landscape units in different parts of a watershed to be simulated as a single unit. APEX offers several characteristics that make it strongly suited for conservation planning at the farm and field scales. Unlike SWAT, that does not spatially represent the connectivity between HRUs, APEX routes water, sediment, and nutrients via overland flow and concentrated\channel flow from one "subarea" (an APEX HRU) to another. This routing allows for the explicit simulation of features like vegetated waterways, buffer strips, and the connectivity between heavy animal use areas, vegetated areas, and streams. In addition, APEX offers capabilities beyond what SWAT provides in terms simulating complex agronomic systems, such as intercropping. This made APEX an ideal tool for conducting an assessment of the environmental benefits that had been achieved at the study site as a result of the voluntary establishment of several BMPs and to evaluate the potential benefits to additional modifications the current agronomic practices.

To simulate the study site farm, the 1.6-m. LiDAR DEM was used to delineate channels and overland flow paths to define the connectivity of different fields on the farm. The flow network delineated from the LiDAR, showing the fields draining the through the grassed waterway is shown in Figure 3.24.

Figure 3.24. LiDAR Delineation of flow connectivity.

STONE ENVIRONMENTAL INC
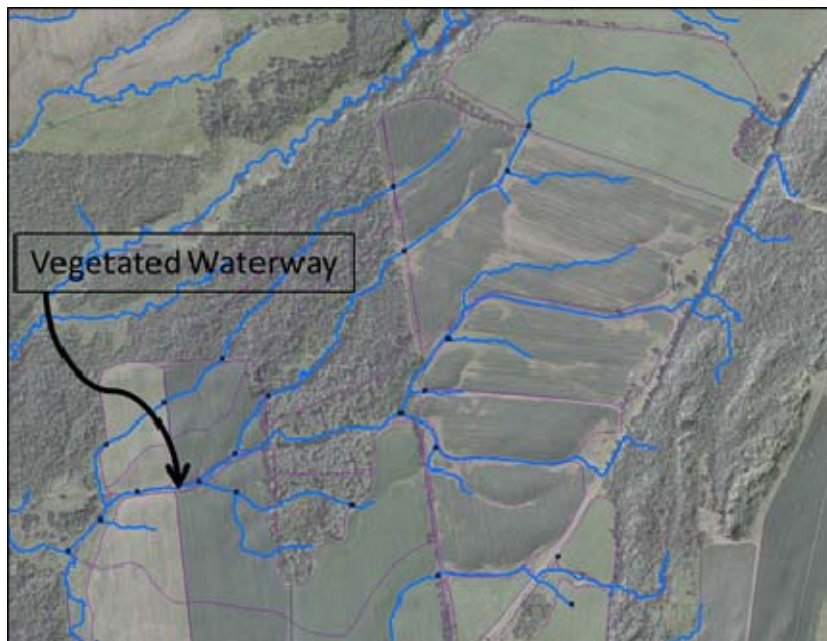
Once the flow network was constructed, the soils and crop rotations for each of the fields were defined. The farmer who manages these fields had five years of extensive records documenting crop planting and harvest dates, fertilizer and manure applications, as well as estimated yields. From this information, a crop rotation and agronomic management schedule for APEX was constructed specifically for each of the farmer's fields. The locations of tile drains, which had been identified by the farmer, allowed for the simulation of sub-surface drainage on a field-by-field basis. Soil P, that had been tested for as part of a nutrient management plan, was used to initialize the soil P levels for each field in the APEX model. A map of the crop historical crop rotations and areas tile drained is shown in Figure 3.25. The group of fields in the northeastern section of the farm which are not tiled have historically been in a continuous corn silage rotation. One of the proposed changes for this farm is to move two years of hay into the rotation on these fields.

All of the agronomic practices that the farmer had been applying over the past five years were used to construct APEX management schedules that reflect the actual conditions on each of the fields. This is the type of approach that could be applied areas identified as critical sources areas based on the strategic level SWAT analysis. By incorporating local data from the farmer, a more refined analysis can be conducted to determine if and where critical source areas exist on the landowner's property.

Figure 3.25. Historical crop rotations and tile drainage (cross-hatched area) for fields in the study farm
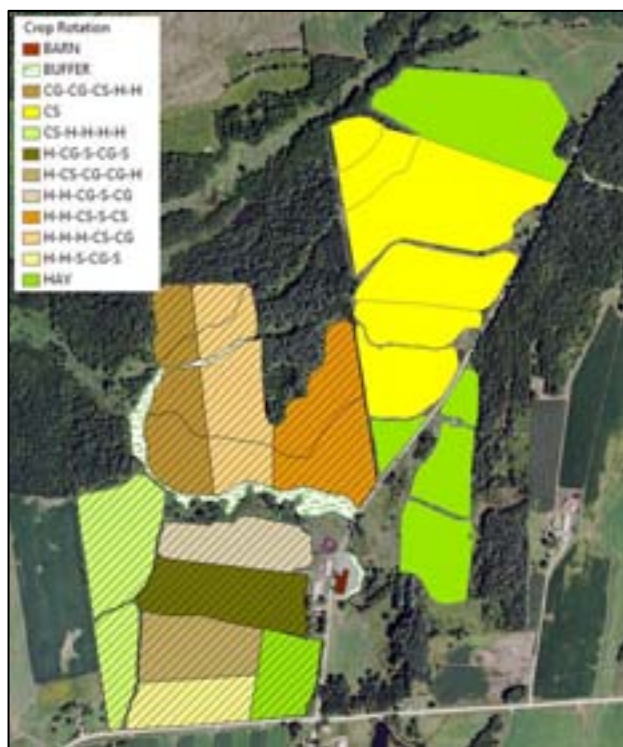
The current location of the barnyard is within 20 m. of a second order stream. Prior to 2009, animals had unconstrained access to the stream. In 2009, the establishment of a variable-width CREP buffer and construction of animal exclusion fencing kept animals a minimum of 5 m from the stream, and often as far as 20 m. There was no longer any direct accumulation of manure within the buffer, and the buffer also provided sediment trapping and nutrient reduction benefits. The APEX simulation of the barnyard area prior to the

STONE ENVIRONMENTAL INC

establishment of the CREP buffer assumed that the entire barnyard area was unvegetated and that direct manure accumulation from the animals occurred over the entire area. In simulating the conditions after the buffer establishment, the unvegetated area and manure accumulation was limited to areas outside of the area between the barn and the buffer. A diagram of these areas is shown in Figure 3.26.

Figure 3.26. Barnyard area of the study farm.

3.3.6. APEX Modeling Results

3.3.6.1. Historical Farming Practices, Field Assessment

APEX was run to simulate the historical crop rotation, for conditions prior to the establishment of the CREP buffer and the vegetated waterway using climate inputs from 1980 – 2009. The field level total P loading rates were assessed to identify the fields that represent the most critical P source areas on the farm. Figure 3.27 provides map showing the fields based on average annual total P export. The fields that produced the highest rates of total P export were the fields in a permanent corn silage rotation (parts of fields B2, B6, and B3). These fields are also ones that are not tile drained, which leads to increased surface runoff and soil erosion, contributing the high P loads. The fields with the lowest P loading rates were those in permanent hay (the B12 fields). The variability in the P loading rates across the different fields is a result of both differences in cropping practices and the field soils and slope characteristics. The fields within the farm study area ranked according to their total P loading rate is provided in Table 3.11. P loading is dominated by sediment on all of the fields, with those fields that included a corn rotation having a higher percentage of the total P as sediment

STONE ENVIRONMENTAL INC

P. It is difficult to identify clear trends in P loading based of hydrologic group or slope due to the variability of the crop rotations, other field specific management practices, and initial soil P levels. These results can be used as guidance to the farmer as to which fields should be considered for changes to crop rotation and management practices that would lead to improvements in the water quality leaving the farm.

Table 3.11. APEX field-level results summary.

Field ID	Rotation	Tile Drained	Soil Hydrologic Group	Average Slope (%)	Soluble P (kg/ha-yr)	Sediment P (kg/ha-yr)	Total P (kg/ha-yr)
B6	CS	No	D	4.7	0.46	5.78	6.24
B3b	CS	No	C	5.7	0.41	5.51	5.92
B3a	CS	No	C	5.5	0.40	5.48	5.88
B2c	CS	No	D	3.5	0.46	4.49	4.95
H3	H-CS-CG-CG-H	Yes	D	5.2	0.41	4.52	4.93
B2b	CS	No	C	3.6	0.40	3.85	4.25
H8	H-H-CS-S-CS	Yes	B	7.0	0.41	3.72	4.13
H6B	H-CG-S-CG-S	Yes	D	5.2	0.64	2.95	3.59
H4	H-H-S-CG-S	Yes	D	5.7	0.61	2.95	3.56
H6A	H-H-CG-S-CG	Yes	D	4.2	0.48	2.95	3.43
H7AN	H-H-H-CS-CG	Yes	D	6.5	0.37	2.82	3.19
H7AS	H-H-H-CS-CG	Yes	D	4.5	0.39	2.78	3.17
H7AN	H-H-H-CS-CG	Yes	D	5.3	0.37	2.76	3.13
B2a	CS	No	C	2.9	0.38	2.61	2.99
H7AS	H-H-H-CS-CG	Yes	D	4.5	0.38	2.46	2.84
H7BN	CG-CG-CS-H-H	Yes	D	4.7	0.51	2.31	2.82
H7BN	CG-CG-CS-H-H	Yes	D	5.9	0.54	2.19	2.73
H8	H-H-CS-S-CS	Yes	B	3.3	0.37	2.24	2.61
H1	CS-H-H-H-H	Yes	D	4.5	0.43	2.16	2.59
H7BS	CG-CG-CS-H-H	Yes	D	4.0	0.54	1.80	2.34
H7BS	CG-CG-CS-H-H	Yes	D	3.6	0.52	1.68	2.20
H2	CS-H-H-H-H	Yes	D	6.7	0.31	1.84	2.15
H5	HAY	Yes	D	9.2	0.36	1.52	1.88
B1	HAY	No	D	3.2	0.29	1.47	1.76
B12a	HAY	No	C	4.6	0.28	1.45	1.73
B12b	HAY	No	C	3.4	0.27	1.27	1.54
B10	HAY	No	C	5.6	0.39	1.13	1.52
B12c	HAY	No	C	3.1	0.27	1.21	1.48

CS = corn, silage; CG = corn, grain; S = soybean; H = hay

STONE ENVIRONMENTAL INC

Figure 3.27. Total P export based on historical agronomic management conditions.
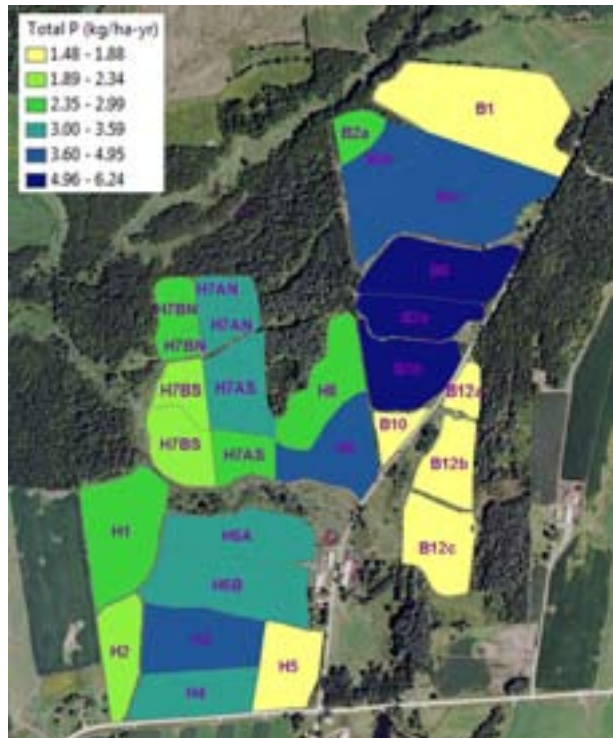
3.3.6.2. Evaluation of Current BMPs

The effectiveness of CREP buffer and vegetated waterway at reducing the total P leaving the farm was evaluated by running two separate APEX simulations, one for past conditions, and one for current conditions. For the past conditions simulation, the vegetated waterway was parameterized to be equivalent to a stream or ditch, with minimal vegetation cover. To simulate P loads entering the stream from fields H8, H7AS and H7BS prior to the CREP buffer establishment, it was assumed that current CREP buffer was unmaintained brush with poor vegetation cover. This type of parameterization results in minimal sediment and nutrient trapping potential, and is appropriate for comparison with a maintained buffer. For the barnyard area, the past conditions were simulated by assuming that there was no vegetated buffer area between the barnyard and the receiving stream.

The results of the comparison between total P losses before and after the current BMP establishment are summarized in Table 3.12. The amount of total P entering the stream from the CREP buffer is divided up to the three sections that drain into the buffer from fields H7BS, H7AS, and H8. The amount of total P leaving the vegetated waterway represents the total amount draining from all upstream fields. The predicted benefits of the CREP buffer and grassed waterway are significant. The grassed waterway provides a 30% reduction in total P leaving the area of the farm that drains through it. The CREP buffers along the field boundaries provides a 50% - 55% reduction in total P leaving the fields that drain through them. The establishment of the buffer along the barnyard boundary was predicted to provide the greatest benefit, reducing the total P load entering the receiving stream by 60%. It should be noted that these reduction numbers assume that the grassed waterway and the CREP buffers are in good condition and are well maintained. The effectiveness of these practices would be reduced if the actual buffer and grassed waterways were in less ideal condition. Even if the

STONE ENVIRONMENTAL INC

reductions in total P were half of what is being predicted by APEX, this still represents a significant benefit that has been achieved by the farmer by establishment of his current BMPs.

Table 3.12. Effectiveness of current BMPs at reducing total P loss.

BMP	Condition	Soluble P (kg/ha-yr)	Sediment P (kg/ha-yr)	Total P (kg/ha-yr)	Total P Reduction (%)
Grassed waterway (GWW)	Current with GWW	0.29	0.74	1.03	-
	Past without GWW	0.32	1.16	1.48	30.4
Buffer, (H7BS)	Current with buffer	0.41	0.38	0.79	-
	Past without buffer	0.44	1.16	1.6	50.6
Buffer (H8)	Current with buffer	0.33	0.34	0.67	-
	Past without buffer	0.35	1.03	1.38	51.4
Buffer (H7AS)	Current with buffer	0.27	0.68	0.95	-
	Past without buffer	0.33	1.8	2.13	55.4
Barnyard	Current with buffer	1.44	17.73	19.17	-
	Past without buffer	1.37	46.88	48.26	60.3

3.3.6.3. Evaluation of Proposed BMPs

The potential benefits of adopting additional BMPs to further reduce the P leaving the farm was evaluated by comparing APEX simulation results based on the current practices with a simulation based on the proposed changes to crop rotations and agronomic practices. The results are summarized in Table 3.13 and are reported based on the benefit realized at both field level, and at the "watershed" level. The "watershed" level results are reported at the outlet of the grassed waterway (which drains many of the fields that received the change in crop rotation) and at the outlets of each of the CREP buffers.

Converting fields that are currently in a permanent silage corn into a five-year rotation that includes two years of hay, results in a reduction in total P leaving the fields from 13% to 40% depending upon the field, with an average of 30%. At the outlet of the grassed waterway, that receives inflow from five of these six fields, the total P load is reduced by almost 8%. This lower percent reduction reported at the grassed waterway outlet reflects the addition areas (both farmed fields and forested areas) that also contribute to flows through the grassed waterway.

The benefits of changing from straight row (rows up and down the slope) to contour farming (rows perpendicular to the slope) results in total P loading reductions from between 20% and 35% over the three fields where this BMP was applied, with an average of 26% reduction. In terms of the total P exiting the CREP buffers, the reduction ranged from 12% to 30%. As was the case with the reported grassed waterway outlet reduction, the lower reductions reported of at the CREP buffer outlets reflects the additional areas draining through the buffer that did not have a change in management practice, as well as the contributions from the buffer areas themselves.

STONE ENVIRONMENTAL INC

Table 3.13. Effectiveness of proposed future BMPs at reducing total P loss.

Field ID / Outlet	BMP	Current Practices			Future Practices			
		Soluble P (kg/ha)	Sediment P (kg/ha)	Total P (kg/ha)	Soluble P (kg/ha)	Sediment P (kg/ha)	Total P (kg/ha)	Total P Red. (%)
B6	Rotation	0.46	5.78	6.24	0.27	3.84	4.11	34.1
B3a	Rotation	0.4	5.48	5.88	0.23	3.8	4.03	31.5
B3b	Rotation	0.41	5.51	5.92	0.23	3.82	4.05	31.6
B2a	Rotation	0.38	2.61	2.99	0.22	1.57	1.79	40.1
B2c	Rotation	0.46	4.49	4.95	0.26	3.22	3.48	29.7
B2b	Rotation	0.4	3.85	4.25	0.22	3.46	3.68	13.4
GWW Outlet	Rotation	0.29	0.74	1.03	0.22	0.73	0.95	7.8
H8	Contouring	0.41	3.72	4.13	0.36	2.93	3.29	20.3
H8-Buff. Outlet	Contouring	0.33	0.34	0.67	0.29	0.3	0.59	11.9
H7BS	Contouring	0.52	1.68	2.2	0.44	1	1.44	34.5
H7BS-Buff. Outlet	Contouring	0.41	0.38	0.79	0.31	0.25	0.56	29.1
H7AS	Contouring	0.38	2.46	2.84	0.36	1.79	2.15	24.3
H7AS-Buff. Outlet	Contouring	0.27	0.68	0.95	0.28	0.47	0.75	21.1

The APEX simulations of modifying the current crop rotation and changing to contour farming on selected fields suggest adopting these practices would further increase the already significant reductions in total P leaving the farm that have been achieved through the addition of grassed waterway and CREP buffers. The farmer has also been considering relocating the barnyard to a new site that is more than 150 m from the stream that it currently borders. Given that the current CREP buffer that was recently established resulted in a predicted reduction in P load of 60%, moving the barn to the proposed new location likely would result in limited additional benefit. Therefore, this potential change on the farm was not simulated. It is suggested that properly maintaining the current buffer between the barnyard and the stream represents the best option for managing the barnyard P source.

3.3.7. Farm Scale Tactical Analysis Summary

The tactical analysis performed on our example farm demonstrated an approach for taking detailed farm management information and using it deepen our understanding of farm-specific critical source areas and the potential benefits of BMPs. The information that went into the APEX model simulations contained a level of detail not available at the watershed scale, and was possible only through the careful records of field information and management activities that the farmer provided. Because the farmer had multiple years of records, the APEX model was able to not only evaluate the benefits of potential management changes, but also estimate the benefits of management practices that have already been implemented. In addition, the APEX model allowed BMPs specifically designed for this farm to be evaluated in terms of their effectiveness at reducing P leaving the farm. For farms where this level of information is available, this approach presents a method by which the P CSAs identified at the strategic level watershed analysis can be refined based on site

STONE ENVIRONMENTAL INC

specific information. The approach is particularly well-suited to the assessment of farmsteads, where limited information was available at the watershed scale.

3.4. Comparison of SWAT-Based CSA Identification to GIS-Based CSA Methods

A simplified CSA analysis was performed using GIS methods for comparison with the SWAT-based CSAs. The following section summarizes the methods used to derive the GIS-based CSA analysis and compares the results to the SWAT-based CSAs.

3.4.1. Method Description

The GIS-based CSA analysis was completed following methods used by Silvertun and Prange (2003) who developed a modified Universal Soil Loss Equation (USLE) model to identify areas of relative risk of sediment and pollution load. The model combines four land use factor maps through multiplication to produce a final risk map. This modified USLE model results in a map indicating relative risk, rather than actual sediment or pollution load, as would the original USLE. The risk map is derived using the following equation:

$$P = K * LS * W * U$$

Where P is the product map of risk of erosion and pollution elution, K is the USLE K-factor, LS is the USLE topographic factor (slope and slope length), W is a watercourse factor, and U is a land use factor. The equation is applied on a grid cell basis.

3.4.2. Application of the Method

GIS datasets for each of the four land use factors were constructed at a 10-m resolution, that was equivalent to the base resolution of the SWAT model.

The K-factor dataset was developed from the NRCS SSURGO-based values that were used as input to the SWAT model. The LS factor dataset was developed using the slope and slope length datasets derived for the 10-m DEM used to define the topographic inputs to the SWAT model. The equations for slope length and slope steepness factors were taken from McCool et al. (1987, 1989) and applied to a grid cell using the approach of Griffin (1988).

The values used for the land use factor (U) map were also based on McElroy et al. (1976) and those used in Silvertun and Prange (2003). The land use factors were adjusted to include land use classes specific to this project and based on local knowledge of the site. The method was originally applied in Sweden and many loading coefficients were quite old; loading coefficients were updated from more up-to-date sources and from local work (e.g., Frink 1991, Meals and Budd 1998). See Table 3.14 below for the land use factor coefficients used in this analysis. The same land use dataset as was used to build the SWAT model was used in mapping of the land use factor (U) map.

STONE ENVIRONMENTAL INC

Table 3.14. Land use (U) factor coefficients used in simple CSA analysis calculation for the CSA assessment area.

LCBP Land Cover Class	U
Barren	0.06
Brush	0.05
Corn	0.15
Corn	0.15
Corn/Hay	0.12
Farmstead, MFO	0.11
Farmstead, SFO	0.13
Forest	0.005
Hay	0.08
Pasture	0.07
Residential, Low	0.07
Residential, Med	0.11
Road, Dirt	0.06
Road, Paved	0.06
Soybean/Corn	0.10
Urban, Open	0.05
Water	0
Wetland	0.01

The watercourse factor map (W) provides information on the distance to streams, weighted to estimate sediment or pollution load reaching stream segments. The enhanced hydrologic network developed for this project was used in the development of this factor map. The same hydrologic flow path distance to the enhanced hydrologic network that was used in the SWAT-based rankings of CSAs (Section 3.2.2.2) was used in the derivation of the water course factor map (W). These distances were then given relative weights representing the percentage of sediment or pollution load that reaches the watercourse using the following weight function, developed by Silvertun and Prange (2003):

$W = (0.6 / (e^{0.002x} - 0.4))$, where x = the distance to the hydrologic network

The values derived from the water course weight function generally correspond to the original USLE values. The four factor maps were combined using simple raster multiplication to derive the final simple CSA analysis raster.

3.4.3. Comparison of the Results with SWAT-Based CSA Identification

The results of the GIS-based CSA analysis are generally as expected, based on knowledge of the study area. Visually, the results appear to be heavily influenced by land use classes. In general, agricultural, farmstead, and developed areas had higher risk values compared with areas of natural vegetation, such as forests and wetlands. Another visual trend is that risk increases as distance to stream decreases. The effect of the soil

STONE ENVIRONMENTAL INC

factor map is less apparent, but in general, areas with clayey or silty soils tend to have higher risk than areas with sandy soil. Visually, high slope steepness (a component of the LS factor) seems to have less influence over the resulting risk map than others, however most areas with high slopes are also in forested areas, that are assigned extremely low land use factor coefficients (0.005), greatly reducing risk for these areas. The results of the GIS-based CSA analysis are shown for the entire CSA assessment area are shown in Map 3.27.

The final results were compared with the SWAT-based CSA rankings. Two versions of the SWAT CSA were used in comparing with the GIS-based CSA results. The first represents SWAT rankings based only on the total P loading rate. The second reflects SWAT rankings weighted by the total P loading rate and hydrologic proximity where total P loading rates were weighted three times that of hydrologic proximity. Percentile rasters were derived for each output CSA layer, resulting in three output rasters with comparable scales of relative risk.

The resulting SWAT CSA percentile and GIS-based CSA percentile rasters were compared using the Band Collection Statistics tool in Spatial Analyst. This tool computes a correlation matrix of the input rasters. The Simple CSA results are positively related to both the SWAT CSA (P Only) (0.36) and SWAT CSA (P & proximity) (0.43) results. The stronger correlation between the SWAT CSA (P and proximity) and GIS-based CSA outputs may be due to the importance of distance to the hydrologic network in the GIS-based CSA analysis.

The CSA results were also summarized by land use class. Figure 3.28 illustrates the average percentile values and standard deviations for each land use class and CSA result. In general, the relative trend between land use classes is consistent for all resulting CSA outputs. There are exceptions, including the results for wetland areas. Both SWAT CSA results indicate relatively high risk in wetland areas (average percentiles of 73 and 77), where the GIS-based CSA method results indicate wetland areas to have the lowest risk (average percentile of 20). For the GIS-based CSA method, wetland areas were assigned a land use factor coefficient (U) of 0.01, one of the lowest U values among land use classes, which may explain the resulting values. While a soils factor map (K) is also used in the GIS-based CSA analysis, the factors are defined by soil texture only. Other factors, such as percent of organic matter, which would inform P loading, are not used. The SWAT model incorporates many additional factors that may explain the higher risk results in wetland areas, including percent organic matter.

STONE ENVIRONMENTAL INC

Figure 3.28: Comparison of the percentile ranking by land use based on the simple GIS approach and the SWAT-based approach.
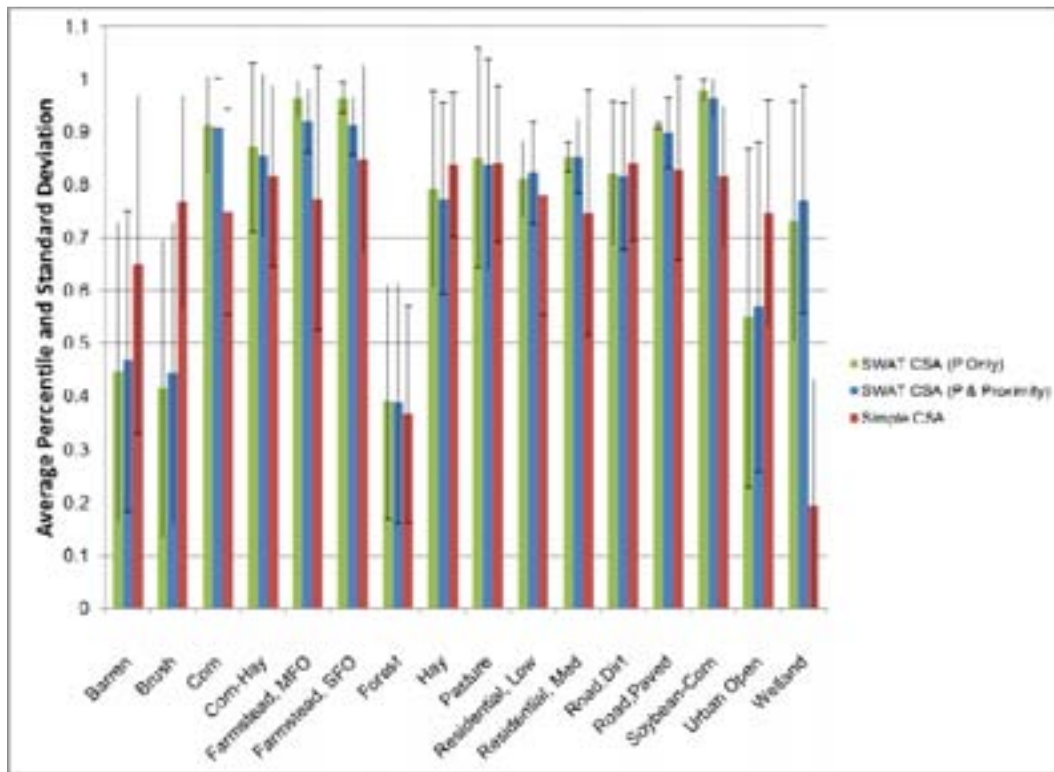
The land use classes brush, and urban open both have lower than average risk values for the SWAT results when compared with the GIS-based CSA results. For brush and urban open, P inputs are limited and runoff and erosion rates are low leading to lower predicted P CSA vulnerability by the SWAT methods.

The GIS-based CSA analysis results compare well with the two SWAT CSA analysis results within agricultural areas, denser urban areas, and forested areas. The comparison of the SWAT CSA and GIS-based CSA results at the land use level may inform potential improvements to the GIS-based CSA model. In particular, the land use factor (U) coefficients for wetland, brush, and urban open land use classes could be changed to reflect total P loading rates predicted by the process based SWAT model.

3.5. Assessment of BMP Targeting

The objective of this task was to assess the effectiveness of targeting BMPs to CSAs by comparing simulated watershed outlet P load reductions under two scenarios: implementation of a specific quantity of BMPs essentially randomly across eligible land units in the MBB and implementation of the same quantity of BMPs only to high-priority CSAs on eligible land units identified in the modeling effort. A secondary benefit of this process was to simulate and compare the potential of some BMPs to reduce P loads from the MBB if fully applied to eligible watershed land. However, because the primary purpose was to test the efficacy of targeting, a systematic evaluation of all possible BMPs was not attempted.

STONE ENVIRONMENTAL INC

3.5.1. BMP Selection

The BMPs used for this evaluation were selected in close consultation with members of the Project Advisory Committee (PAC). Three screening criteria were applied to potential BMPs to determine a list of candidate practices to be applied:

1. Practice can be adequately simulated by SWAT;

2. Practice is reasonably acceptable to farmers in the MBB; and

3. Adequate data exist on the effectiveness of the practice at a field scale.

We identified a preliminary list of practices that met at least one of these criteria:

- Reduced tillage;

- Cover cropping;

- Nutrient management;

- Change in rotations;

- Buffers;

- Conversion of tilled cropland to permanent cover; and

- Pasture management.

Several potentially useful practices had to be eliminated because they did not meet all the criteria. Even though good data exist on the effectiveness of livestock exclusion from streams, for example, SWAT was unable to model this practice because the model did not directly simulate the effects of livestock access to streams to begin with. Aeration of hayland prior to manure application, although popular among MBB farmers, could not be applied because adequate data do not exist to quantify the effectiveness of this practice on P losses from fields. A final list of potential BMPs was developed for review, comment, and priority ranking by PAC members. The result of this process yielded the following three BMPs that were assessed in this task:

1. Reduced manure P;

2. Cover cropping; and

3. Change in crop rotation.

Some fine-tuning and specific assumptions had to be made for each BMP; those are discussed along with results of the assessment in the following sections.

The simulations were done on the basis of implementing the BMPs on 20% of eligible MBB land (e.g., corn land for cover cropping). The overall approach was to identify the 20% highest P loss CSAs in an eligible land category and conduct a model run with the BMP applied only to those CSAs ("targeted scenario"), then repeat the process with the simulated BMPs applied only to an equivalent acreage of fields selected at random from among eligible land ("random scenario"). The SWAT simulations for each of the BMP scenarios were conducted for the same 28-year period as the baseline simulation.

STONE ENVIRONMENTAL INC

3.5.2. Simulation of Reduced Manure P

Nutrient management consists of actions that manage the amount, sources, placement, form, and timing of nutrient application to cropland to provide a nutrient supply adequate for plant production and to minimize nonpoint source pollution of surface and ground water. It is, however, quite difficult to simulate the application of nutrient management across a diverse watershed because the specific parameters of nutrient management – and the expected effects on nutrient losses from crop fields – depend heavily on the starting point on each field. Some fields, for example, may be deficient in P and require more fertilizer or manure, while other field soils may contain excessive P levels and no additional P would be recommended. In this case, specific simulation of nutrient management is impossible because we lack data on initial conditions for each and every field in the MBB.

Instead, we elected to simulate a nutrient management BMP by reducing the total P content of manure by 25% for all manure applications in the MBB. This change approximates an outcome that might be expected if fertilizer and manure nutrients were applied at a rate to supply P at crop removal need, i.e., P-based nutrient management.   Our approximation has the added benefit of also representing several other BMPs that might be applied to reduce the effective quantity of P applied in manure and fertilizer such as changes in livestock feed formulation and treatment of manure before application. In this simulation, we do not specify exactly *how* the P content of manure is reduced; only that 25% less P is applied to cropland.

3.5.2.1. Reduced Manure P BMP SWAT Model Implementation

Under this scenario it was assumed that the adoption of nutrient management practices resulted in the reduction of manure total P content by 25% from the original values assumed in the baseline SWAT scenario. This reduction in total P was applied to all manure – that applied from manure storage facilities to hay, corn, and soybean, as well as the manure applied directly to pasture areas during grazing. This reduction in manure P content was applied in both a random and a targeted implementation strategy. In both implementation strategies, the nutrient management BMP is applied to 20% of the land eligible to receive the BMP.

For the randomized implementation, all SWAT HRUs eligible for the BMP were identified. This included all HRUs with land use classifications of corn, corn-hay, pasture, and soybean-corn. The HRUs were then aggregated to the field level. This resulted in 9,283 fields eligible to receive the nutrient management BMP. Next, the fields were randomly selected until 20% of the total eligible area was reached. The randomized selection was performed using custom-written computer code that used a random number generator to pick values corresponding to the range in field IDs (which ranged from 1 to 9,283). The distribution of the selected fields by land use classification is summarized in Table 3.15. From the table, we see that the selected fields are evenly distributed across the different land uses, and the total area where the BMP was implemented is confirmed to be 20% of the total eligible land area.

STONE ENVIRONMENTAL INC

Table 3.15. Land use distribution of the randomly adopted reduced manure P BMP.

Land Use	Eligible Number of Fields	Selected Number of Fields	Fraction of fields Selected	Eligible Area (ha)	Selected Area (ha)	Fraction of Area Selected
Corn	434	77	0.18	2,637	519	0.20
Corn-Hay	3063	632	0.21	11,142	2,316	0.21
Hay	4075	795	0.20	13,249	2,540	0.19
Pasture	1702	332	0.20	5,387	1,109	0.21
Soybean-Corn	9	2	0.22	118	23	0.20
Total	9,283	1,838	0.20	32,533	6,506	0.20

The distribution of the randomly selected fields by their total P loading rate percentile from the baseline scenario is shown in Figure 3.29. From this figure, we see that the selected fields represent an even distribution of the range in P loading rates simulated over all the eligible fields.

Figure 3.29: Distribution of fields by total P loading rate percentile for fields in the randomly adopted reduced manure P BMP.
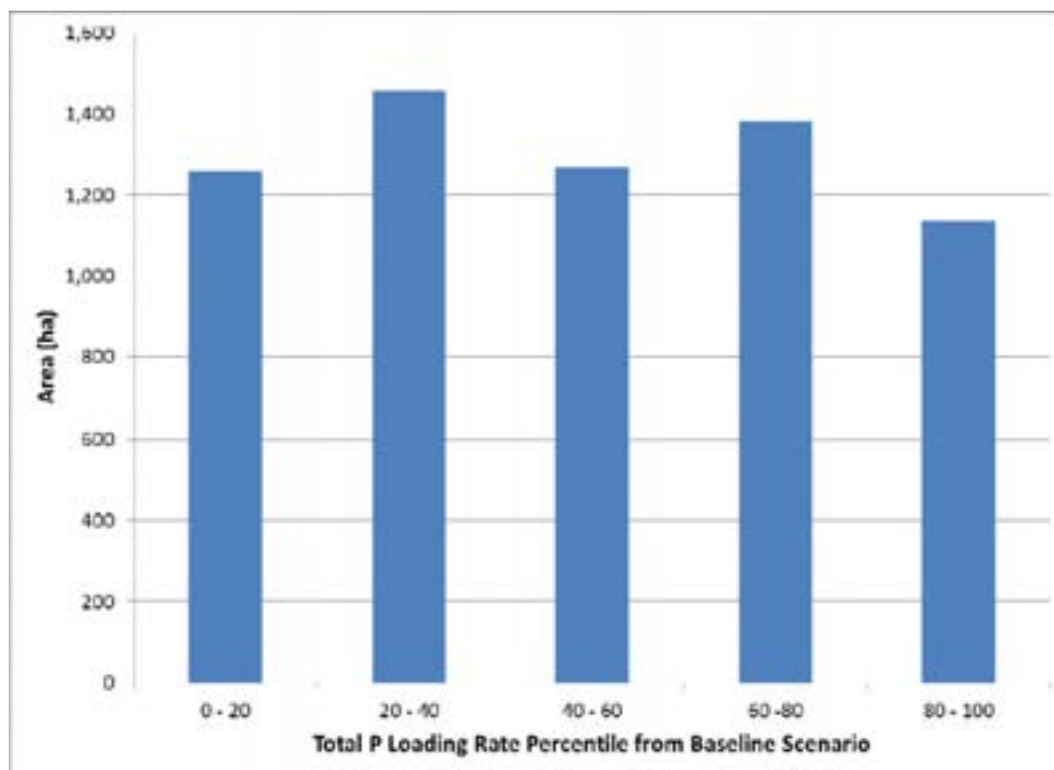
For the targeted implementation of the nutrient management BMP, the population of eligible fields was the same; however the fields selected were those that represented the 20% of the area with the highest annual average total P loading rates. The land use area and field count distribution that this top 20% of the area represents is shown in Table 3.16. Unlike the randomized selection of fields for BMP implementation, the targeted approach does not result in a uniform rate of implementation across all land uses. There is a much

STONE ENVIRONMENTAL INC

higher implementation in the corn, corn-hay, and soybean-corn land uses, which have a higher fraction of fields that are within the top 20% with respect to total P loading rate. For example, 42% of the corn area was selected to receive this BMP while only 7% of the hay and 11% of the pasture was selected.

Table 3.16. Land use distribution of the targeted reduced manure P BMP.

Land Use	Eligible Number of Fields	Selected Number of Fields	Fraction of fields Selected	Eligible Area (ha)	Selected Area (ha)	Fraction of Area Selected
Corn	434	176	0.41	2,637	1,098	0.42
Corn-Hay	3,063	921	0.30	11,142	3,733	0.34
Hay	4,075	293	0.07	13,249	983	0.07
Pasture	1,702	135	0.08	5,387	601	0.11
Soybean-Corn	9	7	0.78	118	95	0.80
Total	9,283	1,532	0.17	32,533	6,510	0.20

The SWAT simulations for the random and targeted reduced manure P BMPs were run with all the same agronomic practices simulated under the baseline conditions, with the only change being the P content of manure applied to the selected fields.

3.5.2.2. Reduced Manure P BMP Simulation Results

The results of the total P loading reductions achieved through random implementation of the reduced manure P BMP is summarized in Table 3.17. The summary is organized by land use, allowing for an assessment of the relative effectiveness of this BMP for different types of cropping practices. In addition, the reductions are presented based on the entire land use area, as well as for only the fields where the BMP was applied. This provides perspective for the effectiveness at the field level in addition to the effectiveness at contributing to total P reductions at the watershed scale.

Effectiveness of the BMP at reducing total P for the selected fields ranges from a low of 6.9% for soybean-corn to a high of 31.6% for hay. Pasture also shows a high P reduction effectiveness. The high effectiveness of this BMP on hay and pasture is due to the dominance of P export from these areas as soluble P that remains largely on the ground surface. The land uses dominated by sediment P export (corn, corn-hay, and soybean-corn) show significantly less P reduction as a result of this BMP, probably because the particulate P loss is also strongly driven by the existing soil test P on the field. The overall impact of adopting this BMP randomly across the watershed was to lower total P export from agricultural lands by 3.4% or 1,593 kg of P.

STONE ENVIRONMENTAL INC

Table 3.17. Summary of total P reductions achieved through random implementation of reduced manure P BMP on 20% of the eligible land.

Land Use	Baseline Total P (kg) All Fields	Baseline Total P (kg) Selected Fields	BMP Total P (kg) All Fields	BMP Total P (kg) Selected Fields	Total P Reduction (%) All Fields	Total P Reduction (%) Selected Fields	Total P Reduction (kg) All Fields
Corn	5,533	975	5,444	886	1.6	9.1	88.5
Corn-Hay	22,214	4,399	21,695	3,879	2.3	11.8	519.8
Hay	11,711	2,078	11,055	1,422	5.6	31.6	656.0
Pasture	7,000	1,407	6,675	1,083	4.6	23.1	324.5
Soybean-Corn	446	67	441	62	1.0	6.9	4.6
Total	46,904	8,925	45,310	7,332	3.4	17.9	1,593

The results from applying the reduced manure P BMP to the 20% of the eligible land with the highest P loading rates are shown in Table 3.18. In comparison to the random implementation, there are several important differences to note. First, the percent reduction in total P for the selected fields (where the BMP is implemented) is slightly less than was predicted for the fields randomly selected. For example, the effectiveness on hay dropped form 31.6% to 24.2% and the effectiveness on corn from 9.1% to 8.6%. This is likely because P availability is not a limiting factor for these highly vulnerable areas. A trend that continues to be seen is that the land uses dominated by soluble P export experience higher levels of P reduction as a result of this BMP than those dominated by sediment P export. The most important trend seen is that when considering the entire population of fields, the percent reduction in total P almost doubles, from 3.4% to 6.0%, or 2,831 kg. This result suggests the significant potential benefits of applying P reduction strategies to the areas identified as critical source areas before expanding implementation to less critical areas.

Table 3.18. Summary of total P reductions achieved through targeted implementation of reduced manure P BMP on 20% of the eligible land with the highest P loading rates.

Land Use	Baseline Total P (kg) All Fields	Baseline Total P (kg) Selected Fields	BMP Total P (kg) All Fields	BMP Total P (kg) Selected Fields	Total P Reduction (%) All Fields	Total P Reduction (%) Selected Fields	Total P Reduction (kg) All Fields
Corn	5,533	3,511	5,232	3,211	5.4	8.6	300.4
Corn-Hay	22,214	13,885	20,768	12,438	6.5	10.4	1,446.7
Hay	11,711	3,032	10,978	2,299	6.3	24.2	732.8
Pasture	7,000	1,512	6,680	1,192	4.6	21.2	320.0
Soybean-Corn	446	400	415	368	7.0	7.8	31.3
Total	46,904	22,340	44,072	19,508	6.0	12.7	2,831

STONE ENVIRONMENTAL INC

3.5.3. Simulation of Cover Cropping

3.5.3.1. Cover Crop BMP SWAT Model Implementation

The cover crop BMP was applicable for all the fields that have been modeled as permanent corn or in a corn-hay rotation (4 years corn followed by 4 years hay). The establishment of a cover crop for the fields selected to receive the cover crop BMP required that the baseline management operations that were established to simulate the permanent corn and corn-hay rotation fields be modified in several respects. The primary changes were as follows:

- A cover crop of cereal rye was planted on October 5th following corn harvest on October 1st.

- On clay soils, fall manure application and tillage was shifted up several days to occur on October 3rd and 4th, prior to the rye planting.

- On non-clay soils, primary tillage that normally would occur in the spring following manure application was shifted to occur on October 4th following corn harvest.

The cover crop BMP was applied to 20% of the eligible land following two different strategies. The first strategy selected 20% of the land randomly, while the second strategy targeted the 20% of the eligible land with the highest total P loading rates.

The fields selected for random BMP implementation were chosen from the total number of eligible fields (3,497) using the same random selection approach that was applied for the nutrient management BMP. The distribution by land use of these selected fields is summarized in Table 3.19. The selection of fields and total area for BMP evenly distributed between the permanent corn and corn-hay rotation areas, with approximately 20% each land use getting selected.

Table 3.19. Land use distribution of the randomly adopted cover cropping BMP.

Land Use	Eligible Number of Fields	Selected Number of Fields	Fraction of fields Selected	Eligible Area (ha)	Selected Area (ha)	Fraction of Area Selected
Corn	434	91	0.21	2,637	507	0.19
Corn-Hay	3063	607	0.20	11,142	2,248	0.20
Total	3,497	698	0.20	13,779	2,756	0.20

The distribution of the selected fields based on the model-estimated total P loading rate from the baseline simulation is shown in Figure 3.30. Given the data shown, we have met the objective of selecting fields that represent a range across the spectrum of total P loading rates.

STONE ENVIRONMENTAL INC

Figure 3.30: Distribution of fields by total P loading rate percentile for fields in the randomly adopted cover cropping BMP.
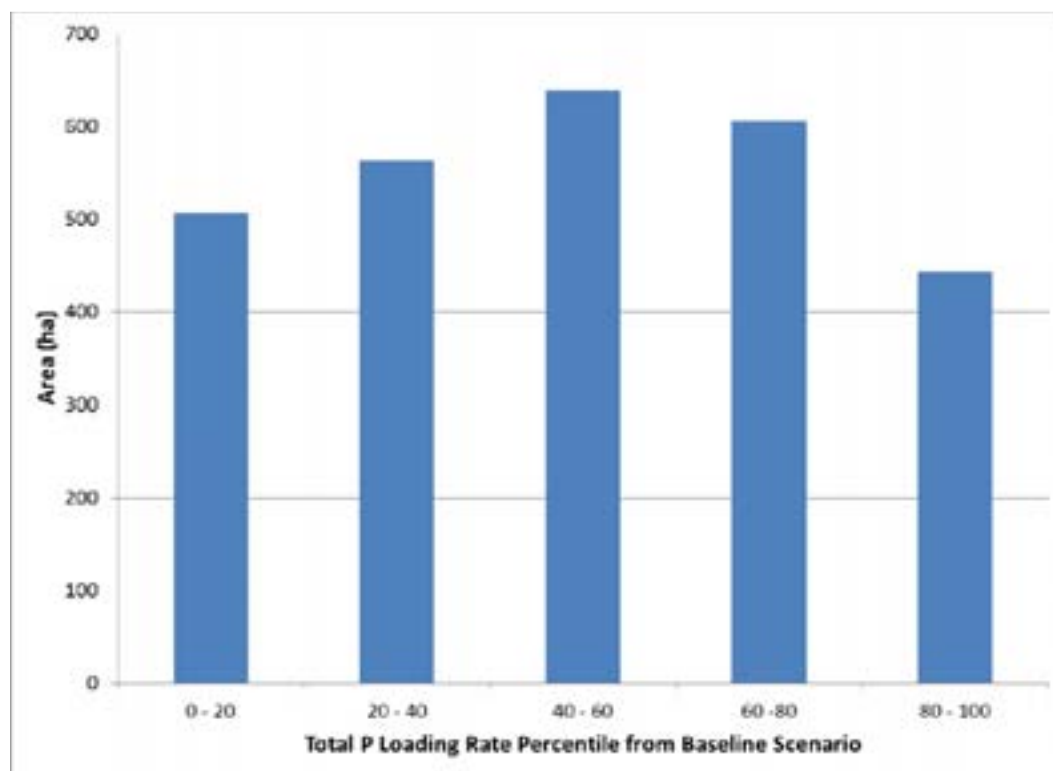
For the targeted implementation of the cover crop BMP, the population of eligible fields was the same; however the fields selected were those that represented the 20% of the area with the highest annual average total P loading rates. The land use area and field count distribution that this top 20% of the area represents is shown in Table 3.20. The land use distribution of the fields falling in the top 20% is generally even, with 21% of corn fields getting selected and 18% of corn-hay fields getting selected. For the targeted selection, there is a slight favor for corn fields over the random selection approach in which 18% of the corn fields were selected. This suggests that overall, the permanent corn fields are slightly more common critical source areas than fields in corn-hay rotation. Table 3.19 also confirms that 20% of the eligible land was selected for the BMP.

Table 3.20. Land use distribution of the targeted cover cropping BMP.

Land Use	Eligible Number of Fields	Selected Number of Fields	Fraction of fields Selected	Eligible Area (ha)	Selected Area (ha)	Fraction of Area Selected
Corn	434	90	0.21	2,637	557	0.21
Corn-Hay	3063	550	0.18	11,142	2,200	0.20
Total	3,497	640	0.18	13,779	2,757	0.20

The SWAT simulations for the random and targeted cover crop BMPs were run with all the same agronomic practices simulated during the baseline simulation, with the only change being the modification in agronomic management at the end of corn years to add a rye cover crop planting on the selected fields.

STONE ENVIRONMENTAL INC

3.5.3.2. Cover Crop BMP Simulation Results

The results of the total P loading reductions achieved through random implementation of the adoption of fall cover cropping following corn for 20% of the eligible land is summarized in Table 3.21. The summary is organized by land use, allowing for an assessment of the relative effectiveness of this BMP permanent corn versus corn-hay rotation. The reductions are presented based on the entire land use area as well as for only the fields where the BMP was applied. This provides perspective for the effectiveness at the field level as well as the effectiveness at reducing total P reductions at the watershed scale.

The effectiveness of the cover crop BMP at reducing total P export from corn and corn-hay rotation is significantly greater (approximately 3 times greater) than the nutrient management BMP applied to the same land uses. For selected fields, the effectiveness at reducing total P export was higher for permanent corn (36.4%) than for land in corn-hay rotation (30.5%). This is to be expected, because permanent corn realizes the benefit of the cover crop following corn every year of the simulation, while the corn-hay rotation benefits every four out of every eight years.

Table 3.21. Summary of total P reductions achieved through random implementation of cover cropping BMP on 20% of the eligible land.

Land Use	Baseline Total P (kg) All Fields	Baseline Total P (kg) Selected Fields	BMP Total P (kg) All Fields	BMP Total P (kg) Selected Fields	Total P Reduction (%) All Fields	Total P Reduction (%) Selected Fields	Total P Reduction (kg) All Fields
Corn	5,533	1,118	5,126	711	7.4	36.4	407
Corn-Hay	22,214	4,347	20,887	3,020	6.0	30.5	1,328
Total	27,747	5,465	26,012	3,730	6.3	31.7	1,735

The results for the cover crop BMP targeted to the 20% of the eligible land with highest total P loading rates is summarized in Table 3.22. The effectiveness of this BMP on the fields where it was applied was similar to what was simulated for the randomly selected fields, increasing slightly for permanent corn and decreasing slightly for corn-hay rotation. As was seen with the simulation of the nutrient management BMP, the overall reduction in total P is much higher when targeted implementation is adopted rather than the random approach. The effectiveness for both land use classes roughly doubles from 7.4% for corn and 6.0% for corn-hay up to 15.3% for corn and 12.6% for corn-hay. This doubling of the benefit by applying the BMPs to fields with the highest P loading rates as opposed to randomly selected fields is similar to what was found for the nutrient management BMP when all the applicable land uses were aggregated, providing more support for the targeted implementation strategy.

Table 3.22. Summary of total P reductions achieved through targeted implementation of cover cropping BMP on 20% of the land with the highest P loading rates.

Land Use	Baseline Total P (kg) All Fields	Baseline Total P (kg) Selected Fields	BMP Total P (kg) All Fields	BMP Total P (kg) Selected Fields	Total P Reduction (%) All Fields	Total P Reduction (%) Selected Fields	Total P Reduction (kg) All Fields
Corn	5,533	2,143	4,689	1,299	15.3	39.4	844
Corn-Hay	22,214	10,114	19,415	7,315	12.6	27.7	2,799
Total	27,747	12,256	24,104	8,613	13.1	29.7	3,643

STONE ENVIRONMENTAL INC

3.5.4. Simulation of Crop Rotation Shift

3.5.4.1. Crop Rotation Shift SWAT Model Implementation

The shift in crop rotation BMP was applicable for all the fields that have been modeled as permanent corn or in a corn-hay rotation (4 years corn followed by 4 years hay). The small area of cropland that was simulated as a soybean-corn rotation was not considered for this BMP. Because the fields simulated as permanent corn had been so-designated because they were on the land most suited for corn cultivation, it was determined unreasonable to replace land taken out of corn with fields that had been in permanent hay or corn-hay rotation, as those areas were already less well suited to corn. Shifting corn production to these less suitable lands would potentially result in no net benefit from adopting this BMP. Therefore, the assumption was made that the selected fields were transitioned to a permanent hay rotation and that the lost corn production area was not replaced. The same implementation assumptions that were applied to the other BMPs were applied to the crop rotation shift BMP. This resulted in applying the crop rotation shift BMP to 20% of the eligible land, both based on random selection of that 20% of land and on targeting the 20% of the eligible land with the highest total P loading rates.

The selection of fields for random implementation of the BMP followed the same approach as was described for the other two BMPs. The fields selected for BMP implementation were randomly chosen from the total number of eligible fields (3,497). The distribution by land use of these selected fields is summarized in Table 3.23. The data in this table confirms that the 20% of the total eligible area was selected, with an even distribution between the permanent corn and corn-hay rotation fields.

Table 3.23. Land use distribution of the randomly adopted crop rotation shift BMP.

Land Use	Eligible Number of Fields	Selected Number of Fields	Fraction of fields Selected	Eligible Area (ha)	Selected Area (ha)	Fraction of Area Selected
Corn	434	80	0.18	2,637	564	0.21
Corn-Hay	3063	608	0.20	11,142	2,192	0.20
Total	3,497	688	0.20	13,779	2,756	0.20

The distribution of the selected fields by their total P loading rate percentile from the baseline scenario is shown in Figure 3.31. This figure confirms that, as intended, the selected fields represent a roughly even distribution of the range in P loading rates simulated over all the eligible fields.

STONE ENVIRONMENTAL INC

Figure 3.31: Distribution of fields by total P loading rate percentile for fields in the randomly adopted crop rotation shift BMP.
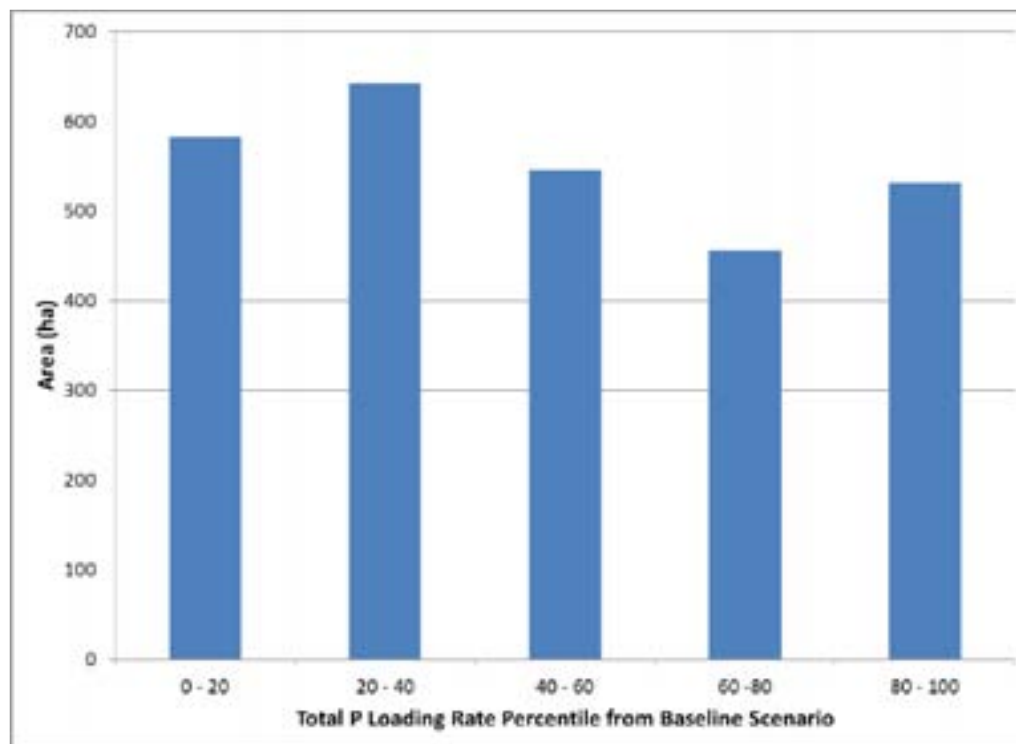
For the targeted implementation of crop rotation shift BMP, the population of eligible fields was the same; however the fields selected were those that represented the 20% of the area with the highest annual average total P loading rates. The land use area and field count distribution represented by this top 20% of the area is shown in Table 3.24. The land use distribution of the fields falling in the top 20% is generally even, with 21% of corn fields and 18% of corn-hay fields selected. For the targeted selection, there is a slight favor for corn fields over the random selection approach in which 18% of the corn fields were selected. This suggests that overall, the permanent corn fields are slightly more common critical source areas than fields in corn-hay rotation. This pattern was previously noted in section 3.1.1.1. Table 3.24 also confirms that the BMP was applied to 20% of the eligible land, as was intended.

Table 3.24. Land use distribution of the targeted crop rotation shift BMP.

Land Use	Eligible Number of Fields	Selected Number of Fields	Fraction of fields Selected	Eligible Area (ha)	Selected Area (ha)	Fraction of Area Selected
Corn	434	90	0.21	2,637	557	0.21
Corn-Hay	3063	550	0.18	11,142	2,200	0.20
Total	3,497	640	0.18	13,779	2,757	0.20

STONE ENVIRONMENTAL INC

The SWAT simulations for the random and targeted crop rotation shift BMPs were run with all the same agronomic practices as were used during the baseline simulation, with the only change being the change in crop rotation for the selected fields.

3.5.4.2. Crop Rotation Shift BMP Simulation Results

The results of the total P loading reductions achieved through random implementation of the shift to permanent hay for 20% of the eligible land are summarized in Table 3.25. The summary is organized by land use, allowing for an assessment of the relative effectiveness of this BMP for different types of cropping practices. In addition, the reductions are presented based on the entire land use area as well as for only the fields where the BMP was applied. This provides perspective for the effectiveness at the field level as well as the effectiveness at contributing to total P reductions at the watershed scale.

Switching to a permanent hay rotation results in very large total P loading reductions, even when applied to randomly selected fields. For those fields where the crop rotation BMP was applied, effectiveness ranged from 77.7% for corn-hay rotation land to 85% for land rotated out of permanent corn. This results in a reduction in total export over all of the eligible land of 15.2%, or 4,227 kg. This is significant given that only 20% of randomly selected fields received the BMP.

Table 3.25. Summary of total P reductions achieved through random implementation of crop shift rotation BMP on 20% of the eligible land.

Land Use	Baseline Total P (kg)		BMP Total P (kg)		Total P Reduction (%)		Total P Reduction (kg)
	All Fields	Selected Fields	All Fields	Selected Fields	All Fields	Selected Fields	All Fields
Corn	5,533	1,035	4,653	155	15.9	85.0	879
Corn-Hay	22,214	4,308	18,867	961	15.1	77.7	3,347
Total	27,747	5,343	23,520	1,116	15.2	79.1	4,227

The results from adopting the crop rotation shift BMP on the 20% of the eligible land with the highest P loading rates are shown in Table 3.26. The shift to permanent hay was slightly more effective for the selected fields than was the random implementation of the BMP, with the reductions increasing from 79.1% to 83.1%. However, the total P reduction when considering all of the eligible fields increased by nearly 3 times, from 15.2% to 44.7%, or 12,393 kg. This is equivalent to total P export of reductions of 4,227 kg/yr and 12,393 kg/yr respectively. The reduction achieved by the targeted implementation to the most critical 20% of eligible land is equal to 16.3 % of the model-estimated total P load from all land uses within the Vermont sector of the MBB (75,626 kg/yr). The BMP of moving corn rotations into permanent hay is the most effective of the three BMPs evaluated, and also shows the greatest benefit from implementation on the fields with highest P loading rates.

STONE ENVIRONMENTAL INC

Table 3.26. Summary of total P reductions achieved through random implementation of crop shift rotation BMP on 20% of the land with the highest P loading rates.

Land Use	Baseline Total P (kg)		BMP Total P (kg)		Total P Reduction (%)		Total P Reduction (kg)
	All Fields	Selected Fields	All Fields	Selected Fields	All Fields	Selected Fields	All Fields
Corn	5,533	2,143	3,643	253	34.1	88.2	1,889
Corn-Hay	22,214	10,114	11,711	1,819	47.3	82.0	10,504
Total	27,747	12,256	15,354	2,072	44.7	83.1	12,393

Table 3.27 summarizes the six different BMP scenarios simulated. The effectiveness on the fields where the BMPs were implemented ranged from a low of 12.7% - 17.9% for the reduced manure P BMP, up to 79.15 – 83.1% for the crop rotation shift BMP. This translated into a range of total P reduction over the entire CSA assessment area from 2.1% - 16.4% of average annual P load (75,626 kg/yr). For each BMP tested, significant benefit was realized by implementing the BMP on a targeted area representing the eligible land with the simulated highest P loading rates from the baseline simulation. The improvements in total P reduction following the targeted as opposed to random implementation were by factors of 1.8, 2.1, and 2.9 for the reduced manure P, cover crop, and crop rotation shift BMPs respectively. From both an environmental quality and an economic perspective, choosing a targeted BMP implementation strategy offers clear benefits.

Table 3.27. Summary of total P reductions achieved through six BMP scenarios evaluated.

BMP Scenario	Average Field Effectiveness (%)	Total Area Implemented (ha)	Avg. Annual Total P Reduction (kg)	Reduction in Total P, CSA Assessment Area (%)
Reduced Manure P, Random	17.9	6,506	1,593	2.1
Reduced Manure P, Targeted	12.7	6,510	2,831	3.7
Cover Cropping, Random	31.7	2,756	1,735	2.3
Cover Cropping, Targeted	29.7	2,757	3,643	4.8
Crop Rotation Shift, Random	79.1	2,756	4,227	5.6
Crop Rotation Shift, Targeted	83.1	2,757	12,393	16.4

As the model shows, the transition of land from corn into permanent hay offers the greatest potential reductions in total P loading per treated acre. Although there are numerous farm management decisions that would have to factor into any such transition, targeted efforts to install permanent hay on those most sensitive fields could yield substantial and meaningful improvements in water quality in the Missisquoi Bay.

3.6. Assessment of Climate Change Impacts on P Loading

The potential effects of climate change on P critical source areas within the MBB was evaluated by running the MBB SWAT with weather inputs based on projected climate change scenarios. The focus of the assessment was on the broader watershed and land use level scale and did not consider the HRU-level changes under future climate conditions. In addition, the spatial resolution of and availability of future climate time series

STONE ENVIRONMENTAL INC

data required that a new "baseline" SWAT simulation be generated to represent current climate conditions. The development of the climate inputs and modeling results will be discussed in the following sections.

3.6.1. Future Climate Scenarios Evaluated

Two different future climate scenarios were simulated in order to evaluate the possible change in P loading within the MBB under projected climate change. Both climate scenarios represent the projected climate conditions for the period form 2041 – 2070. The climate scenarios were taken from the North American Regional Climate Change Assessment Program (NARCCAP; http://www.narccap.ucar.edu). The NARCCAP data includes higher resolution regional climate models (RCM) to downscale the output from the global climate models (GCMs) to a more localized. The downscaling approach results in a spatial resolution of climate output of 50 km. The carbon dioxide emission used in the NARCAP projections is the A2 emissions scenario (described in Nakicenvoic et al. (2000)). This emissions scenario corresponds to $CO2$ concentrations by the middle and end of the 21tst century of about 575 ppm and 870 ppm respectively.

The two future climate scenarios represent projections from two GCM/RCM model combinations. Because there can be great variability in output predictions from different GCMs, evaluation of two scenarios representative of the range in predicted changes would place upper and lower bounds on the predicted effects on P loading. The selection of climate scenarios that represent the upper and lower bounds of projected changes in P loading was based on recent work in the LaPlatte River watershed in central Vermont (Perkins, 2011). The first climate scenario selected was Hadley Centre Coupled Model, Version 3(HadCM3) GCM with downscaling from the Hadley Region Model 3 (HRM3), known as the HRM3_HadCM3 scenario. The second scenario selected was the Community Climate System Model (CCSM0 GCM with downscaling from the Weather Research and Forecasting Model (WRFP), known as the WRFP_CCSM scenario. The HRM3_HadCM3 represented the climate scenario with resulting in the highest projections of P loading, while the WRFP_CCSM scenario resulted in P loading projections the lower end.

The GCM/RCM climate change predictions from the two scenarios selected were used to generated monthly climate change statistics. These monthly change statistics were then used to perturb historical hourly time series of precipitation and temperature from a local climate station. This analysis was performed as part of a recent study of climate change effects on water quantity and water quality in 20 large US watersheds. This study, that is part of the US EPA's Global Change Research Program (GCRP), is described in Johnson et al. (2011).

Daily time series of precipitation and temperature representative of each future climate scenario, as well as the "baseline" current conditions was provided by the EPA's "20 watersheds" project study team (Parker 2011). The daily time series provided as for the Enosburg Falls, Vermont observing station. Enosburg Falls is one of the 16 stations used in the development of precipitation and temperature time series for the MBB SWAT model. Recall that the process followed in the weather time series development for the MBB SWAT model calibration, validation and application involved a kriging interpolation that accounted for both spatial variability as a function of x-y coordinates and as a function of annual average variability based on elevation and topography (see Section 2.2.2). The future climate scenarios provided were representative of just a single location (Enosburg Falls) within the MBB study area. In consultation with the "20 watersheds" project study team, it was decided that a similar extrapolation of the single Enosburg Falls station using the 1971-2000 PRISM annual averages may not be a valid approach, as the same relationship between elevation\topography and precipitation/temperature may not hold for the future climate conditions. Therefore, it was decided that the best approach would be to simulate a new "baseline" scenario using the current climate "baseline" Enosburg

STONE ENVIRONMENTAL INC

Falls climate time series as input to all subbasins within the MBB study area. This option would result in P loading results that are not directly comparable to the MBB P loading results presented thus far. The approach does, however, offer consistency of inputs with the GCRP project, and allows the relative changes in P load to be compared between the new "baseline" and the two future climate scenarios.

A summary of the basin-average annual precipitation and evapotranspiration characteristics for the baseline and two future climate scenarios is presented in Table 3.28. This table shows that the total precipitation for the WRFG scenarios is only 7 mm higher than the baseline. However, the amount of snowfall is reduced by a third. The precipitation increase under the HRM3 scenario is considerably greater, with 12% increase over the baseline. Snowfall reduction is similar to the WRFG scenario, with a roughly one third decrease. This change in snowfall is significant in both scenarios, as it means that additional precipitation is occurring in the cold season with saturated soils and less vegetation to protect the soil. In both future climate scenarios, ET increases by approximately 4%.

Table 3.28. Change in land-use level sediment loads under future climate scenarios, CSA assessment area.

Climate Scenario	Mean Annual Precipitation (mm)	Mean Annual Snowfall, Liquid Equivalent (mm)	Mean Annual ET (mm)
Baseline	1090	155	575
WRFG ccsm	1097	102	596
HRM3 hadcm3	1223	110	600

3.6.2. Climate Change Scenario Results

The MBB SWAT model was run for a 30 year simulation representative of the new "baseline" scenario (referred to now as the "climate change baseline"). This baseline time period was taken as the most recent 30 years in the time series data provided by the GCRP project, plus an additional 2 years model warm-up period. This resulted in a MBB SWAT simulation period from 1/1/1975- 12/31/2006. Simulations representing the HRM3_HadCM3 and WRFP_CCSM scenarios were run for the same 32 year simulation period (however the future climate time series included perturbations representative of the 2041-2070 climate conditions). The results for changes in simulated sediment and total P load between the climate change baseline and the 2 future climate scenarios are provided in Tables 3.29 and 3.30 respectively.

STONE ENVIRONMENTAL INC

Table 3.29. Change in land-use level sediment loads under future climate scenarios, CSA assessment area.

Land Use Classification	Area (ha)	Sediment Load Rate (ton/ha-yr)			Total Sediment Load (ton/yr)			Percent Change (%)	
		Baseline	WRFG ccsm	HRM3 hadcm3	Baseline	WRFG ccsm	HRM3 hadcm3	WRFG ccsm	HRM3 hadcm3
Barren	354	0.86	0.93	1.32	305	329	469	8.0	54.0
Brush	15,762	0.18	0.19	0.27	2,909	3,069	4,289	5.5	47.5
Corn	2,637	5.24	6.52	7.77	13,826	17,204	20,487	24.4	48.2
Farmstead, MFO	113	0.44	0.45	0.50	50	51	56	1.0	11.7
Farmstead, SFO	489	0.36	0.37	0.41	178	181	200	1.4	12.4
Forest	114,449	0.12	0.13	0.19	13,712	14,499	21,199	5.7	54.6
Hay	13,249	0.41	0.57	0.97	5,386	7,533	12,891	39.9	139.4
Pasture	5,387	0.74	1.08	1.57	3,994	5,809	8,467	45.5	112.0
Residential, Low	1,310	0.61	0.69	0.78	798	904	1,025	13.3	28.5
Residential, Med	308	0.51	0.56	0.62	157	173	190	10.3	21.1
Road, Dirt	1,007	7.72	8.07	10.41	7,766	8,123	10,479	4.6	34.9
Road, Paved	709	0.50	0.52	0.54	357	371	383	4.0	7.4
Soybean-Corn	118	9.01	11.24	13.48	1,063	1,326	1,590	24.7	49.5
Urban Open	4,431	0.61	0.72	0.84	2,712	3,171	3,711	16.9	36.8
Corn-Hay	11,142	4.46	5.57	6.83	49,663	62,016	76,098	24.9	53.2
Wetland	5,843	0.10	0.11	0.15	608	653	872	7.5	43.5
Total	177,307	0.58	0.71	0.92	103,483	125,412	162,408	21.2	56.9

STONE ENVIRONMENTAL INC

Table 3.30. Change in land-use level total P loads under future climate scenarios, CSA assessment area.

Land Use Classification	Area (ha)	Total P Load Rate (ton/ha-yr)			Total P Load (ton/yr)			Percent Change (%)	
		Baseline	WRFG ccsm	HRM3 hadcm3	Baseline	WRFG ccsm	HRM3 hadcm3	WRFG ccsm	HRM3 hadcm3
Barren	354	0.25	0.25	0.33	87	87	116	0.0	33.0
Brush	15,762	0.19	0.18	0.23	2,988	2,868	3,589	-4.0	20.1
Corn	2,637	2.21	2.74	3.20	5,838	7,234	8,443	23.9	44.6
Farmstead, MFO	113	3.28	3.09	3.57	370	349	403	-5.8	8.7
Farmstead, SFO	489	3.16	2.98	3.45	1,547	1,456	1,688	-5.9	9.1
Forest	114,449	0.09	0.09	0.12	10,228	10,492	14,115	2.6	38.0
Hay	13,249	0.80	1.00	1.60	10,637	13,249	21,143	24.6	98.8
Pasture	5,387	1.30	1.37	1.76	7,015	7,380	9,474	5.2	35.0
Residential, Low	1,310	0.62	0.64	0.69	807	843	910	4.4	12.7
Residential, Med	308	0.77	0.79	0.84	236	245	257	3.7	9.1
Road, Dirt	1,007	0.76	0.77	0.93	762	773	933	1.3	22.3
Road, Paved	709	1.24	1.30	1.33	881	919	942	4.3	6.9
Soybean-Corn	118	4.10	4.93	5.77	484	582	680	20.2	40.6
Urban Open	4,431	0.32	0.35	0.40	1,420	1,557	1,770	9.6	24.6
Corn-Hay	11,142	2.05	2.49	3.04	22,873	27,793	33,880	21.5	48.1
Wetland	5,843	0.88	0.82	0.92	5,137	4,806	5,398	-6.4	5.1
Total	177,307	0.40	0.45	0.59	71,312	80,633	103,743	13.1	45.5

Over the full CSA assessment area, the total sediment load increased by 21.2% and 56.9% over the baseline for the WRFG and HRM3 climate scenarios respectively. This load increase did not occur uniformly over the different land uses with the study area. The farmstead and road land use classes saw the lowest increases in

STONE ENVIRONMENTAL INC

sediment (<5% for the WRFG scenario). Hay and pasture land uses saw the largest increases in sediment load both showing greater than 100% increases under the HRM3 scenario. For total P, the load at the full CSA assessment area increased by 13.1% and 45.5% over the baseline for the WRFG and HRM3 climate scenarios respectively. This is 8%-11% less than the increase in sediment load. As was the case with sediment, the amount of change over the baseline varied widely over the different land uses. For the WFRG scenario, several land uses saw decreased in total P load (both farmstead classes, brush, and wetlands), with the greatest increase seen on hay, at 24.6%. For the HRM3 scenario, increases in total P load were significantly higher, ranging from a low of 5.1% for wetland up to a high of 98.8% for hay.

Although the magnitudes of the change in P loading rates does show variability across the land uses classes, a ranking of the land uses based on the average annual P loading rate shows that the land uses that ranked as highest P CSAs in the baseline scenario did not change for the future climate scenarios we considered. Those land uses that ranked lowest in P loading also stayed the same between the baseline conditions and the future scenarios, while for the uses in the middle range of P loading rates, there were some differences in rankings. This rankings comparison is shown graphically in Figure 3.32, where a rank of "1" signifies the highest total P loading rate and a value of 16 indicates the lowest loading rate. The data in Figure 3.32 suggest that designing BMPs and P reduction strategies based on an analysis if current climate conditions should target the same groups of P CSAs that will be important in reducing well into the future.

Figure 3.32: Comparison of total P loading rate rankings for baseline and future climate scenarios.
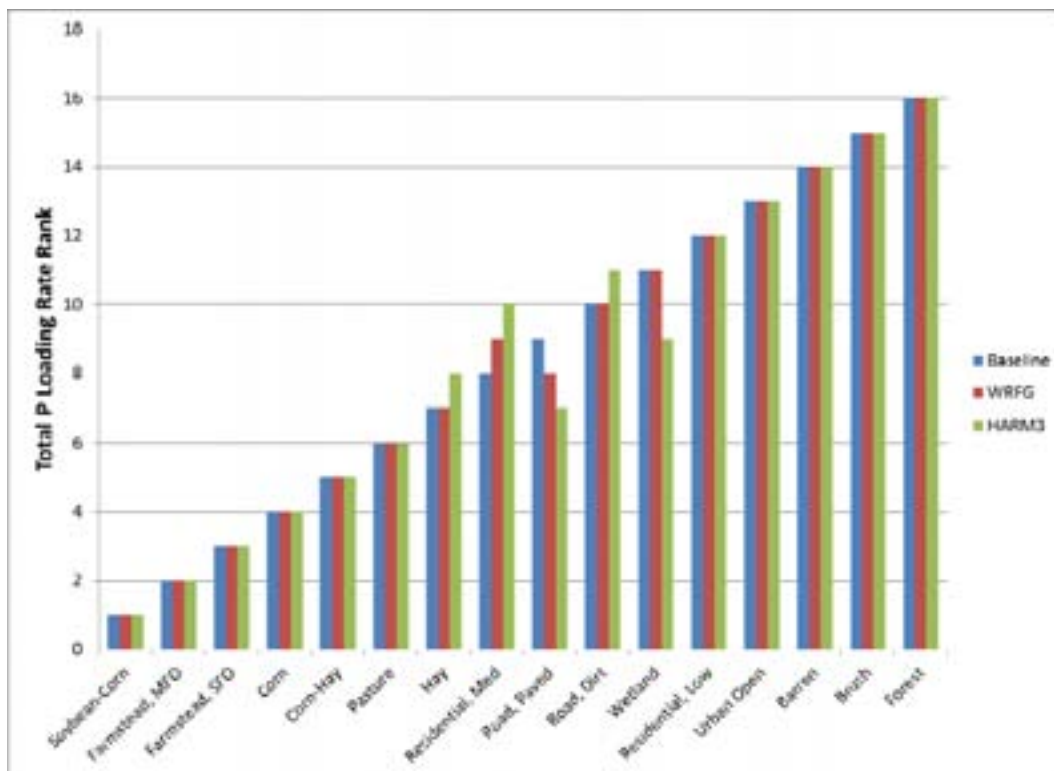
The distribution of sediment and P sources between upland and channel sources was also assessed for the baseline and future climate scenarios. These results are summarized in Table 3.31 and 3.32 for sediment and P respectively. While the total upland sediment and P contributions increase for both future climate scenarios,

STONE ENVIRONMENTAL INC

the channel bank contributions decrease for the WRFG scenario, but increase for the HARM3 scenario. For both sediment and P, the fraction of total load coming from upland sources is projected to rather consistent between the baseline and future climate scenarios, ranging between 69% and 75% for sediment and 70% and 74% for P.

Table 3.31. Change in upland and channel sediment sources under future climate scenarios, CSA assessment area.

| | Average Annual Load (tons) | | | Percent of Total Load (%) | | | Load Change (%) | |
| | | WRFG | HRM3 | | WRFG | HRM3 | WRFG | HRM3 |
Source	**Baseline**	**ccsm**	**hadcm3**	**Baseline**	**ccsm**	**hadcm3**	**ccsm**	**hadcm3**
Uplands	103,483	125,412	162,408	68.8	74.8	70.8	21.2	56.9
Channel Bank	47,036	42,188	67,135	31.2	25.2	29.2	-10.3	42.7
Total	150,519	167,599	229,543	100.0	100.0	100.0	11.3	52.5

Table 3.32. Change in upland and channel P sources under future climate scenarios, CSA assessment area.

| | Average Annual Load (kg) | | | Percent of Total Load (%) | | | Load Change (%) | |
| | | WRFG | HRM3 | | WRFG | HRM3 | WRFG | HRM3 |
Source	**Baseline**	**ccsm**	**hadcm3**	**Baseline**	**ccsm**	**hadcm3**	**ccsm**	**hadcm3**
Uplands	71,312	80,633	103,743	69.7	74.4	70.2	13.1	45.5
Channel Bank	30,957	27,760	43,947	30.3	25.6	29.8	-10.3	42.0
Total	102,269	108,392	147,690	100.0	100.0	100.0	6.0	44.4

Assessing the potential impacts of projected climate change on P loading and P critical source areas in the Vermont sector of the has shown a range in projected increases under the specific climate change scenarios evaluated, from between 6% and 44% for combined upland and channel P sources. The ranking of P loading by land use suggests that the land uses targeted for mitigation based on current climate conditions will provide similar benefit under a changing climate scenario.

3.7. Future MBB SWAT Model Assessments

The MBB SWAT model was developed for the explicit purpose of identifying the locations of P critical source areas at the field and sub-field level. The data collection, model development, and model calibration efforts were focused on sediment and phosphorus. As such, use of the model in the assessment of other pollutants, such as nitrogen and pesticides, would not be appropriate without the consideration of additional inputs and parameters. The MBB model is, however, well suited to further P-based assessments that may be of interest in the future. This includes basin-wide assessments of alternative BMPs, such as vegetated filter strips, grassed waterways, or modified tillage practices. It may also include the assessment of alternative strategies for BMP implementation, or the beneficial effects of combined BMPs. In addition to basin-wide studies, the model could be used to conduct refined analysis at the sub-watershed scale using site specific data, were it to become

STONE ENVIRONMENTAL INC

available for a broader group of farms. Finally, given the interest in global change, the model could be used to both further evaluate future climate conditions, as well as to assess the impacts of land use change.

The MBB SWAT model has been provided to the LCBP as a work product from this project. The model is on the higher end of complexity for SWAT model applications. It requires considerable resources, both computational and human, to manage. Building the model, populating its inputs, and processing the outputs required custom methods that are beyond those available in the standard SWAT interfaces. The MBB SWAT model has the potential for continued use in addressing questions concerning environmental quality and phosphorus source areas within the MBB; however, in its current form, future application of the model will only be practical for expert SWAT modelers. The possibility does exist for the development of management tools that integrate with the MBB SWAT model to allow natural resource managers, agronomists, and crop consultants to evaluate alternative management practices through a streamlined and simplified user interface. This approach would enable the non-expert user to address a pre-defined set of alternative land management scenarios and obtain output that helps enable data-driven, informed decisions.

STONE ENVIRONMENTAL INC

4. SUMMARY AND CONCLUSIONS

The restoration of Missisquoi Bay is not a short-term proposition that will be measured in months of even a handful of years. Reducing excessive phosphorus inputs to Missisquoi Bay in order to address the most critical and controllable case of algae blooms is a matter of steady, deliberate action to improve the health of the watershed. Because the technical and financial resources available for this work are limited, it is essential to have high quality information that can help target and set priorities at a variety of scales. The MBB SWAT allows for an "apples-to-apples" comparison of different land-use categories at a number of different scales.

The model offers a watershed-scale view that assesses the total contributions of P from various sources. Reviewing results at this scale shows that some land uses within the watershed produce a disproportionately high amount of P relative to the fraction of the total watershed area they represent. For example, while agricultural land uses represent 17% of the total land area in the MBB, they contribute nearly 65% of the total P load. Similarly, developed land uses (residential areas and roads) account for less than 3% of the watershed area, but contribute approximately 6% of the total P load.

The MBB SWAT model is also able to evaluate the P load associated with more discrete landscape units, beginning with major sub-watersheds, through smaller subbasins that were represented in the SWAT model, continuing down to the highest resolution landscape representation—the unique combinations of land use, soils, topographic characteristics that form a SWAT HRU. Identifying CSAs at multiple scales allows future management activities to be defined in terms of the major sub-watershed, subbasin, and field scale goals.

Working at these finer scales required that certain agronomic management operations such as tillage, planting, and harvest dates, manure or fertilizer application rates, and crop rotations be specified for each unit of cropland. And although information is available from AAFM about the number and types of conservation practices that have been implemented by HUC-12 watershed, the data could not be explicitly assigned to individual farmsteads or fields in the MBB. In considering options, we were reluctant to create a bias by assuming different practices/conditions for different fields in the watershed without complete data for all farms and all fields. As such, reasonable descriptions of agronomic operations, based on known conditions in the MBB, were developed and applied basin-wide.

Although this approach may tend to over-estimate the contribution of individual farmsteads and fields that currently receive a high level of management, the long-term simulation and uniform assumptions provide field-specific risk predictions that should hold great value for program managers in targeting the use of certain BMP interventions.

The model also clearly demonstrates the value of targeting BMPs to the areas of highest risk. For each BMP tested, significant benefit was realized by implementing the BMP on a targeted area representing the eligible land with the simulated highest P loading rates from the baseline simulation. The improvements in total P reduction following the targeted as opposed to random implementation were two to three-fold for the three BMP scenarios tested.

As would be expected, model results also demonstrated that the proximity of a particular critical source area to a surface water feature is quite important in estimating its relative impact. Specifically, giving consideration to proximity was able to allow important distinctions within an otherwise uniform ranking class that was largely driven by land use and soils to be made.

STONE ENVIRONMENT INC

A separate modeling analysis was also conducted of a single farm operation in the MBB. This model was designed to identify CSAs at the level necessary to determine individual management measures that could be expected to have the greatest success in reducing P loads. In addition, the farmer was interested in using the farm-specific model to quantify the benefits of practices he has already installed. The ability to produce meaningful results at this scale was heavily influenced by the agronomic records the farmer made available for the project. Without detailed, farm-specific data the value of this modeling analysis would have been greatly reduced.

In conclusion, the method used to identify CSAs in the MBB is a carefully constructed analytical approach that should have value to other efforts in the Champlain basin. That said, the MBB represents a unique set of land use, soil, slope, receiving water conditions and relied on a suite of data (e.g., LiDAR, CLU boundaries) that is not currently available basin-wde. Although it would be imprudent to simply extend the SWAT MBB model results to the rest of the Champlain basin, there are several key observations from this effort that should have broad application. These include:

- There is enormous value to long-term simulation. Wet weather events drive the annual phosphorus loads delivered to Missisquoi Bay, and are subject to a significant amount of year-to-year variability; coupled with on-going crop rotations, it is ensured that no two years will look the same. The value of a long-term simulation (in this case 30 years) is that it can smooth the variability, and identify particular land units will contribute the greatest pollution load over the long term.

- The model also demonstrates the value of targeting BMPs to the areas of highest risk. For each BMP tested, significant benefit was realized by implementing the BMP in the areas identified as having the highest P loading rates in the baseline scenario. From both an environmental quality and an economic perspective, choosing a targeted BMP implementation strategy offers clear benefits.

- Although it can be tempting to use all available data, it is important to avoid introducing bias into the model by relying on incomplete datasets. For example, farmers who have invested heavily in conservation practices are understandably interested in having these investments reflected in the model. The challenge, however, is that complete, spatially-referenced datasets of all of the conservation practices that have been implemented in the MBBare simply not available. To incorporate data on a case-by-case into the model is neither practical, nor particularly useful for improving model results.

- Higher resolution data on the location of surface water features has important influence on identifying the most significant CSAs. Land use, soils and slope tend to be the critical drivers in identifying CSAs, introducing more detailed information on the location of surface water features created important distinctions within an otherwise uniform ranking class.

The predicted effects of climate change do not appear to reorder implementation priorities. Although the magnitude of P loading rates are predicted to increase as a result of the changing climate, the land areas that ranked as the most significant P CSAs under current conditions did not change with future climate scenarios. The data suggest that designing BMPs and P reduction strategies based on an analysis of current climate conditions will target the same groups of P CSAs that will also be the most important under future climate conditions.

STONE ENVIRONMENTAL INC

5. REFERENCES

Abbaspour, M. C. 2009. SWAT-CUP2: SWAT Calibration and Uncertainty Programs - A User Manual. Department of Systems Analysis, Integrated Assessment and Modeling (SIAM), Eawag, Swiss Federal Institute of Aquatic Science and Technology, Duebendorf, Switzerland. 95pp.

American Sheep Industry Association, Inc. 2011. Website Directory of US Breeds of Sheep. Accessed March 2011. (http://www.sheepusa.org/resource/shbreeds.htm).

American Dairy Goat Association Website. 2011. Dairy Goat Facts. Accessed March 2011. (http://www.adga.org/facts.htm)

Arnold, J.G., P.M. Allen, R. Muttiah, and G. Bernhardt. 1995. Automated base flow separation and recession analysis techniques. Ground Water 33(6):1010-1018.

Arnold, J.G. and P.M. Allen. 1999. Automated methods for estimating baseflow and ground water recharge from streamflow records. J. Am. Water Resour. Assoc. 35(2):411-424.

Arnold, J. G., and N. Fohrer. 2005. SWAT2000: Current capabilities and research opportunities in applied watershed modeling. Hydrol. Process. 19(3):563-572.

Arnold, J.G., J.R. Williams, A.D. Nicks, and N.B. Sammons. 1990. SWRRB: A basin scale simulation model for soil and water resources management. Texas A&M Univ. Press, College Station, TX

Arnold, J. G., R. Srinivasan, R. S. Muttiah, and J. R. Williams. 1998. Large-area hydrologic modeling and assessment: Part I. Model development. J. American Water Resour. Assoc. 34(1): 73-89.

Allen, P.M., J.G. Arnold. 2005. SWAT-DEG Channel Stability Assessment. USDA/ARS Half Associates, Inc. Available at: http://www.brc.tamus.edu/swat/3rdswatconf/PDF/Session_III/Allen.pdf.

Bagnold, R.A. 1977. Bed load transport by natural rivers. Water Resour. Res. 13:303-312.

Band, L. E.1986. Topographic partition of watersheds with digital elevation models. Water Resour. Res. 22(1):15-24.

Beaudin, I. 2010a. Watershed boundary recommendation for Québec. IRDA, Québec, Québec, personal communication.

Beaudin, I. 2010b. Interpretation of agricultural land use classification in Québec, IRDA, Québec, Québec, personal communication.

Bekele, E.G., and J.W. Nicklow. 2007. "Multi-objective automatic calibration of SWAT using NSGA-II." J. Hydrol. 341(3-4):165–176.

Beven, K. J. 1986. Hillslope runoff processes and flood frequency characteristics. In Hillslope Processes, edited by A.D. Abrahams. pp. 187-202.

Beven, K. and Binley, A., 1992. The future of distributed models - model calibration and uncertainty prediction. Hydrological Processes, 6(3): 279-298.

Beven, K.J. and Kirkby, M.J., 1976. Towards a simple physically-based variable contributing model of catchment hydrology. School Geogr., Univ. of Leeds, Leeds, Work. Pap. No. 154.

Beven, K.J., and M.J. Kirkby. 1979. A physically-based, variable contributing area model of basin hydrology. Hydrol. Sci. Bull. 24:43–69.

STONE ENVIRONMENTAL INC

Borah, D.K., Bera, M., 2004. Watershed-scale hydrologic and nonpoint-source pollution models: review of applications. Trans. ASAE 47:789–803.

Boyle, D.P., H.V. Gupta, and S. Sorooshian. 2000. "Toward improved calibration of hydrologic models: Combining the strengths of manual and automatic methods." Water Resour. Res. 36(12):3663–3674.

Brown, M.P., P. Longabucco, M.R. Rafferty, P.D. Robillard, M.F. Walter, and D.A. Haith. 1989. Effects of animal waste control practices on nonpoint-source phosphorusP loading in the West Branch of the Delaware River Watershed. J.Soil Water Cons. 44:67-70.

Budd, L. and D. W. Meals. 1994. Lake Champlain Nonpoint Source Assessment. Lake Champlain Basin Program, Technical Report 6a. 138 pp.

Bunte, K. and S. R. Abt, 2001. Sampling Surface and Subsurface Particle-Size Distributions in Wadeable Gravel- and Cobble-Bed Streams for Analyses in Sediment Transport, Hydraulics, and Streambed Monitoring. RMRS-GTR-74. Rocky Mountain Research Station, Fort Collins, CO.

Busteed, P. R., D. E. Storm, M. J. White, and S. H. Stoodley. 2009. Using SWAT to target critical source sediment and phosphorus areas in the Wister Lake basin, USA. American J. Environ. Sci.5(2): 56-163.

CADMUS. 2010. Total Maximum Daily Load and Watershed Management Plan for Total Phosphorus and Total Suspended Solids in the Lower Fox River Basin and Lower Green Bay.

Cassell, E.A., R.L. Kort, D. Braun. 1998. Dynamic Simulation Modeling for Watershed Ecosystem Analysis of Phosphorus Budgets. School of Natural Resources, University of Vermont. 230 pp.

Center for Rural Studies. 2004. Colchester Residential Survey. Center for Rural Studies, University of Vermont, Burlington.

Daly, C., R.P. Neilson, and D.L. Phillips, 1994: A Statistical-Topographic Model for Mapping Climatological Precipitation over Mountanious Terrain. J. Appl. Meteor., 33:140-158.

Daniel, T.C., Sharpley, A.N., Edwards, D.R., Wedepohl, R., Lemunyon, J.L., 1994. Minimizing surface water eutrophication from agriculture by phosphorus management. J. Soil Water Cons. 49:30–38.

Darby, H. 2011a. Recommendation for a common grass species for simulation of hay crops. University of Vermont Extension, St. Albans, VT, personal communication.

Darby, H. 2011b. Recommended crop rotation and agronomic practices for soybeans. University of Vermont Extension, St. Albans, VT, personal communication.

Di Luzio, M., and J.G. Arnold. 2004. "Formulation of a hybrid calibration approach for a physically based distributed model with NEXRAD data input." J. Hydrol. 298(1-4):136–154.

Diodato, N. 2005. "The influence of topographic co-variables on the spatial variability of precipitation over small regions of complex terrain." International Journal of Climatology 25(3):351–363.

DiPietro, L. 2011a. Verification of farmstead classifications. Vermont Department of Agriculture, Food, & Markets, Montpelier, VT, personal communication.

DiPietro, L. 2011b. Estimation of animal grazing frequency. Vermont Department of Agriculture, Food, & Markets, Montpelier, VT, personal communication.

Duan, Q., V. K. Gupta, and S. Sorooshian. 1992. Effective and efficient global optimization for conceptual rainfall-runoff models, Water Resour. Res. 28:1015–1031.

STONE ENVIRONMENTAL INC

Dunne, T., and Black, R. D. 1970. "Partial area contributions to storm runoff in a small New England watershed." Water Resour. Res. 6:1296–1311.

Dunne, T., 1978. Field studies of hillslope flow processes. In: M.J. Kirkby (Editor), Hill slope Hydrology, Ch. 7. Wiley, London, pp. 227-293.

Easton, Z.M., Foka, D.R., Walter, M.T., Cowan, D.M., Schneiderman, E.M., Steenhuis, T.S., 2008. Re-conceptualizing the soil and water assessment tool (SWAT) model to predict runoff from variable source areas. J. Hydrol.348, 279–291.

Eckhardt K, Haverkamp S, Fohrer N, Frede HG. 2002. SWAT-G a version of SWAT99Đ2 modified for application to low mountain range catchments. Physics and Chemistry of the Earth 27(9/10): 641–644.

Engman, E.T. 1983. Roughness coefficients for routing surface runoff. Proc. Spec. Conf. Frontiers of Hydraulic Engineering.

Engman, E.T. 1986. Roughness coefficients for routing surface runoff. J. Irrigation and Drainage Eng. ASCE 112(1): 39-53.

ESRI. 2010. ArcHYDRO Tools.

Feyereisen, GW, TC Strickland, DD Bosch, and DG Sullivan. 2007. "Evaluation of SWAT manual calibration and input parameter sensitivity in the Little River watershed." Trans. ASAE. 50(3):843–855.

Fischenich, J. C., 2001. Stability Thresholds for Stream Restoration Materials. ERDC TN-EMRRP-SR-29. US Army Engineer Research and Development Center, Vicksburg, MS.

FISRWG, 1998. Stream Corridor Restoration: Principals, Processes, and Practices. The Federal Interagency Stream Restoration Working Group (FISRWG) (15 Federal Agencies of the US Government). GPO Item No. 0120-A; SuDocs No. A 57.6/2:EN 3/PT.653. ISBN-0-934213-59-3.

Frankenberger, J.R., E.S. Brooks, M.T. Walter, M.F. Walter, and T.S. Steenhuis. 1999. A GIS-based variable source area hydrologic model. Hydrol. Process. 13:805–822.

Fredlund, M.D., D.G. Fredlund, and G.W. Wilson. 2000. An equation to represent grain-size distribution. Can. Geotech. J. 37:817–827.

Frink, C.R. 1991. Estimating nutrient exports to estuaries. J. Environ. Qual. 20:717-724.

Gaddis, E.J.B. 2007. Landscape modeling and spatial optimization of watershed interventions to reduce phosphorus load to surface waters using a process-oriented and participatory research approach: A case study in the St. Albans Bay watershed, Vermont. Ph.D. Dissertation, Rubenstein School of Environment and Natural Resources, University of Vermont, Burlington.

Gassman, P.W., M.R. Reyes, C.H. Green, and J.G. Arnold, 2007. The Soil and Water Assessment Tool: Historical Development, Applications, and Future Research Directions. Trans. ASABE 50(4):1211-1250.

Gassman P.W., Arnold J.G., Srinivasan R., Reyes M. 2010. The worldwide use of the SWAT Model: Technological drivers, networking impacts, and simulation trends. In Proceedings of the Watershed Technology Conference, February 21-24. Costa Rica: American Society of Agricultural and Biological Engineers, Earth University.

Gburek, W.J., A.N. Sharpley, and G.J. Folmar, 2000a. Critical areas of phosphorus exportfrom agricultural watersheds. In: Sharpley, A.N. (Ed.), Agriculture and Phosphorus Management. Lewis Publishers, Boca Raton, pp. 83–104.

STONE ENVIRONMENTAL INC

Gburek, W.J., Sharpley, A.N., Heathwaite, L., Folmar, G.J., 2000b. Phosphorus management at the watershed scale: a modification of the phosphorus index. J. Environ. Qual. 29:130–144.

Gessler, P., I. Moore, N. McKenzie and P. Ryan. 1995. Soil-landscape modelling and spatial prediction of soil attributes. Int. J. Geogr. Inf. Sci. 9:421-432.

Ghebremichael, L. T., T. L. Veith, M. C. Watzin. 2010. Determination of critical source areas for phosphorus loss: Lake Champlain basin, Vermont. Trans. ASABE 53(5): 1595-1604.

Giroux, M., M. Duchemin, A. Michaud, I. Beaudin, C. Landry, P. Enright, C. Madromootoo, and M. Laverdiere, 2008. Relation Entre Les Concentrations En Phosphore Particulaire Et Dissous Dans Les Eaux De Ruissellement Et Les Teneurs En P Total Et Assimilable Des Sols Pour Differentes Cultures Agrosolutions 19(1).

Gitau, M.W., W.J. Gburek, and P.L. Bishop. 2008. Use of the SWAT model to quantify water quality effects of agricultural BMPs at the farm-scale level. Trans. ASABE. 51:1925-1936.

Griffin, M.L., Beasley, D.B., Fletcher, J.J and Foster, G.R. (1988) Estimating soil loss on topographically non-uniform field and farm units. J. Soil Water Cons. 43:326-331.

Gupta, H. V., S. Sorooshian, and P. O. Yapo. 1999. Status of automatic calibration for hydrologic models: Comparison with multilevel expert calibration. J. Hydrologic Eng. 4(2):135-143.

Harmel, R. D., R. J. Cooper, R. M. Slade, R. L. Haney, and J. G. Arnold. 2006. Cumulative uncertainty in measured streamflow and water quality data for small watersheds. Trans. ASABE 49(3): 689-701.

Harmel, R. D., and P. K. Smith. 2007. Consideration of measurement uncertainty in the evaluation of goodness-of-fit in hydrologic and water quality modeling. J. Hydrology 337(3-4): 326-336.

Heathewaite, A.L., A.N Sharpley, and W.J Gburek. 2000. A conceptual approach for integrating phosphorus and nitrogen management at watershed scales. J. Environ. Qual. 29:159–166.

Heinrichs J, Lammers B. 1998. Monitoring Dairy Heifer Growth. University Park, PA: Pennsylvania State University College of Agricultural Sciences. 16 pp.

Hewlett, J.D. and Hibbert, A.R. 1967. Factors affecting the response of small watersheds to precipitation in humid regions. IN Forest Hydrology (eds. W.E. Sopper and H.W. Lull). Pergamon Press, Oxford. pp. 275-290.

Hewlett, J.D. and W.L. Nutter. 1970. The varying source area of streamflow from upland basins. Proceedings of the Symposium on Interdisciplinary Aspects of Watershed Management. held in Bozeman, MT. August 3-6, 1970. pp. 65-83. ASCE. New York

Hill, C.M., J. Duxbury, L. Geohring, and T. Peck. 2000. Designing constructed wetlands to remove phosphorus from barnyard runoff: A comparison of four alternative substrates. Journal of Environmental Science and Health, Part A. 35:1357-1375.

Hively W.D., P. Gerard-Marchant, and T.S. Steenhuis. 2006. Distributed hydrological modeling of total dissolved phosphorus transport in an agricultural landscape, Part II: dissolved phosphorus transport. Hydrol. and Earth System Sci. 10:263-276.

Hively, W.D., R.B. Bryant, and T.J. Fahey. 2005. Phosphorus concentrations in overland flow from diverse locations on a New York dairy farm. J.Environ.Qual. 34:1224-1233.

Horton, R. E. 1933. The role of infiltration in the hydrologic cycle. Eos Trans. AGU. 14: 446-460.

STONE ENVIRONMENTAL INC

James, W., L.E. Rossman, W.C. Huber, R.E. Dickinson, W.R.C. James, L.A. Roesner, and J.A. Aldrich. 2008. User's Guide to SWMM 5. CHI, Guelph, Ontario, Canada.

Jokela, W.E., F. Magdoff, R. Bartlett, S. Bosworth, and D. Ross. 2004. Nutrient Recommendations for Field Crops in Vermont. University of Vermont Extension, University of Vermont, Burlington.

Johnson, T. E., J.B. Butcher, A. Parker, and C.OP. Weaver. 2011. Investigating the Sensitivity of US Streamflow and Water Quality to Climate Change: The USEPA Global Change Research Program's "20 Watersheds" Project. J. Water Resour. Planning Manage. (In press).

Julian, J. P. and R. Torres. 2006. Hydraulic Erosion of Cohesive river banks. Geomorphology, 76:193-206.

Ketterings, Q.M. 2005. Soil Test Conversion Tool for New York v. 7 www.nmsp.cals.cornell.edu/software/Morganequiv7.xls [accessed October 19, 2011]

Kim, N.W., I.M. Chung, Y.S. Won, J.G. Arnold. 2008. Development and application of the integrated SWAT-MODFLOW model. J. Hydrology. 356: 1-16.

Knisel, W. G. 1980. CREAMS: A field-scale model for chemicals, runoff and erosion from agricultural management systems. USDA Conservation Research Report 640pp.

IRDA 2010a. Daily weather data for Québec sites near the MBB. personal communication.

IRDA 2010b. Land cover data for the Québec portion of the MBB. personal communication.

IRDA. 2011a. Soils Inputs for the Québec portion of the MBB. Québec, Québec, personal communication.

IRDA. 2011b. Animal Unit Data for Québec. Québec, Québec, personal communication.

Lake Champlain Committee. 2004. A Survey of Citizen Awareness of Stormwater Pollution Issues in Chittenden County. Final 319 Grant Project Report, Grant #: WQ2003-319-SWMP-01.

Lake Champlain Sea Grant, University of Vermont, and City of Burlington. 2003. Englesby Brook Restoration Residential Survey.

LCBP. 2010. Opportunities for Action Management Plan. Lake Champlain Basin Program, Grand Isle, VT http://plan.lcbp.org/

Leonard, R.A., W.G. Knisel, and D.A. Still. 1987. GLEAMS: Groundwater loading effects on agricultural management systems. Trans. ASAE 30(5):1403-1428.

Manning , M.J., R.H. Sullivan, and T.M. Kipp. 1977. Nationwide Evaluation of Combined Sewer Overflows and Urban Stormwater Discharges, Volume III: Characterization of Discharges. EPA-600/2-77-064c. US Environmental Protection Agency, Office of Research and Development. Cincinnati, OH.

McCool, D.K., L.C. Brown, and G.R. Foster.1987.Revised slope steepness factor for the Universal Soil Loss Equation. Trans. ASAE 30:1387-1396.

McCool, D.K., G.R. Foster, C.K. Mutchler, and L.D. Meyer. 1989. Revised slope length factor for the Universal Soil Loss Equation. Trans. ASAE, 32: 1571-1576.

McDowell, R. W. and R. J. Wilcock, 2007. Sources of Sediment and Phosphorus in Stream Flow of a Highly Productive Dairy Farmed Catchment. J. Environ. Qual. 36(2):540-548.

McElroy, A.D., S.Y. Chiu, J.W. Negben, A. Aleti, and F.W. Bennett. 1976. Loading functions for assessment of water pollution from non-point sources. EPA 600/2-76-151, Midwest Research Institute, Kansas City,MO, USA.

STONE ENVIRONMENTAL INC

Meals, D.W. and L.F. Budd. 1998. Lake Champlain Basin nonpoint source assessment. J. Am. Water Resour. Assoc. 34(2):251-265.

Michaud, A. R., I. Beaudin, J. Deslandes, F. Bonn, and C. A. Madramootoo. 2007. SWAT-predicted influence of different landscape and cropping system alterations on phosphorus mobility within the Pike River watershed of south-western Québec, Can. J. Soil Sci. 87:329-344.

Michaud, A. 2011a. Recommendation for agronomic practices in Québec. IRDA, Québec, Québec, personal communication.

MN Dept Ag. 1995. Useful Nutrient Management Data. Minnesota Department of Agriculture, St. Paul, MN.

Moore, I., P. Gessler, G. Nielsen and G. Peterson. 1993. Soil attribute prediction using terrain analysis. Soil Sci. Soc. Am. J. 57:443-443.

Moriasi, D.N., J.G. Arnold, M.W. Van Liew, R.K. Bingner, R.D. Harmel, T. Veith. 2007. Model evaluation guidelines for systematic quantification of accuracy in watershed simulations. Trans. ASABE. 50(3):885-900.

Muleta, M.K., and J.W. Nicklow. 2005. "Sensitivity and uncertainty analysis coupled with automatic calibration for a distributed watershed model." J.Hydrol. 306(1-4):127–145.

Nakicenvoic et al., 2000. Special Report on Emissions Scenarios. A Special Report of Working Group III of the Intergovernmental Panel on Climate Change. Cambridge University Press: Cambridge. 599 pp.

Narasimhan, B. 2011. Modification to the SWAT 2009 code to address bank erosion. Department of Civil Engineering, Indian Institute of Technology Madras, Tamil Nadu, India. personal communication.

National Agricultural Statistics Service. 2010. 2009 Cropland Data Layer. Available at http://www.nass.usda.gov/research/Cropland/SARS1a.htm.

Nash, J. E., and J. V. Sutcliffe. 1970. River flow forecasting through conceptual models: Part 1. A discussion of principles. J. Hydrology 10(3): 282-290.

National Pork Producers Council. 1998-99 Pork Facts. Des Moines, IA. June 1998.

NCDC. 2010. National Climatic Data Center, weather data download web site. http://www.ncdc.noaa.gov/oa/ncdc.html.

Neitsch, S.L., J. G. Arnold, J. R. Kiniry, and J. R. Williams. 2011. Soil and Water Assessment Tool theoretical documentation version 2009. Texas Water Resources Institute. TR-406. 647 pp..

Neitsch, S. L., J. G. Arnold, J. R. Kiniry R. Srinivasan, and J. R. Williams. 2009. Soil and Water Assessment Tool input/output documentation version 2009. Available at http://swatmodel.tamu.edu/documentation.

Noll, M. R., A. E. Szatkowski, and E. A. Magee, 2009. Phosphorus Fractionation in Soil and Sediments Along a Continuum from Agricultural Fields to Nearshore Lake Sediments: Potential Ecological Impacts. Journal of Great Lakes Research 35:56-63.

NRCS. 2007. National Engineering Handbook, Part 630 Hydrology. pp. 7-2 – 7-3.

O'Loughlin, E. M. 1981. Saturation regions in catchments and their relations to soil and topographic properties. J. Hydrol. 53: 229-246.

Ouyang, W., F. Hao, and X. Wang. 2007. Regional nonpoint-source organic pollution modeling and critical area identification for watershed best environmental management. Water Air Soil Pollution 187: 251-261.

STONE ENVIRONMENTAL INC

Parker, A. 2011. Daily weather time series representative of baseline and future climate scenarios for Enosburg Falls, Vermont. Tetra Tech, Fairfax, VA. personal communication.

Perkins, E. 2011. Recommendations on climate change scenarios representing the range is projected P loading. USEPA, Region I, Boston, MA, personal communication.

Peuker, T. K. and D. H. Douglas. 1975. Detection of surface-specific points by local parallel processing of discrete terrain elevation data. Comput. Graphics Image Process. 4:375-387.

Pionke, H.B., W.J. Gburek, and A.N. Sharpley. 2000. Critical source area controls on water quality in an agricultural watershed located in the Chesapeake Basin. Ecol. Eng. 14:325–335.

Pitt, R., D. Williamson, J. Voorhees, and S. Clark. 2004. Chapter 12: Review of historical street dust and dirt accumulation and washoff data. *In* Effective Modeling of Urban Water Systems, Monograph 13. W. James, K.N. Irvine, E.A. McBean, and R.E. Pitt eds. CHI, Guelph, Ontario, Canada.

Pote, D.H., Daniel, T.C., Sharpley, A.N., Moore, P.A., Edwards, D.R., Nichols, D.J., 1996. Relating extractablesoil phosphorus to phosphorus losses in runoff. Soil Sci. Soc. Am. J. 60:855–859.

Potter, K. 2011. Recommendations for tile drainage identification in Missisquoi Basin sub-watersheds. USDA-NRCS-VT, Colchester, VT, personal communication.

Potter, K. 2011b. Classification of pasture land cover. USDA-NRCS-VT, Colchester, VT, personal communication.

PRISM Climate Group at Oregon State University. 2006a. United States Average Monthly or Annual Precipitation, 1971 – 2000. Corvallis, Oregon, USA.

PRISM Climate Group at Oregon State University. 2006b. Average Monthly or Annual Maximum Temperature, 1971-2000. Corvallis, Oregon, USA.

PRISM Climate Group at Oregon State University. 2006c. United States Average Monthly or Annual Minimum Temperature, 1971 - 2000. Corvallis, Oregon, USA.

Quinn, P., Beven, K., Chevallier, P., Planchon, O., 1991. The prediction of hillslope flow paths for distributed hydrological modeling using digital terrain models. Hydrol. Proc. 5:59–79.

Refsgaard, JC, and B. Storm. 1996. Construction, calibration and validation of hydrological models, In: Distributed Hydrological Modelling. pp 41-54. .

Refsgaard, J.C., R. Grayson, and G. Bloschl. 2001. Towards a formal approach to calibration and validation of models using spatial data. Cambridge University Press, Journals, 40 West 20 th Street New York NY 10011-4211 USA.

Regional Stormwater Education Program, Center for Rural Studies, University of Vermont. 2007. Stormwater Opinions and Behaviors in Chittenden County, Vermont. Center for Rural Studies, University of Vermont, Burlington.

Regional Stormwater Education Program, Lake Champlain Committee, Center for Rural Studies, University of Vermont. 2008. Awareness, Knowledge, Opinions, and Behaviors Related to Stormwater in Chittenden County, Vermont. Center for Rural Studies, University of Vermont, Burlington.

Runkel, R.L., Crawford, C.G., and Cohn, T.A. 2004. Load Estimator (LOADEST): A FORTRAN Program for Estimating Constituent Loads in Streams and Rivers: US Geological Survey Techniques and Methods Book 4, Chapter A5, 69 p.

STONE ENVIRONMENTAL INC

Sammons, N. 2010. SWAT 2009 source code. USDA Grassland Soil and Water Research Laboratory, Temple, TX, personal communication.

Beaudin, I. 2010a. Watershed boundary recommendation for Québec. IRDA, Québec, Québec, personal communication.

Sartor, J.D. and G.B. Boyd. 1972. Water Pollution Aspects of Street Surface Contaminants. EPA-R2-72-081 (NTIS PB-214408). US Environmental Protection Agency, Washington, D.C.

Schellinger, G.R. and J.C. Clausen. 1992. Vegetative filter treatment of dairy barnyard runoff in cold regions. J. Environ. Qual. 21:40-45.

Sekely, A. C., D. J. Mulla, and D. W. Bauer, 2002. Streambank Slumping and Its Contribution to the Phosphorus and Suspended Sediment Loads of the Blue Earth River, Minnesota. Journal of Soil and Water Conservation 57(5):243-250.

Soil Conservation Service Engineering Division. 1986. Urban Hydrology for Small Watersheds. US Department of Agriculture. Technical Release 55.

Sharpley, A.N. 1995. Dependence of runoff phosphorus on extractable soil phosphorus. J. Environ. Qual. 24:920–926.

Sharpley, A. 1999. Agricultural phosphorus, water quality, and poultry production: Are they compatible? Poult. Sci. 78:660–673.

Sharpley, A.N., Chapra, S.C., Wedepohl, R., Sims, J.T., Daniel, T.C., Reddy, K.R., 1994. Managing agricultural phosphorus for protection of surface waters: issues and options. J. Environ. Qual. 23:437–451.

Simon, A., Bingner, R. L. Langendoen, E. J. and C.V. Alonso. 2002. Actual and reference sediment yields for the James Creek Watershed –Mississippi. Channel and Watershed Processes Research Unit, National Sedimentation Laboratory. Oxford, Mississippi. 202 pp.

Simon A. 2011. Bank Stability and Toe Erosion Modeling of the Missisquoi Basin in Vermont. Presentation to the Lake Champlain Basin Program, September 19, 2011. Personal communication.

Sims, J.T., Edwards, A.C., Schoumans, O.F., Simard, R.R. 2000. Integrating soil phosphorus testing into environmentally based agricultural management practices. J. Environ. Qual. 29:60–71.

Sivertun, A. and L. Prange. 2003. Non-point source critical area analysis in the Gisselo¨ watershed using GIS. Environ. Modelling Software 18:887–898.

Smith, C., and B. Croke. 2005. "Sources of uncertainty in estimating suspended sediment load." P. 136 in Sediment budgets: proceedings of the International Symposium on Sediment Budgets: held during the Seventh Scientific Assembly of the International Association of Hydrological Sciences (IAHS) at Foz do Iguaço, Brazil, 3-9 April, 2005, vol. 2.

Solomon MF. 2010. Swat modeling of sediment, nutrients and pesticides in the Le-Sueur River watershed, south-central Minnesota. Ph.D. Thesis Dissertation. University of Minnesota Digital Conservancy.

Sonnen, M.B. 1980. Urban runoff quality: Information needs. J.Tech. Councils. ASCE, 106:29-40.

Sonneveld M.P.W., J.M. Schoorl, and A. Veldkamp. 2006. Mapping hydrological pathways of phosphorus transfer in apparently homogeneous landscapes using a high-resolution DEM. Geoderma 133:32–42.

Srinivasan, M.S., Gburek, W.J., Hamlett, J.M., 2002. Dynamics of stormflow generation – a hillslope-scale field study in east-central Pennsylvania, USA. Hydrol. Proc. 16:649–665.

STONE ENVIRONMENTAL INC

Srinivasan, M. S., P. Gerard-Marchant, T. L. Veith, W. J. Gburek, and T. S. Steenhuis. 2005. Watershed scale modeling of critical source areas of runoff generation and phosphorus transport. J. American Water Resour. Assoc.41(2): 361-375.

Srinivasan, R. 2010. SWAT PCP tool for interpolation of weather time series to SWAT subbasins. Texas A&M University, College Station, TX. personal Communication.

Statistics Canada. 2006. 2006 Census of Agriculture. http://www.statcan.gc.can/ca-ra2006/index-eng.htm.

Stuntebeck, T.D. 1995. Evaluating barnyard best management practices in Wisconsin using upstream-downstream monitoring. USGS Fact Sheet FS-221-95.

Stuntebeck, T.D. 2011. USGS, Madison, WI, personal communication,.

Tarboton, D. G. 1997. "A New Method for the Determination of Flow Directions and Contributing Areas in Grid Digital Elevation Models. Water Resources Research, 33(2):309-319.

Tarboton DG. 2010: Hydrology Research Group-Terain Analysis Using Digital Elevation Models (TauDEM)." Accessed October, 2010 (http://hydrology.usu.edu/taudem/taudem5.0/downloads.html).

Texas A&M University. 2011. SWAT Model Web Site. http://swatmodel.tamu.edu/.

Tilley, J. 2011.. Agricultural Testing Laboratory, Plant & Soil Science Department, University of Vermont, Burlington, personal communication.

Tomer M., M. Dosskey, M. Burkart, D.James, M. Helmers, and D. Eisenhauer, 2005. Placement of Riparian Forest Buffers to Improve Water Quality. *In Proceedings of:* Moving Agroforestry into the Mainstream, Proceedings of the 9th North American Agroforest Conference. K. Brooks and P. Ffolliot (Editors), Department of Forest Resources, University of Minnesota, St. Paul, MN, Rochester, MN.

Troy, A., D. Wang, D. Capen.2007. Updating the Lake Champlian Basin Land Use Data to Improve Prediction of Phosphorus Loading, Lake Champlain Basin Program Technical Report No. 54. 116 pp.

US Department of Agriculture. 1992. Chapter 4, Agricultural Waster Characteristics. Agricultural Waste Management Field Handbook. 28 pp.

USDA-NASS. 2009. Census of Agriculture - 2007 Census Publications for the VT State Counties. Accesssed October, 2010 (http://www.agcensus.usda.gov/Publications/2007/).

USDA-NRCS 2008. Missisquoi area wide plan. A Watershed Approach to Improving Water Quality in Lake Champlain, VT.

USDA-NRCS, 2009. Soil Data Mart. Soil Survey Geographic (SSURGO) database for VT, Accessed July 2009. (http://soildatamart.nrcs.usda.gov/).

USGS. 1998. Evaluation of a method for comparing phosphorus loads from barnyards and croplands in the Otter Creek Watershed, Wisconsin. USGS Fact Sheet FS-168-98.

USGS. 2010. LiDAR Data for the Missisquoi Bay Basin, Eastern Section.

UVM Spatial Analysis Lab. 2006. Suburban and Pasture Fields, Grassland Study Area.

UVM Spatial Analysis Lab. 2007. 2001 Land Use Land Cover Dataset for Lake Champlain Basin.

UVM Spatial Analysis Lab. 2010. LiDAR Data for the Missisquoi Bay Basin, Rock River and Western Franklin County.

STONE ENVIRONMENTAL INC

van Griensven A, Bauwens W. 2005. Application and evaluation of ESWAT on the Dender basin and the Wister Lake basin. Hydrological Processes 19:827–838.

van Griensven, A., Meixner, T., 2006. Methods to quantify and identify the sources of uncertainty for river basin water quality models. Water Science and Technology. 53(1):51-59.

VTAAFM. 2008. Report to the Vermont Legislature 2009 pursuant to Sec. 1. 6 V.S.A. § 370 CONSUMER INFORMATION REGARDING FERTILIZER USE ON NONARICULTURAL TURF.

VTANR, 2009. Vermont Stream Geomorphic Assessment Protocol Handbooks: Remote Sensing and Field Surveys Techniques for Conducting Watershed and Reach Level Assessments (Http://Www.Anr.State.Vt.Us/Dec/Waterq/Rivers/Htm/Rv_Geoassesspro.Htm). Acquired via the internet May 17, 2007. Vermont Agency of Natural Resources, Department of Environmental Conservation, Division of Water Quality, River Management Program, Waterbury, VT.

Vermont Center for Geographic Information. 2010. E911 Road centerlines. Available at: http://www.vcgi.org/dataware/search_tools/moreinfo.cfm?catalog_id=1&layer_id=43&layer_name=EmergencyE911_RDS.

Vermont Methane Pilot Project. 2011. Vermont Department of Public Service. Accessed March, 2011. (http://publicservice.vermont.gov/energy-efficiency/ee_files/methane/methane.htm)

VT DEC. 2004. Basin 6, Missisquoi River watershed water quality and aquatic habitat assessment report. Vermont Agency of Natural Resources, Department of Environmental Conservation, Water Quality Division, Waterbury, VT.

VT DEC and NYS DEC. 2002. Lake Champlan Phosphorus TMDL. Vermont Agency of Natural Resources, Department of Environmental Conservation, Water Quality Division, Waterbury, VT.

Walter, M.T., Walter, M.F., Brooks, E.S., Steenhuis, T.S., Boll, J., Weiler, K., 2000. Hydrologically sensitive areas: variable source area hydrology implications for water quality risk assessment. J. Soil Water Cons. 55 (3):277–284.

Wang, F S; Roddick, F A ; Richardson, A J ; Curnow, R C. 1994. SWIM - interactive software for continuous improvement of solid waste management . J. Resour. Manage. Technol. 22(2):63-72.

Ward, R.C., 1984. On the response to precipitation of headwater streams in humid areas. J. Hydrol. 74:171–189.

Waschbusch, R.J., W.R. Selbig, and R.T. Bannerman. 2000. Sources of phosphorus in stormwater and street dirt from two urban residential basins in Madison, Wisconsin, 1994-95. *In* Proceeding of the National Conference on Tools for Urban Water Resource Management and Protection. February 7-10, 2000. EPA/625/R-00/001. US Environmental Protection Agency, Office of Research and Development, Cincinnati, OH.

Watson BM, McKeown RA, Putz G, MacDonald JD. 2009. Modification of SWAT for modelling streamflow from forested watersheds on the Canadian Boreal Plain. J. Environ. Eng. Sci. 7 (In press).

Western, A.W., R.B. Grayson, G. Bloschl, G.R. Willgoose and T.A. McMahon. 1999. Observed spatial organization of soil moisture and its relation to terrain indices. Water Resour. Res. 35:797-810.

White, M. 2011a. Initialization of SWAT soil P pools from Mehlich III soil test values. USAD-ARS, Grassland Soil and Water Research Laboratory. Personal communication.

White, M. 2011b. Biomass harvest operation modifications for SWAT code. USAD-ARS, Grassland Soil and Water Research Laboratory. Personal communication.

STONE ENVIRONMENTAL INC

Williams, J. R. 1969. Flood routing with variable travel time or variable storage coefficients. Trans. ASAE 12(1):100-103.

Williams, J.R. 1975. Sediment-yield prediction with universal equation using runoff energy factor. In Present and prospective technology for predicting sediment yield and sources: Proceedings of the sediment-yield workshop, USDA Sedimentation Lab., Oxford, MS, November 28-30, 1972. ARS-S-40. p. 244-252.

Williams, J.R. 1995. Chapter 25: The EPIC model. p. 909-1000. In V.P. Singh (ed). Computer models of watershed hydrology. Water Resources Publications, Highlands Ranch, CO.

Williams, J. R., C. A. Jones and P. T. Dyke. 1984. A Modeling Approach to Determining the Relationship between Erosion and Soil Productivity. Transactions of the ASAE 27(1):129-144.

Williams, J. R., R. C. Izaurralde, and E. M. Steglich. 2008. Agricultural Policy/Environmental eXtender model: Theoretical documentation version 0604. BREC Report # 2008-17. Temple, TX: Texas AgriLIFE Research, Texas A&M University, Blackland Research and Extension Center. Available at: http://epicapex.brc.tamus.edu/downloads/user-manuals.aspx. Accessed 31 January 2010.

Winchell, M., R. Srinivasan, M. Di Luzio, J. Arnold. 2010. ArcSWAT Interface for SWAT 2009. Blackland Research and Extension Center, Temple, TX. 495 pp.

Yang, W., and A. Weersink. 2004. Cost-effective targeting of riparian buffers. Can. J. Agric. Econ. 52:17–34.

Zhang, X., Srinivasan, R., 2009. GIS based spatial precipitation estimation: a comparison of geostatistical approaches. J. Am. Water Resour. Assoc. 45:894-906.

STONE ENVIRONMENTAL INC

APPENDICES

STONE ENVIRONMENTAL INC

Lake Champlain Basin Program / Identification of Critical Source Areas of Phosphorus Within the Vermont Sector of the Missisquoi Bay Basin / December 15, 2011   159

APPENDIX A: INITIAL MODEL PARAMETERIZATION

A.1. Definition of Upland Model Parameters

The following section provides information regarding key parameter choices made for initial upland parameters in the MBB SWAT model.

The SCS runoff curve numbers is one of the more important hydrologic parameters in SWAT. The adjustment of standard CN2 values based on the Compound Topographic Index (CTI) was described in Section 2.4.4. The baseline CN2 values selected for each land use and soil group are provided here in Table A.1.

Table A.1. Baseline CN2 values by land use and hydrologic group for the MBB SWAT model.

SWAT Land Use	CN-A	CN-B	CN-C	CN-D	Land Use Description from SWAT Manual, Tables 20-1, 20-2, 20-3
Barren	77	86	91	94	Fallow, Bare soil
Corn (grain)	64	75	82	85	Row Crop, Straight row, good condition, with residue
Corn (silage)	67	78	85	89	Row Crop, Straight row, good condition, no residue
Developed, Low Intensity (pervious fraction)	49	69	79	84	Open spaces (fair condition)
Developed, Med/High Intensity (pervious fraction)	49	69	79	84	Open spaces (fair condition)
Developed, Open	39	61	74	80	Open spaces (good condition)
Farmstead, MFO/LFO (pervious fraction)	49	69	79	84	Open spaces (fair condition)
Farmstead, SFO (pervious fraction)	49	69	79	84	Open spaces (fair condition)
Forest	30	55	70	77	Woods, good condition
Hay	30	58	71	78	Meadow, continuous grass, mowed for hay
Impervious areas	98	98	98	98	Roofs, roads, driveways, paved roads
Pasture	39	61	74	80	Pasture, good condition
Roads, Dirt (with right-of-way)	76	85	89	91	Gravel streets and roads (including right-of-way)
Roads, Paved (pervious fraction)	49	69	79	84	Open spaces (fair condition)
Soybean	64	75	82	85	Row Crop, Straight row, good condition, with residue
Un-managed Ag, Brush	30	48	65	73	Brush, brush-weed-grass mixture, good condition
Wetland	49	69	79	84	SWAT Crop Database Default, Wetlands/Mixed

STONE ENVIRONMENTAL INC

The Manning's N for overland flow was adjusted from the SWAT default values for each land use as shown in Table A.2.

Table A.2. Overland flow Manning's N values by land use.

SWAT Land Use	Manning's N	Source
Barren	0.05	Engman 1986, Fallow
Corn	0.09	Engman 1983, Conventional Tillage No Residue
Corn/Hay rotation	0.17	Engman 1983, Average of corn and hay
Developed, Low Intensity (pervious fraction)	0.15	Engman 1983, Grass, Short
Developed, Med/High Intensity (pervious fraction)	0.15	Engman 1983, Grass, Short
Developed, Open	0.15	Engman 1983, Grass, Short
Farmstead, MFO/LFO (pervious fraction)	0.15	Engman 1983, Grass, Short
Farmstead, SFO (pervious fraction)	0.15	Engman 1983, Grass, Short
Forest	0.8	Engman 1986, Woods Dense Underbrush
Hay	0.24	Engman 1983, Dense Grass
Pasture	0.24	Engman 1983, Dense Grass
Roads, Dirt (pervious fraction)	0.15	Engman 1983, Grass, Short
Roads, Paved (pervious fraction)	0.15	Engman 1983, Grass, Short
Soybean/Corn rotation	0.14	Engman 1983, average of Conventional Tillage with Residue and No Residue
Un-manged Ag, Brush	0.24	Engman 1983, Dense Grass
Wetland	0.4	Engman 1986, Woods light Underbrush

The initialization of inorganic soil phosphorus was based on the soil P analysis described in Section 2.2.4.2. The Mehlich III soil test P values were taken to represent the total of the SWAT labile and active mineral P pools (White 2011a). The fraction of the soil P in the labile pool versus the active mineral pool is a function of the phosphorus availability index parameter (PSP). Based on the SWAT default value for PSP (0.4) the SWAT initial soluble P values (SOL_SOLP) for each land use were determined. These are summarized in Table A.3. These labile P values were assigned to the first 3 soil layers in the SWAT soil profile. For undeveloped land and non-agricultural land uses, the value recommended in the SWAT manual (5 ppm) was assigned to all soil layers. The initial organic soil P in the MBB SWAT model was calculated by the model and was based upon the soil organic carbon fraction of the soil.

STONE ENVIRONMENTAL INC

It is acknowledged that the initial values assigned for labile soil P represent average conditions and that variability will exist across different areas with the same land use. It should be notes that this variability will occur in the SWAT model over time as the effects of the local land use, soils, topography, weather, and management effect the dynamic state of soil P. Over a long simulation period as was conducted with the MBB SWAT model, the effects of initial conditions become less important.

Table A.3. SWAT initial soluble P by land use.

SWAT Land Use	Crop 1 Median Mehlich III P (ppm)	Crop 2 Median Mehlich III P (ppm)	Crop Avg. Median Mehlich III P (ppm)	SOL_SOLP (ppm)
Corn	55.8	N/A	55.8	22.3
Corn/Hay rotation	55.8	38.7	47.3	18.9
Hay	38.7	N/A	38.7	15.5
Pasture	36	N/A	36	14.4
Soybean/Corn rotation	31.1	55.8	43.5	17.4
Residential lawns open space	30	N/A	30	12

The organic carbon fraction of the soil was initialized using a combination of the SSURGO soils database organic matter and organic matter data collected from the same UVM Agricultural Testing Laboratory from which the soil test P analysis was conducted (see Section 2.2.4.2). Soil organic carbon is calculated directly from soil organic matter using the standard conversion that organic carbon (%) = organic matter (%) / 1.724. Two constraints were put on the initial organic carbon fraction of the soil in the SWAT model. The first constraint addressed cases where the surface soil layer organic carbon was greater than 10 times the second soil layer. In these cases, the second layer organic carbon was assigned to the surface layer. This situation was found to occur mostly where a shallow (< 50 mm) litter layer was represented in a soil description. These situations have been found to result in excessive simulated organic nutrient transport, which was the reason for the adjustment. For deep organic soils, this process resulted in no adjustment. The second constraint was to use the UVM Agricultural Testing Laboratory data to constrain the organic matter and organic carbon from soils under agricultural use. The 75th percentile of organic matter and organic carbon was calculated for each land use reported in the UVM dataset. This 75th percentile value was set as the maximum allowed for the surface soil layer for a given land use in the SWAT model. This constraint was imposed in order to adjust for soils with reported high organic matter in a shallow surface layer that would have been lowered over time due to cultivation and mixing within the plow zone. The data from the UVM lab used in setting initial soil organic carbon values is shown in Table A.4.

STONE ENVIRONMENTAL INC

Table A.4. Soil organic matter/organic carbon by agricultural land use.

SWAT Land Use	Crop 1 75th Percetile OM (%)	Crop 2 75th Percetile OM (%)	Crop Avg. 75th Percetile OM (%)	Soil Orgainc Carbon (%)
Corn	5.9	N/A	5.9	3.4
Corn/Hay rotation	5.9	7.3	6.6	3.8
Hay	7.3	N/A	7.3	4.2
Pasture	8.7	N/A	8.7	5
Soybean/Corn rotation	5.4	5.9	5.7	3.3

Additional SWAT model parameters were initially set based on modeler experience and best judgment. Those parameters which different from the ArcSWAT default values are provided in Table A.5.

Table A.5. Initial values for general SWAT parameters.

Parameter Name	Parameter Description	Initial Value
SFTMP	Snowfall temp (C)	0
SMTMP	Snow melt base temp (C)	0.5
SMFMX	Max snow melt factor (mm/C-day)	4.5
SMFMN	Min snow melt factor (mm/C-day)	1.5
TIMP	Snow pack temperature lag factor	0.2
SNOCOVMX	Min snow water corresponding to 100% snow cover (mm)	50
PET Method	Method for calculating potential evapotranspiration	Hargreaves
SURLAG	Surface runoff lag coefficient	2
ALPHA_BF	Baseflow recession constant	0.04, 0.05, 0.06
GW_DELAY	Time delay from recharge to occur as baseflow (days)	3
REVAPMN	Threshold depth of water in shallow aquifer for revap to occur (mm)	250
DDRAIN	Depth to tile drains (mm)	914
TDRAIN	Time for tile to drain soil to field capacity (hr)	48
GDRAIN	Tile drain lag time (hr)	24

Notes:

1.) ALPHA_BF varied by subbasin elevation

STONE ENVIRONMENTAL INC

A.2. Definition of Channel Parameters

A.2.1. Mainstem Channel Data

This section describes the data collection and setting of initial parameter values for mainstem channels.

CH_W (m) – Channel Width

- Phase 2 data variable "bankfull_width" was averaged for the subbasin and assigned if available. In the Phase 2 assessment the bankfull width was measured in the field at multiple cross sections and the representative cross section bankfull width was chosen.

- If Phase 2 data were not available the cumulative drainage area at the outlet of the subbasin was used to estimate the width using the Vermont Hydraulic Geometry Curves (VTANR, 2009). The equation is W(ft) = 13.1*(DA(sq.mi.))^0.44. Subbasin mainstem channel width values estimated with this equation were found to be 17% larger than bankfull width values measured during the Phase 2 assessment. It is expected that the HGR estimate would be larger because the geomorphic assessment location is located further upstream larger than the SWAT subbasin drainage outlet used in the calculation.

- Phase 1 SGA width data were not used because it is also an estimate calculated using the Vermont Hydraulic Geometry Curves and calculating this variable based on subbasin drainage area is more accurate.

CH_D (m) – Channel Depth

- Phase 2 data variable "mean_depth" was averaged for the subbasin and assigned if available. In the Phase 2 assessment the depths were measured in the field at multiple cross sections and the representative value was reported.

- If Phase 2 data were not available the cumulative drainage area at the outlet of the subbasin was used to estimate the depth using the Vermont Hydraulic Geometry Curves (VTANR, 2006). The equation is D(ft) = 0.96*(DA(sq.mi.))^0.30. Subbasin mainstem channel depth values estimated with this equation were found to be 3% smaller than bankfull mean depth values measured during the Phase 2 assessment. This shows good agreement for this estimation method.

- The Phase 1 assessment does not have an estimation of depth.

CH_N – Manning's N-value

- Effective FEMA FIS studies were referenced to find n-values used (Table 1).

- If a specific stream was referenced in the FIS, the average n-value was assigned to the subbasin.

- Mainstem Missisquoi River n-values were assigned based on specific town n-value average or for towns not listed the average value of 0.041 was assigned for all but the Upper Missisquoi reaches which were assigned the average tributary value of 0.045.

- These estimates were in line with our initial guess from field work in the basin of a range between 0.040 to 0.045.

STONE ENVIRONMENTAL INC

- Estimates also were similar to a hydraulic study on the Black Creek using a range of 0.028 and 0.050.

- Geomorphic data of dominant bed particle appear to stratify by elevation (Figure A.1). This follows the general trend of decreasing particle size and channel roughness moving towards the outlet of a watershed (i.e., with decreasing elevation) (FISRWG, 1998). N-values were assigned based on this spatial distribution of bed particles in conjunction with typical values in the FEMA and other hydraulic studies. Subbasins with elevation <= 100 m were assigned an n of 0.040, elevation between 100 and 200 m were assigned an n of 0.045, and higher subbasins were assigned n-values of 0.050.

Table A.6. FEMA FIS Manning's N-values.

Municipality	FIS Date	River	Channel Min	Channel Max	Average
Enosburg	July 2, 1980	Missisquoi River	0.015	0.028	0.0215
Swanton	October 18, 1982	Missisquoi River	0.025	0.085	0.055
Richford	April 1, 1980	Missisquoi River	0.028	0.05	0.039
Berkshire	December 1, 1982	Missisquoi River	0.029	0.041	0.035
Highgate	October 4, 1982	Missisquoi River	0.025	0.08	0.0525
Average Min/Max			**0.024**	**0.057**	
Average			**0.041**		
Richford	April 1, 1980	Mountain Brook	0.038	0.048	0.043
Richford	April 1, 1980	North Branch	0.03	0.044	0.037
Richford	April 1, 1980	Stanhope Brook	0.043	0.053	0.048
Montgomery	July 5, 2001	Trout River	0.03	0.055	0.0425
Montgomery	July 5, 2001	Black Falls Brook	0.05	0.065	0.0575
Richford	April 1, 1980	Loveland Brook	0.03	0.055	0.0425
Richford	April 1, 1980	Lucas Brook	0.04	0.055	0.0475
Average Min/Max			**0.037**	**0.054**	
Average			**0.045**		

STONE ENVIRONMENTAL INC

Figure A.1. Geomorphic data extrapolation by elevation.
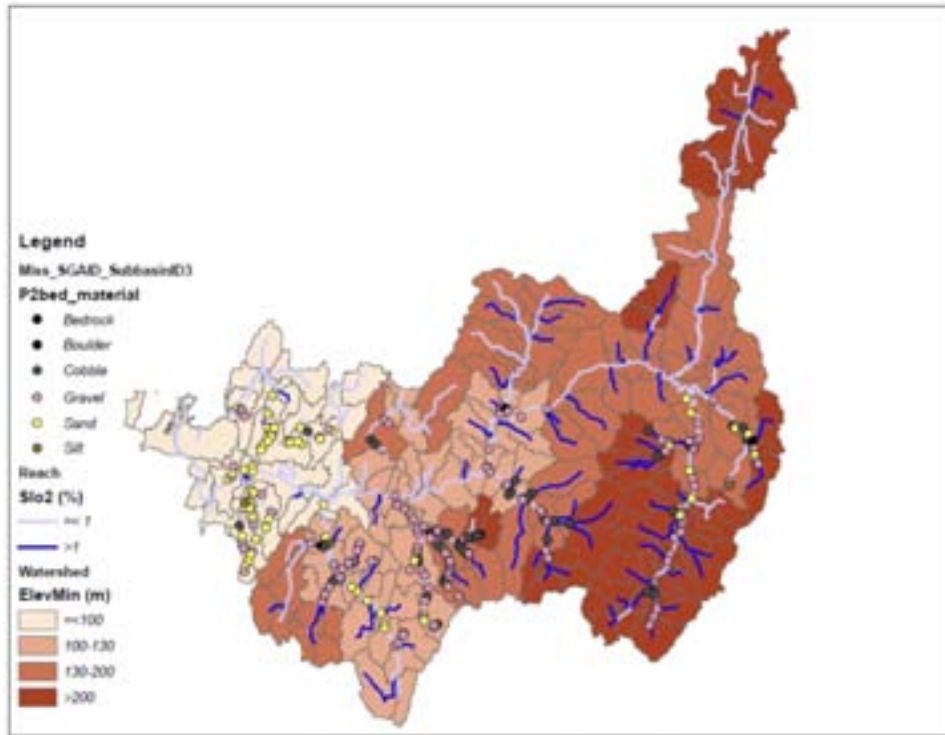
CH_K – Hydraulic Conductivity

- Mainstem streams are not "losing streams". All channels were assigned the value of 0.

CH_COV1 – Channel BANK vegetation coefficient (none=1, grassy=2.5, sparse trees 3.4, dense trees=6.8)

- Vegetation data exist for 28 sites from ANR-ARS study. This information listed vegetation species and indicated if they were dominant (~60% coverage). Dominant species were used to assign a bank vegetation coefficient as indicated above to both banks that were then averaged.

- If data were not available from the ANR-ARS study, Phase 2 geomorphic assessment data on dominant bank vegetation was used. The categorical values were assigned numerical values (Table A.7). Left and Right bank values were averaged, and then averaged for the subbasin. The numerical values are based upon a condensed range from that described in the SWAT manual.

- For subwatersheds with no field data the GIS land cover data derived for the CSA project were used to assign the bank vegetation coefficient based on dominant mapped vegetation adjacent to the channel. GIS was used to identify the dominant landuse within 50 meters on each side of the stream centerline. Landuse was assigned the required values of bank vegetation coefficient (Table A.8).

STONE ENVIRONMENTAL INC

Table A.7. Phase2 Data Bank Vegetation Coefficients.

Dominant Bank Vegetation	COV_1
Bare	1
Lawn	2.5
Pasture	2.5
Herbaceous	2.5
Invasives	2.5
Shrubs-Sapling	3.4
Coniferous	6.8
Deciduous	6.8

Table A.8. Land Cover Data Bank Vegetation Coefficients.

Dominant Land Cover	COV_1
Barren	1
Perm Corn	2.5
Perm Hay	2.5
Corn Hay Rotation	2.5
Pasture	2.5
Ag, Generic Cultivated	2.5
Soybean	2.5
Dev/Low Intensity	3.4
Developed/Open	3.4
Ag, Unmanaged/Brush	3.4
Forest	6.8
Wetland	6.8

CH_COV2 Channel BED vegetation coefficient

- Channels in MBB typically are not vegetated with dense grasses or trees. Assume value of 1 indicative of no vegetation.

CH_OPCE (ppm) – organic phosphorus concentration

- 15 NRCS soil samples were analyzed by UVM for total phosphorus and Mehlich-3 extracted Phosphorus. Sample horizons were composited by volume based on their bulk density prior to

STONE ENVIRONMENTAL INC

analysis. Total phosphorus values were assigned to appropriate subbasins to represent the organic / particulate form required for SWAT modeling.

- For the portion of the basin in the United States where no samples were collected, TP values were assigned based on the dominant soil type adjacent to the stream in the 50-meter buffer on each side of the stream using GIS. The median TP values for each soil series sampled during this project were first used to define TP levels for dominant soils in other locations in the basin. If the series was not sampled and analyzed in the basin, the TP level was assigned based on the dominant soil texture.

- For the Canadian portion of the basin, a listing of natural total phosphorus based on soil series was used to assign values throughout the basin (Giroux et al., 2008). The list was provided by A. Michaud of IRDA. TP values were assigned based on the dominant soil type or texture adjacent to the stream in the 50-meter buffer on each side of the stream using GIS.

CH_SIDE – Channel Side Slope (H:V)

- Phase 2 variable "Typical_bank_slope" is used. This is a categorical dataset that needed to be converted to numbers within the accepted range (Table A.9). The H:V slopes assigned are comparable to the slopes used in defining the Phase 2 categories.

- Phase 1 does not have a similar variable.

- Where data do not exist, a value of 1.1 is used as this is the mean of the most common measurements of during stream assessments.

Table A.9. Channel Side Slope Values.

typical_bank_slope	slope H:V
Undercut	0.0
Steep	1.0
Moderate	2.0
Shallow	3.0
No SGA Value	NO DATA

CH_BNK_BD (g/cm3) – Dry Bulk Density of <u>Bank</u> Sediment

- Values exist for 28 sites from the ANR-ARS study. Values have a tight distribution around a mean value of 1.30 g/cm^3 with a standard deviation of 0.13.

- For banks with median particle size of less than gravel size (16,000 um), the mean value form the 28 ARS sites was applied.

- For banks with median particle size of greater than gravel size (16,000 um), values from Table A.10 (Bunte and Abt 2001) were used.

STONE ENVIRONMENTAL INC

CH_BED_BD (g/cm3) – Dry Bulk Density of <u>Bed</u> Sediment

■ Bulk density of the bed was not measured. Typical values were selected based on measured or estimated bed particle type (Table A.10) (Bunte and Abt, 2001).

Table A.10. Bed Bulk Density.

Bed Material	Bulk Density (g/cc)
Bedrock	2.7
Boulder	2.7
Cobble	2.4
Gravel	2.1
Sand	1.2
Silt	1.2

CH_BNK_KD (cm3/N-s) – Jet Test Erodability of <u>Bank</u>

■ Values were calculated from the estimates of bank critical shear stress (T_c) based on the equation from the SWAT manual, (kd=0.2 x T_c^-0.5).

CH_BED_KD (cm3/N-s) - Jet Test Erodability of <u>Bed</u>

■ Values were calculated from the estimates of bed critical shear stress (T_c) based on the equation from the SWAT manual, (kd=0.2 x T_c^-0.5)

CH_BNK_D50 (um) – D50 of <u>bank</u> in microns

■ Use measured values in ANR-ARS study.

■ Phase2 variables of either "material_type_lower" or an average of "material_type_lower_left" and "material_type_lower_right" were used if no bank study data were available. This variable is categorical, and converted to representative particle size for the bed material type in microns (Table A.11).

■ In SWAT reaches where data from both the ARS study and Phase 2 data were available, the average of the two values was assigned to the reach

■ For each major sub-watershed, the median of the d50 was calculated for mainstem and headwater reaches. When no field data was available for a reach, the median value for the local sub-watershed was assigned to that reach (mainstem or headwater reaches). In sub-watersheds where no data was available, the median d50 values from a nearby and similar sub-watershed was applied. Guidance for median particle for different bed and bank materials if provided in Table A.11 (Tomer et al. 2005).

STONE ENVIRONMENTAL INC

Table A.11. Bank and Bed Material Sizes.

Bed Material	Size (um)
Bedrock	4,096,000
Boulder	1,024,000
Cobble	128,000
Gravel	16,000
Sand	500
Silt	50

CH_BED_D50 (um) – D50 of <u>bed</u> in microns

- The Phase2 variable "P2_bed_material" was used if available and categories were assigned a size representing the mean particle size for the class (Table 6).

- If Phase 2 data were not available the Phase 1 variable "bed_material" was used and values were assigned with the same method as the Phase 2 data.

- If no data were available, the subbasins were assigned values based on elevation following the observed trends in bed sediment and roughness. Subbasins with elevation <= 100 m were assigned a value of sand, elevation between 100 and 200 m were assigned gravel, and higher subbasins were assigned cobble.

CH_BNK_TC (N/m^2) – Critical Shear of Bank

- For reaches with estimated bank d50 values of <= 2,000 um (sand sized), the silt and clay fractions of the bank material were estimated using the equations provided in the latest SWAT sediment routing algorithms (Fredlund et al. 2000). The equation for calculating Tc as a function of silt and clay fraction presented in the SWAT model (Julien and Torres 2006) was applied to estimate the Tc of the reach.

- For reaches with estimated bank d50 values of > 2,000 um (sand sized), the Tc values were estimated based on the data provided in Table A.12 (Fischenich 2001).

- Tc values were then multiplied by the channel bank cover factor (CH_COV1) to obtain the final Tc value.

STONE ENVIRONMENTAL INC

Table A.12. Material Critical Shear Stress.

Material	Critical Shear Stress (N/m2)
None	NO DATA
Bedrock	478 (400 max)
Boulder	445 (400 max)
Cobble	81
Gravel	5.7
Sand	0.5
Silt	0.05
Clay	12

CH_BED_TC (N/m2) – Critical Shear of Bed

- The Phase2 variable "P2_bed_material" was used if available and categories were assigned a critical shear value for the class (Table 7).

- If the Phase 2 data were not available the Phase 1 variable "bed_material" was used and values were assigned the same way as the Phase 2 data.

- If no field data were available, a critical shear value was set based on the estimated dominant particle size and tabulated critical shear stress values (Fischenich, 2001).

A.2.2. Subbasin Tributary Channels

This section describes the data collection and setting of initial parameter values for tributary channels.

CH_W (m) – Channel Width

- Phase 2 data variable "bankfull_width" was averaged for the subbasin and assigned if available. In the Phase 2 assessment the bankfull width was measured in the field at multiple cross sections and the representative cross section bankfull width was chosen.

- If Phase 2 data were not available the Phase 1 data variable "channel _width" were averaged for the subbasin and assigned. In the Phase 1 assessment the channel width data were estimated using the reach/segment point drainage area and the Vermont Hydraulic Geometry Curves. Note that this approach is required rather than performing a direct calculation of width from the equations since there is no delineation of a single tributary subbasin area for the SWAT model.

- The measured data have a mean value of 3.6 meters and a standard deviation of 1.5 m. Where no other data are available the value of 4.0 meters was assigned. If the mainstem reach had a drainage area less than 4.0 meters, the tributary was assigned a value of 2.5 m, or the mean minus one standard deviation.

STONE ENVIRONMENTAL INC

CH_N – Manning's N-value

- Refer to data sources described in detail in Mainstem Data Section.

- Tributaries are generally smaller and rougher than downstream reaches and thus n-values were assigned by adding 0.010 to the n-values assigned to the mainstem for the subbasin.

CH_K – Hydraulic Conductivity

- It is assumed that all of the tributaries are gaining streams for most of the hydrologic year and thus all values were assigned as 0.

A.3. SWAT Model Modifications

Several modifications were made to the SWAT model code. Each of these is described here. The source code for SWAT2009 that was used as the foundation for the LCBP model was Revision 477. This version was packaged with the official release of ArcSWAT 2009.93.6.

1. Modification of tile drainage calculations: Changes to the tile drainage was made according to changes made by the IRDA group in Quebec (Michaud 2007). These changes modified the order in which water moves vertically and horizontally in the soil in order to achieve a higher amount of tile flow, which was observed in agricultural land in southern Quebec. The method is based on the approach used in SWAT 2000. The subroutines modified were, *permain.f*, *permicro.f*, and *percmacro.f*. Changes incorporated by IRDA regarding the modification to initial abstraction term in the SCS curve number runoff equations were not made in the MBB application.

2. Modification of snow routines: The subroutine, *snom.f* was updated to include snowfall adjustment and groundmelt.

   a. A parameter called "sfadj" was added. This is a snowfall adjustment factor is used in the National Weather Service Snow-17 model and takes into account the under-catch of snowfall by precipitation gages. The parameter was hard-coded at a value of 1.10.

   b. A parameter called "grmlt" was added. This is the daily ground melt. Ground melt is a parameter used by the National Weather Service Snow-17 mode and is common in areas with deeper snowpacks that insulate the ground from the cold. The parameter was hard-coded a value of 1 mm/day.

   c. The calculation of subbasin precip for the day was also adjusted in snom.f so that it is reported correctly.

3. Addition of Subbasin-level Hargreaves PET coefficient: The Hargreaves PET coefficient is available in the SWAT code through the use of special projects. In addition, this is a parameter available for adjustment in the APEX model as well. The parameter acts to adjust the PET predicted by the Hargreaves equations.

STONE ENVIRONMENTAL INC

a. In the subroutine, *readsub.f*, the code was modified to read in the subbasin-level harg_petco parameter. The parameter is read in on line 3 of the sub file.

4. Addition of subbasin-level SURLAG: The change was made so that SURLAG could vary by subbasin.

    a. In the subroutine, *hydroinit.f*, the code was modified to use the variable "surlag_sub" in place of "surlag".

    b. In the subroutine, *readsub.f*, the code was modified to read in the subbasin-level surlag parameter. The parameter is read in on line 4 of the sub file.

5. Subbasin level snow parameters: This was added as part of the standard SWAT2009 rev477 code. However, a change to the code in the *etact.f* subroutine was required in order for the sublimation to occur correctly. The issue was how the original code was checking for elevation bands. The modification corrected for the case where there was a single elevation band without the elevation specified.

6. Flow Routing: The subroutine *rtmusk.f* was modified by Jaehak Jong (Backland Texas AgriLife Research & Extension Center) to produce a numerically stable solution to the Muskingum flow routing.

7. Sediment Routing:

    a. In consultation with the SWAT channel process development team (Narasimhan 2011), an updated set of sediment routing subroutines was incorporated into the model. This updated set of subroutines addressed an issue in the algorithms that restricted bank erosion from occurring unless the sediment transport capacity is high enough to enable transport of addition sediment, regardless of the availability of excess shear stress. The updated sediment routing subroutines allowed bank erosion to occur regardless of the availability of excess transport capacity. This resulted in a new code file called, *rtesednew.f*.

    b. The parameters controlling the sediment transport capacity for the Bagnold equation were allowed to vary by reach. The standard SWAT code has these parameters constant for the entire watershed. A modification to the *readrte.f* was made to read in the reach level SPEXP, SPCON, and PRF parameters. These reach level parameters were then used in the transport capacity calculation in the *rtesednew.f* subroutine.

    c. A parameter that represents that fraction of the channel bank that is actively eroding was added to the *readrte.f* file. This new parameter was incorporated to the bank erosion equations in the *rtesednew.f* subroutine. The standard version of SWAT assumes that 100% of one bank (50% of combined left and right banks) is actively eroding. The use of the new reach level parameter allows the extent of channel bank erosion to be controlled based on observed fractions of areas eroding.

8. Biomass Harvest Operation Modification: With the standard SWAT model, it is possible for a biomass harvest operation to remove an excessive amount of biomass. To address this, a modified *harvestop.f* subroutine was provided by the SWAT development team in Temple Texas (White

STONE ENVIRONMENTAL INC

2011b). The modified algorithm will not remove biomass below a defined minimum threshold. This is necessary so that the ground cover is not completely removed.

9. Fertilizer File: The *readfrt.f* was modified to increase the precision of fertilizer nutrient contents that are read in from the fert.dat file.

10. Initialization of Plant Biomass Nutrient Content: The *plantop.f* subroutine was modified so that plant operations for existing plants (transplants) would not result in plants with nutrient contents of 0. This was corrected to prevent a large uptake of nutrients form the soil occurring after the vegetation is transplanted.

11. Plant Nutrient Uptake: It was found that the SWAT Rev 477 code resulted in plant nutrient uptake occurring even when plants were not growing due to temperature or water stress. This was occurring because the algorithms for calculating nutrient uptake considered only if the plant was out of the dormant season and whether the plant was at or below optimal nutrient content. The *nup.f*, *npupf*, and *grow.f* subroutines were updated so that nutrient uptake did not occur when plant growth was zero.

12. Sediment Yield Reduction for Snow Cover: The SWAT Theoretical Manual, section 4.1.3 (Neitsch et al. 2011) describes an algorithm used to reduce sediment yield predicted by the MUSLE equation when snow is present on the ground. A walkthrough of the Rev 477 code showed that this algorithm was not properly being executed. The *ysed.f* subroutine was modified so that the algorithm would be properly executed. It was subsequently determined that the degree of sediment yield reduction that was occurring was too high; therefore, an adjustment factor was added to lower the impact of snow cover.

13. WWQ CHLA_SUBCO Parameter: Upon reviewing the Rev 477 code, it was found that the watershed water quality parameter, CHLA_SUBCO, was being correctly read into the model, but was not being used correctly for its intended purpose of adjusting upland chlorophyll-a loading. The *subwq.f* subroutine was modified to fix this.

Many of the model updates described in this section have been shared with the SWAT development team and will likely appear in future releases of the model.

STONE ENVIRONMENTAL INC

Lake Champlain Basin Program / Identification of Critical Source Areas of Phosphorus Within the Vermont Sector of the Missisquoi Bay Basin / December 15, 2011   174

APPENDIX B: CALIBRATED MODEL PARAMETERIZATION

The Table B.1 summarizes the SWAT model parameters that were adjusted during calibration. The parameters that did not change from their initial values described in Appendix A or within the main body of the report are not included in the table. Further discussion regarding some parameters that require additional information is provided following the summary table.

Table B.1. Calibrated Model Parameter Summary.

Parameter Name	Parameter Description	Calibrated Value	Comments
GWQMN	Threshold depth of water in shallow aquifer for return flow (mm)	0, 750, 1050	Varied by subbasin elevation\sub-watershed
ESCO	Soil evaporation compensation factor	0.90, 0.98, 1.0	Varied by subbasin elevation\sub-watershed
EPCO	Plant evaporation compensation factor	0.5	
HARG_PETCO	Hargreaves equation coefficient	0.0019, 0.002, 0.0023	Varied by subbasin elevation.
CN2	SCS curve number for soil moisture condition II	lowered by 6 for all HRUs	Reduction from CTI-based CN2 value.
SLSUBBSN	Slope length (m)	Reduced for slopes < 12%	Varies as a function of HRU slope
SLSOIL	Lateral flow slope length (m)	0.5 * SLSUBBSN	Minimum value of 15 m.
TDRAIN	Time for tile to drain soil to field capacity (hr)	36	
GDRAIN	Tile drain lag time (hr)	2	
DEP_IMP	Depth to impermeable layer (mm)	Hydro Group C: SOL_ZMX+2000; Hydro Group D: SOL_ZMX+1000	Varied by hydrologic soil group and soil profile depth
SFTMP	Snowfall temp (C)	-1.5	
SMFMX	Max snow melt factor (mm/C-day)	3.5, 4.0, 4.5	Varied by subbasin forest cover.
SMFMN	Min snow melt factor (mm/C-day)	0.5, 1, 1.5	Varied by subbasin forest cover.
TIMP	Snow pack temperature lag factor	0.2, 0.4, 0.6	Varied by subbasin elevation.
SURLAG	Surface runoff lag coefficient	1.0, 1.2, 1.5, 2.0, 2.5	Varied by sub-watershed
USLE_C (corn)	USLE crop cover factor (corn)	0.15	Only corn was adjusted from initial value
ERORGP	Enrichment ratio for P	1	
PSP	Phosphorus availability index	0.5	
P_UPDISP	Phosphorus uptake distribution parameter	75	
MUK_X	Muskingum weighting factor	0.25	
MUK_CO1	Muskingum coef. 1	4.5, 0	Varied by sub-watershed
MUK_CO2	Muskingum coef. 2	0.5, 5	Varied by sub-watershed

STONE ENVIRONMENTAL INC

Parameter Name	Parameter Description	Calibrated Value	Comments
SPCON	Linear parameter for sediment transport	0.00014 - 0.0004	Varied by sub-watershed
SPEXP	Exponent parameter for sediment transport	1.2, 1.4	Varied by sub-watershed
PRF	Peak rate adjustment factor for sediment transport	1.5	
CN_N2	Manning's N for main channel	0.037 - 0.05	Varied by reach
CH_BNK_TC	Critical sheer stress of channel bank (N/m2)	30 - 463	Varied based on particle size, vegetation cover, and a minimum threshold
CH_BNK_KD	Erodibility of channel bank (cm3/N-s)	0.003 - 0.009	Calculated as a function of adjusted critical sheer stress
AI2	Fraction of algal biomass that is P	0.01	
K_P	Half saturation constant for P	0.01	
RHOQ	Algal respiration rate	0.05	
TFACT	Fraction of solar radiation that is photosynthetically active	0.05	
RS5	Organic P settling rate (1/day)	0.01	
CHLA_SUBCO	Regional chlorophyll loading adjustment	0.5	

SLSUBBSN: Slope Length (m)

The default values for SLSUBBSN were judged to be too long for the lower slopes. The lower slope values were adjusted down, while the higher slope values were left the same as the ArcSWAT default values. The following is the summary SLSUBBSN for all the slope ranges:

1. 0-2%: 76.2 m (modified)

2. 2-5%: 70.0 m (modified)

3. 5-12%: 45.7 m (modified)

4. 12-16%: 24.4 m (default)

5. 12-20%: 18.3 m (default)

6. 20-25%: 15.2 m (default)

7. > 25%: 9.1 m (default)

CH_N2: Manning's N for Main Channel

Of the 223 channels in the MBB, 5 were initially assigned with Manning's N values of less than 0.037 and 5 were assigned values of greater than 0.05. These 10 reaches on the extremes of the distribution of values

STONE ENVIRONMENTAL INC

throughout he MBB were adjusted up (or down) to so that they fell within the range of 95% of the reaches (between 0.037 and 0.05).

CH_BNK_TC, and CH_BNK_KD: Bank critical sheer stress and erodibility

During sediment calibration the SWAT model, one of the goals was to achieve bank erosion rates within the same range as that which was predicted by the BSTEM model. The initial parameterization of the SWAT model resulted in excessive rates of bank erosion compared to the BSTEM model. This required that, in some cases, significant adjustments to the bank critical sheer stress (and the bank erodibility) be made. In addition, the initial parameterization of the bank vegetation cover coefficient (CH_COV1) resulted in a particularly wide range in effective critical sheer stress. The adjustment of CH_BNK_TC during calibrating consisted of the following steps:

1. The vegetation cover coefficient was adjusted to a range of 1 to 6.8 (as opposed to the original 1 to 19.2)

2. The CH_BNK_TC was calculated as a function of the bank mean particle size and adjusted vegetation cover coefficient.

3. Calculated values of CH_BNK_TC that were less than 50 N/m2 were set at 50.

4. The CH_BNK_KD was calculated as a function of the CH_BNK_TC using the original equation presented in Appendix A, and then reduced by an additional 75%.

5. Independent adjustments to approximately 20 reaches were made during calibration based on observed sediment and P load.

As discussed in 2.5.4, the resulting parameterization of the channel banks resulted good agreement with total sediment load at the monitoring locations and was in good agreement with predicted bank erosion rates generated by the BSTEM modeling project.

STONE ENVIRONMENTAL INC

APPENDIX C: CALIBRATION AND VALIDATION RESULTS

C.1. Hydrology Calibration/Validation

Figure C1. Missisquoi at North Troy, daily flow calibration, 10/2005-9/2010.
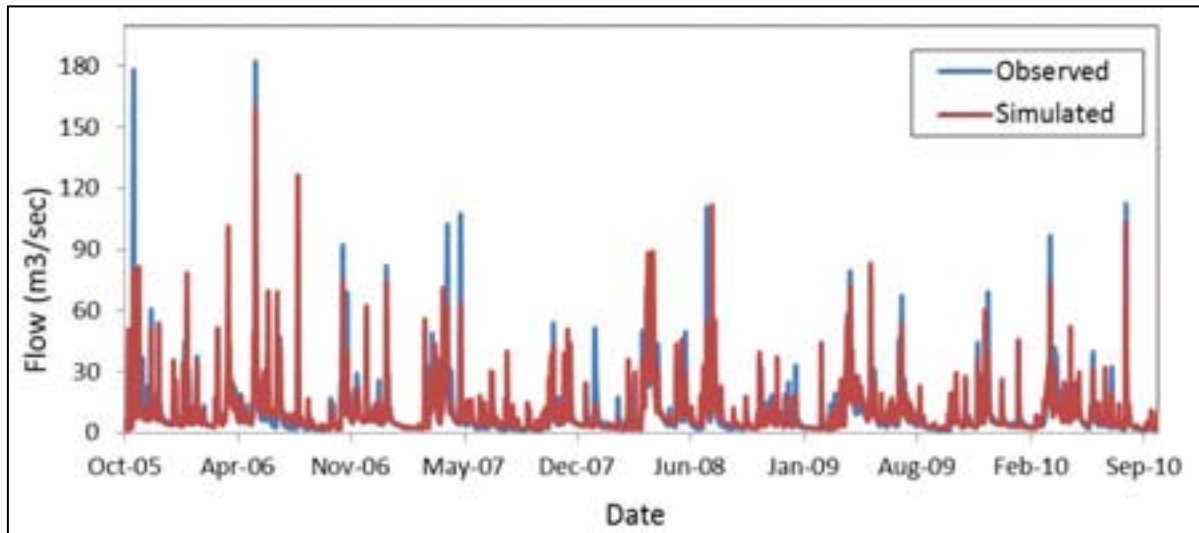
Figure C2. Missisquoi at North Troy, monthly flow calibration, 10/2005-9/2010.

STONE ENVIRONMENTAL INC
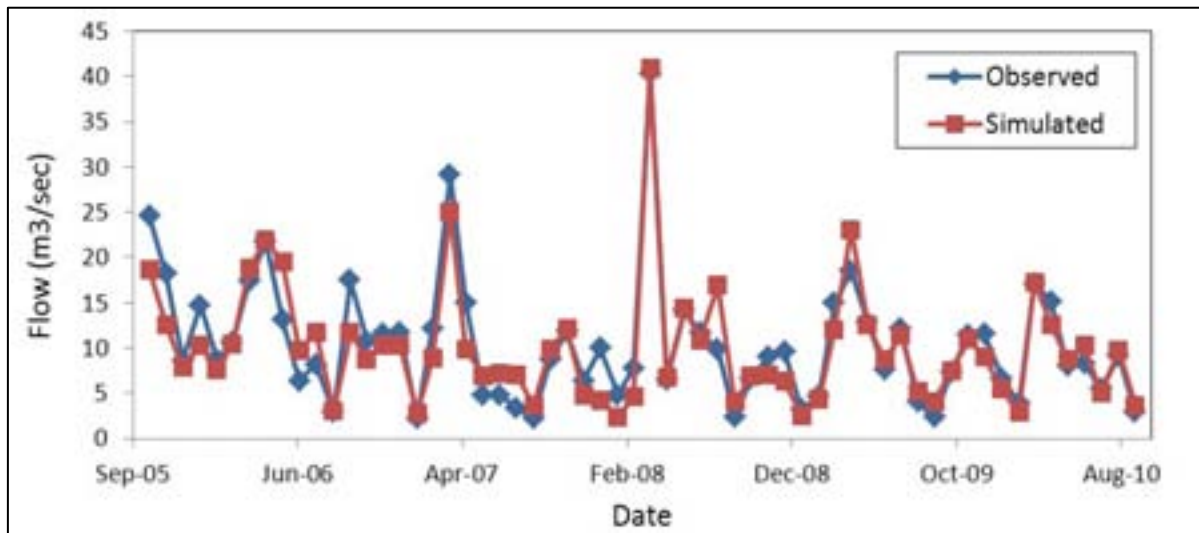
Figure C3. Missisquoi at North Troy, daily flow validation, 10/2001-9/2005.
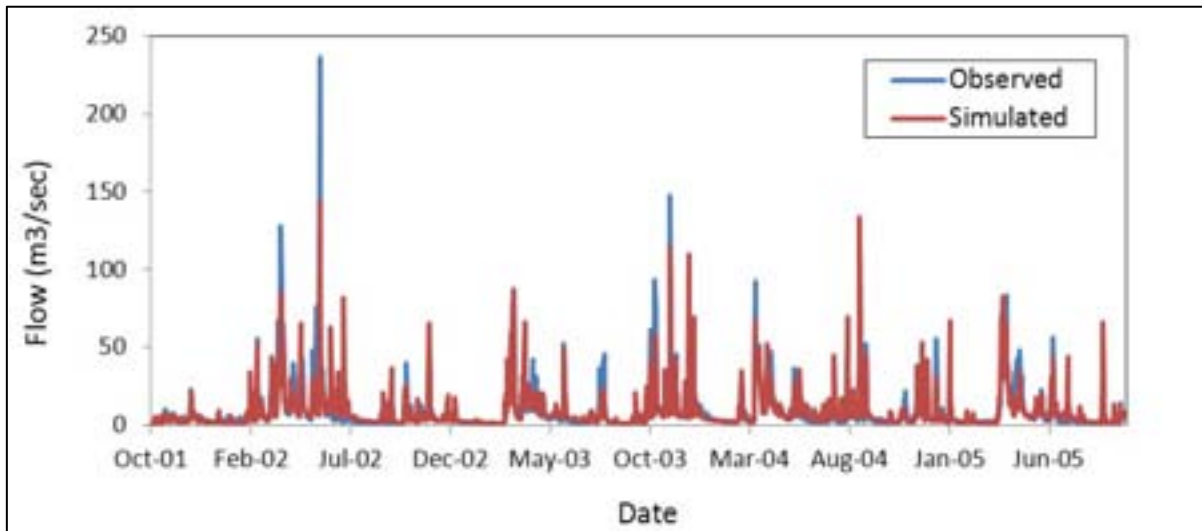
Figure C4. Missisquoi at North Troy, monthly flow validation, 10/2001-9/2005.

STONE ENVIRONMENTAL INC
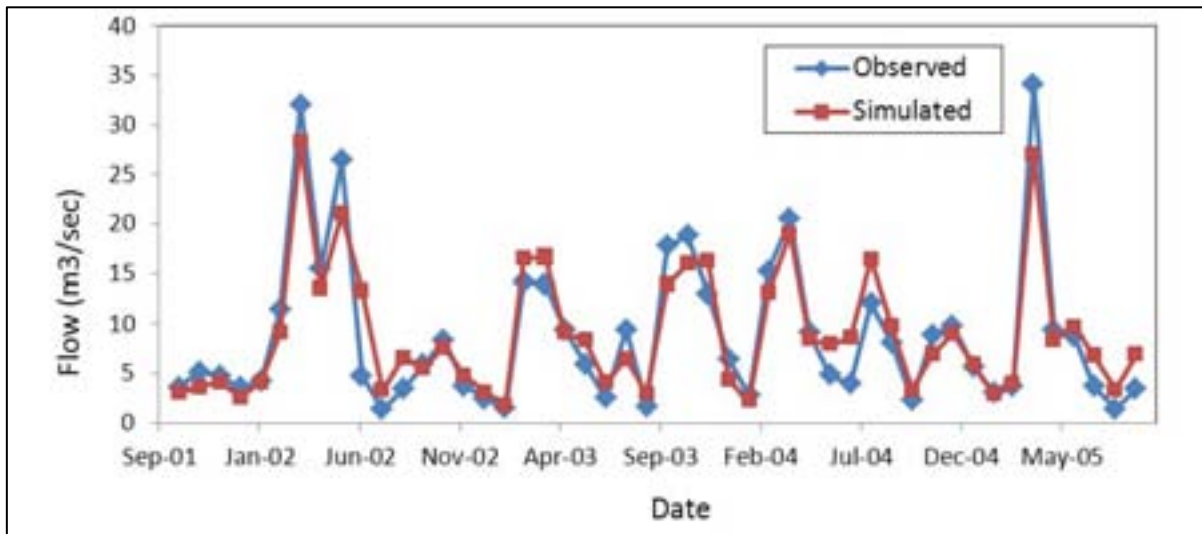
Figure C5. Missisquoi at East Berkshire, daily flow calibration, 10/2005-9/2010.
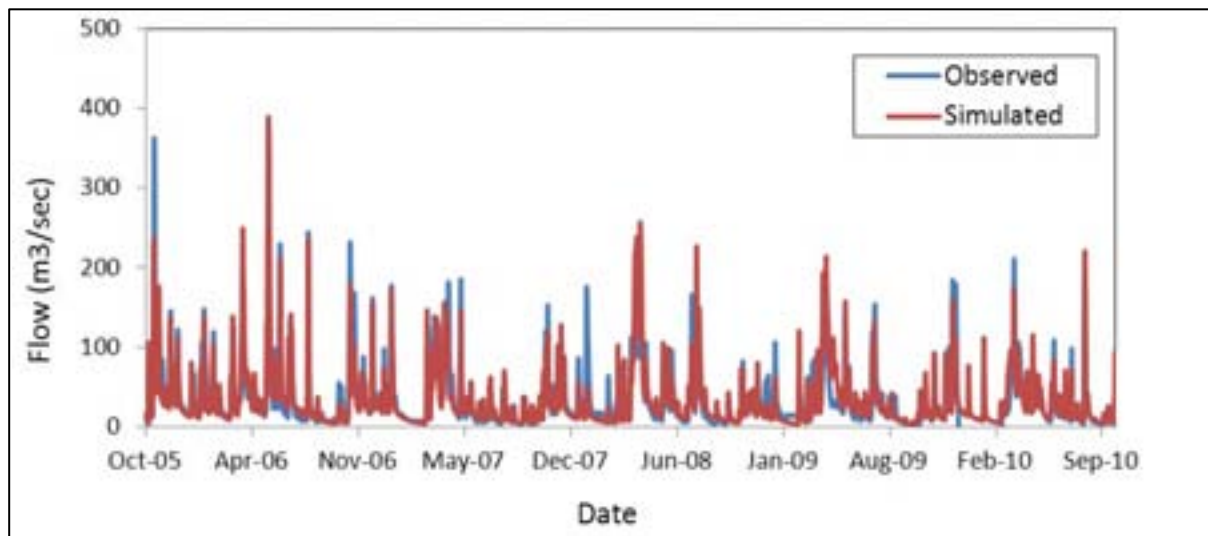
Figure C6. Missisquoi at East Berkshire, monthly flow calibration, 10/2005-9/2010.

STONE ENVIRONMENTAL INC
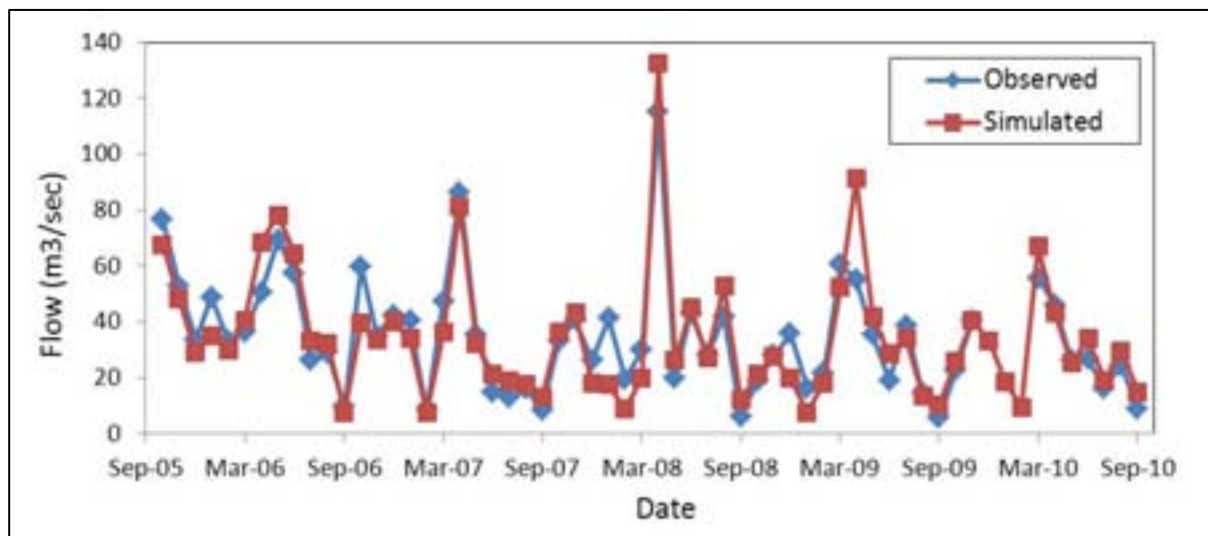
Figure C7. Missisquoi at East Berkshire, daily flow validation, 10/2001-9/2005.
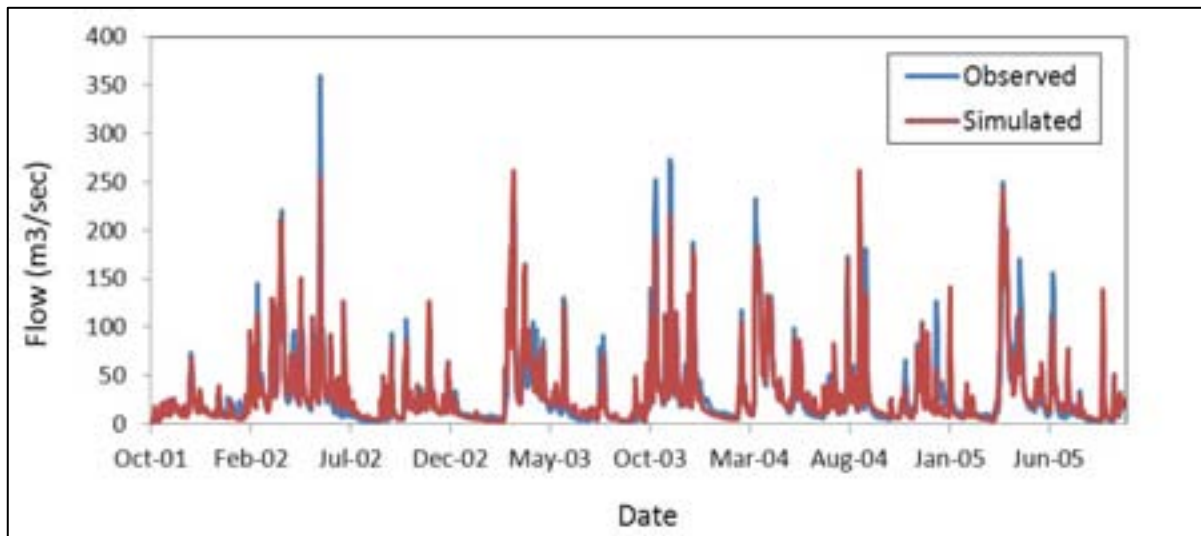
Figure C8. Missisquoi at East Berkshire, monthly flow validation, 10/2001-9/2005.

STONE ENVIRONMENTAL INC
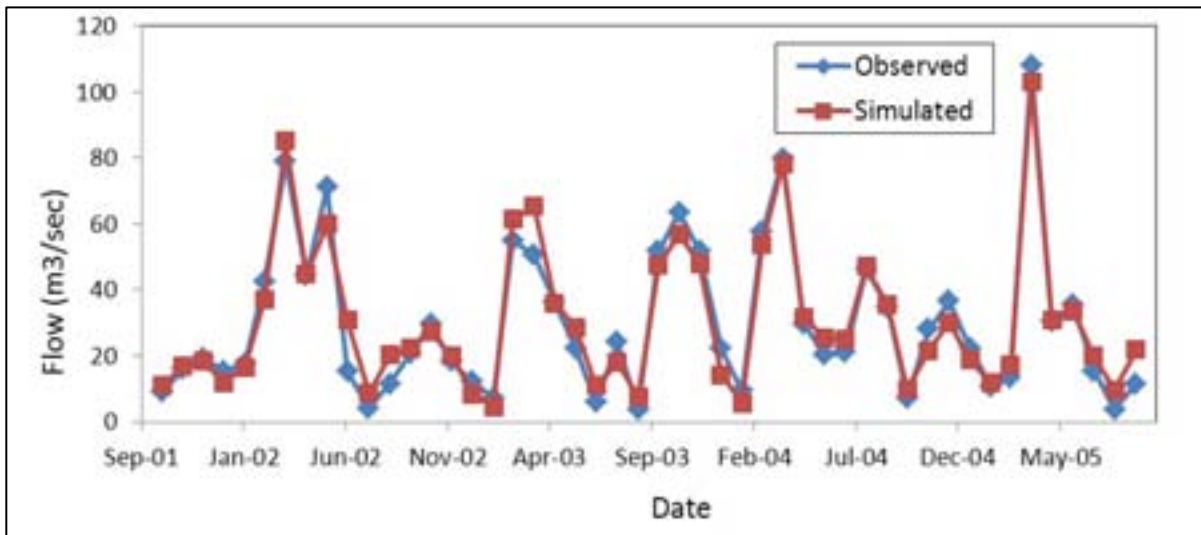
Figure C9. Missisquoi at Swanton, daily flow calibration, 10/2005-9/2010.
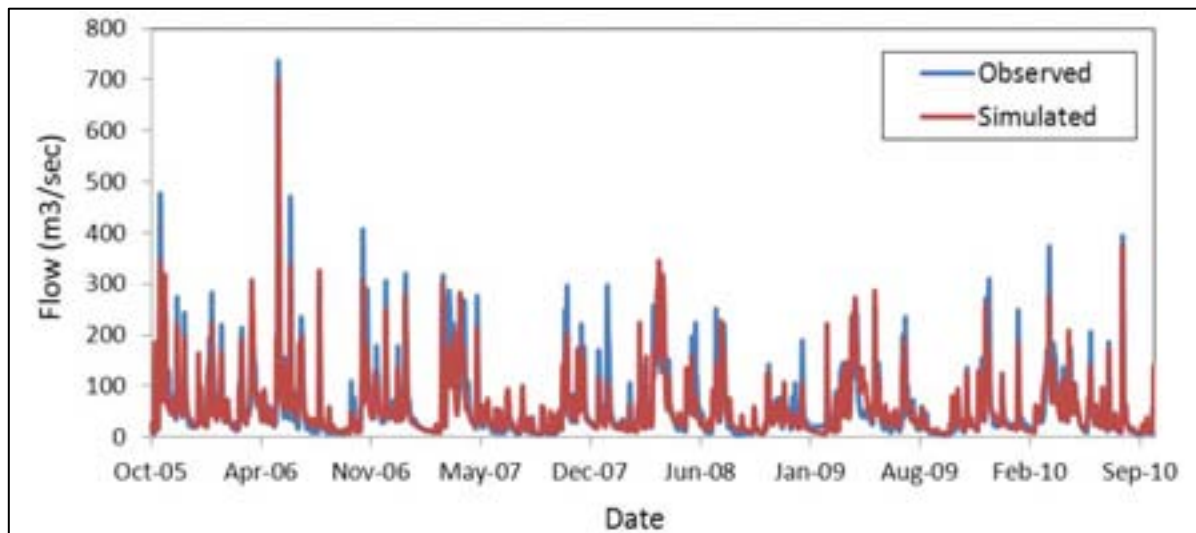
Figure C10. Missisquoi at Swanton, monthly flow calibration, 10/2005-9/2010.

STONE ENVIRONMENTAL INC
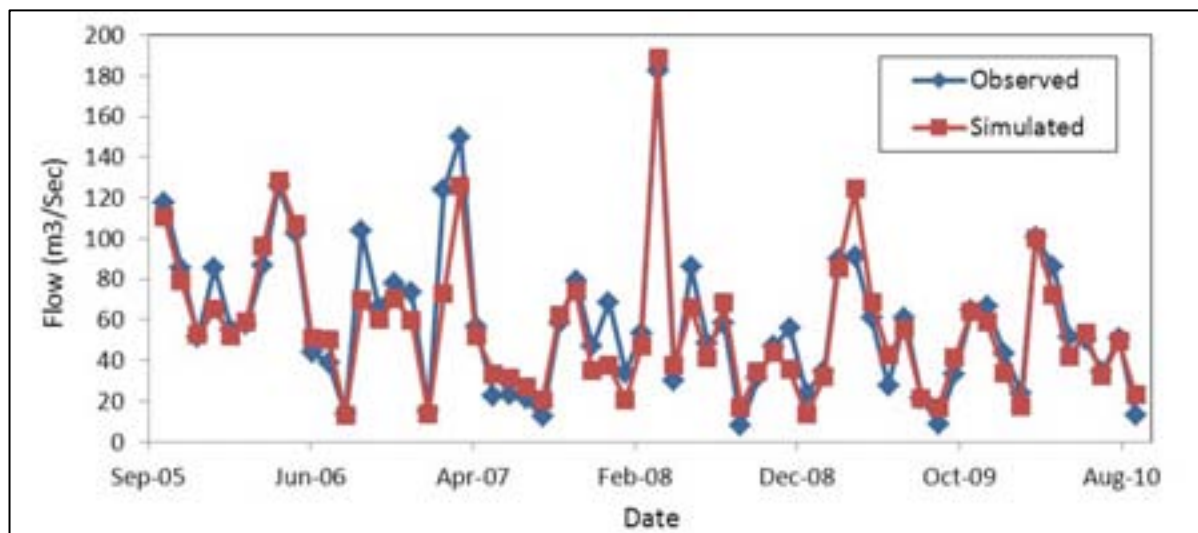
Figure C11. Missisquoi at Swanton, daily flow validation, 10/2001-9/2005.
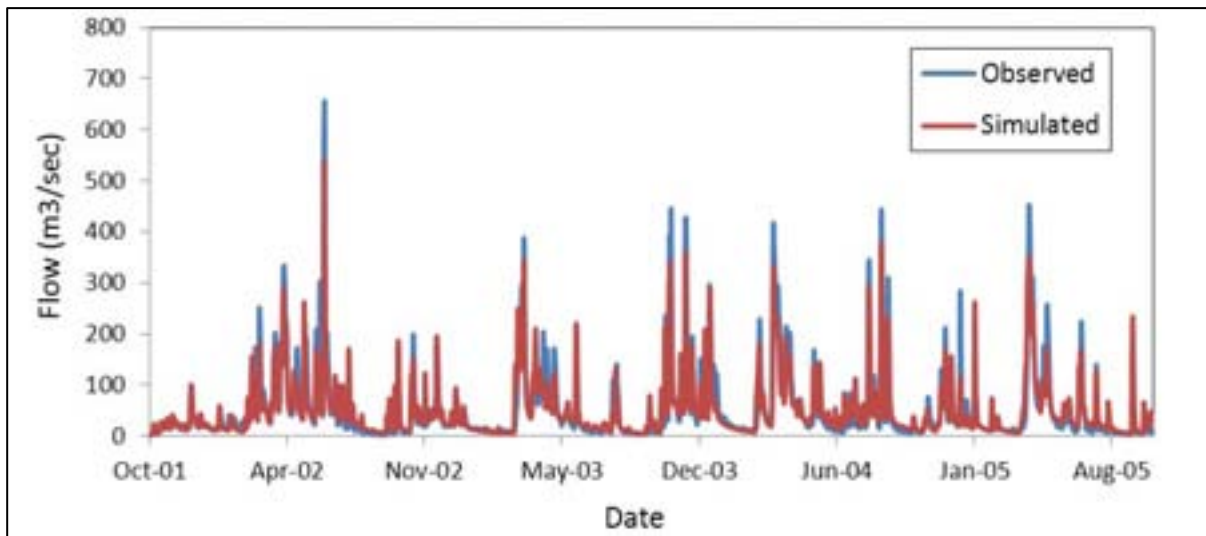
Figure C12. Missisquoi at Swanton, monthly flow validation, 10/2001-9/2005.

STONE ENVIRONMENTAL INC
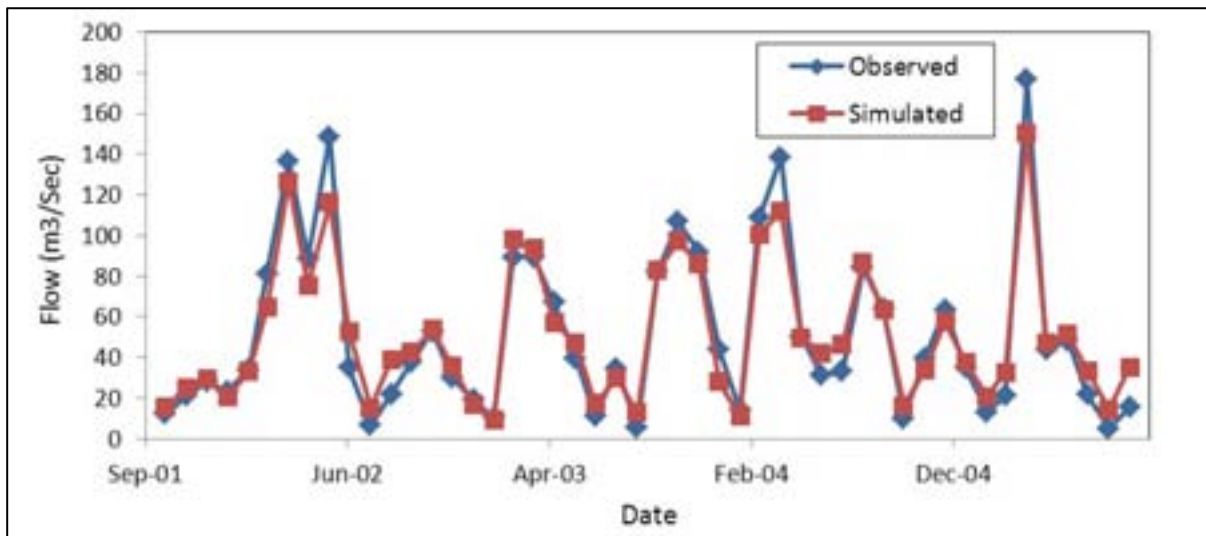
Figure C13. Rock River at Saint Armand, daily flow calibration, 10/2005-9/2009.
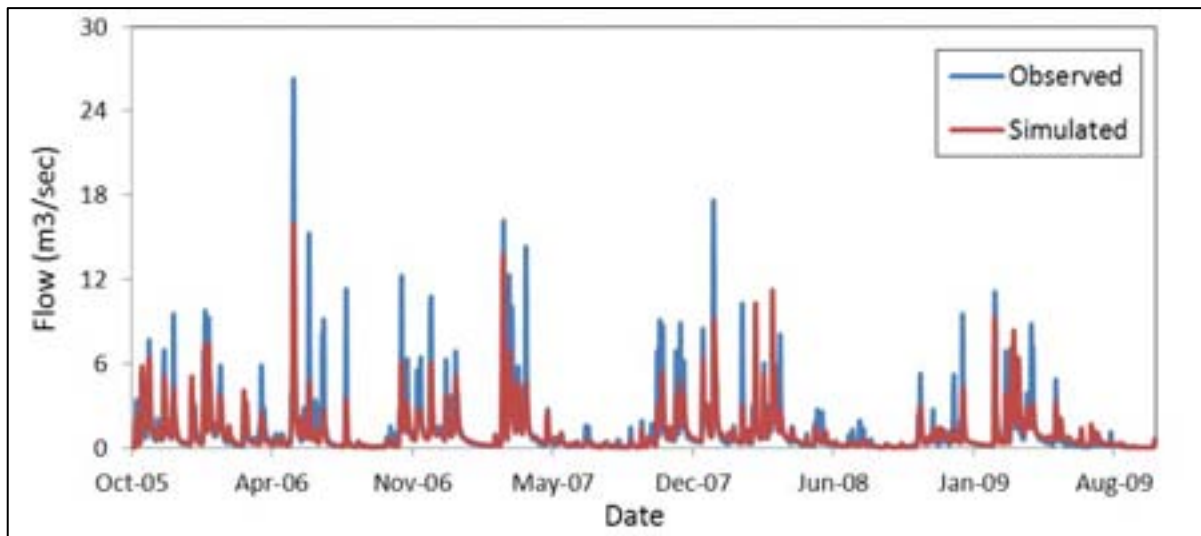
Figure C14. Rock River at Saint Armand, monthly flow calibration, 10/2005-9/2009.

STONE ENVIRONMENTAL INC
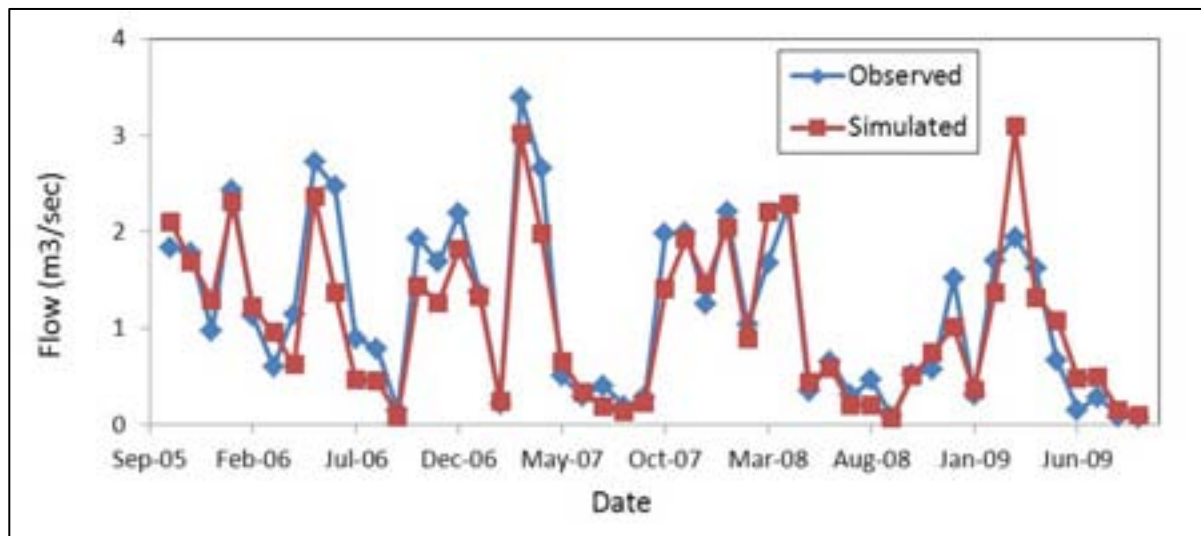
Figure C15. Rock River at Saint Armand, daily flow validation, 10/2001-9/2005.
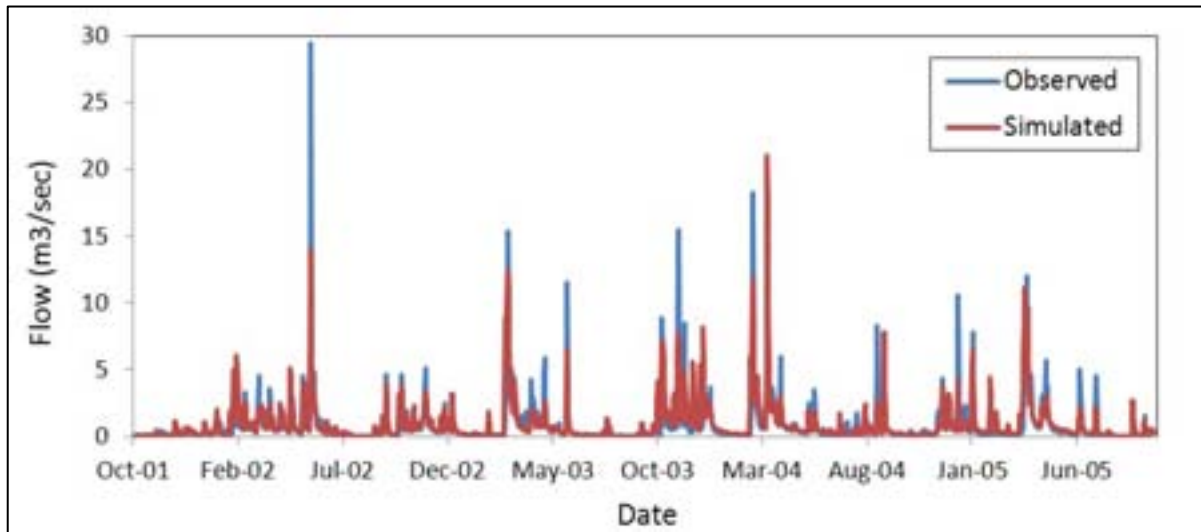
Figure C16. Rock River at Saint Armand, monthly flow validation, 10/2001-9/2005.

STONE ENVIRONMENTAL INC
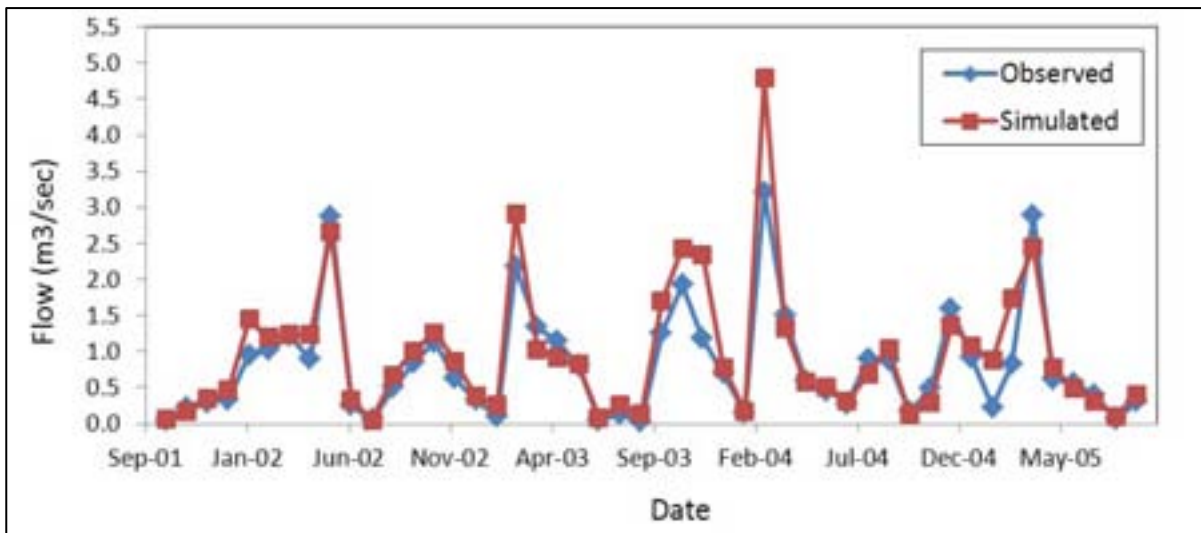
Figure C17. Mud Brook, daily flow calibration, 8/2009-9/2010.
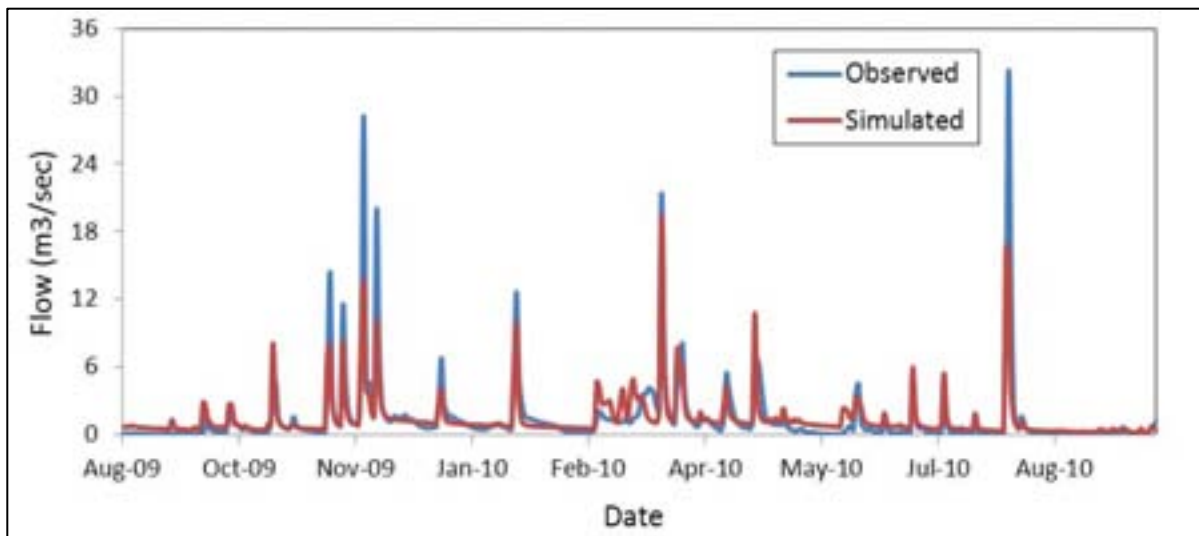
Figure C18. Mud Brook, monthly flow calibration, 8/2009-9/2010.

STONE ENVIRONMENTAL INC
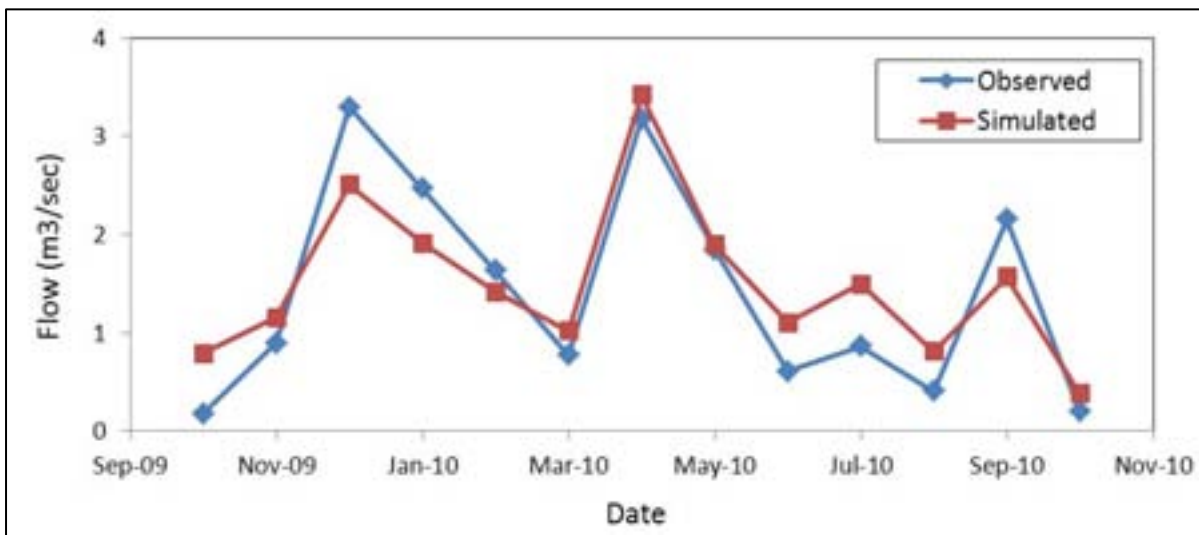
Figure C19. Trout River, daily flow calibration, 8/2009-9/2010.
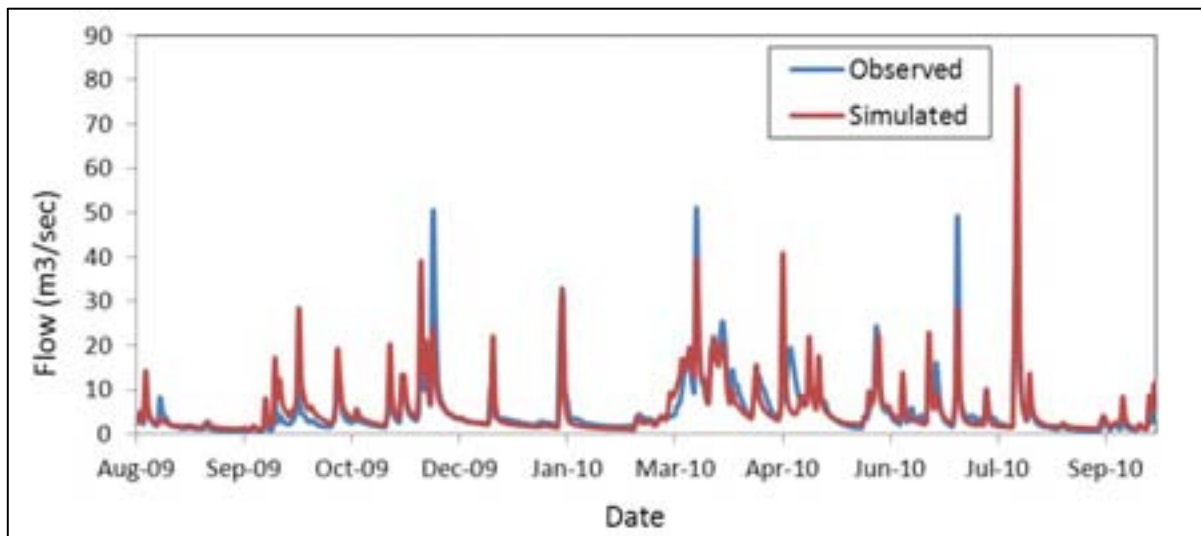
Figure C20. Trout River, monthly flow calibration, 8/2009-9/2010.

STONE ENVIRONMENTAL INC
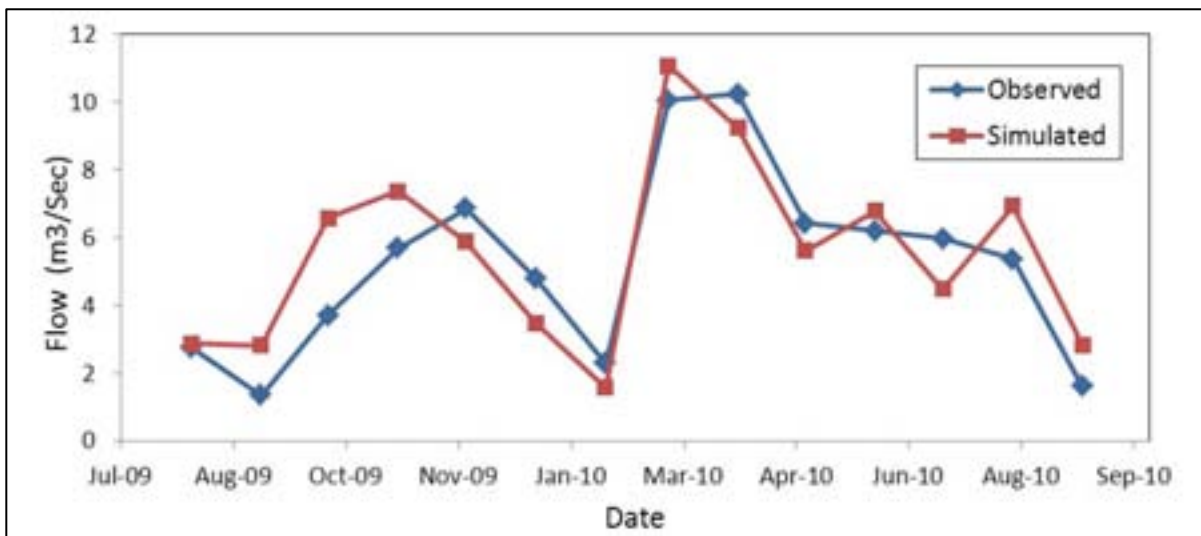
Figure C21. Tyler Branch, daily flow calibration, 8/2009-9/2010.
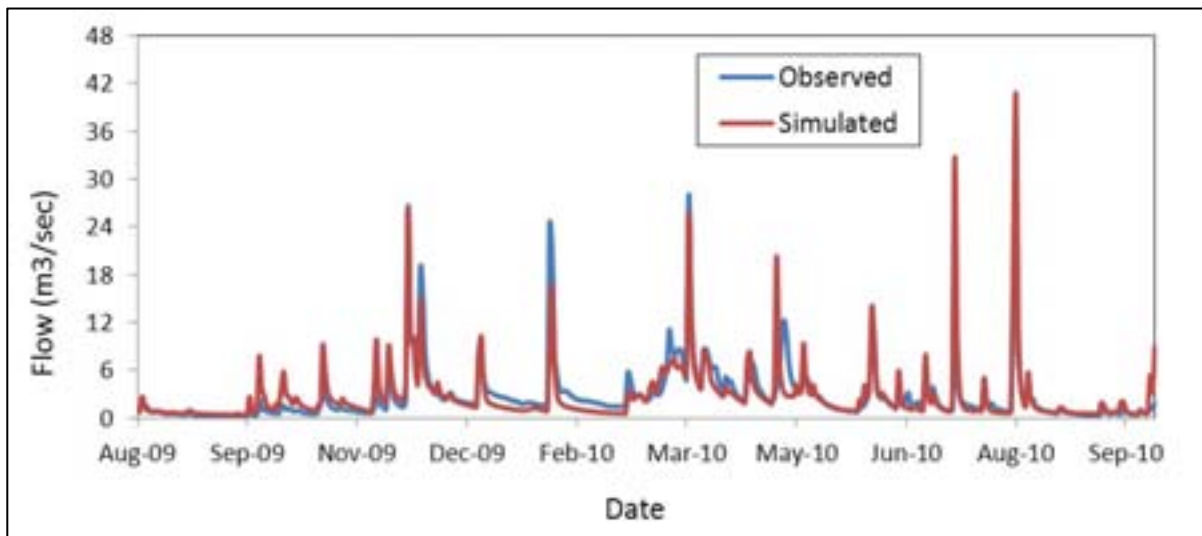
Figure C22. Tyler Branch, monthly flow calibration, 9/2009-9/2010.

STONE ENVIRONMENTAL INC
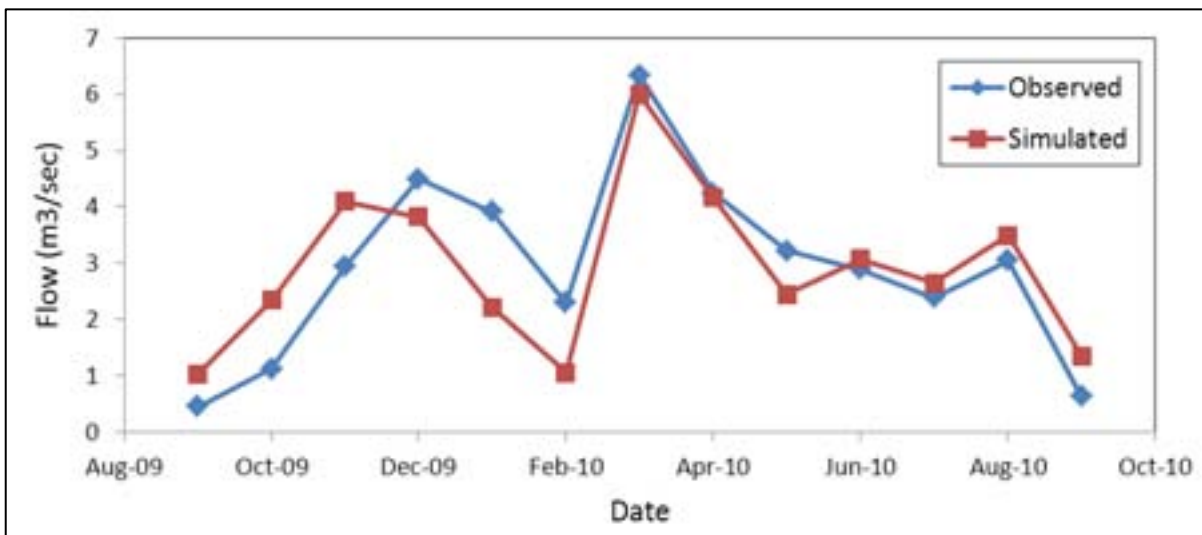
Figure C23. Black Creek, daily flow calibration, 7/2009-9/2010.
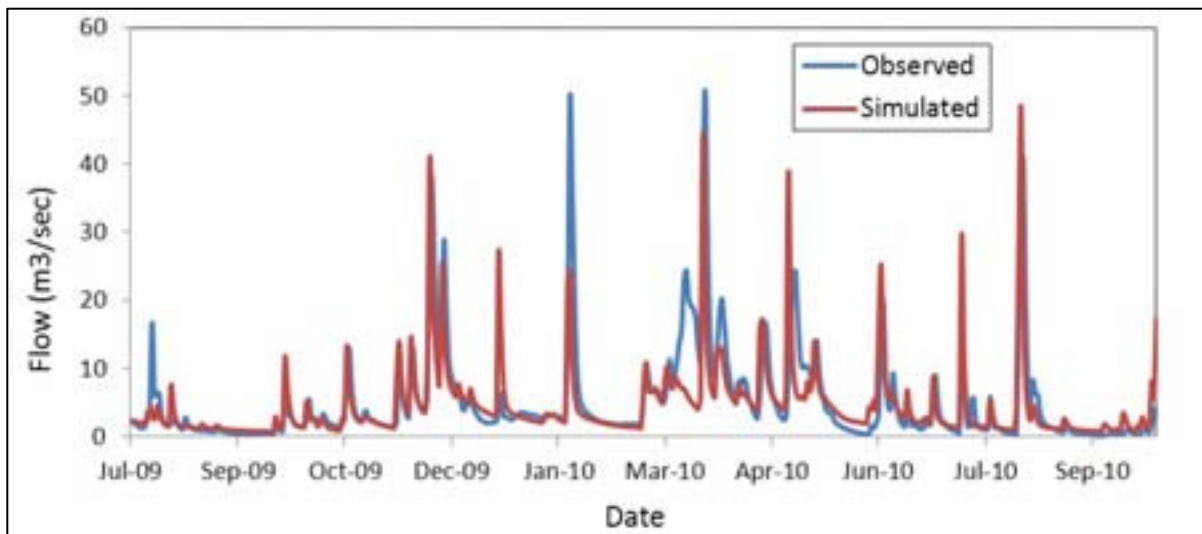
Figure C24. Black Creek, monthly flow calibration, 8/2009-9/2010.
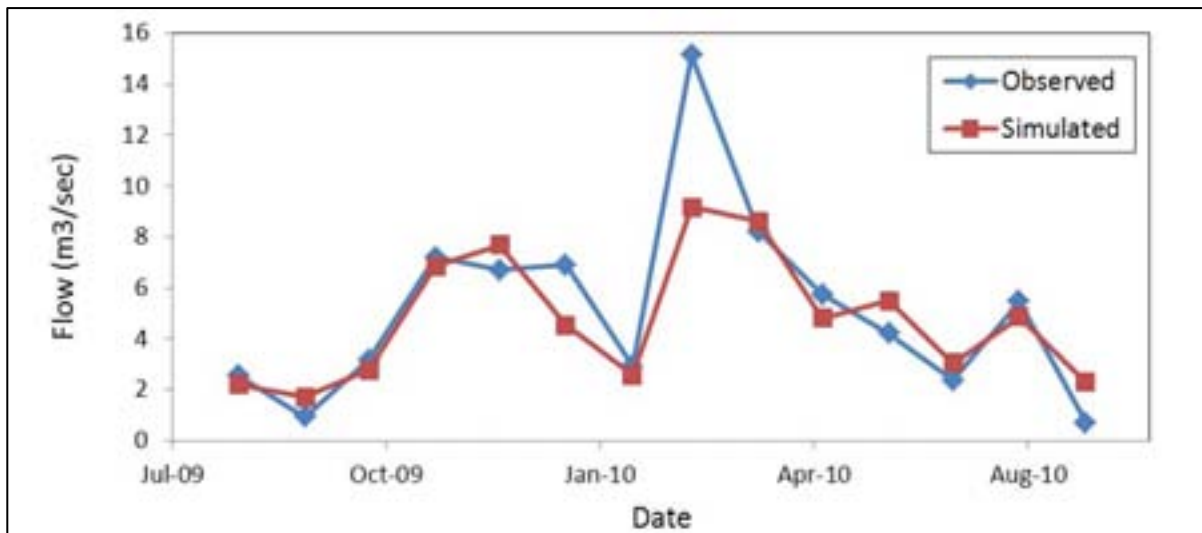
Figure C25. Hungerford Brook, daily flow calibration, 9/2009-9/2010.
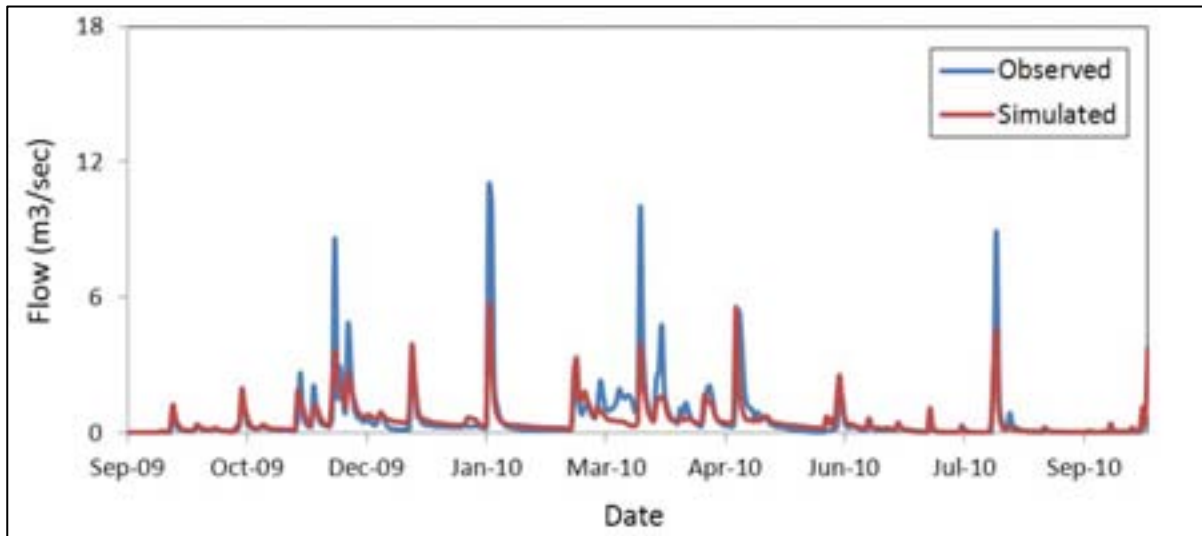
Figure C26. Hungerford Brook, monthly flow calibration, 10/2009-9/2010.

STONE ENVIRONMENTAL INC
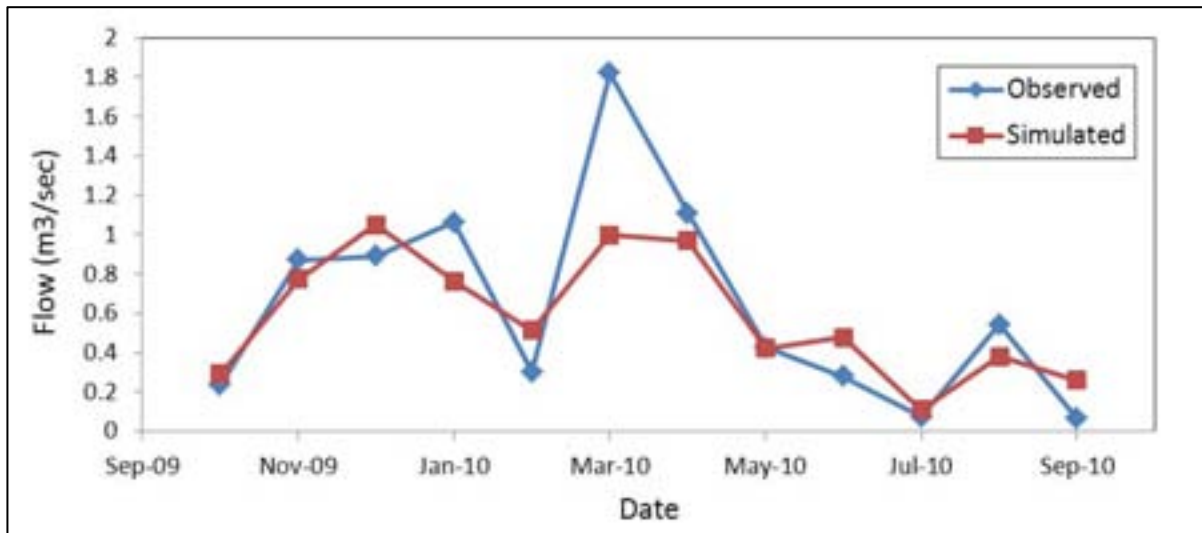
C.2. Sediment Calibration/Validation

Figure C27. Upper Missisquoi upstream of Mud Brook, monthly sediment calibration, 10/2005 – 9/2009.
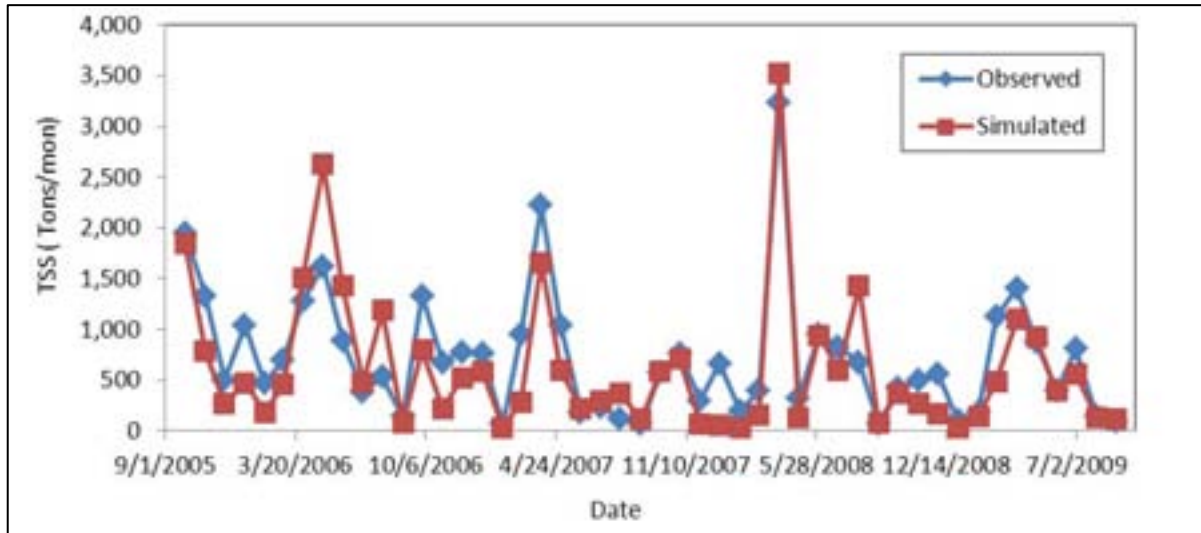
Figure C28. Upper Missisquoi upstream of Mud Brook, monthly sediment validation, 10/2001 – 9/2005.

STONE ENVIRONMENTAL INC
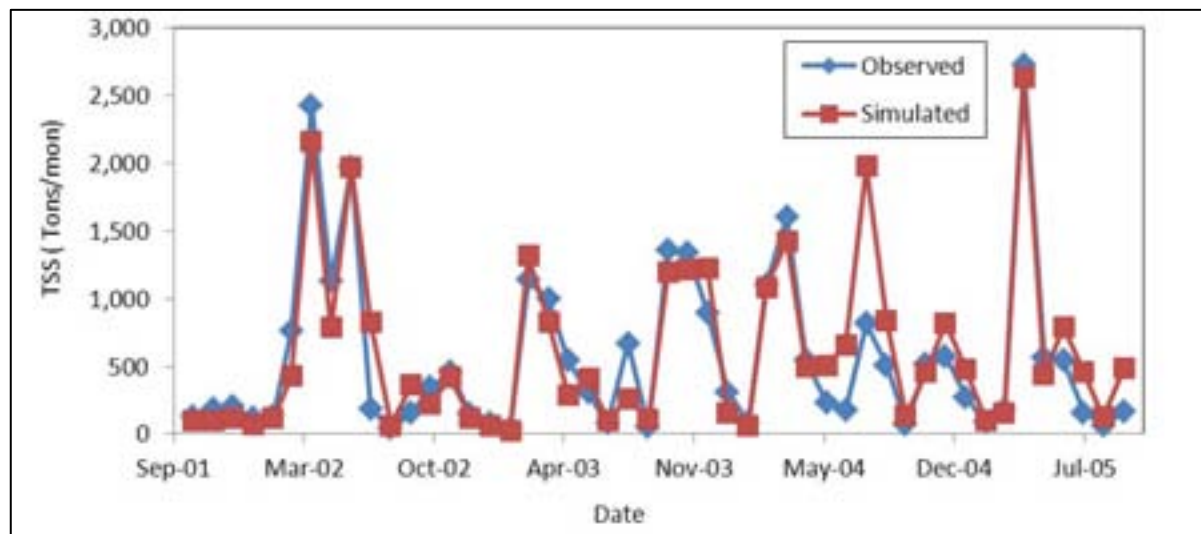
Figure C29. Missisquoi Nord near East Richford, monthly sediment calibration, 10/2005 – 9/2009.
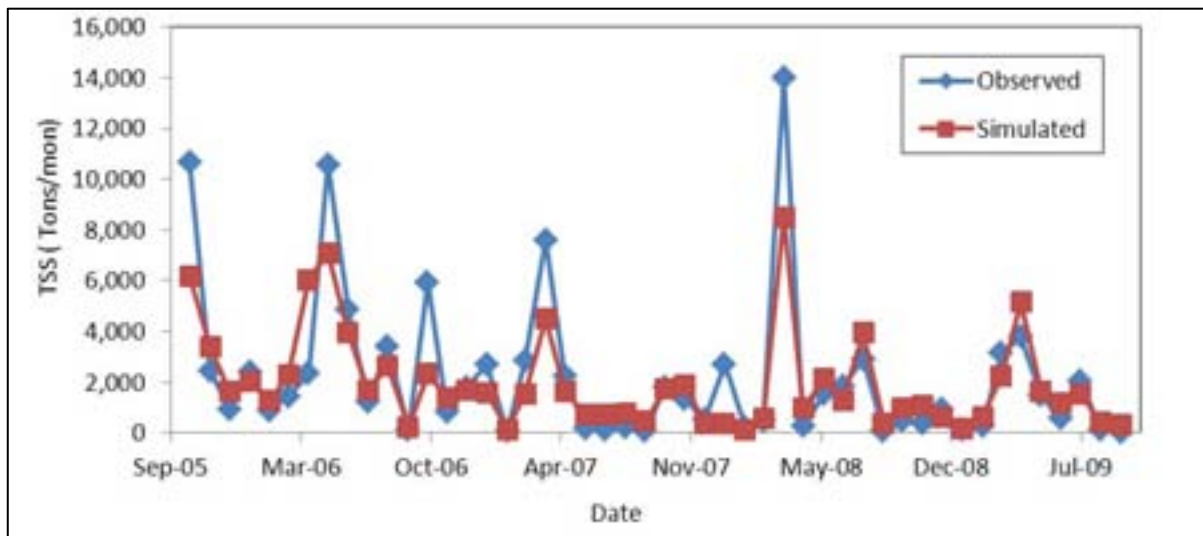
Figure C30. Missisquoi Nord near East Richford, monthly sediment validation, 10/2001 – 9/2005.

STONE ENVIRONMENTAL INC
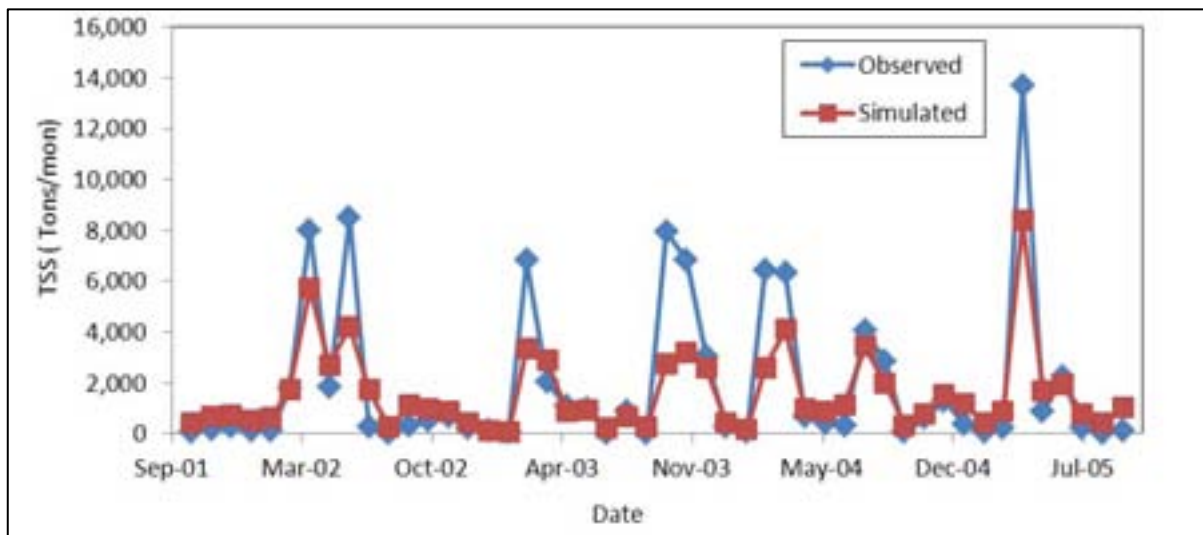
Figure C31. Missisquoi at Swanton, monthly sediment calibration, 10/2005 – 9/2009.
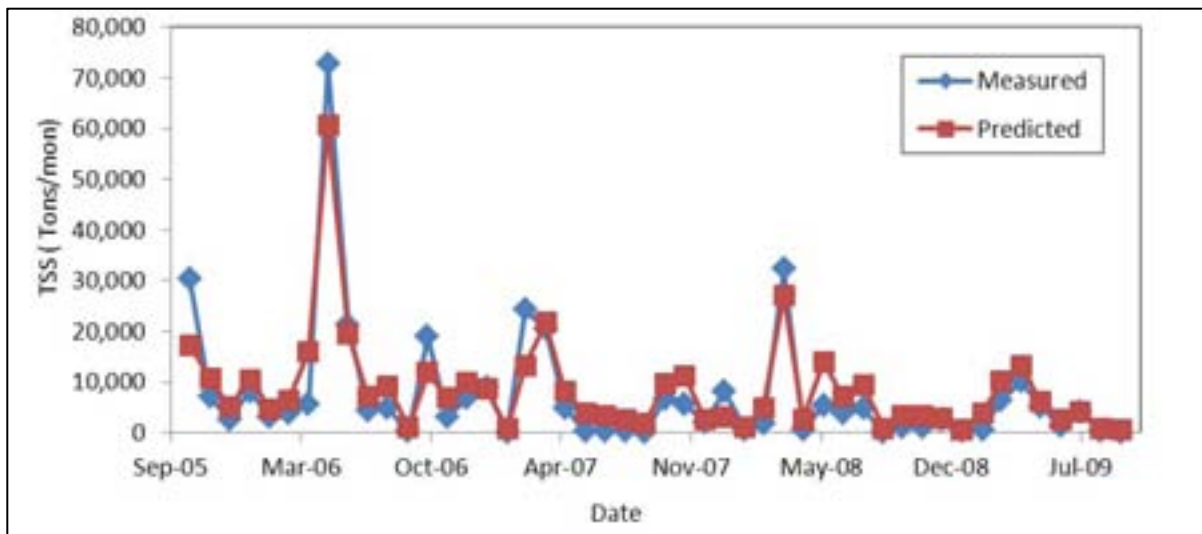
Figure C32. Missisquoi at Swanton, monthly sediment validation, 10/2001 – 9/2005.

STONE ENVIRONMENTAL INC
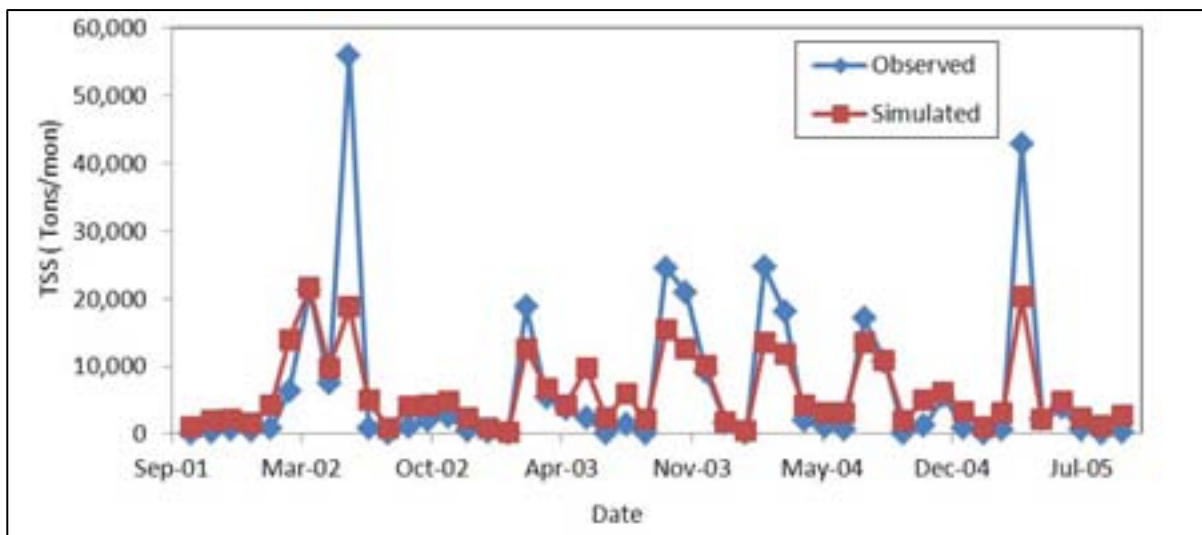
Figure C33. Upper Rock at S. Armand, monthly sediment calibration, 10/2005 – 9/2009.
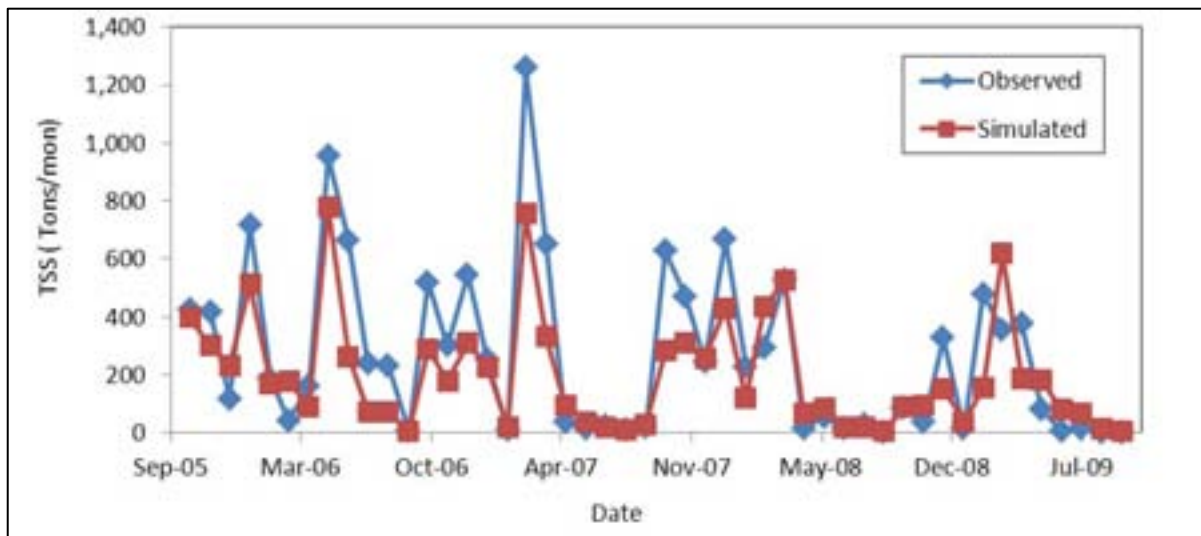
Figure C34. Upper Rock at S. Armand, monthly sediment validation, 10/2001 – 9/2005.

STONE ENVIRONMENTAL INC
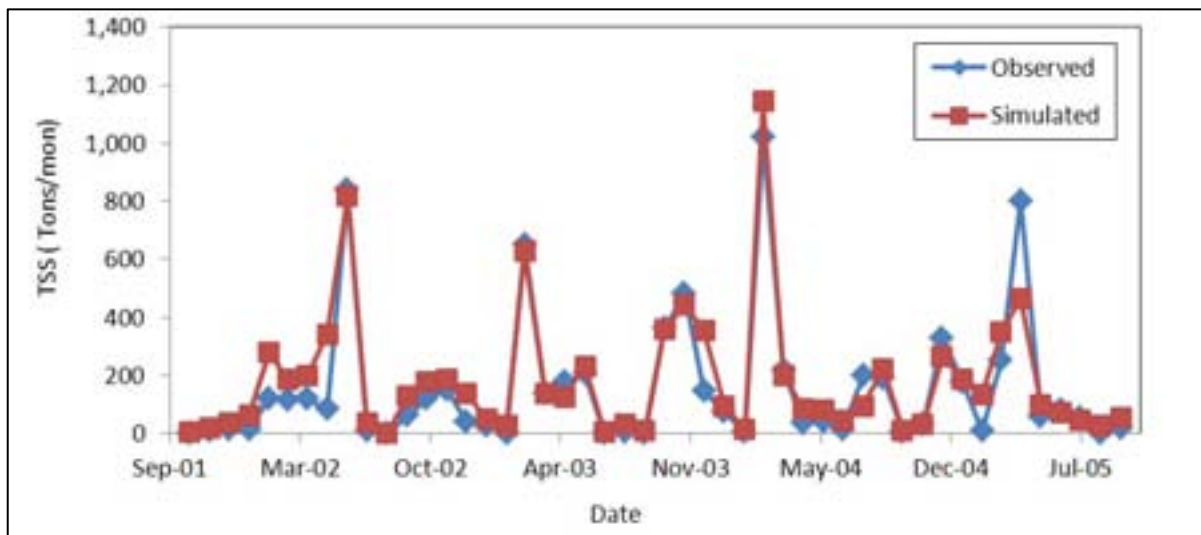
Figure C35. Lower Rock (north of border), monthly sediment calibration, 10/2005 – 9/2009.
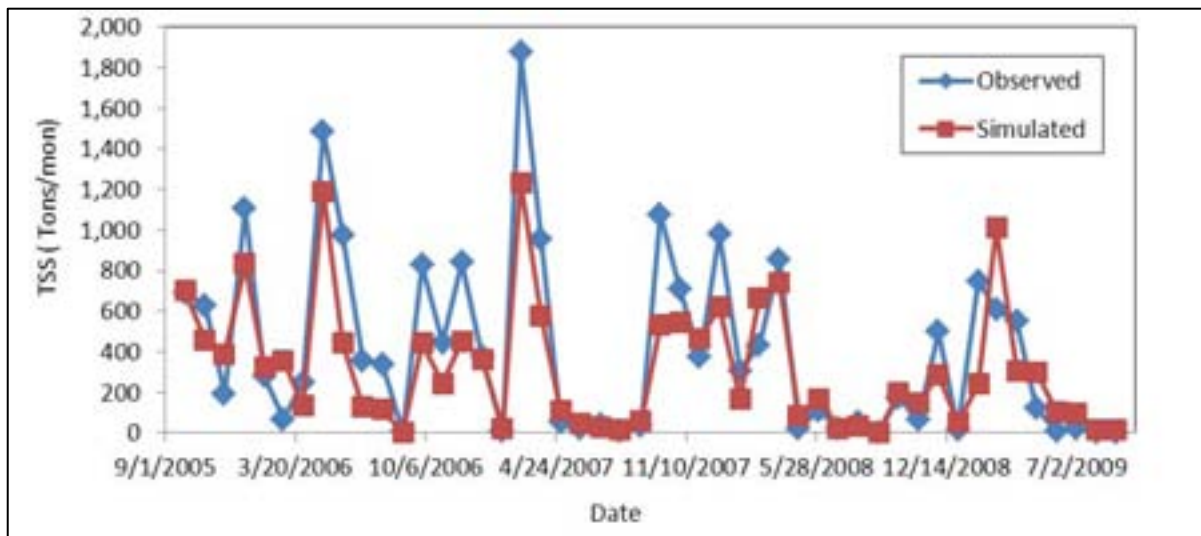
Figure C36. Lower Rock (north of border), monthly sediment validation, 10/2001 – 9/2005.

Stone Environmental Inc
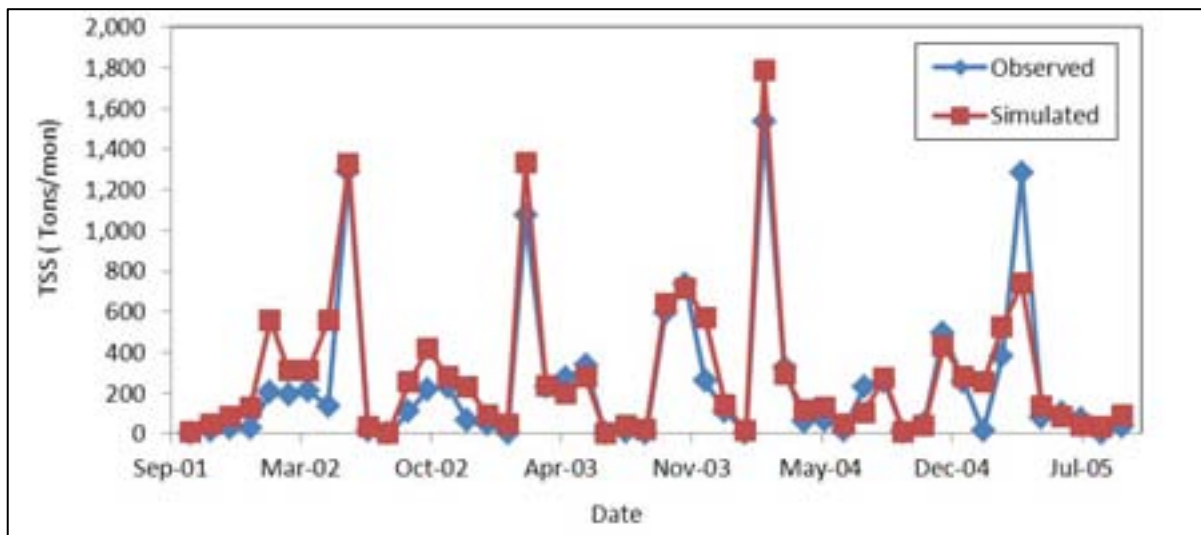
C.3. Phosphorus Calibration/Validation

Figure C37. Upper Missisquoi upstream of Mud Brook, monthly phosphorus calibration, 10/2005 – 9/2009.
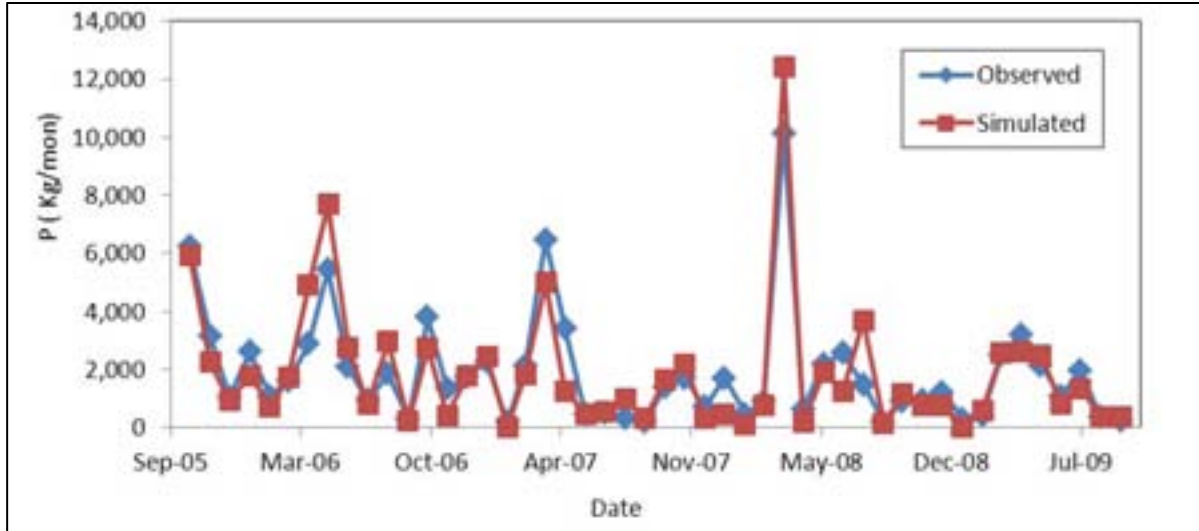
Figure C38. Upper Missisquoi upstream of Mud Brook, monthly phosphorus validation, 10/2001 – 9/2005.

STONE ENVIRONMENTAL INC
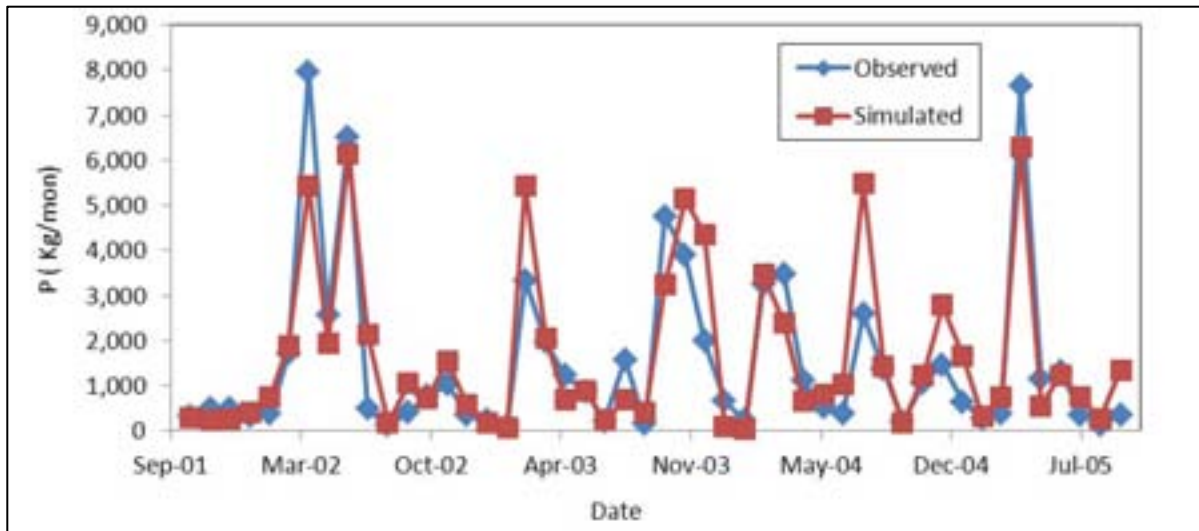
Figure C39. Missisquoi Nord near East Richford, monthly phosphorus calibration, 10/2005 – 9/2009.
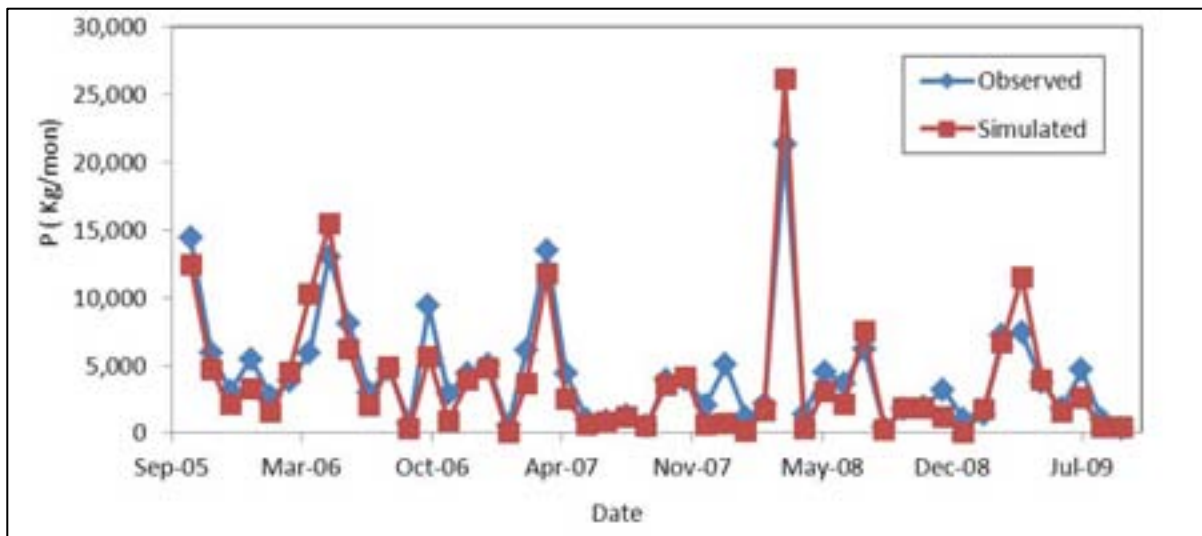
Figure C40. Missisquoi Nord near East Richford, monthly phosphorus validation, 10/2001 – 9/2005.

STONE ENVIRONMENTAL INC
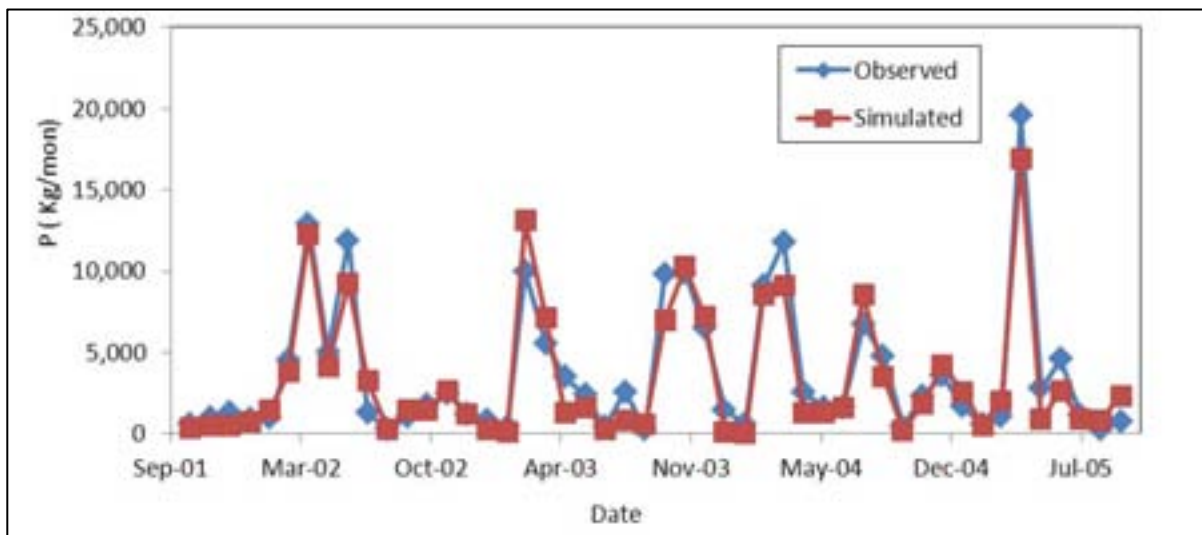
Figure C41. Missisquoi at Swanton, monthly phosphorus calibration, 10/2005 – 9/2009.
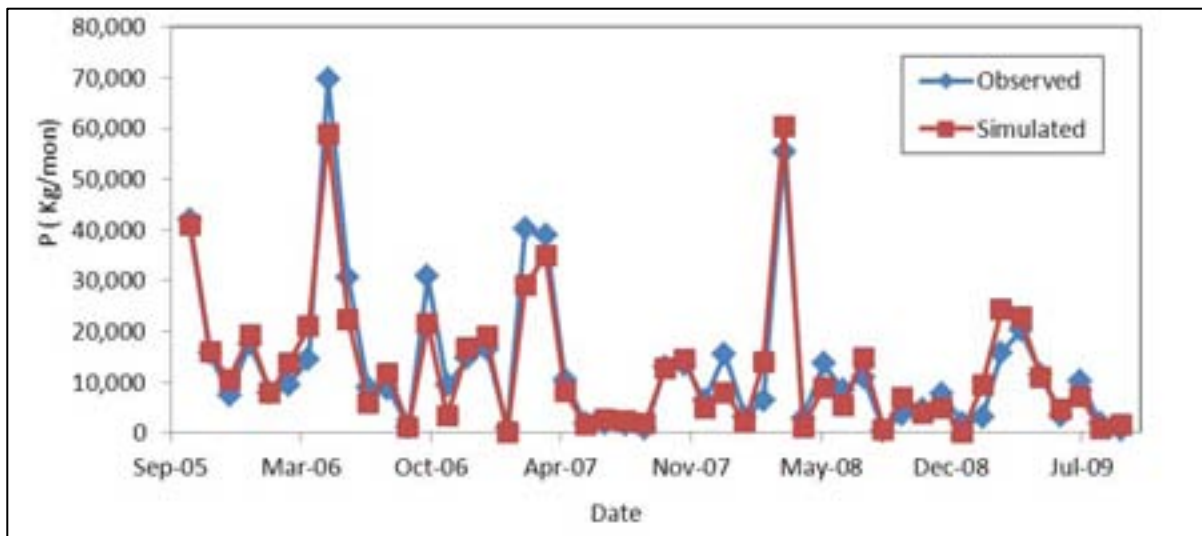
Figure C42. Missisquoi at Swanton, monthly phosphorus validation, 10/2001 – 9/2005.

STONE ENVIRONMENTAL INC
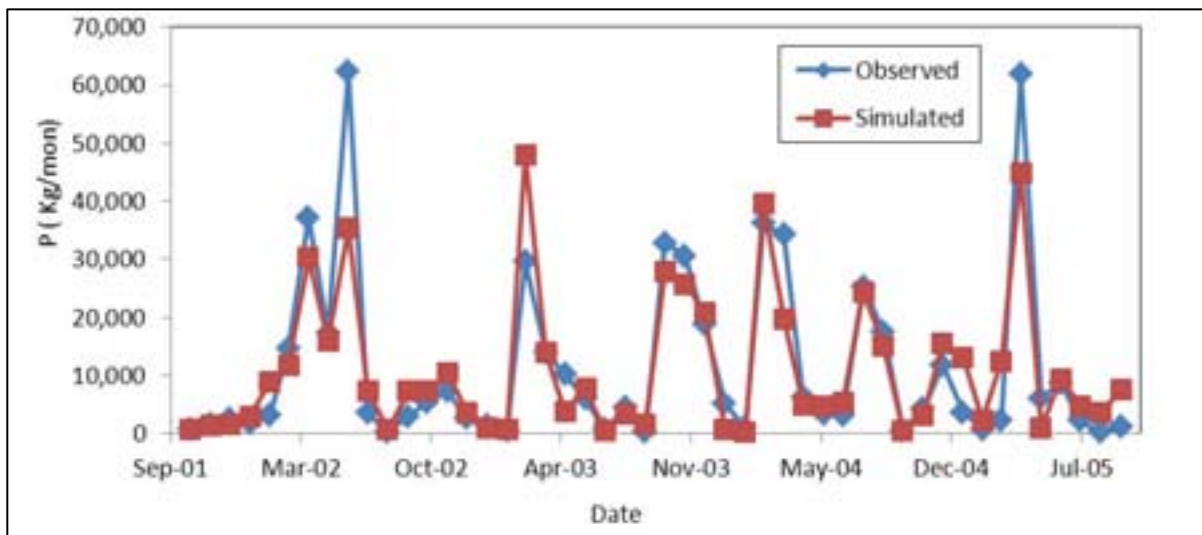
Figure C43. Upper Rock at S. Armand, monthly phosphorus calibration, 10/2005 – 9/2009.
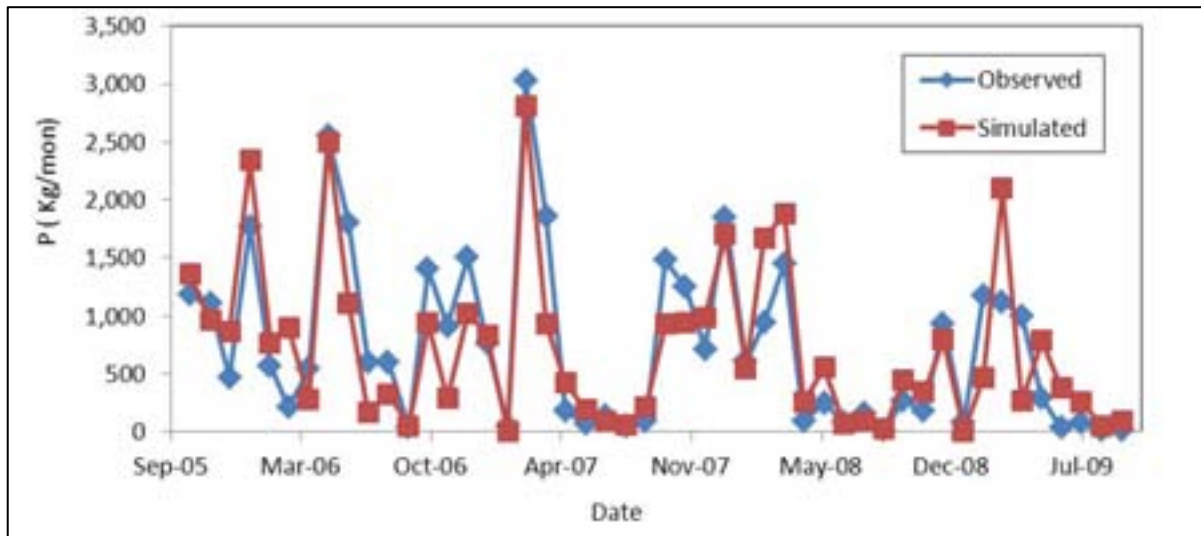
Figure C44. Upper Rock at S. Armand, monthly phosphorus validation, 10/2001 – 9/2005.

STONE ENVIRONMENTAL INC
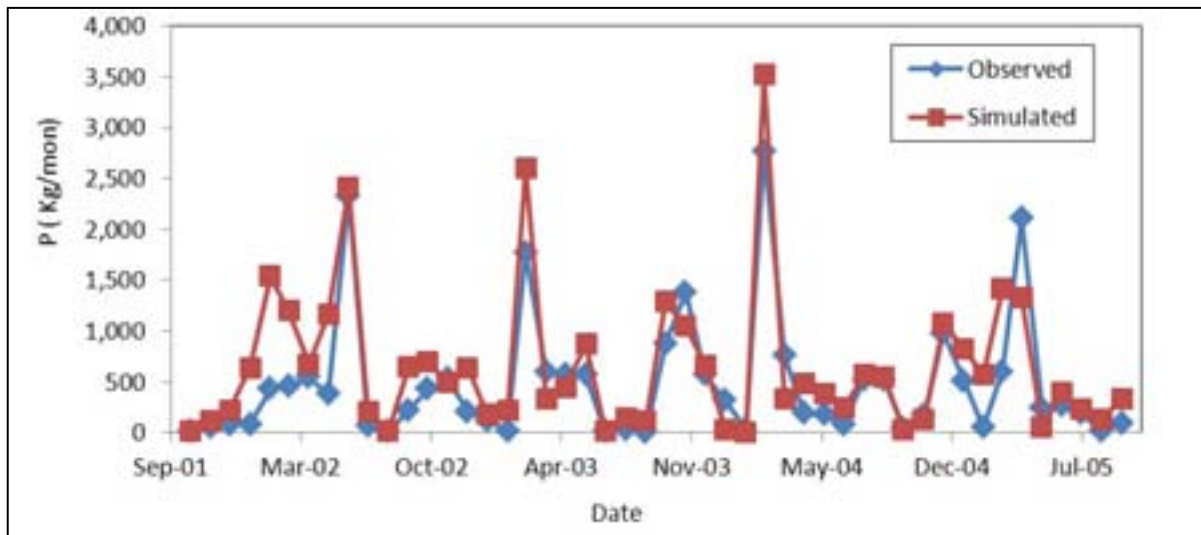
Figure C45. Lower Rock (north of border), monthly phosphorus calibration, 10/2005 – 9/2009.
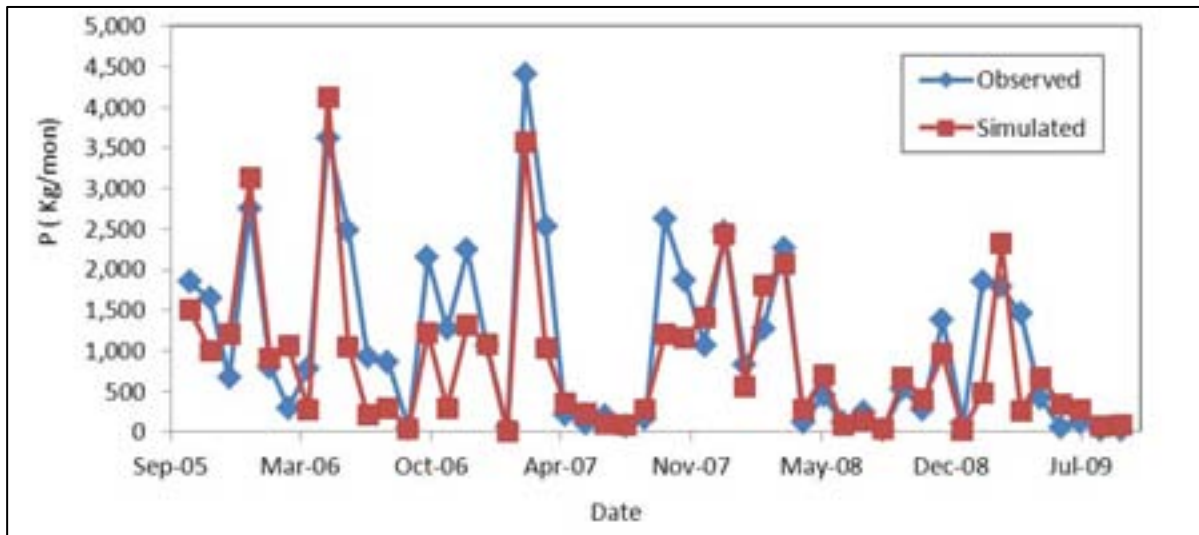
Figure C46. Lower Rock (north of border), monthly phosphorus validation, 10/2001 – 9/2005.
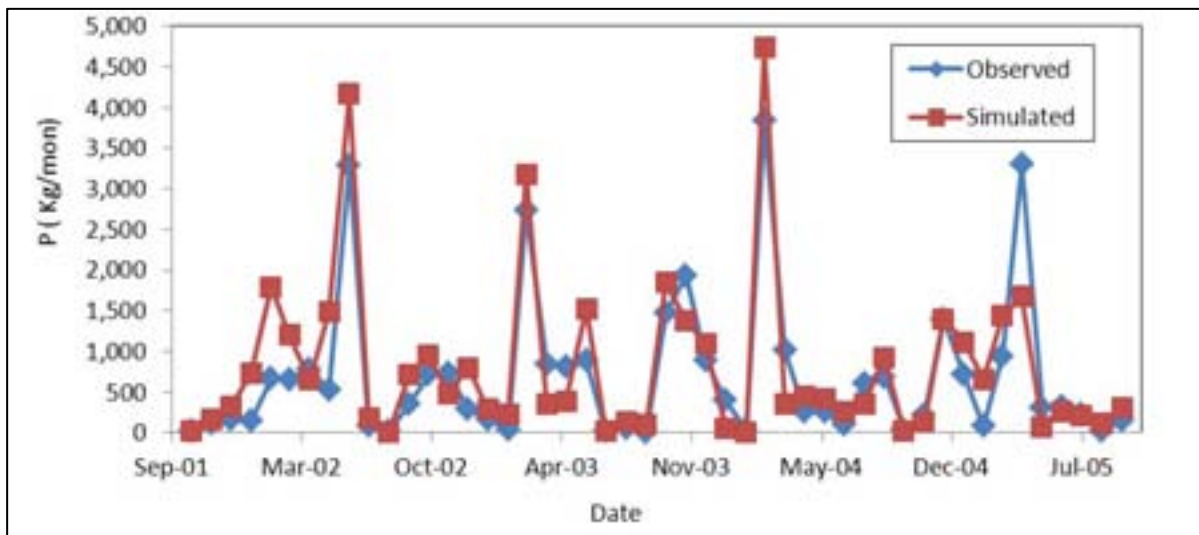
STONE ENVIRONMENTAL INC

APPENDIX D: MAPS

Identification of Critical Source Areas of Phosphorus Pollution within the Vermont Sector of the Missisquoi Bay Basin

Missisquoi Bay Basin Study Area

Compiled SWAT Model DEM

Map 2.1

Sources: DEM: Stone Environmental (2010); HUC 12 Watersheds: USGS; Imagery (2009): esri.

Elevation
High : 1175
Low : 2
Rivers and Streams
HUC (12) Watersheds
DEM Sources

Miles
0   5   10

N

QC CDED1

VT HYDRODEM

East LiDAR

West LiDAR

STONE ENVIRONMENTAL INC

Identification of Critical Source
Areas of Phosphorus Pollution
within the Vermont Sector of
the Missisquoi Bay Basin
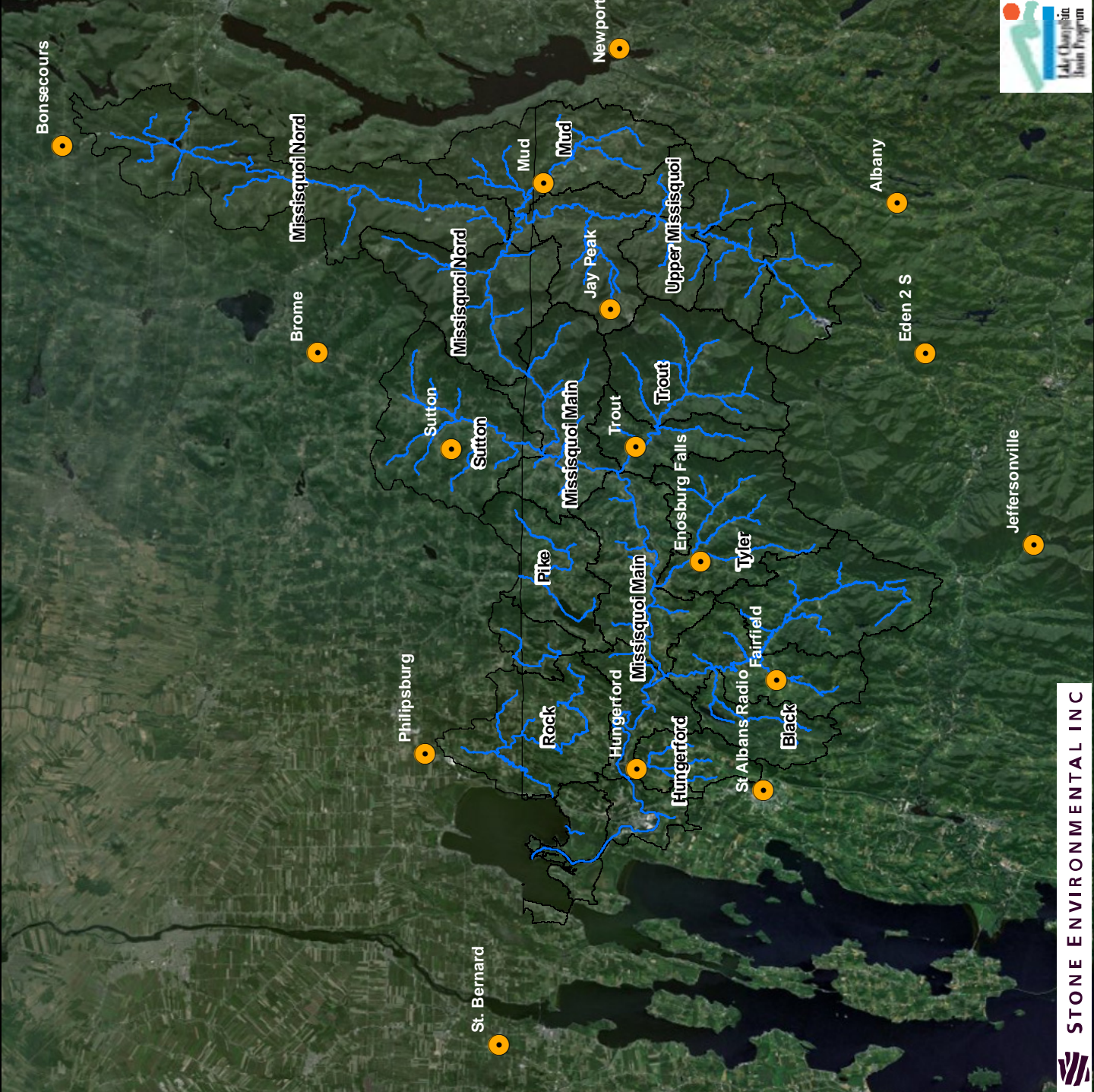
Missisquoi Bay
Basin Study Area

Weather Station
Locations

Map 2.4

Weather Stations
Rivers and Streams
HUC (12) Watersheds

N

Miles
0   5   10

STONE ENVIRONMENTAL INC

Lake Champlain
Basin Program

O:\Proj-09\AIM2156-G LCBP Phosphorus Critical Source Areas\Data\MapDocuments\PresentationsAndReports\FinalReport\Map2.4_ClimateStations.mxd

Bonsecours

Brome

Sutton

Missisquoi Nord

Missisquoi Nord

Mud

Mud

Jay Peak

Upper Missisquoi

Newport

Albany

Eden 2 S

Trout

Trout

Sutton

Missisquoi Main

Pike

Enosburg Falls

Tyler

Jeffersonville

Philipsburg

Rock

Hungerford

Missisquoi Main

Hungerford

Fairfield

St Albans Radio

Black

St. Bernard

205

Average Annual Precipitation (in.)

35 - 38
39 - 40
41 - 42
43 - 44
45 - 48
49 - 52
53 - 56
57 - 60
61 - 64
65 - 75

Rivers and Streams

HUC (12) Watersheds

Map 2.5

Average Annual
Precipitation, 1971-2000

Missisquoi Bay
Basin Study Area

Identification of Critical Source
Areas of Phosphorus Pollution
within the Vermont Sector of
the Missisquoi Bay Basin

N

Miles

0   5   10

Missisquoi Nord

Mud

Missisquoi Nord

Upper Missisquoi

Sutton

Missisquoi Main

Trout

Pike

Missisquoi Main

Tyler

Black

Rock

Hungerford

STONE ENVIRONMENTAL INC

Average Annual Max Temp (F)

Average Annual Max Temp (F)

- 44.2 - 46.4
- 46.5 - 47.5
- 47.6 - 48.4
- 48.5 - 49.3
- 49.4 - 50.1
- 50.2 - 50.8
- 50.9 - 51.5
- 51.6 - 52.1
- 52.2 - 52.8
- 52.9 - 54

— Rivers and Streams

☐ HUC (12) Watersheds
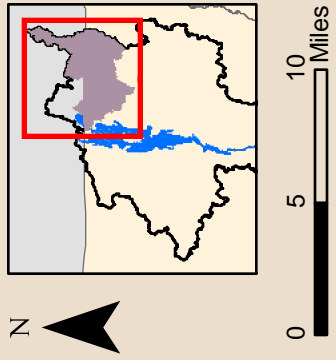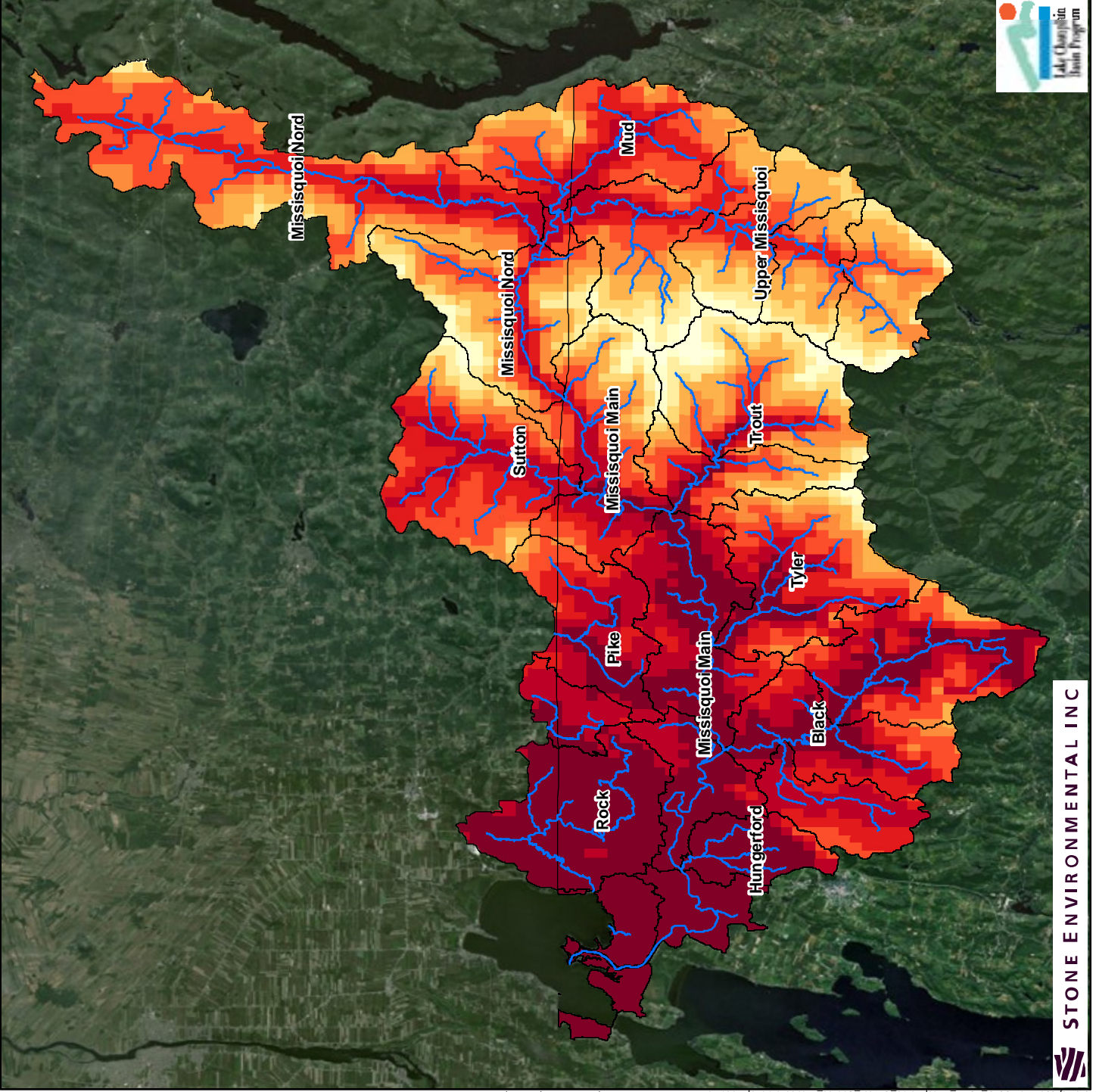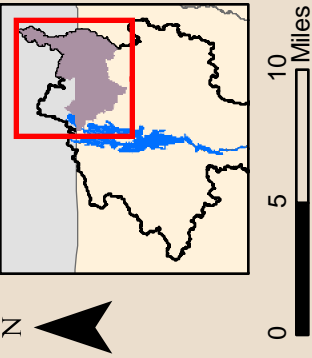
Map 2.6

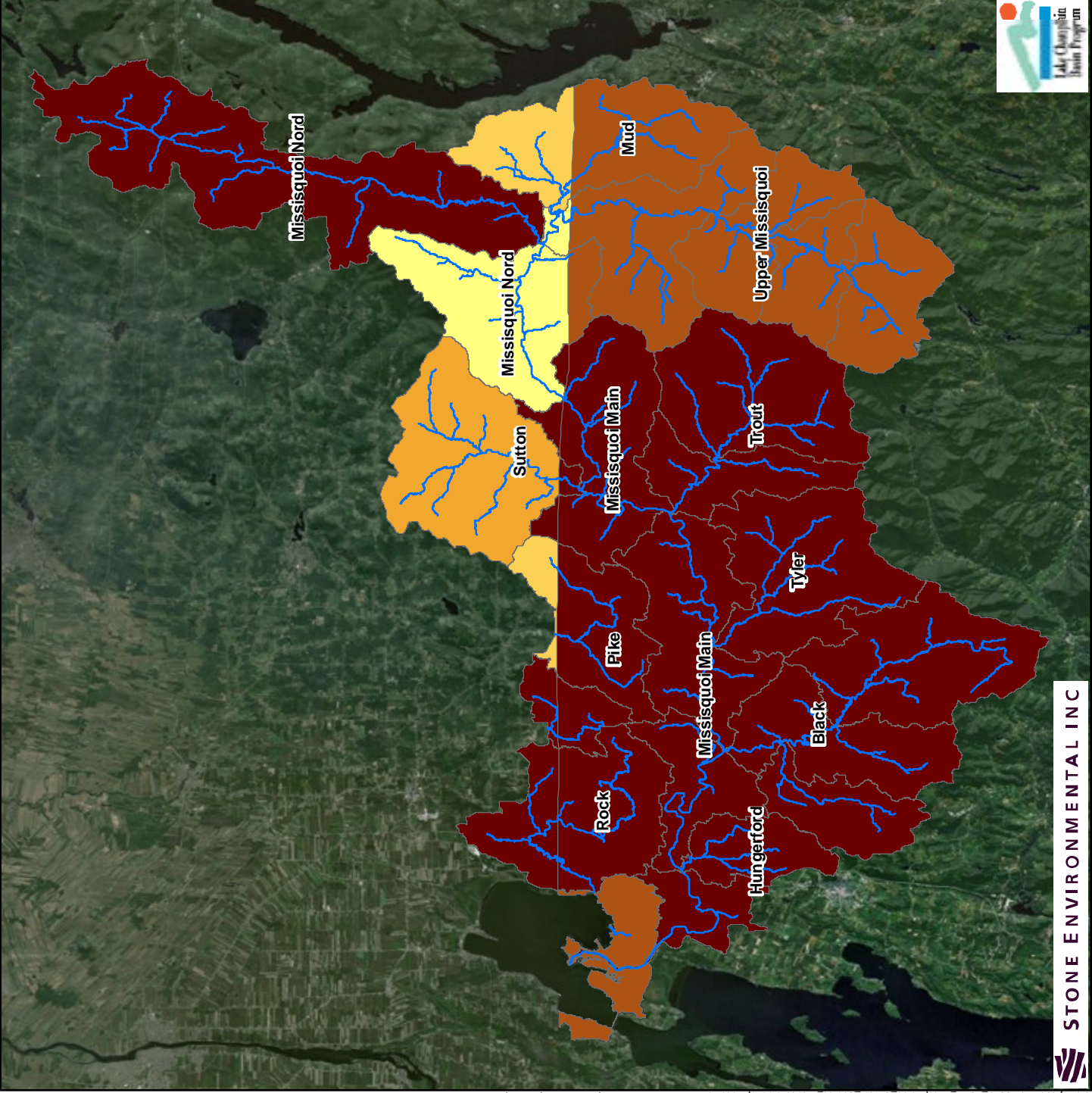Average Annual Maximum Temperature, 1971-2000

Missisquoi Bay Basin Study Area

Identification of Critical Source Areas of Phosphorus Pollution within the Vermont Sector of the Missisquoi Bay Basin

STONE ENVIRONMENTAL INC

Missisquoi Nord

Mud

Upper Missisquoi

Missisquoi Nord

Sutton

Missisquoi Main

Trout

Tyler

Pike

Missisquoi Main

Black

Rock

Hungerford

O:\Proj-09\AIM2156-G LCBP Phosphorus Critical Source Areas\Data\MapDocuments\Presentations\AndReports\FinalReport\Map2.6_PRISM_TMax.mxd

207

Average Annual Min Temp (F)

26.4 - 28.4
28.5 - 29.4
29.5 - 30.2
30.3 - 30.9
31 - 31.7
31.8 - 32.3
32.4 - 33
33.1 - 33.9
34 - 34.6
34.7 - 35.5

Rivers and Streams

HUC (12) Watersheds

N

Miles
0   5   10

Sources: Average Annual Min Temp:
PRISM Climate Group; HUC 12 Watersheds:
USGS; Imagery (2009): esri.
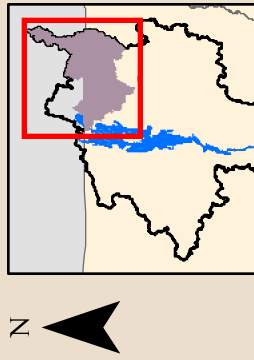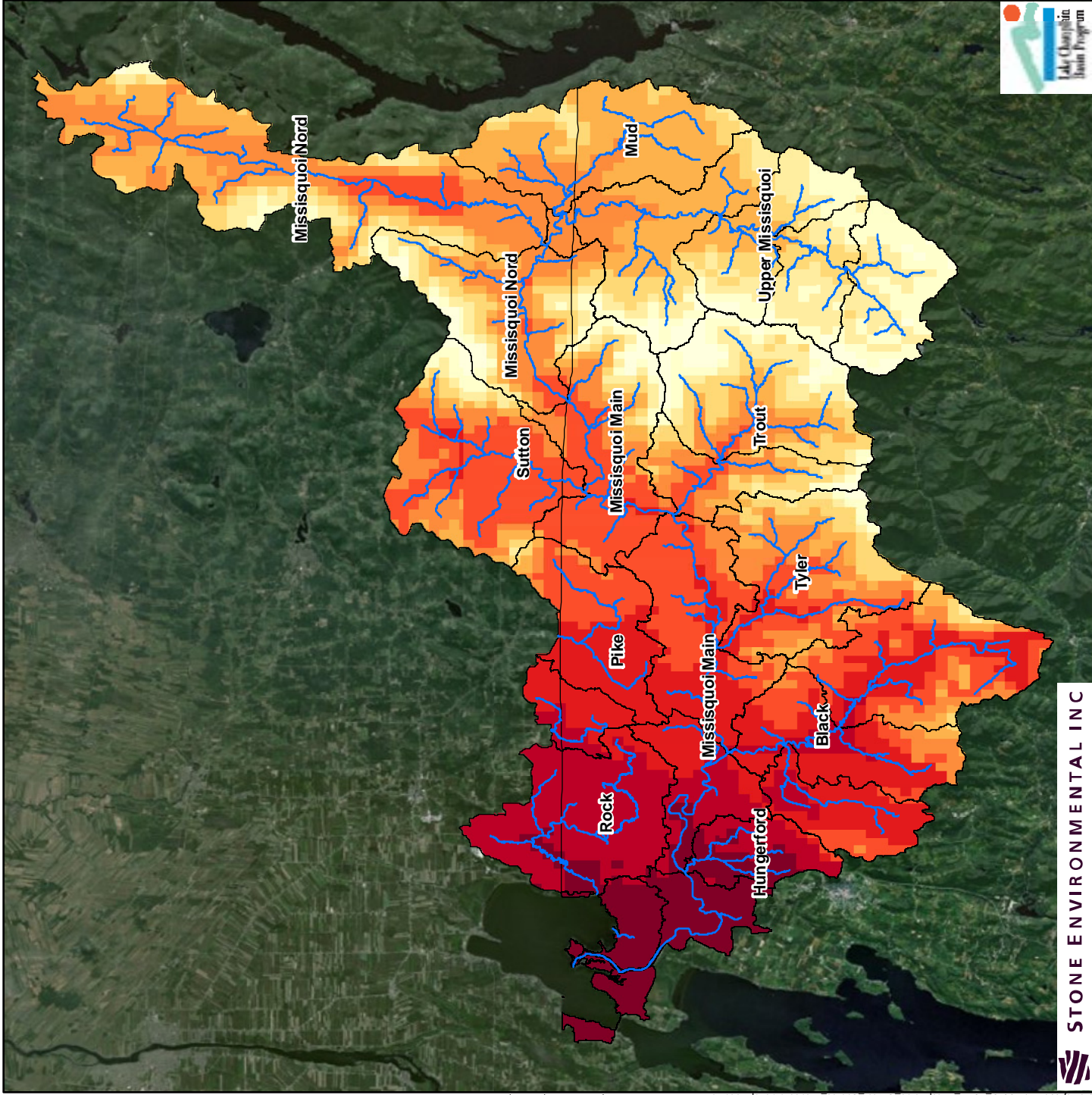
Map 2.7

Average Annual
Minimum Temperature,
1971-2000

Missisquoi Bay
Basin Study Area

Identification of Critical Source
Areas of Phosphorus Pollution
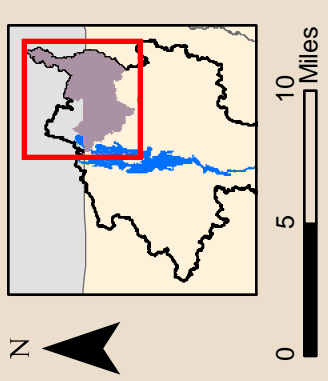within the Vermont Sector of
the Missisquoi Bay Basin

STONE ENVIRONMENTAL INC

Missisquoi Nord

Mud

Upper Missisquoi

Missisquoi Nord

Sutton

Missisquoi Main

Trout

Pike

Tyler

Missisquoi Main

Black

Rock

Hungerford

Identification of Critical Source Areas of Phosphorus Pollution within the Vermont Sector of the Missisquoi Bay Basin

Map 2.8

Hybrid Land Use

Missisquoi Bay Basin Study Area
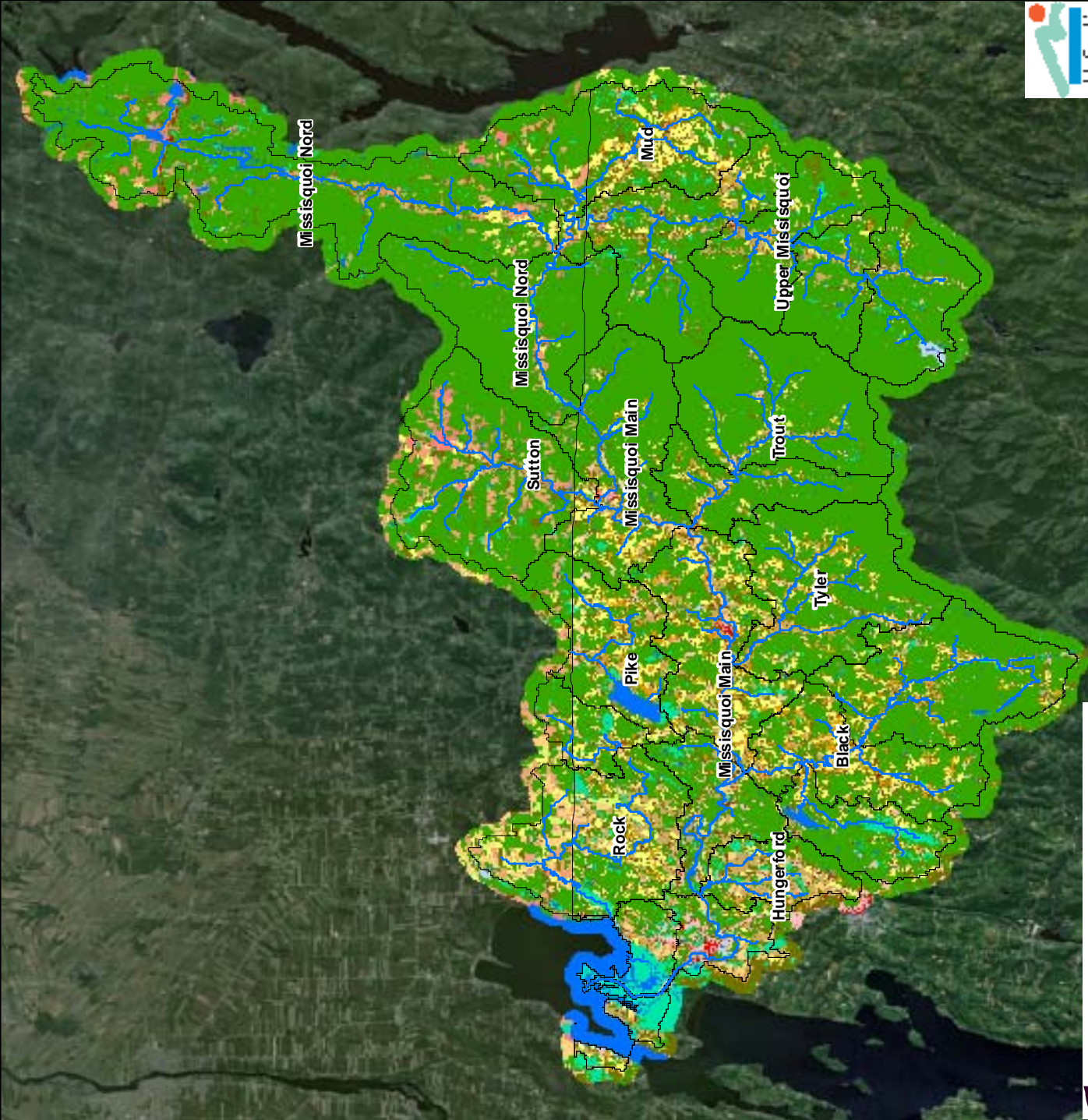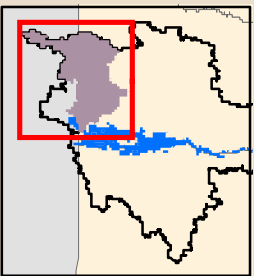
Hybrid Land Use
- Water
- Developed, Med/High Intensity
- Developed, Low Intensity
- Farmstead, SFO
- Farmstead, MFO/LFO
- Roads, Paved
- Roads, Unpaved
- Developed, Open
- Unmanaged Ag, Brush
- Continuous Corn
- Continuous Hay
- Corn/Hay Rotation
- Soybeans
- Pasture
- Cultivated Ag, General
- Forest
- Barren
- Wetland
- Rivers and Streams
- HUC (12) Watersheds

Sources: Hybrid Land Use : Stone Environmental; HUC 12 Watersheds: USGS; Imagery (2009) : esri.

N

Miles
0   5   10

STONE ENVIRONMENTAL INC

O:\Proj09\AiM2156-G_LCBP_Phosphorus_Critical_Source_AreasDataMapDocumentsPresenationsAndReports\FinalReports\Map2.8_HybridLandUse.mxd
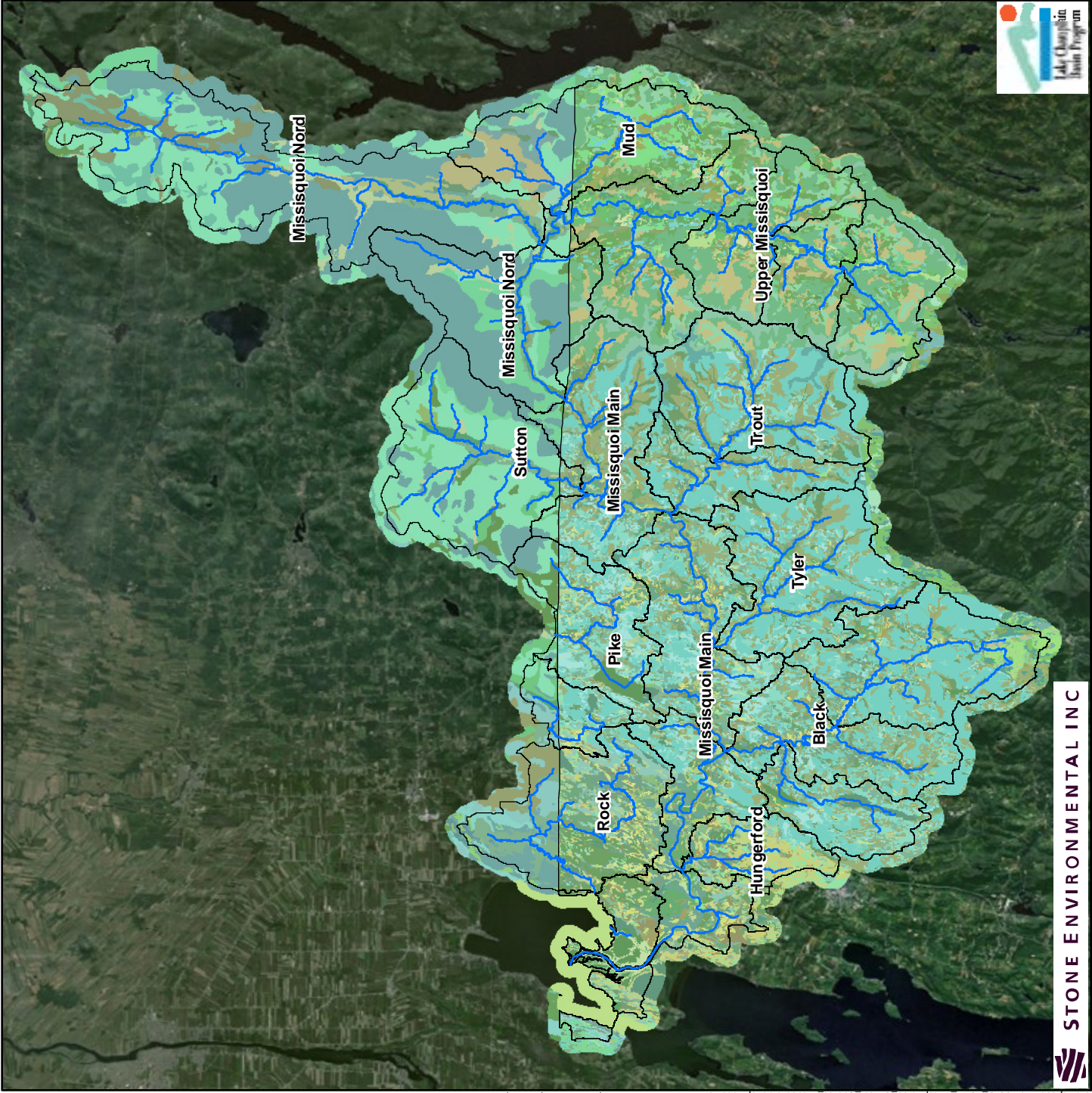
Map 2.9

Soils

Missisquoi Bay
Basin Study Area

Identification of Critical Source
Areas of Phosphorus Pollution
within the Vermont Sector of
the Missisquoi Bay Basin

Soil Mapping Units
Rivers and Streams
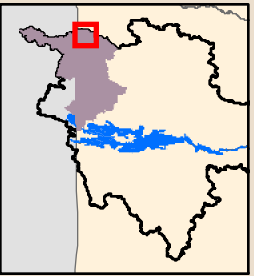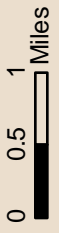HUC (12) Watersheds

Sources: Source: US Soils: NRCS
SSURGO; Quebec Soils: IRDA;
HUC 12 Watersheds: USGS;
Imagery (2009): esri.

N

0   5   10
Miles

STONE ENVIRONMENTAL INC

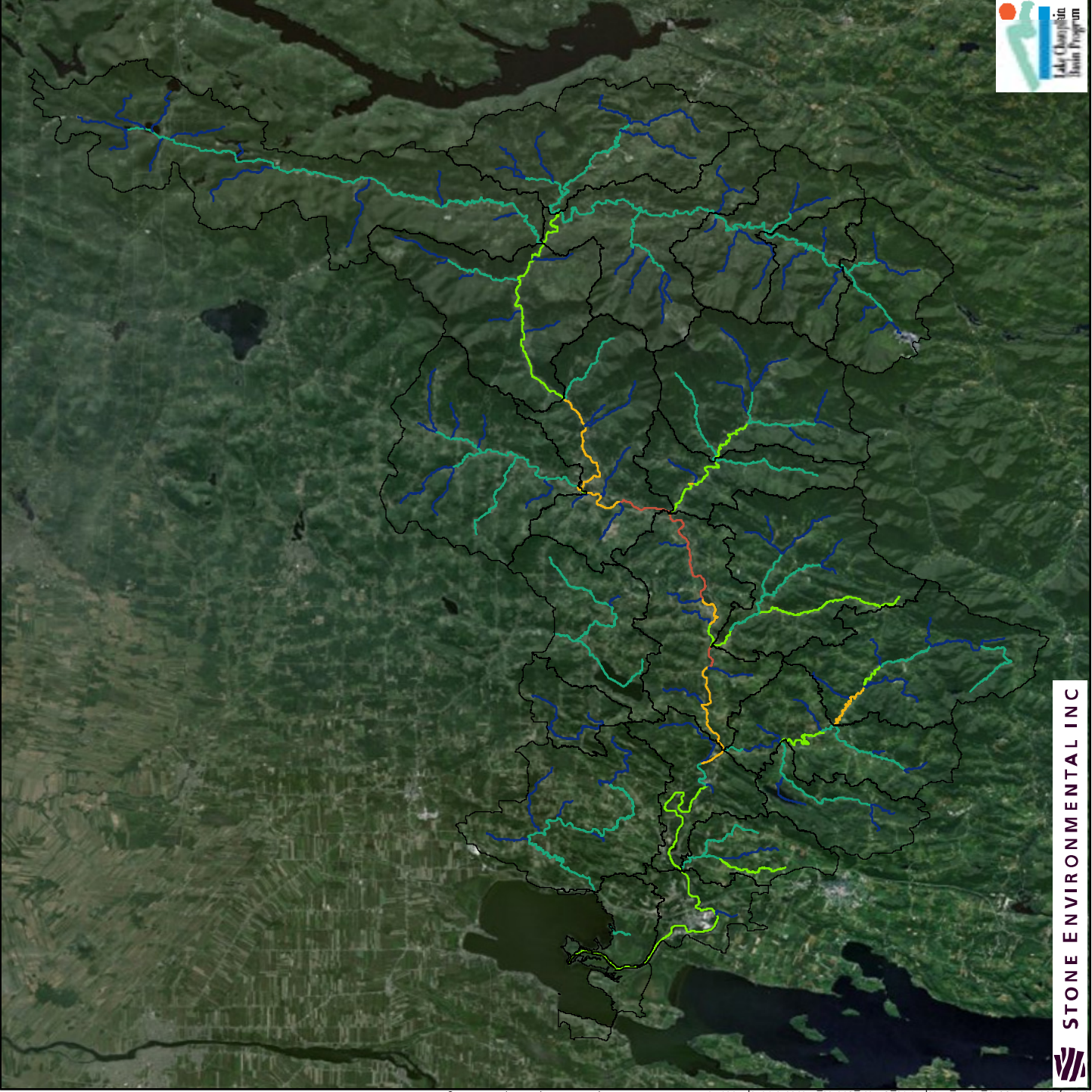O:\Proj-09\AIM2156-G LCBP Phosphorus Critical Source Areas\Data\MapDocuments\PresentationsAndReports\FinalReport\Map2.9_Soils.mxd

Map 2.10

Identification of Critical Source
Areas of Phosphorus Pollution
within the Vermont Sector of
the Missisquoi Bay Basin

Missisquoi Bay
Basin Study Area

Manure P Application Rate
on Cropland

Sources: Source: Manure P Rates:
Stone Environmental;
HUC 12 Watersheds: USGS;
Imagery (2009): esri.

Manure P on Cropland
(kg-P/ha-yr)
3 - 5
6 - 10
11 - 15
16 - 20
21 - 26
Rivers and Streams
HUC (12) Watersheds

N

Miles
0   5   10

STONE ENVIRONMENTAL INC

O:\Proj-09\AIM2156-G LCBP Phosphorus Critical Source Areas\Data\MapDocuments\Presentations\AndReports\FinalReport\Map2.10_ManureP.mxd

211
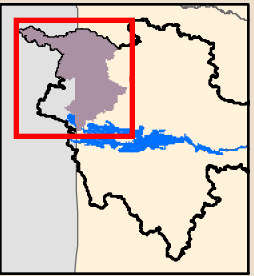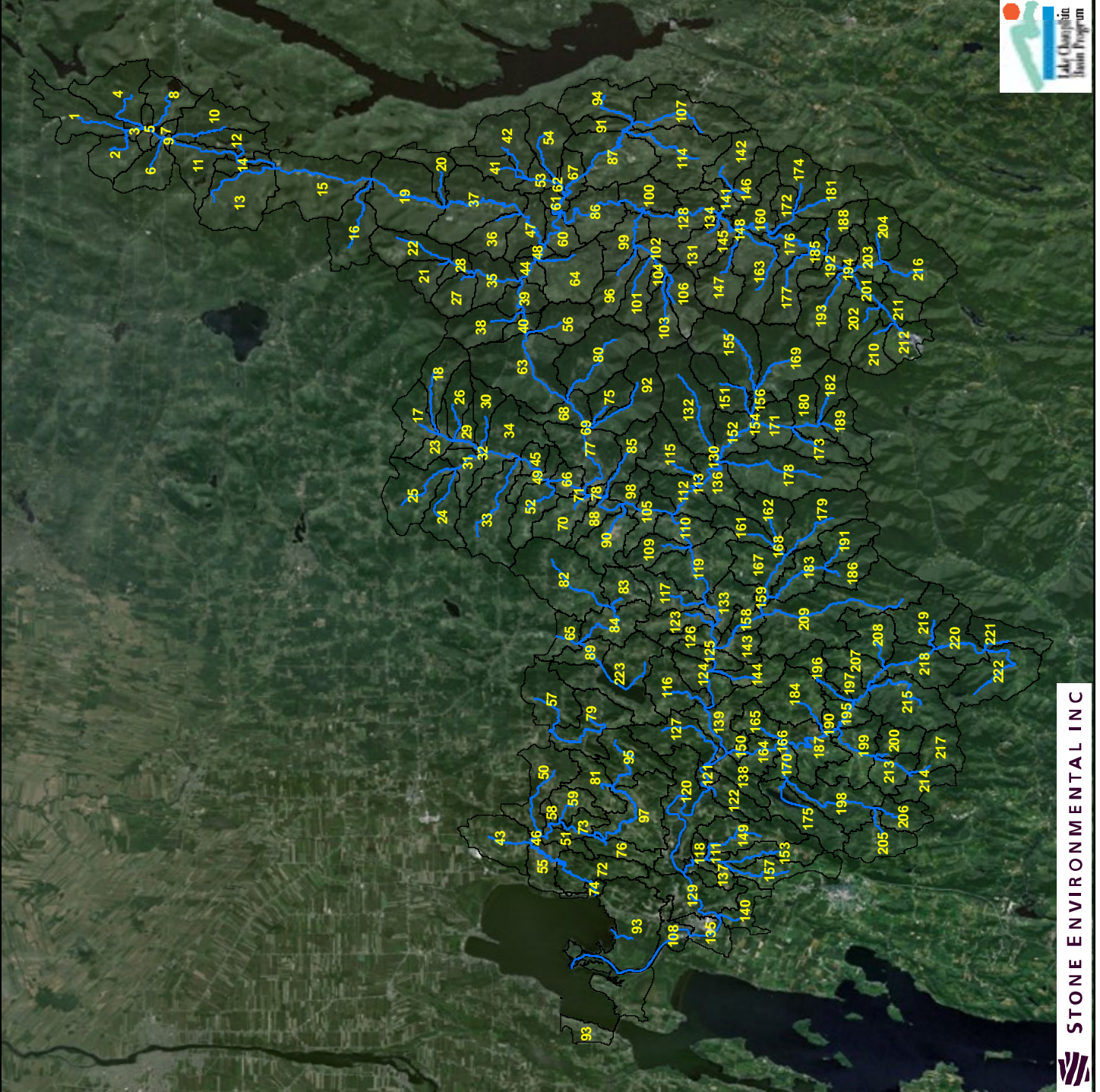
SWAT Reaches
☐ SWAT Subbasins

Sources: Source: SWAT Subbasins
and SWAT Reaches: Stone
Environmental; Imagery (2009); esri.
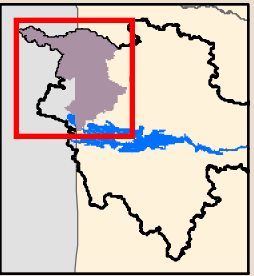
SWAT Subbasin and Reach
Delineation

Missisquoi Bay
Basin Study Area

Identification of Critical Source
Areas of Phosphorus Pollution
within the Vermont Sector of
the Missisquoi Bay Basin

Map 2.11

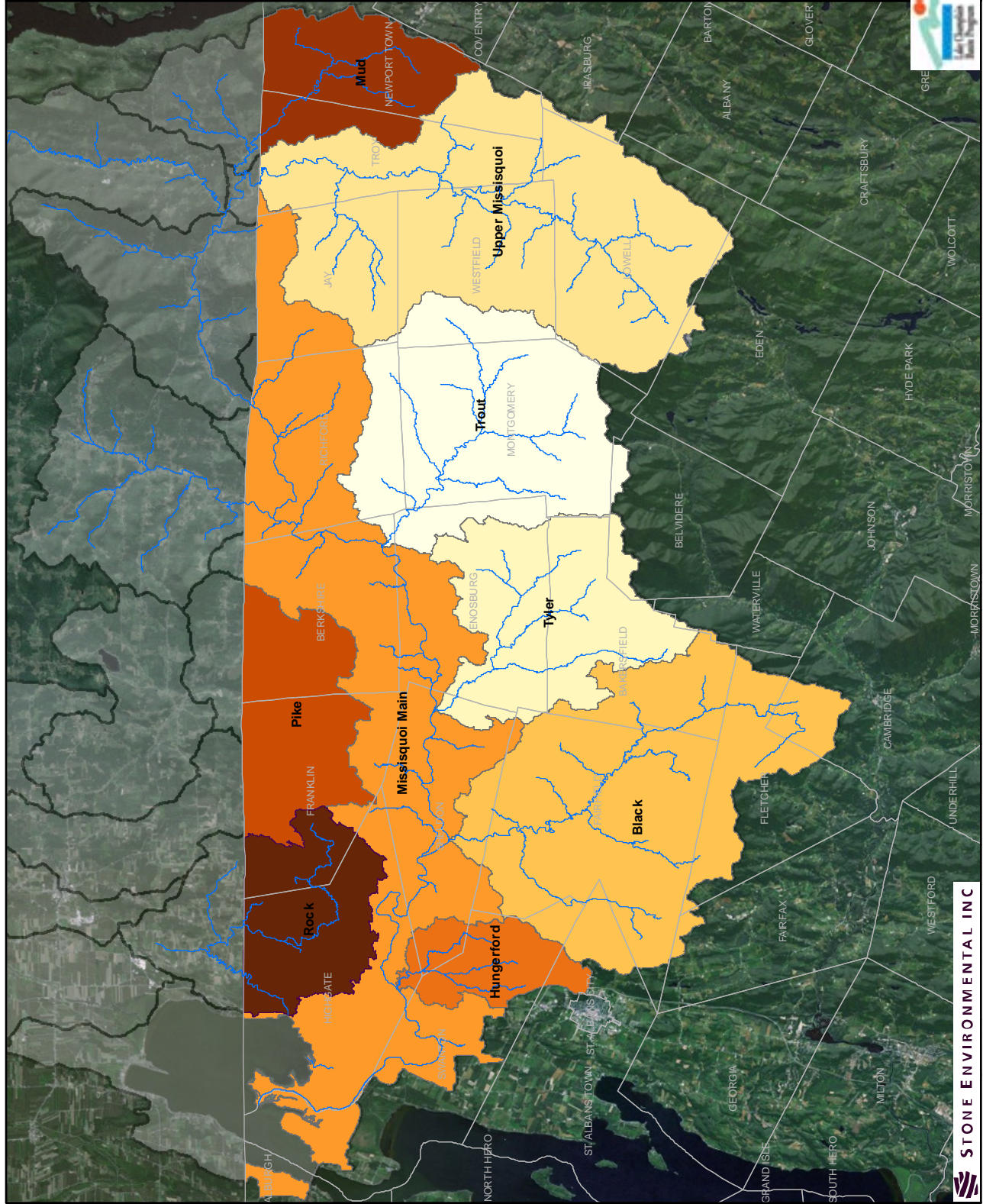STONE ENVIRONMENTAL INC

N

Miles
0 0.5 1

SWAT Reaches
SWAT Subbasins
HRU Delineation

Sources: Source: SWAT HRUs,
Subbasins and Reaches: Stone
Environmental; Imagery (2009): esri.

Map 2.12

SWAT HRU Delineation

Mud Brook Sub-Watershed

Identification of Critical Source
Areas of Phosphorus Pollution
within the Vermont Sector of
the Missisquoi Bay Basin

STONE ENVIRONMENTAL INC

Lake Champlain
Basin Program

O:\Proj-09\AIM2156-G LCBP Phosphorus Critical Source Areas\Data\MapDocuments\PresentationsAndReports\FinalReport\Map2.12_HRUDelin.mxd

Map 2.13

Bank Erosion Fraction
- 0.10 - 0.15
- 0.16 - 0.22
- 0.23 - 0.30
- 0.31 - 0.40
- 0.41 - 0.53
- ▢ HUC (12) Watersheds

Sources: Source: SWAT Reaches: Stone Environmental (2010); Bank Fraction Failing; ANR_USDA BSTEM Study, and Stone Environmenta (2011)\; Imagery (2009): esri.

Fraction of Bank Failing by SWAT Reach

Missisquoi Bay Basin Study Area

Identification of Critical Source Areas of Phosphorus Pollution within the Vermont Sector of the Missisquoi Bay Basin
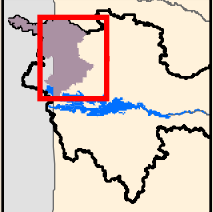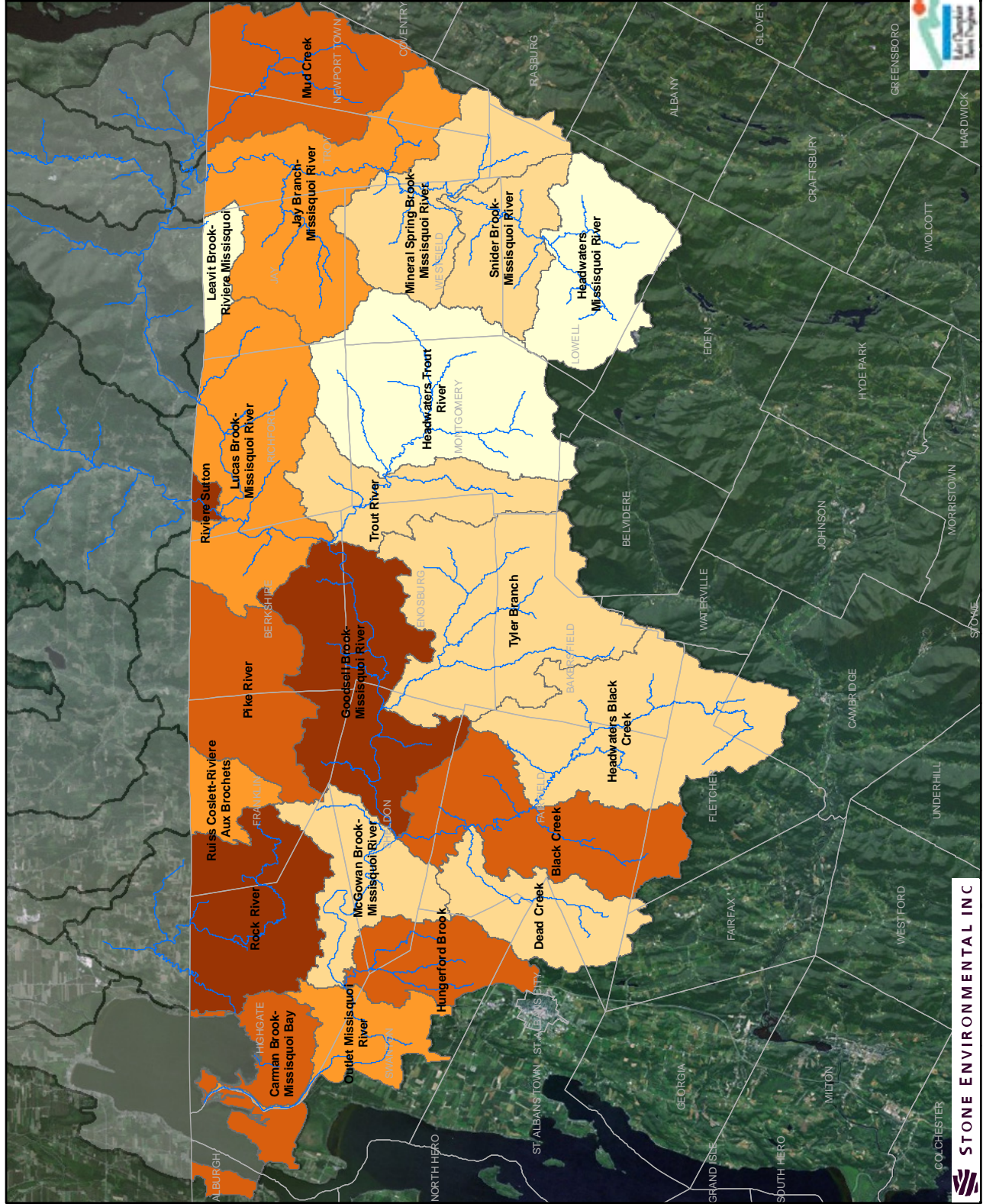
STONE ENVIRONMENTAL INC

Map 3.1

Average Annual Model
Estimated Total P Loading
by Sub-Watershed

Full Watershed

Identification of Critical Source
Areas of Phosphorus Pollution
within the Vermont Sector of
the Missisquoi Bay Basin

Avg. Annual Total P (kg/ha)

- 0.250
- 0.323
- 0.323
- 0.393
- 0.482
- 0.547
- 0.577
- 0.644
- 0.811

Rivers and Streams

HUC (12) Watersheds

N

Miles
0   2.5   5

Mud

Upper Missisquoi

Trout

Tyler

Pike

Missisquoi Main

Black

Rock

Hungerford

NEWPORT TOWN
COVENTRY
IRASBURG
BARTON
GLOVER
GRE
ALBANY
CRAFTSBURY
WOLCOTT
TROY
JAY
WESTFIELD
LOWELL
EDEN
HYDE PARK
MONTGOMERY
BELVIDERE
MORRISTOWN
NICHOLS
ENOSBURG
WATERVILLE
JOHNSON
MORRISTOWN
BERKSHIRE
BAKERSFIELD
CAMBRIDGE
FRANKLIN
FLETCHER
UNDERHILL
HIGHGATE
FAIRFAX
WESTFORD
FAIRFIELD
ST ALBANS TOWN
GEORGIA
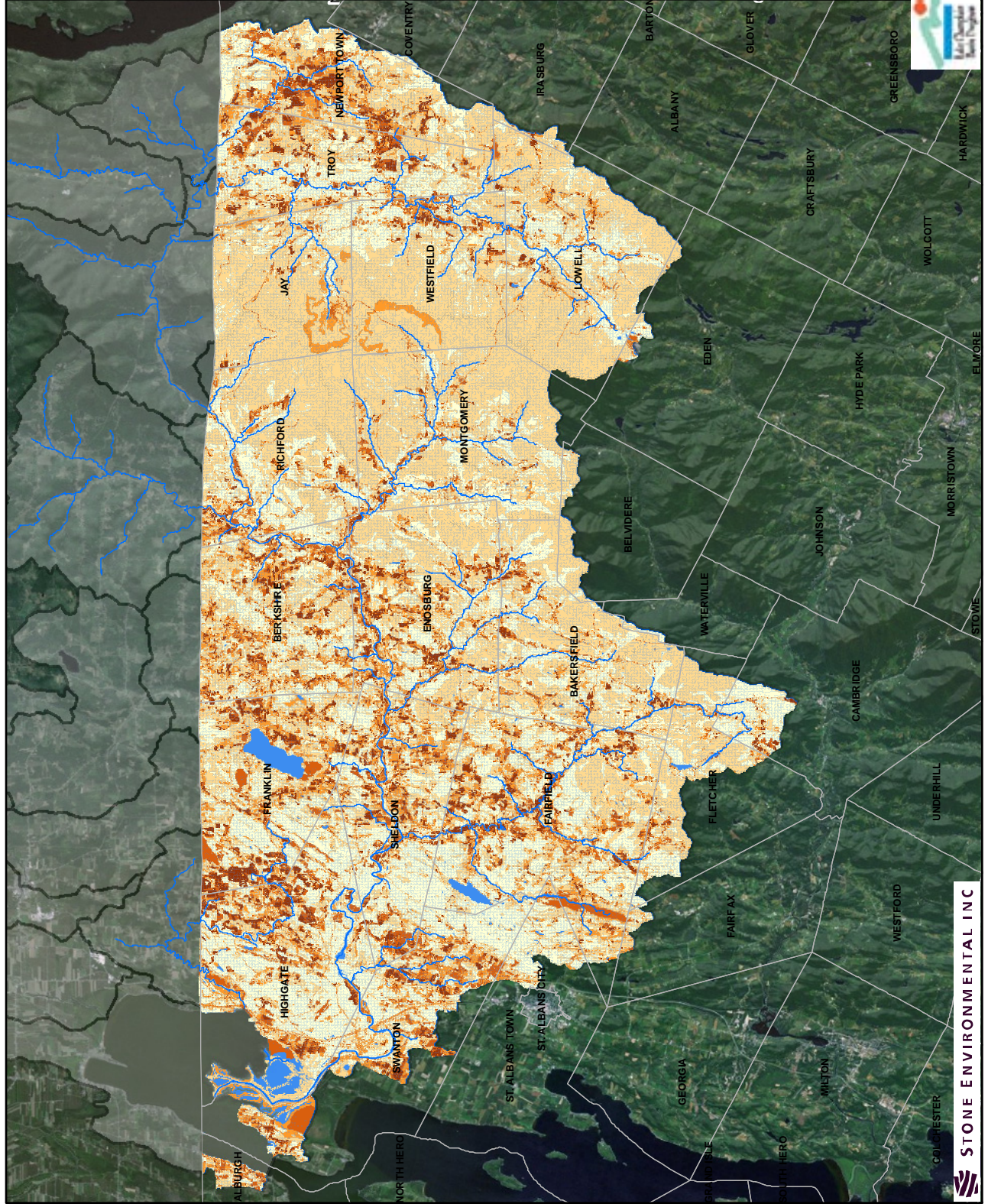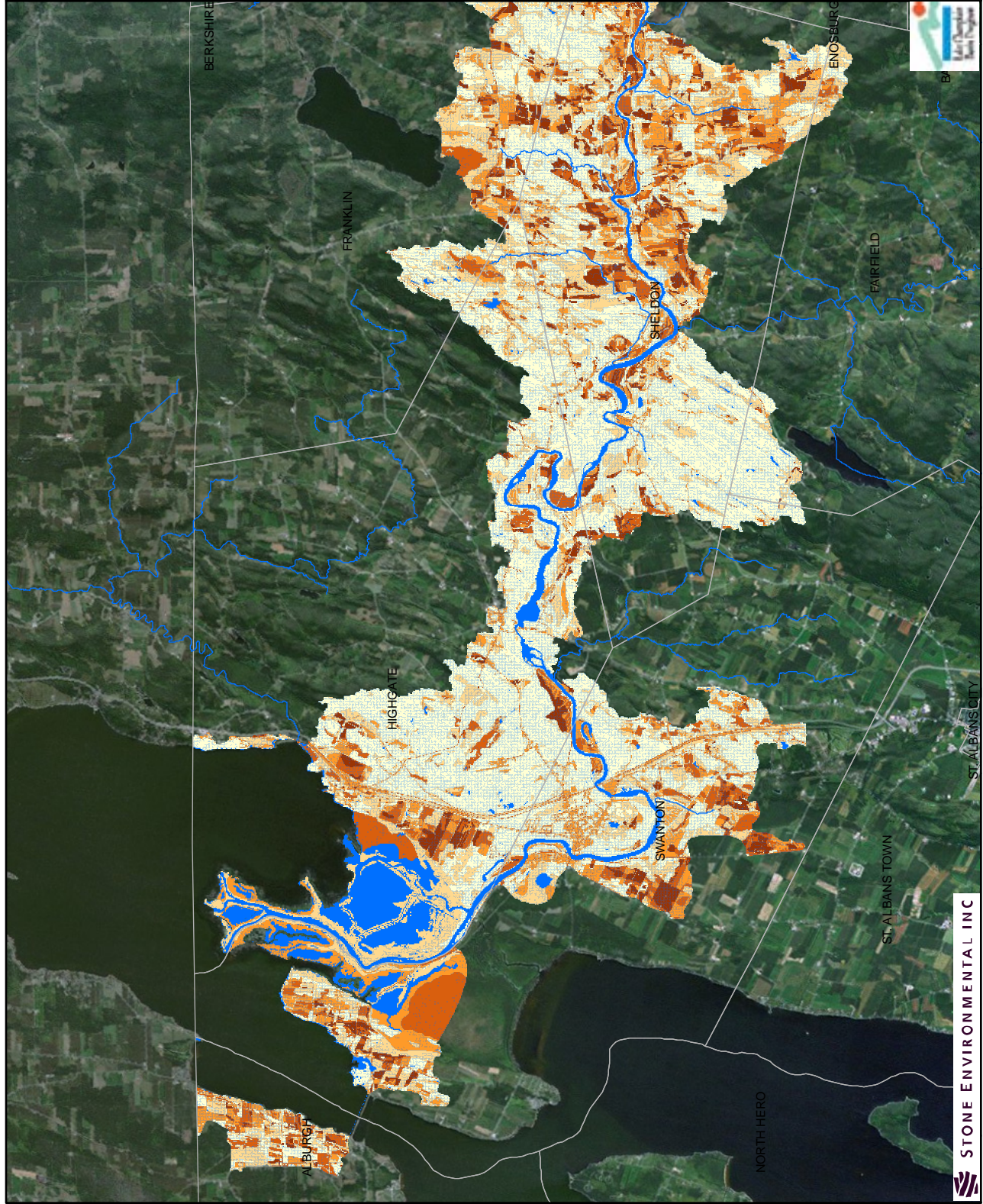MILTON
NORTH HERO
GRAND ISLE
SOUTH HERO

Map 3.2

Average Annual Model
Estimated Total P Loading
by HUC12

Full Watershed

Identification of Critical Source
Areas of Phosphorus Pollution
within the Vermont Sector of
the Missisquoi Bay Basin

Sources: Rivers and Streams; Subwatersheds;
& Avg. Annual Model Estimated Total P.: Stone
Environmental; HUC 12 Watersheds: USGS;
Town Boundaries: VCGI; Imagery (2009): esri.

Avg. Annual Total P (kg/ha)
<= 0.25
0.26 - 0.35
0.36 - 0.50
0.51 - 0.70
> 0.7
Rivers and Streams
HUC (12) Watersheds

N

0   2.5   5
Miles

STONE ENVIRONMENTAL INC

Q\Proj09\IAMC156-G_LCBP_Phosphorus_Critical_Source_Areas\MapDocuments\Presentations\AndReports\FinalReport\Map3.2_HUC12TotalP.mxd

Map 3.3

Average Annual Model
Estimated Total P Loading
by SWAT Subbasin

Full Watershed

Identification of Critical Source
Areas of Phosphorus Pollution
within the Vermont Sector of
the Missisquoi Bay Basin

Sources: Rivers and Streams; Sub Basins;
& Avg. Annual Model Estimated Total P: Stone
Environmental; HUC 12 Watersheds: USGS;
Town Boundaries: VCGI; Imagery (2009): esri.

Avg. Annual Total P (kg/ha)

<= 0.15
0.16 - 0.25
0.26 - 0.35
0.36 - 0.50
0.51 - 0.75
0.76 - 1.00
> 1

Rivers and Streams
HUC (12) Watersheds

0   2.5   5
Miles

N

STONE ENVIRONMENTAL INC

217

Avg. Annual Total P (kg/ha)

- <= 0.10
- 0.11 - 0.50
- 0.51 - 1.00
- 1.01 - 2.00
- > 2.00

Rivers and Streams

- Water
- HUC (12) Watersheds

N

0   2.5   5
Miles

Map 3.4

Average Annual Model
Estimated Total P Loading
by SWAT HRU

Full Watershed

Identification of Critical Source
Areas of Phosphorus Pollution
within the Vermont Sector of
the Missisquoi Bay Basin

STONE ENVIRONMENTAL INC

Identification of Critical Source
Areas of Phosphorus Pollution
within the Vermont Sector of
the Missisquoi Bay Basin

Western Missisquoi
Main Stem

Average Annual Model
Estimated Total P Loading
by SWAT HRU

Map 3.5

Sources: Rivers and Streams; & Avg. Annual
Model Estimated Total P: Stone Environmental;
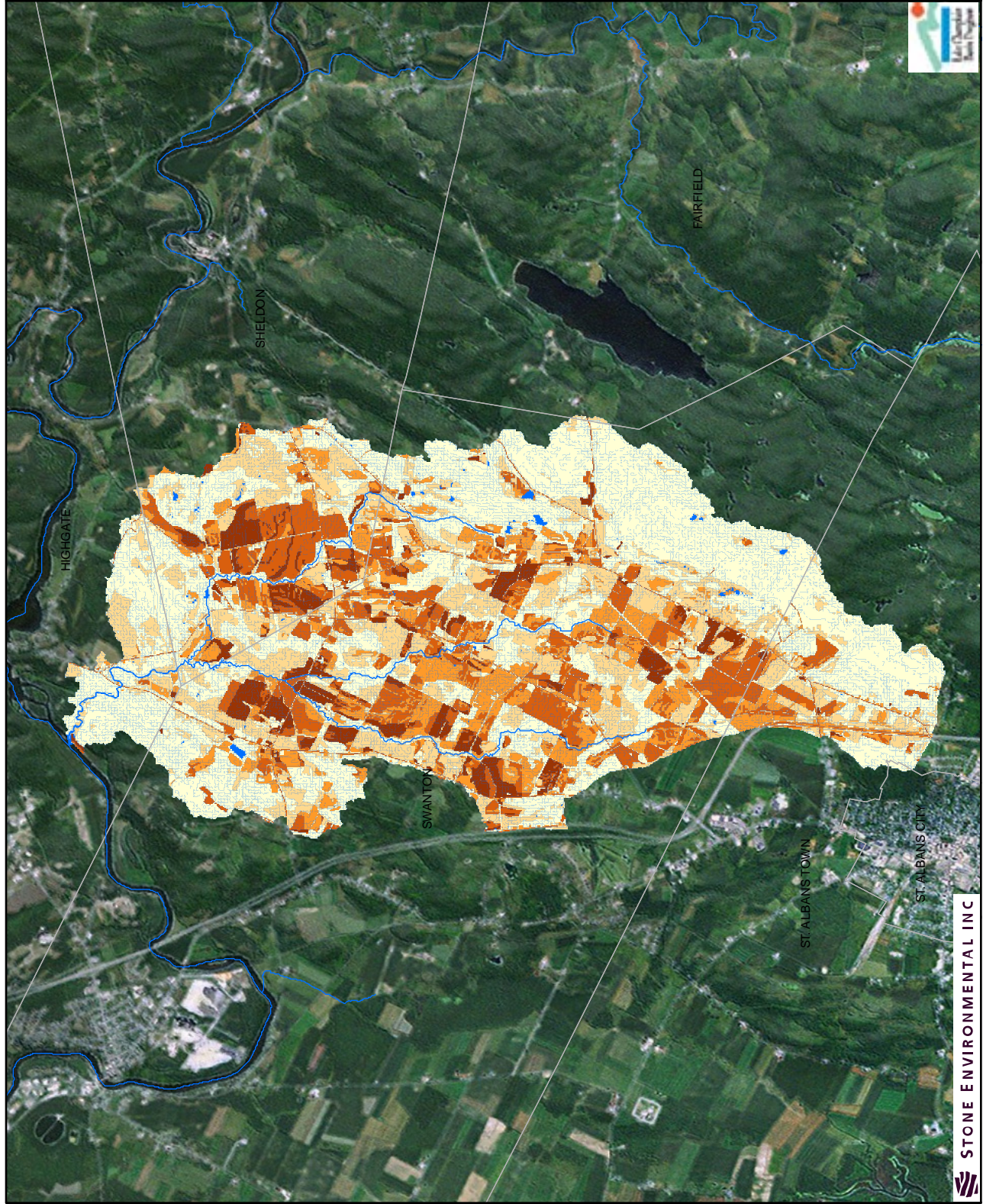Town Boundaries: VCGI; Imagery (2009): esri.

Avg. Annual Total P (kg/ha)

<= 0.10
0.11 - 0.50
0.51 - 1.00
1.01 - 2.00
> 2.00

Rivers and Streams

Water

N

0   1   2
Miles

STONE ENVIRONMENTAL INC

O:\Projects\MMZ\156-G_LCBP_Phosphorus_Critical_Source_Areas\Data\MapDocuments\Presentations\AndReports\FinalReport\Map3.5_WMM_HRU_TotalP.mxd
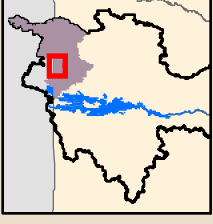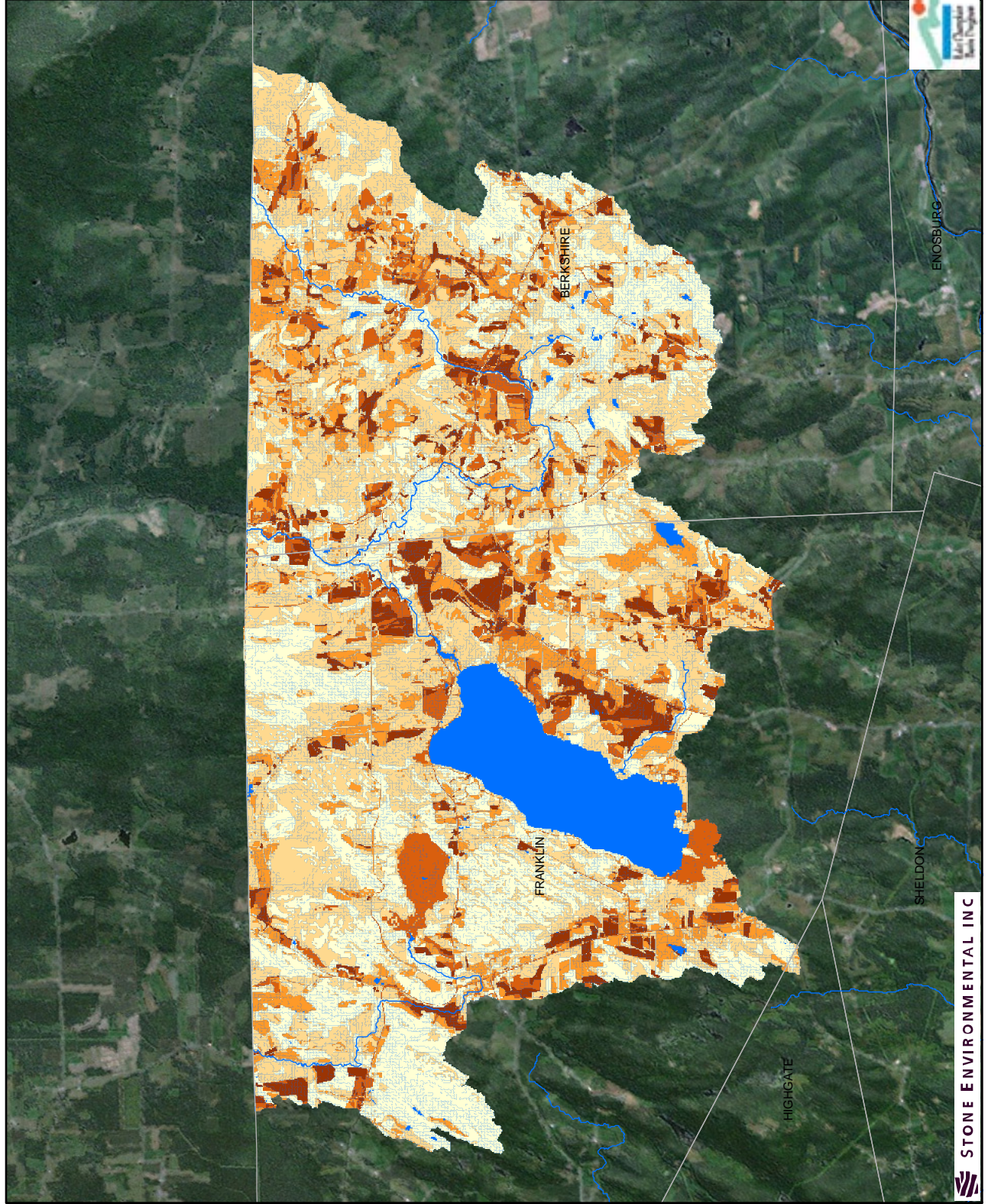
Map 3.6

Average Annual Model
Estimated Total P Loading
by SWAT HRU

Rock River
Sub-Watershed

Identification of Critical Source
Areas of Phosphorus Pollution
within the Vermont Sector of
the Missisquoi Bay Basin

Avg. Annual Total P (kg/ha)

<= 0.10
0.11 - 0.50
0.51 - 1.00
1.01 - 2.00
> 2.00

Rivers and Streams

Water

N

0   0.5   1
Miles

Sources: Rivers and Streams & Avg. Annual
Model Estimated Total P: Stone Environmental;
Town Boundaries: VCGI; Imagery (2009): esri.

FRANKLIN

SHELDON

HIGHGATE

SWANTON

Map 3.7

Average Annual Model
Estimated Total P Loading
by SWAT HRU

Hungerford Brook
Sub-Watershed

Identification of Critical Source
Areas of Phosphorus Pollution
within the Vermont Sector of
the Missisquoi Bay Basin

Sources: Rivers and Streams & Avg. Annual
Model Estimated Total P: Stone Environmental;
Town Boundaries: VCGI; Imagery (2009): esri.

Avg. Annual Total P (kg/ha)

<= 0.10
0.11 - 0.50
0.51 - 1.00
1.01 - 2.00
> 2.00

Rivers and Streams

Water

Miles
0   0.5   1

N

FAIRFIELD

SHELDON

HIGHGATE

SWANTON

ST. ALBANS TOWN

ST. ALBANS CITY

STONE ENVIRONMENTAL INC

O:\Proj09\IMMC2156-G_LCBP_Phosphorus_Critical_Source_Areas\Data\MapDocuments\Presentations AndReports\FinalReportMap3.7_Hunger_HRU_TotalP.mxd

221

Avg. Annual Total P (kg/ha)
- <= 0.10
- 0.11 - 0.50
- 0.51 - 1.00
- 1.01 - 2.00
- > 2.00

Rivers and Streams

Water

Map 3.8

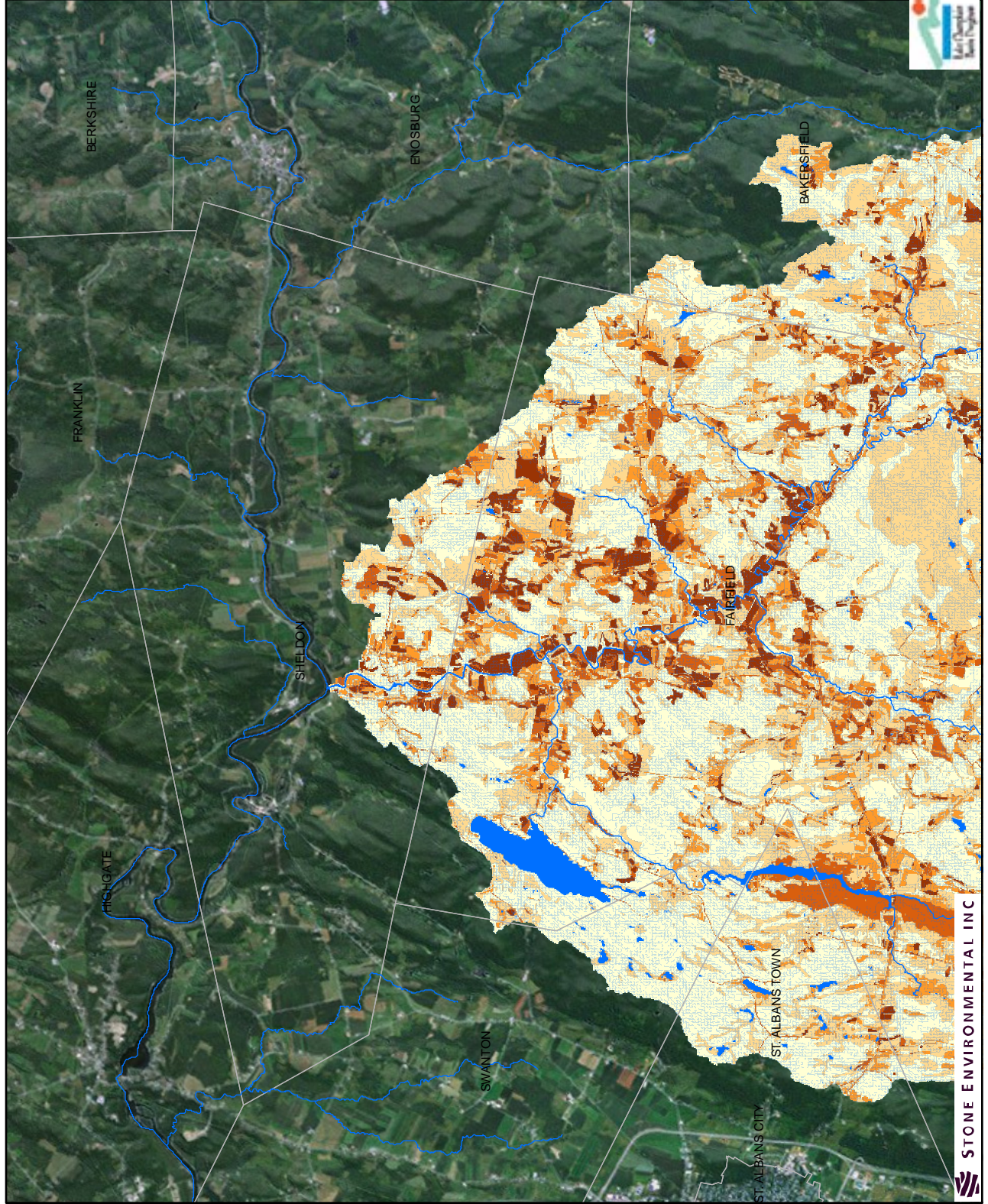Average Annual Model Estimated Total P Loading by SWAT HRU

Pike River Sub-Watershed

Identification of Critical Source Areas of Phosphorus Pollution within the Vermont Sector of the Missisquoi Bay Basin

STONE ENVIRONMENTAL INC

Map 3.9

Average Annual Model
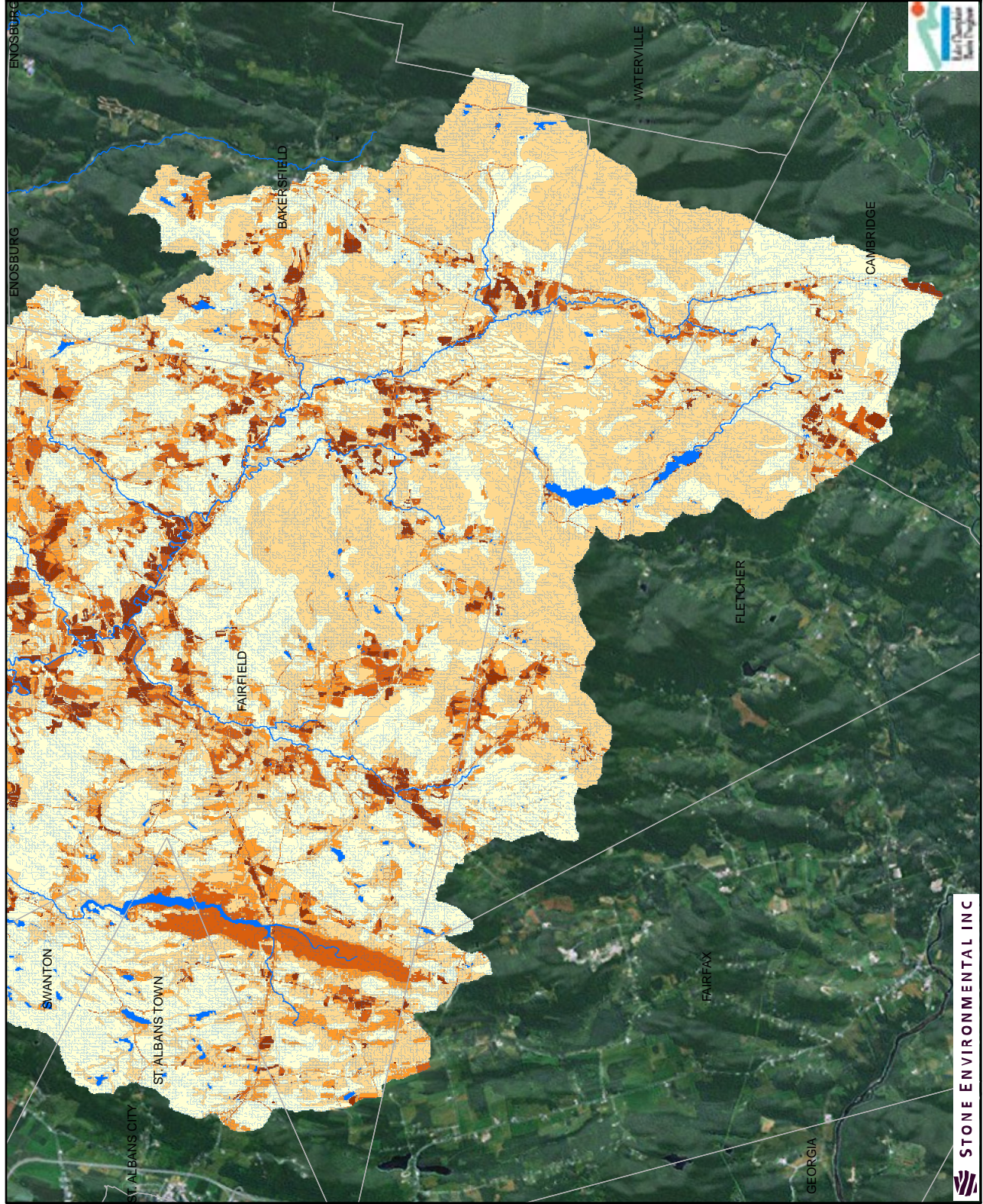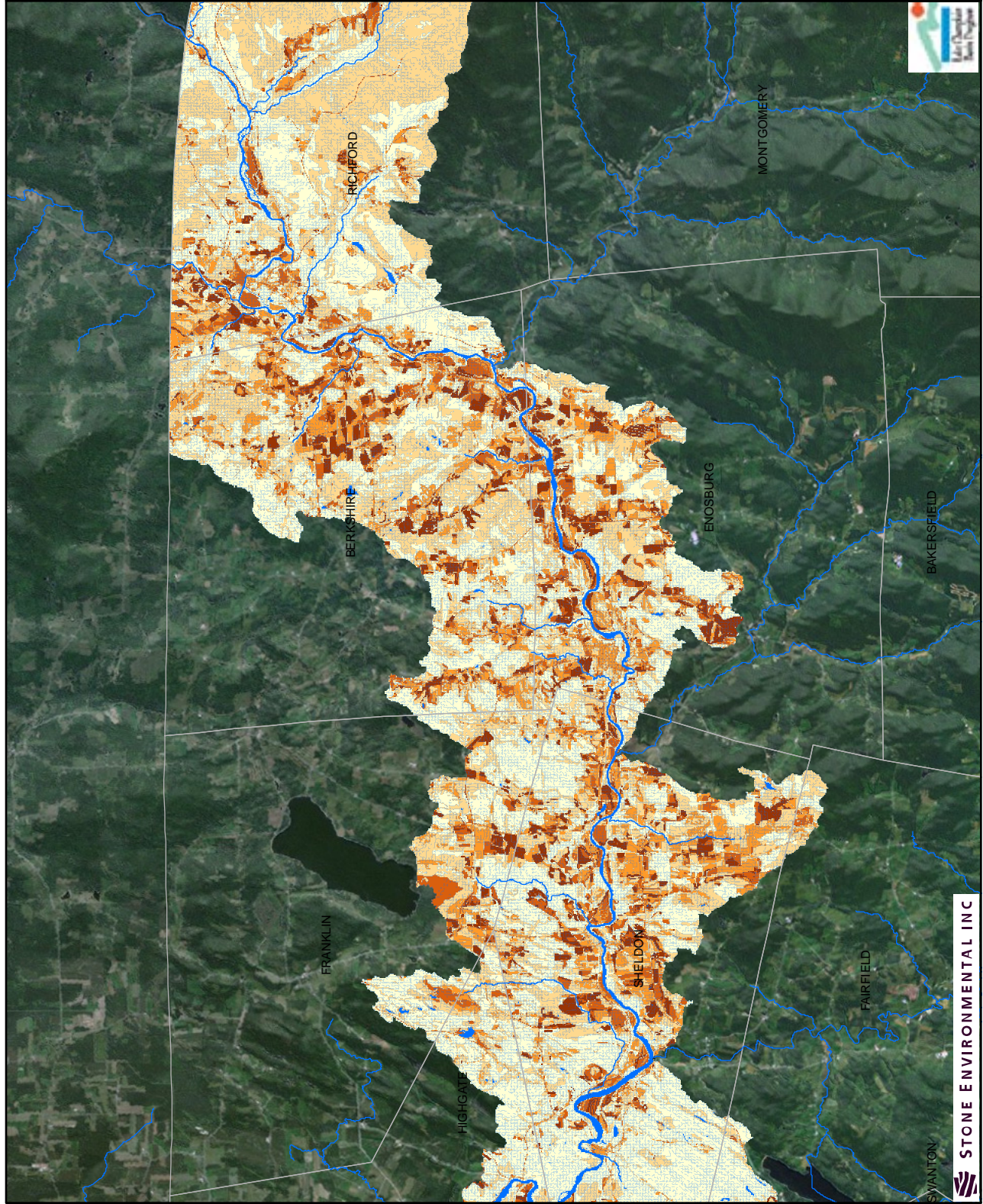Estimated Total P Loading
by SWAT HRU

North Black Creek
Sub-Watershed

Identification of Critical Source
Areas of Phosphorus Pollution
within the Vermont Sector of
the Missisquoi Bay Basin

Avg. Annual Total P (kg/ha)

<= 0.10
0.11 - 0.50
0.51 - 1.00
1.01 - 2.00
> 2.00

Rivers and Streams

Water

Sources: Rivers and Streams & Avg. Annual
Model Estimated Total P: Stone Environmental;
Town Boundaries: VCGI; Imagery (2009): esri.

N

Miles
0   1   2

BERKSHIRE

ENOSBURG

BAKERSFIELD

FRANKLIN

SHELDON

FAIRFIELD

HIGHGATE

SWANTON

ST. ALBANS TOWN

ST. ALBANS CITY

STONE ENVIRONMENTAL INC

O:\Proj09\AMM21156-G_LCBP_Phosphorus_Critical_Source_Areas\Data\MapDocuments\Presentations\AndReports\FinalReport\Map3.9_NBlack_HRU_TotalP.mxd

223

Map 3.10

Average Annual Model
Estimated Total P Loading
by SWAT HRU

South Black Creek
Sub-Watershed

Identification of Critical Source
Areas of Phosphorus Pollution
within the Vermont Sector of
the Missisquoi Bay Basin

Sources: Rivers and Streams & Avg. Annual
Model Estimated Total P: Stone Environmental;
Town Boundaries: VCGI; Imagery (2009); esri.

Avg. Annual Total P (kg/ha)

<= 0.10
0.11 - 0.50
0.51 - 1.00
1.01 - 2.00
> 2.00

Rivers and Streams

Water

N

0   1   2
Miles

O:\Proj-09\AIMG\156-G_LCBP_Phosphorus_Critical_Source_Areas\Data\MapDocuments\AndReports\FinalReport\Map3.10_SBlack_HRU_TotalP.mxd

224

Map 3.11

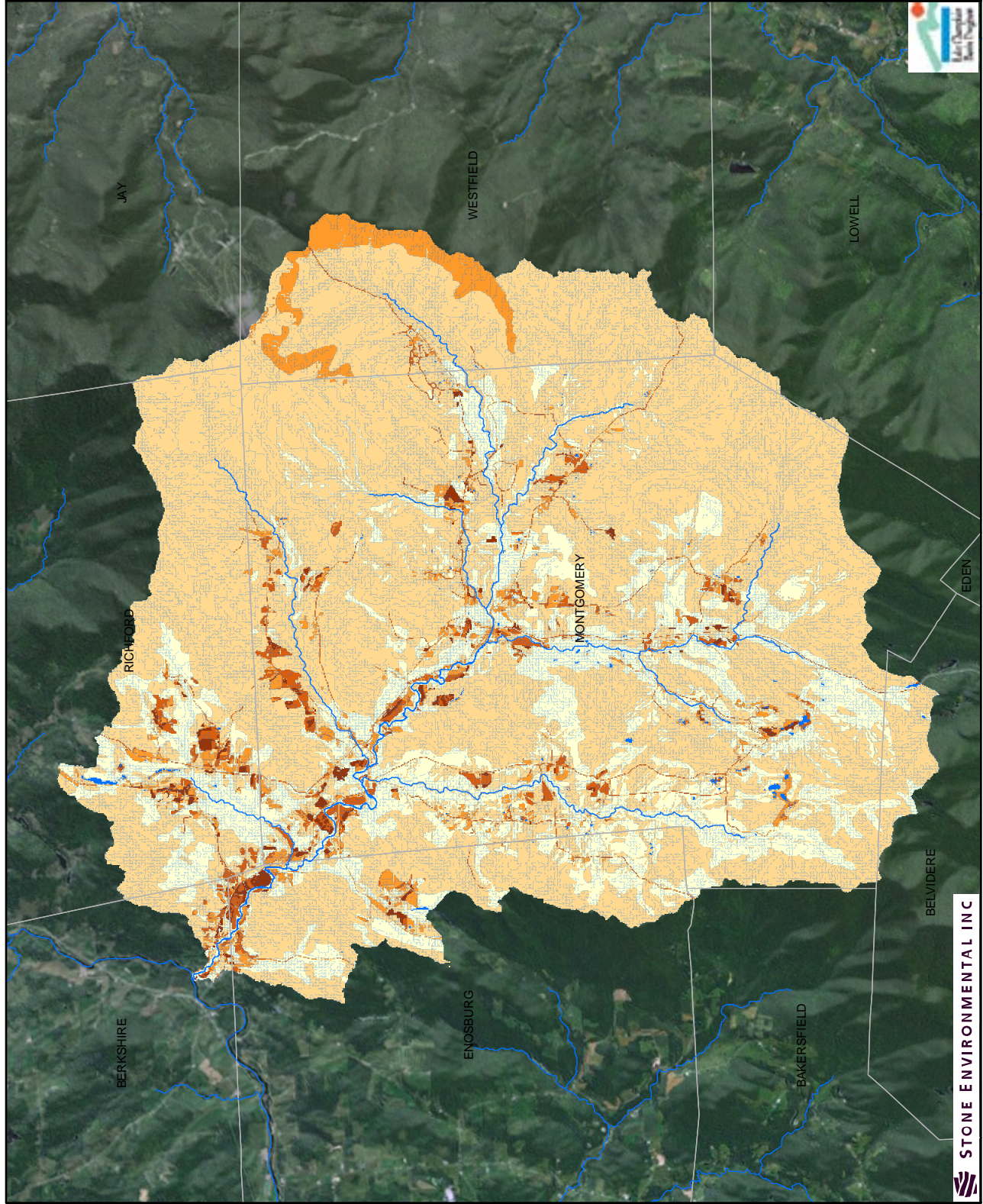Average Annual Model
Estimated Total P Loading
by SWAT HRU

Central Missisquoi
Main Stem

Identification of Critical Source
Areas of Phosphorus Pollution
within the Vermont Sector of
the Missisquoi Bay Basin

Avg. Annual Total P (kg/ha)
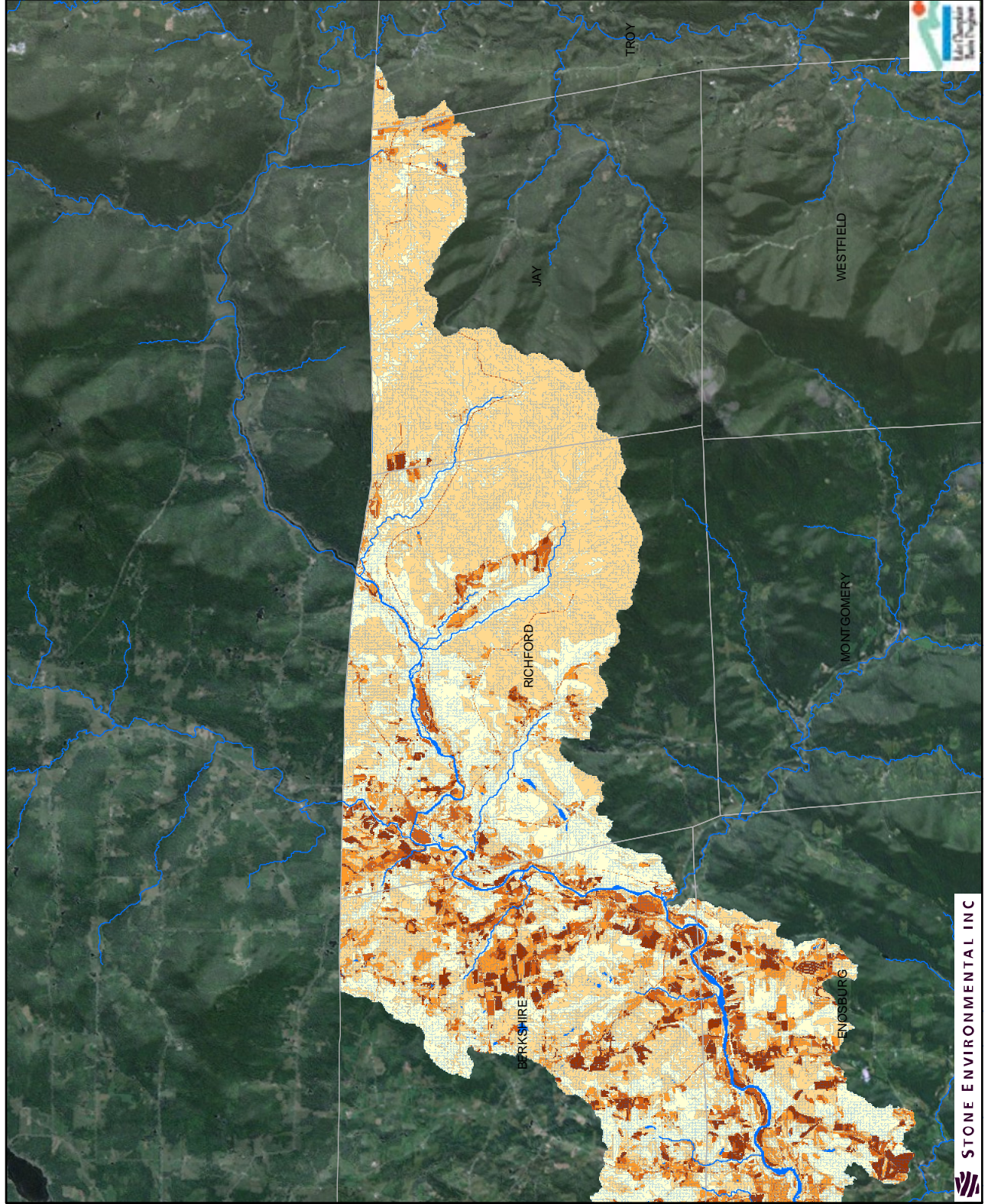
<= 0.10
0.11 - 0.50
0.51 - 1.00
1.01 - 2.00
> 2.00

Rivers and Streams
Water

Sources: Rivers and Streams & Avg. Annual
Model Estimated Total P: Stone Environmental;
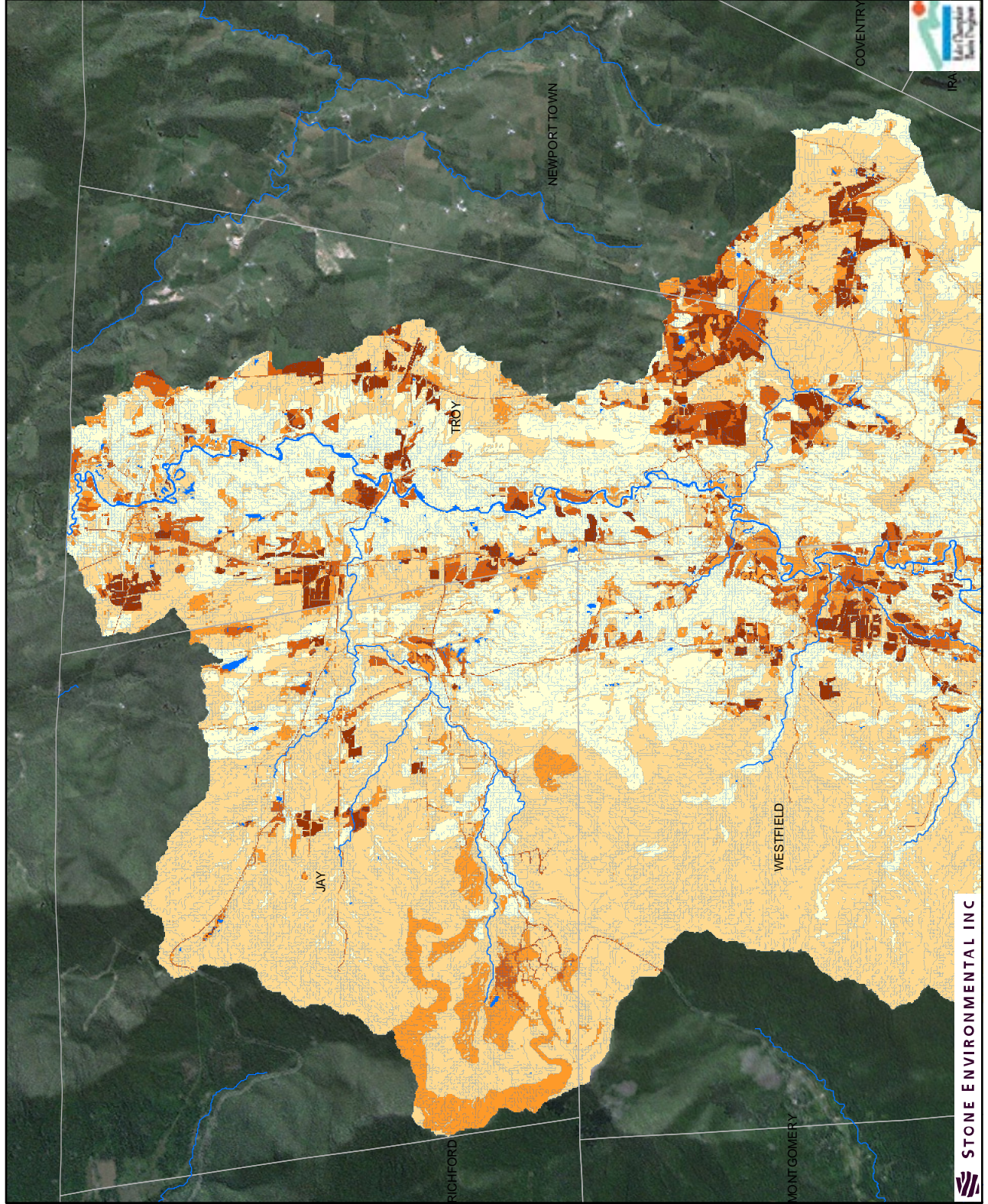Town Boundaries: VCGI; Imagery (2009): esri.

N

0   1   2
Miles

RICHFORD

MONTGOMERY

BERKSHIRE

ENOSBURG

BAKERSFIELD

FRANKLIN

SHELDON

FAIRFIELD

HIGHGATE

SWANTON

STONE ENVIRONMENTAL INC

O:\Project\91\IAM\2156-G_LCBP_Phosphorus_Critical_Source_Areas\Data\MapDocuments\MapDocumentsForFinalReportsAndReports\FinalReport\Map3.11_CMM_HRU_TotalP.mxd

Map 3.12

Average Annual Model
Estimated Total P Loading
by SWAT HRU

Tyler Branch
Sub-Watershed

Identification of Critical Source
Areas of Phosphorus Pollution
within the Vermont Sector of
the Missisquoi Bay Basin

Sources: Rivers and Streams & Avg. Annual
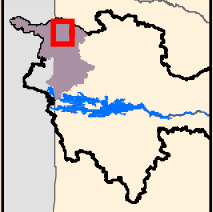Model Estimated Total P: Stone Environmental;
Town Boundaries: VCGI; Imagery (2009); esri.

N

Avg. Annual Total P (kg/ha)
<= 0.10
0.11 - 0.50
0.51 - 1.00
1.01 - 2.00
>2.00

Rivers and Streams
Water

Miles
0   1   2

STONE ENVIRONMENTAL INC

O:\Proj-09\IMM21156-G_LCBP_Phosphorus_Critical_Source_Areas\Data\MapDocuments\Presentations\AndReports\FinalReport\Map3.12_Tyler_HRU_TotalP.mxd

226

Map 3.13

Average Annual Model
Estimated Total P Loading
by SWAT HRU

Trout River
Sub-Watershed

Identification of Critical Source
Areas of Phosphorus Pollution
within the Vermont Sector of
the Missisquoi Bay Basin

Sources: Rivers and Streams & Avg. Annual
Model Estimated Total P: Stone Environmental;
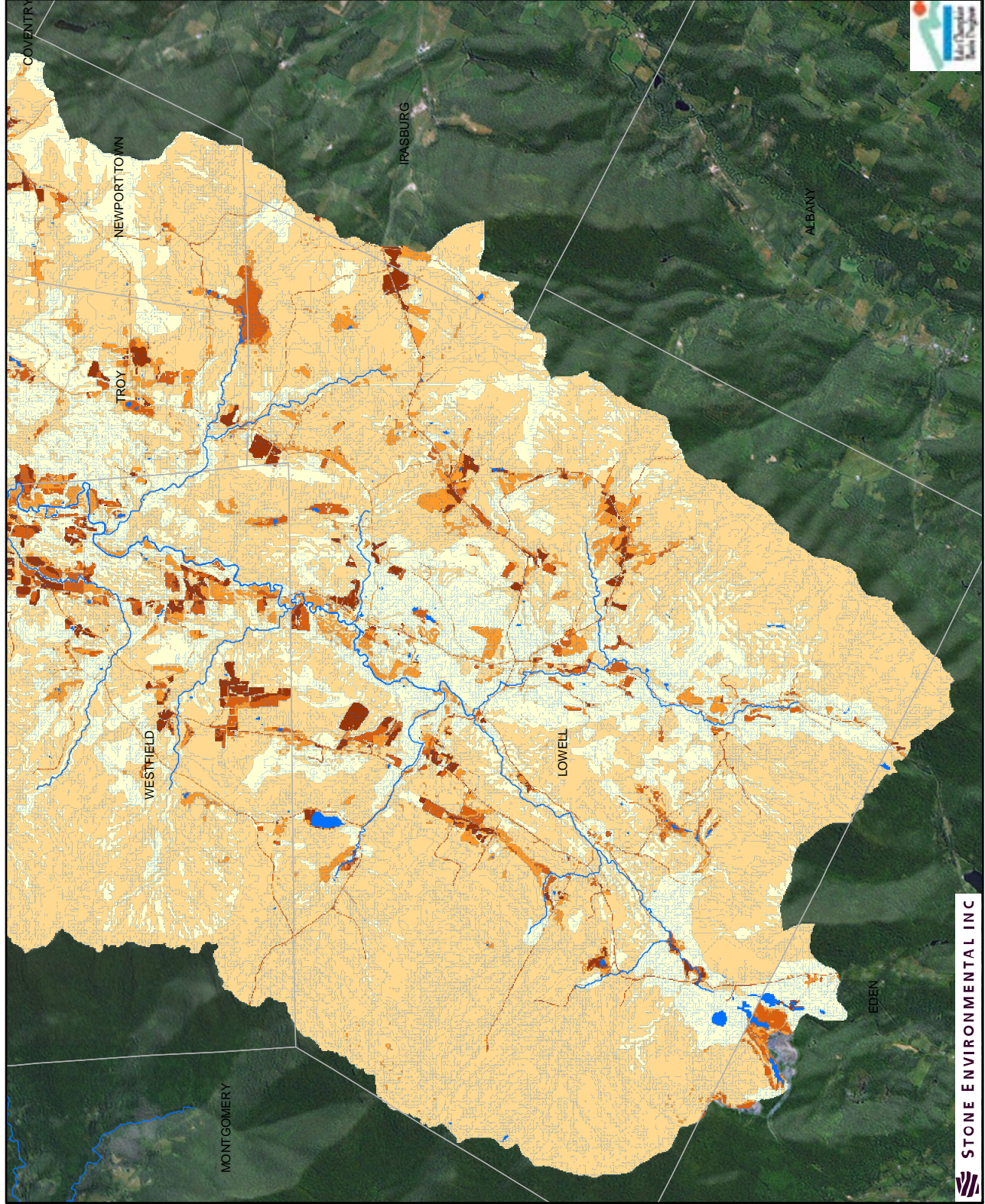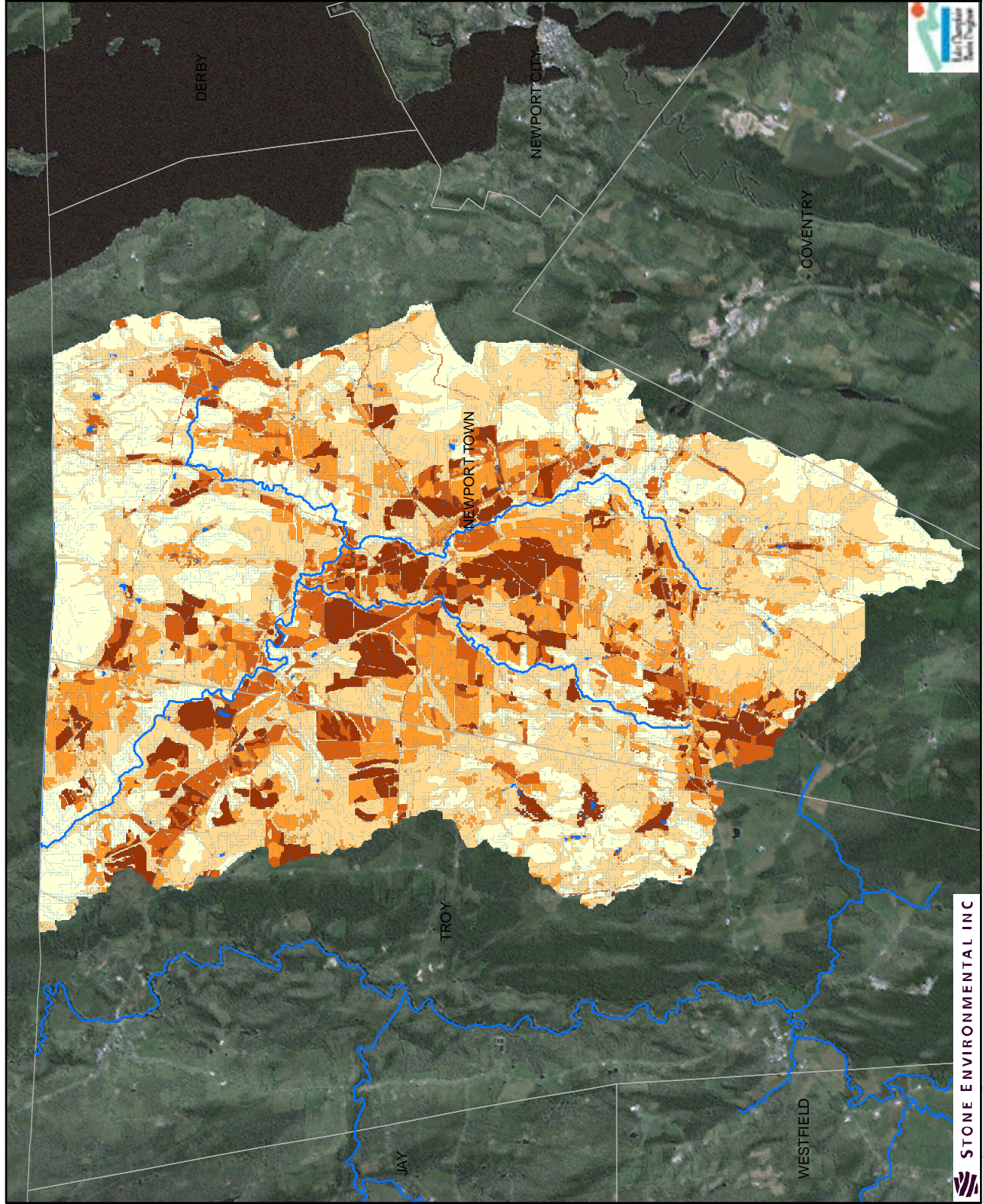Town Boundaries: VCGI; Imagery (2009): esri.

Avg. Annual Total P (kg/ha)

<= 0.10
0.11 - 0.50
0.51 - 1.00
1.01 - 2.00
> 2.00

Rivers and Streams

Water

Miles
0   1   2

N

STONE ENVIRONMENTAL INC

JAY

WESTFIELD

LOWELL

RICHFORD

MONTGOMERY

EDEN

BERKSHIRE

ENOSBURG

BAKERSFIELD

BELVIDERE

Avg. Annual Total P (kg/ha)

<= 0.10
0.11 - 0.50
0.51 - 1.00
1.01 - 2.00
> 2.00

Rivers and Streams

Water

N

0   1   2
Miles

Map 3.14

Average Annual Model
Estimated Total P Loading
by SWAT HRU

Eastern Missisquoi
Main Stem

Identification of Critical Source
Areas of Phosphorus Pollution
within the Vermont Sector of
the Missisquoi Bay Basin

STONE ENVIRONMENTAL INC

TROY

WESTFIELD

JAY

MONTGOMERY

RICHFORD

BERKSHIRE

ENOSBURG

O:\Proj09\IAMC156-G_LCBP_Phosphorus_Critical_Source_Areas\Data\MapDocuments\PresentationsAndReports\FinalReport\Map3.14_EMM_HRU_TotalP.mxd

228

Average Annual Total P (kg/ha)

<= 0.10
0.11 - 0.50
0.51 - 1.00
1.01 - 2.00
> 2.00

Rivers and Streams
Water

N

0 0.5 1 Miles

Map 3.15

Average Annual Model
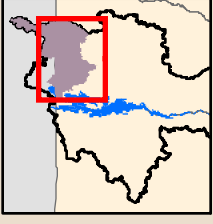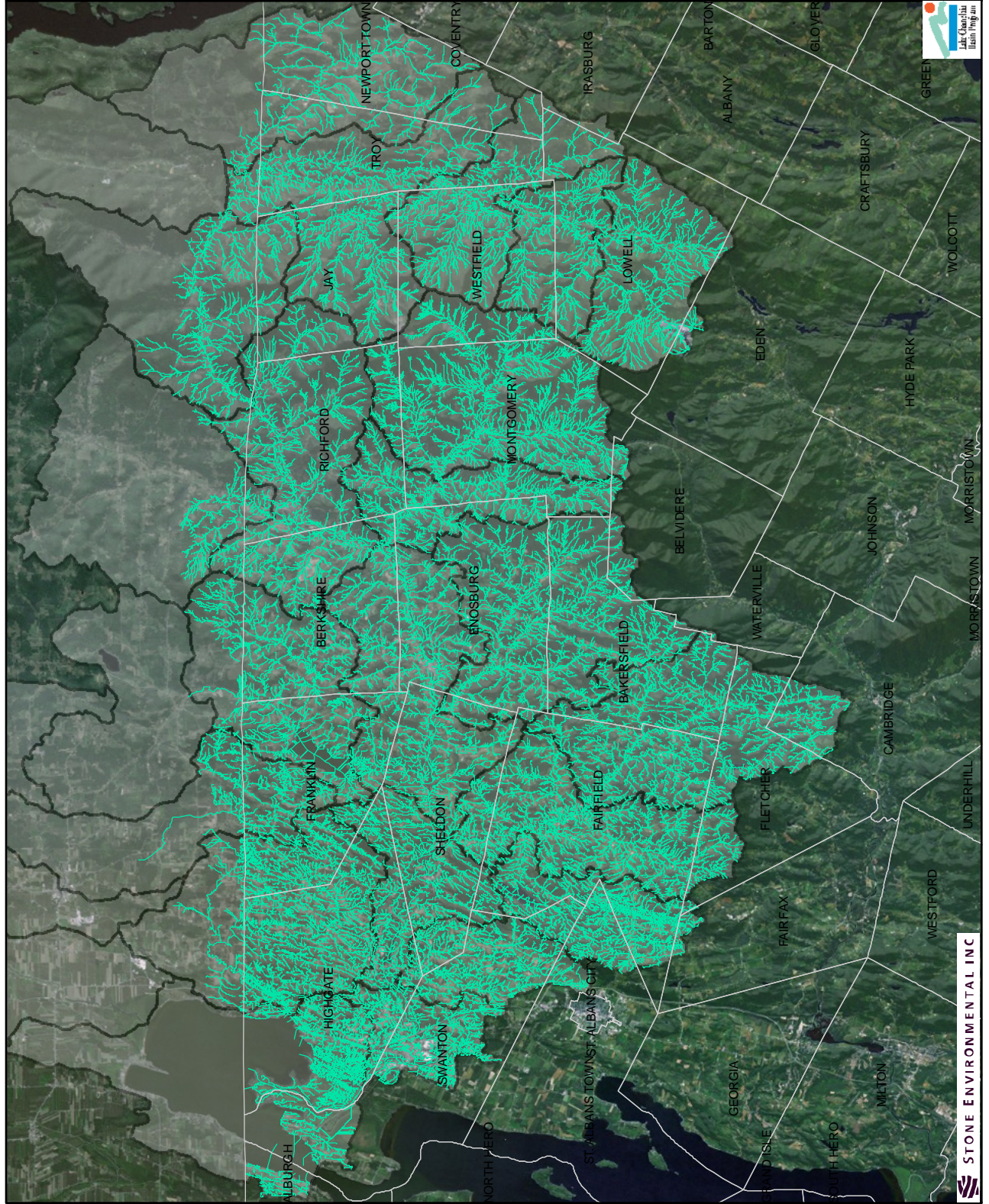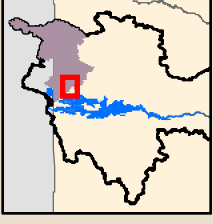Estimated Total P Loading
by SWAT HRU

Northern Upper Missisquoi
Sub-Watershed

Identification of Critical Source
Areas of Phosphorus Pollution
within the Vermont Sector of
the Missisquoi Bay Basin

NEWPORT TOWN
COVENTRY
IRA
TROY
WESTFIELD
JAY
RICHFORD
MONTGOMERY

STONE ENVIRONMENTAL INC

O:\Proj09\IAMC156-G_LCBP_Phosphorus_Critical_Source_Areas\Data\MapDocuments\Presentations And Reports\FinalReport\Map3.15_NUpMiss_HRU_TotalP.mxd

229

Avg. Annual Total P (kg/ha)

<= 0.10
0.11 - 0.50
0.51 - 1.00
1.01 - 2.00
> 2.00

Rivers and Streams

Water

Sources: Rivers and Streams & Avg. Annual
Model Estimated Total P: Stone Environmental;
Town Boundaries: VCGI; Imagery (2009): esri.

Map 3.16

Average Annual Model
Estimated Total P Loading
by SWAT HRU

Southern Upper Missisquoi
Sub-Watershed

Identification of Critical Source
Areas of Phosphorus Pollution
within the Vermont Sector of
the Missisquoi Bay Basin

N

0   0.5   1
Miles

COVENTRY
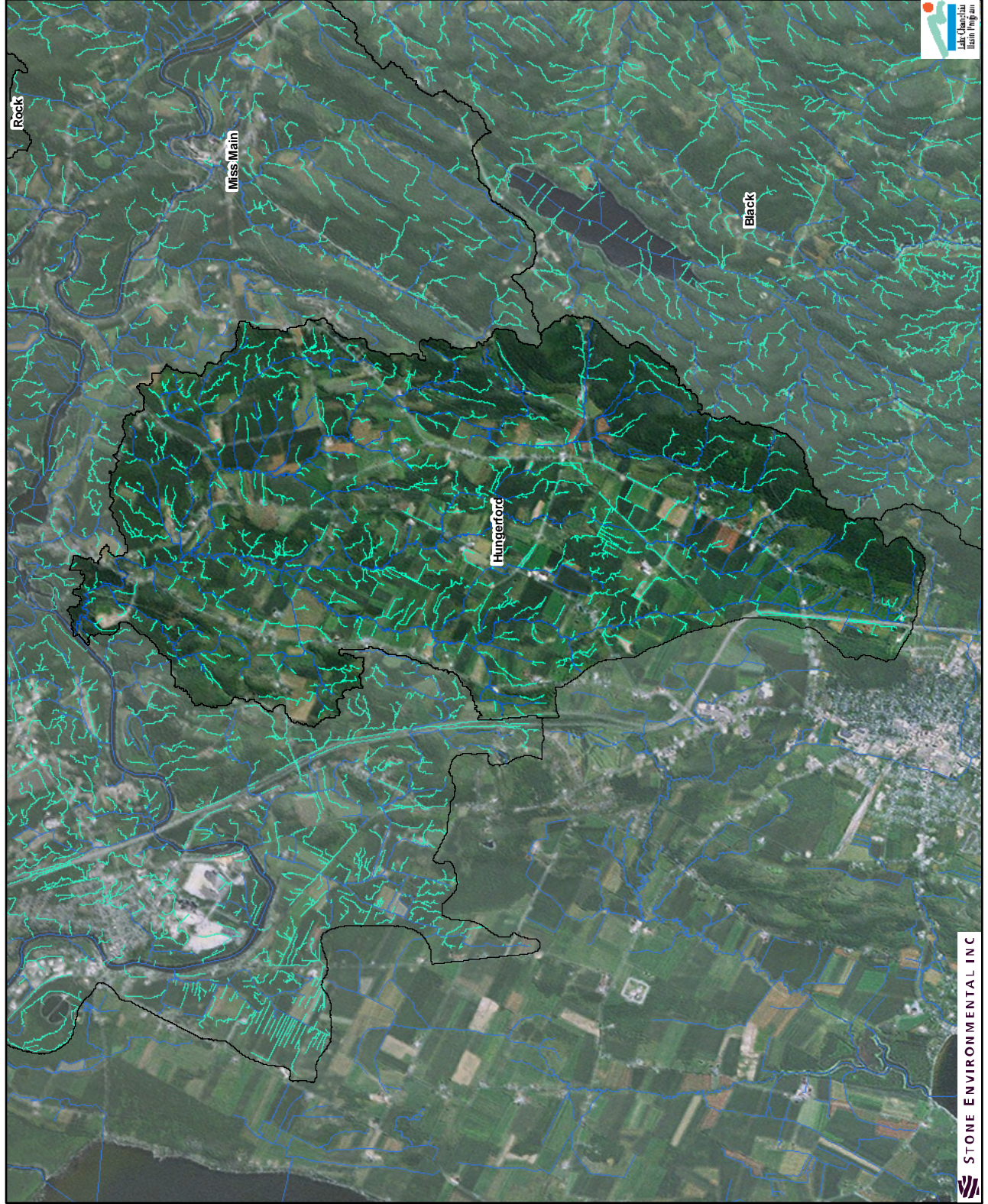
NEWPORT TOWN

IRASBURG

ALBANY

TROY

WESTFIELD

LOWELL

EDEN

MONTGOMERY

STONE ENVIRONMENTAL INC

O:\Proj\091\IMM2156-G_LCBP_Phosphorus_Critical_Source_Areas\Data\MapDocuments\PresentationsAndReports\FinalReport\Map3.16_SUPAes_HRU_TotalP.mxd

Avg. Annual Total P (kg/ha)
<= 0.10
0.11 - 0.50
0.51 - 1.00
1.01 - 2.00
> 2.00

Rivers and Streams
Water

N

0   0.5   1   Miles

Map 3.17

Average Annual Model
Estimated Total P Loading
by SWAT HRU

Mud Creek
Sub-Watershed

Identification of Critical Source
Areas of Phosphorus Pollution
within the Vermont Sector of
the Missisquoi Bay Basin

DERBY

NEWPORT CITY

COVENTRY

NEWPORT TOWN

TROY

WESTFIELD

JAY

STONE ENVIRONMENTAL INC

231

Map 3.18

Enhanced Hydrography
Network

Full Watershed

Identification of Critical Source
Areas of Phosphorus Pollution
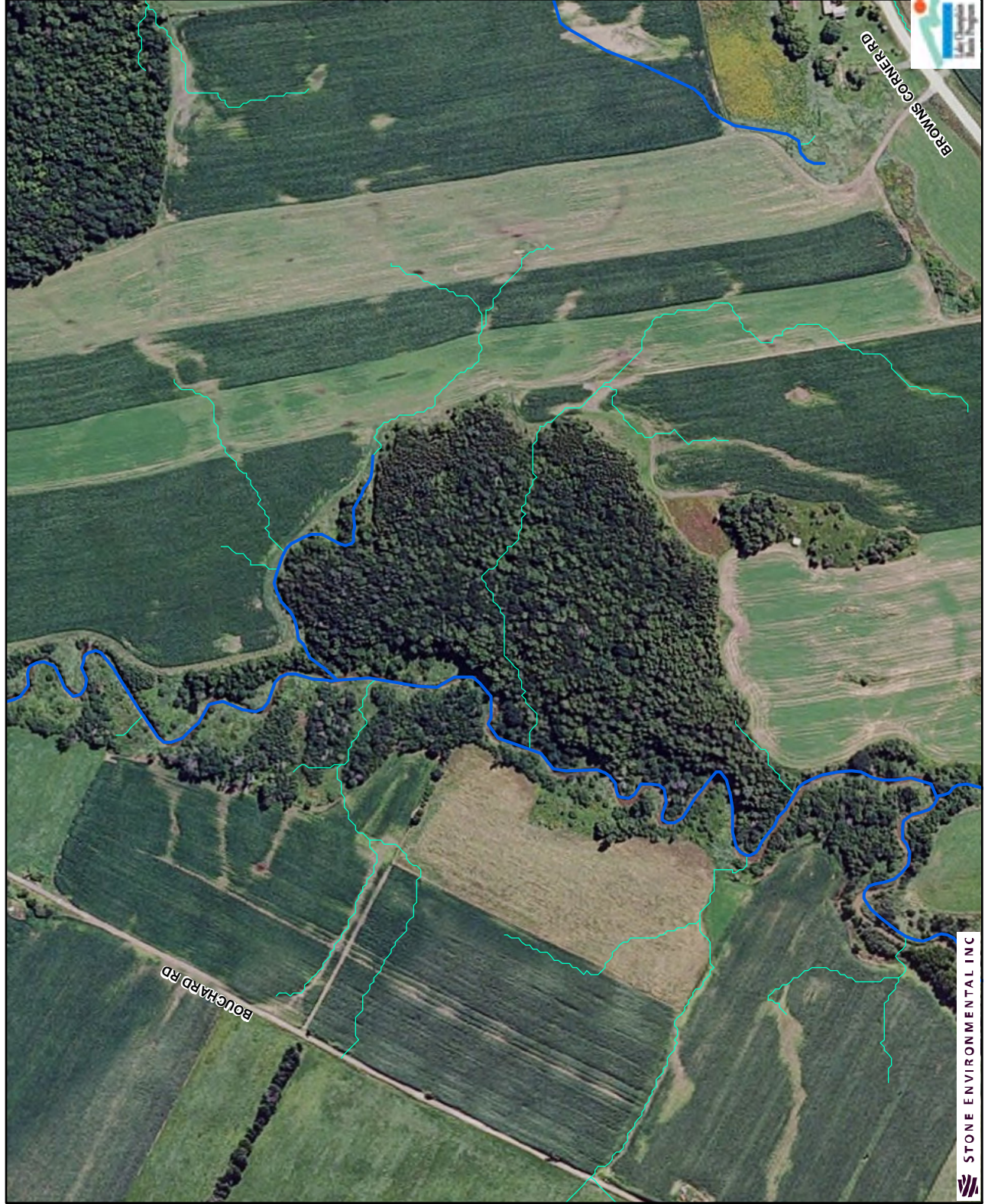within the Vermont Sector of
the Missisquoi Bay Basin

Enhanced Hydrography
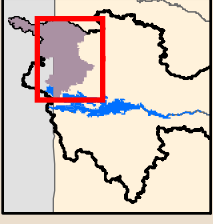HUC (12) Watersheds

Sources: Rivers and Streams; Subwatersheds
& Enhanced Hydrography Network: Stone
Environmental; HUC 12 Watersheds: USGS;
Town Boundaries: VCGI, Imagery (2009): esri.

N

0   2.5   5
Miles

STONE ENVIRONMENTAL INC

O:\proj\94\LMM2\156-G_LCBP_Phosphorus_Critical_Source_Areas\Data\MapDocuments\Presentations AndReports\FinalReportMap3.18_Enhanced_Hydro_FullWatershed.mxd

Identification of Critical Source
Areas of Phosphorus Pollution
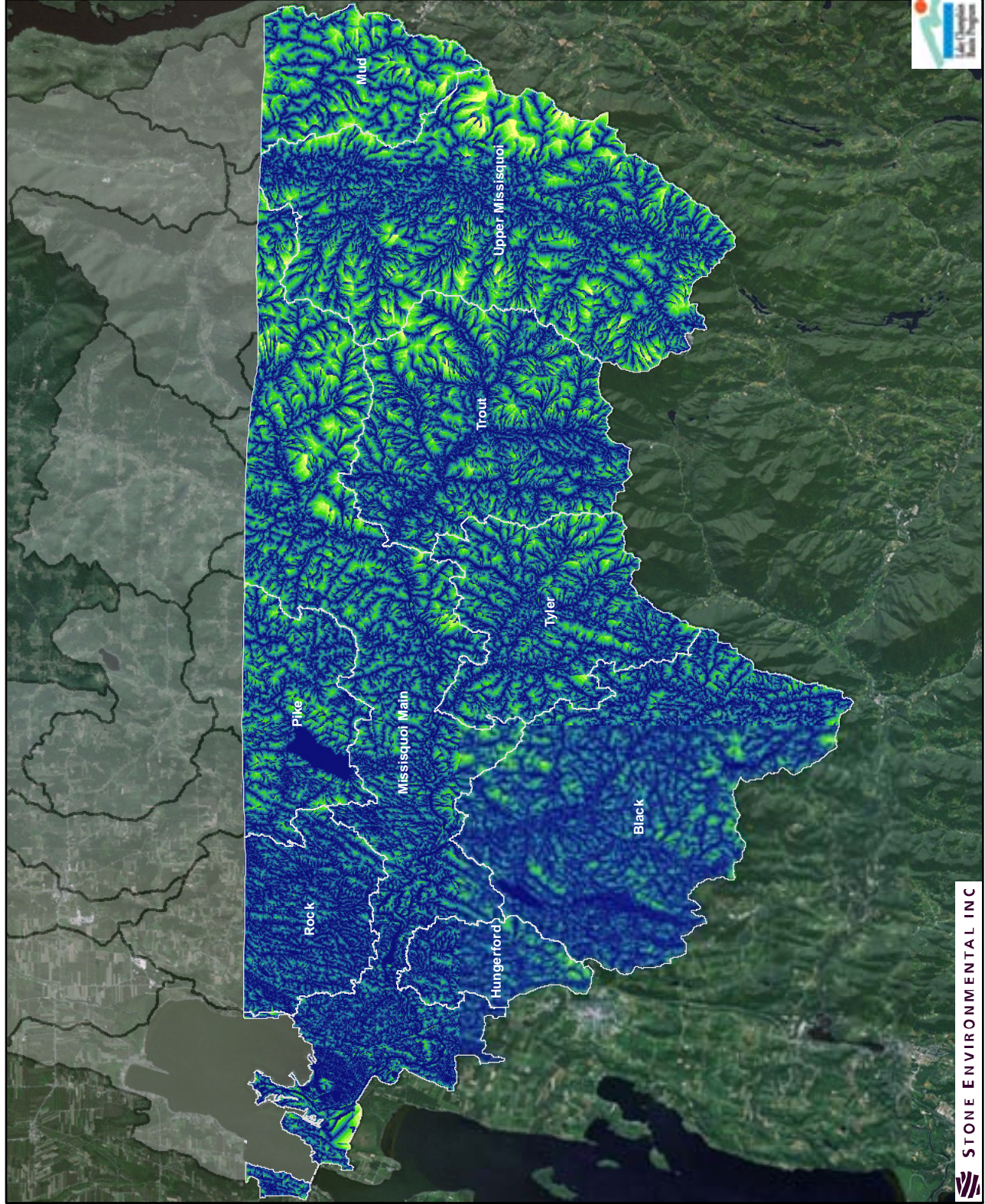within the Vermont Sector of
the Missisquoi Bay Basin

Hungerford Brook
and Tributaries

Enhanced Hydrography
Network

Map 3.19
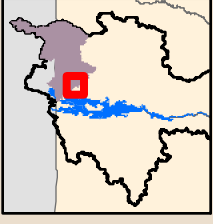
—— VHD Hydrography
—— Enhanced Hydrography

Sources: Enhanced Hydrography &
Subwatersheds: Stone Environmental;
Vermont Hydrography Dataset: USGS;
Imagery (2009): esri.

N

0   0.5   1
Miles

Rock

Miss Main

Black

Hungerford

STONE ENVIRONMENTAL INC

Map 3.20

Enhanced Hydrography Network

Rock River, Field Level

Identification of Critical Source Areas of Phosphorus Pollution within the Vermont Sector of the Missisquoi Bay Basin

Sources: Enhanced Hydrography: Stone Environmental; Vermont Hydrography Dataset: USGS; VT Road Network: VCGI; Imagery (2009): esri.

— VHD Hydrography
— Enhanced Hydrography

N

0   280   560
Feet

BROWNS CORNER RD

BOUCHARD RD

STONE ENVIRONMENTAL INC

O:\Projdir\...WMG2156-G_LCBP_Phosphorus_Critical_Source_Areas\Data\MapDocuments\Presentations\AndReports\FinalReport\Map3.20_Enhanced_Hydro_Local.mxd

234

Proximity to Hydrologic Network (m)

- 0 - 56
- 57 - 124
- 125 - 198
- 199 - 281
- 282 - 378
- 379 - 497
- 498 - 650
- 651 - 862
- 863 - 1,193
- 1,194 - 2,920
- HUC (12) Watersheds

Miles
0 2.5 5

N

Sources: Subwatersheds & Proximity to Hydrologic Network: Stone Environmental; HUC 12 Watersheds: USGS; Imagery (2009): esri.

Map 3.21

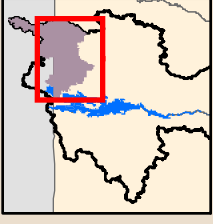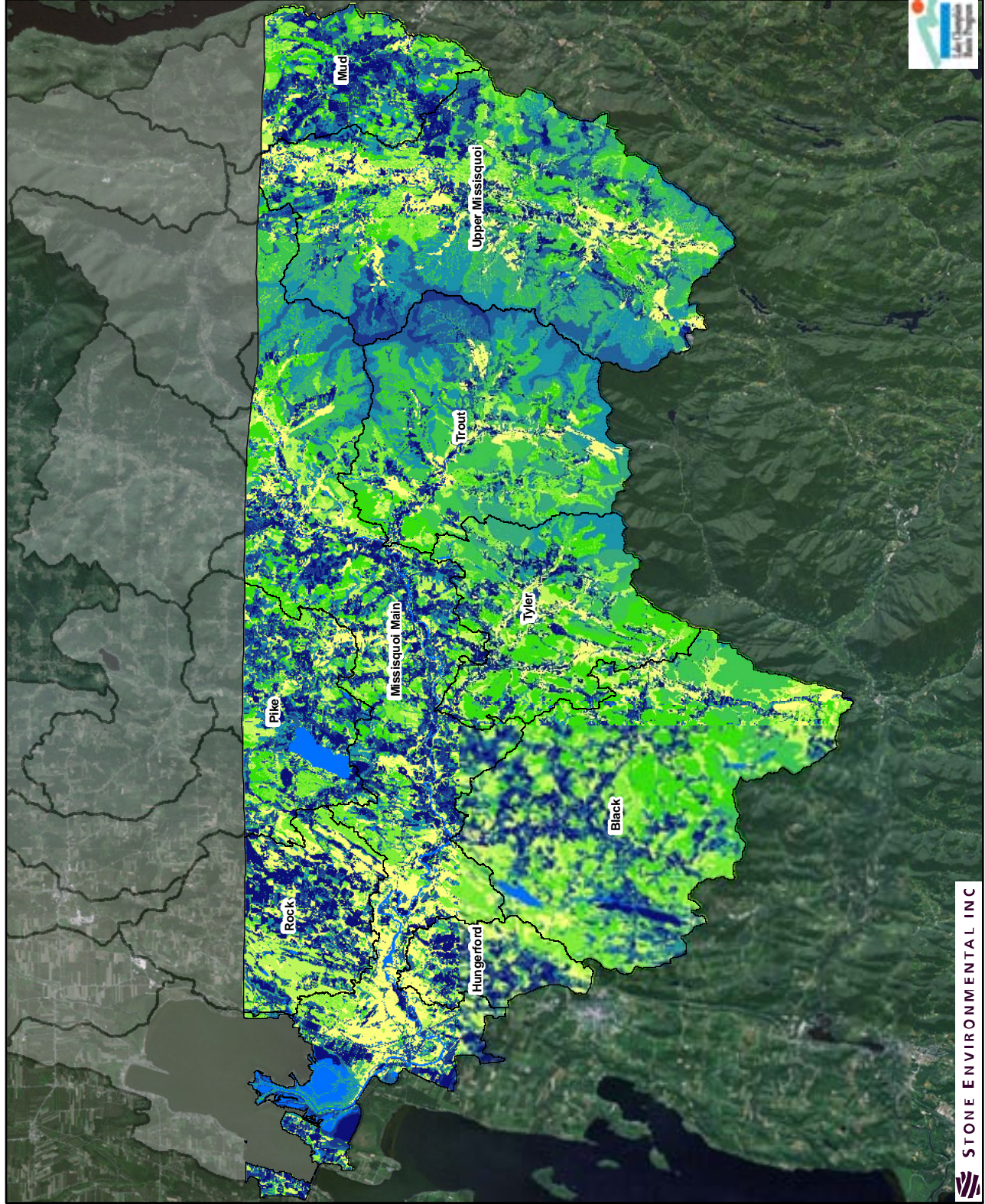Proximity to Hydrologic Network

Full Watershed

Identification of Critical Source Areas of Phosphorus Pollution within the Vermont Sector of the Missisquoi Bay Basin

STONE ENVIRONMENTAL INC

Identification of Critical Source Areas of Phosphorus Pollution within the Vermont Sector of the Missisquoi Bay Basin

Map 3.22

Hydrologic Network Proximity
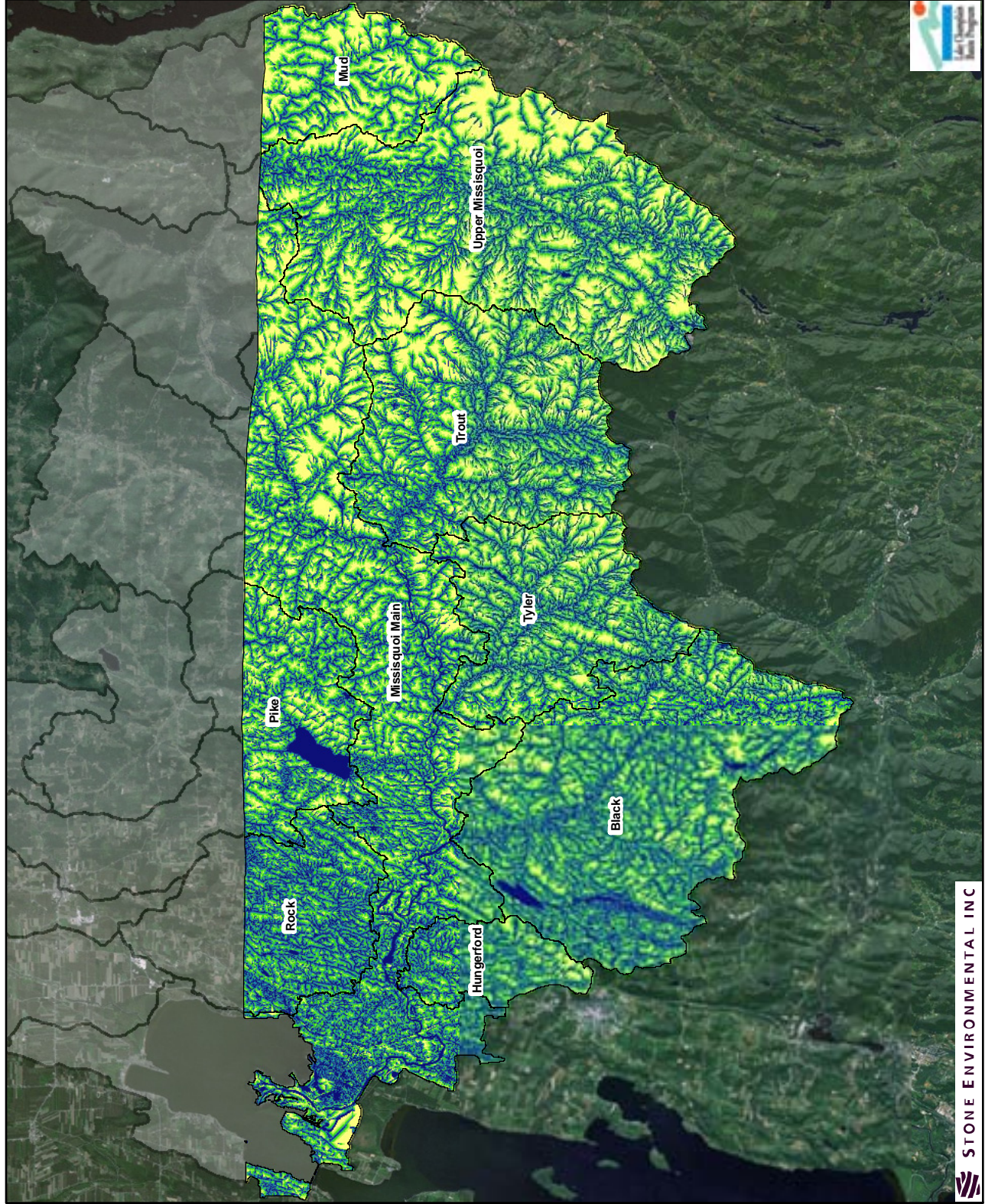
Full Watershed

Hydrologic Network Proximity (Percentile)

- < 0.1
- 0.1 - 0.2
- 0.2 - 0.3
- 0.3 - 0.4
- 0.4 - 0.5
- 0.5 - 0.6
- 0.6 - 0.7
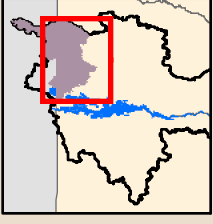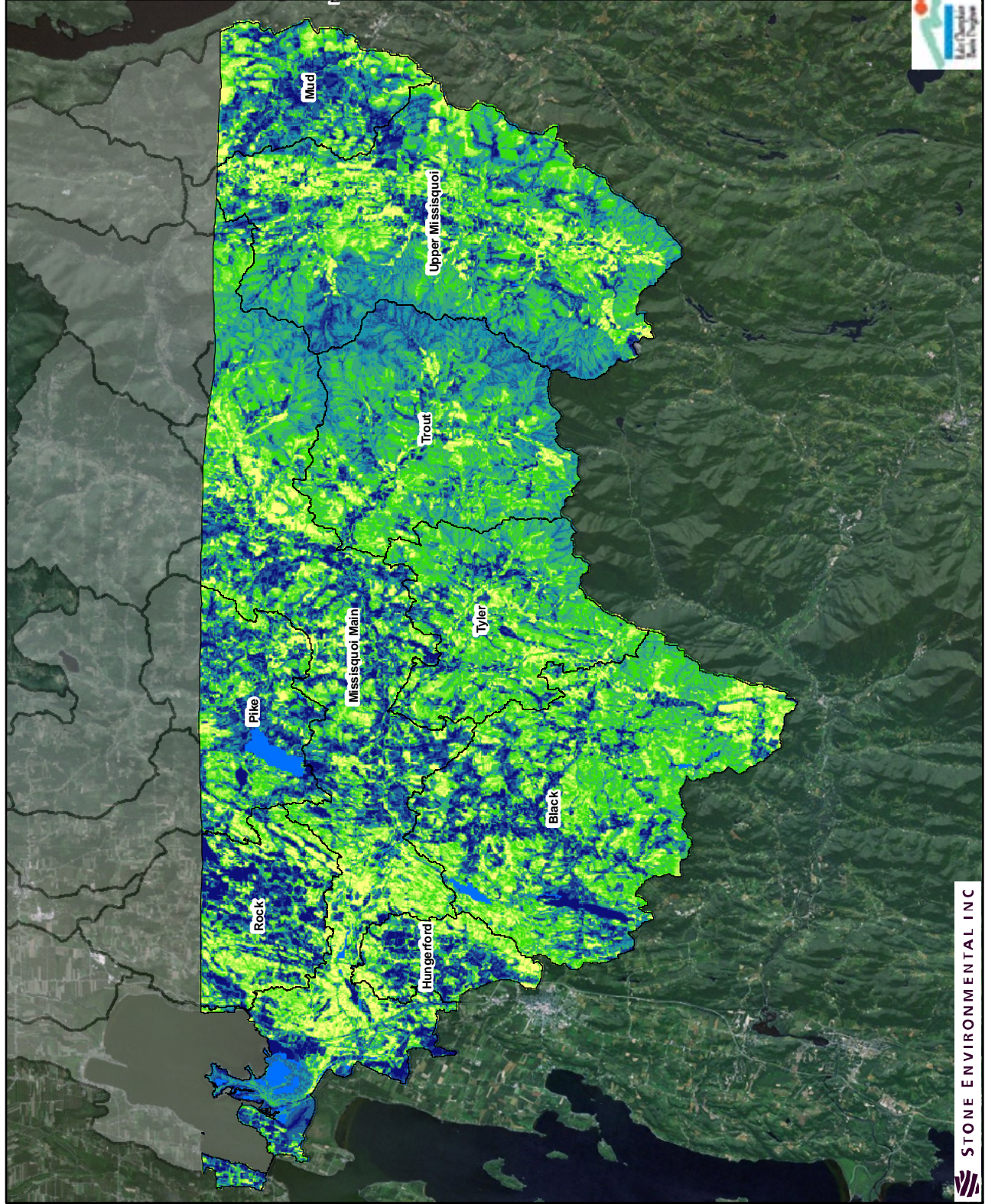- 0.7 - 0.8
- 0.8 - 0.9
- 0.9 - 1
- HUC (12) Watersheds

Sources: Subwatersheds & Hydrologic Network Proximity: Stone Environmental; HUC 12 Watersheds: USGS; Imagery (2009): esri.

STONE ENVIRONMENTAL INC

Identification of Critical Source Areas of Phosphorus Pollution within the Vermont Sector of the Missisquoi Bay Basin

Full Watershed

Total P Loading Percentile by HRU

Map 3.23

Total P Loading Percentile

< 0.1
0.1 - 0.2
0.2 - 0.3
0.3 - 0.4
0.4 - 0.5
0.5 - 0.6
0.6 - 0.7
0.7 - 0.8
0.8 - 0.9
0.9 - 1
HUC (12) Watersheds
Water

Sources: Subwatersheds & Total P Loading Percentile: Stone Environmental; HUC 12 Watersheds: USGS; Imagery (2009): esri.

STONE ENVIRONMENTAL INC

Map 3.24

Weighted CSA Ranking

Percentile
- < 0.1
- 0.1 - 0.2
- 0.2 - 0.3
- 0.3 - 0.4
- 0.4 - 0.5
- 0.5 - 0.6
- 0.6 - 0.7
- 0.7 - 0.8
- 0.8 - 0.9
- 0.9 - 1
- HUC (12) Watersheds
- Water

Miles

0   2.5   5

N

Sources: Rivers and Streams & Weighted
CSA Ranking: Stone Environmental; HUC 12
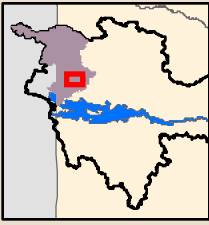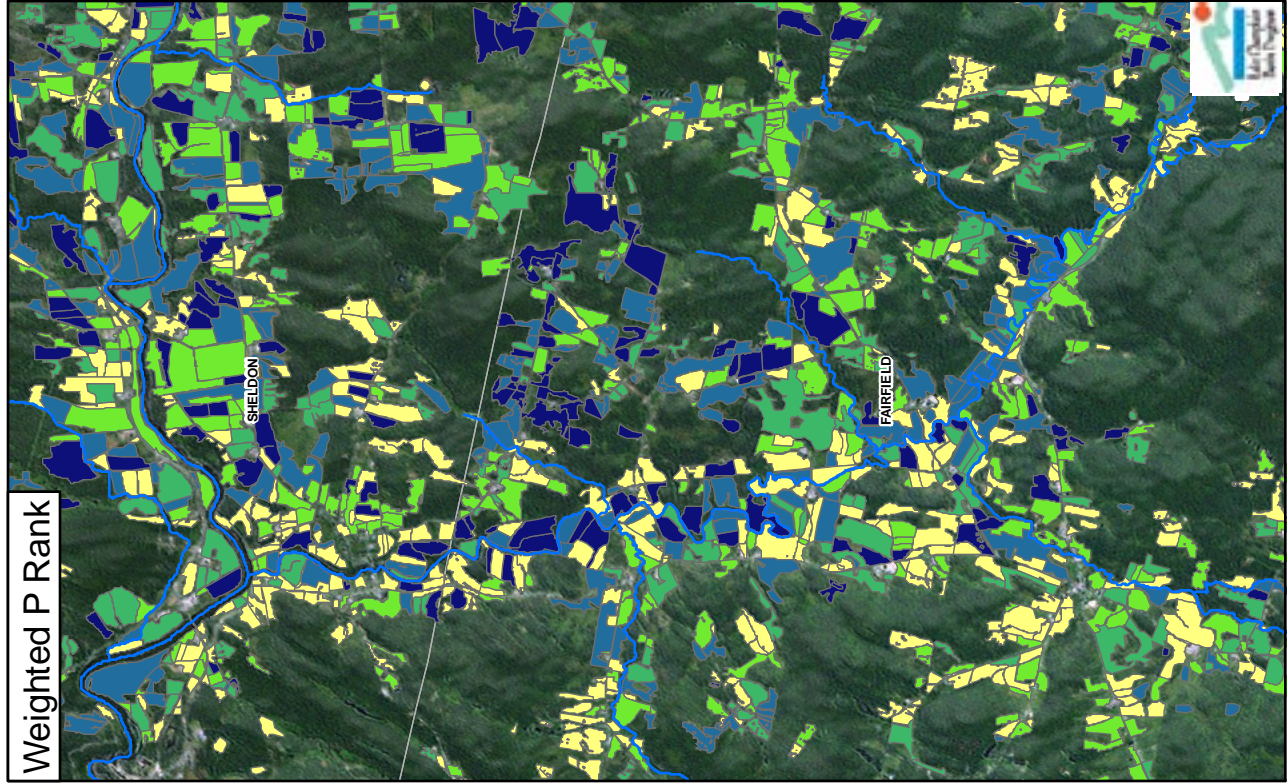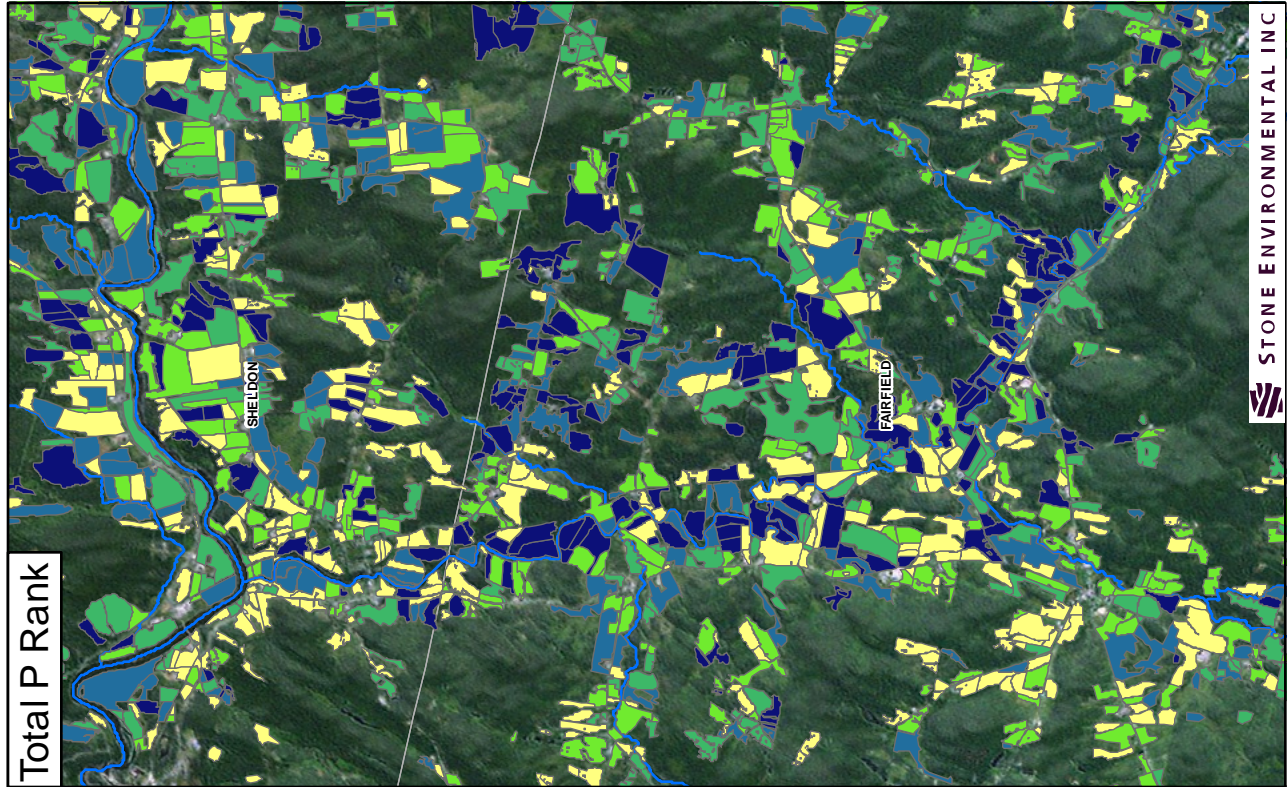Watersheds: USGS; Town Boundaries:
VCGI; Imagery (2009): esri.

CSA Ranking Based on
Weighting Total P Load and
Proximity to Hydrologic Network

Full Watershed

Identification of Critical Source
Areas of Phosphorus Pollution
within the Vermont Sector of
the Missisquoi Bay Basin

STONE ENVIRONMENTAL INC

Mud

Upper Missisquoi

Trout

Tyler

Missisquoi Main

Pike

Black

Rock

Hungerford

O:\Proj09\IMMQ\156-G_LCBP_Phosphorus_Critical_Source_Areas\Data\MapDocuments\Presentations\FinalReport\Map3.24_WeightedRankPercentile.mxd

238

Total P Rank

Weighted P Rank

Total P Rank and
Weighted P Rank, Percentile

< 0.2
0.2 - 0.4
0.4 - 0.6
0.6 - 0.8
0.8 - 1

Rivers and Streams

Map 3.25

Total P Rank and Weighted
P Rank by Percentile

Full Watershed

Identification of Critical Source
Areas of Phosphorus Pollution
within the Vermont Sector of
the Missisquoi Bay Basin

N

0   0.5   1
Miles

SHELDON

FAIRFIELD

STONE ENVIRONMENTAL INC

Locations of Field Verification

Low Rank CLUs
High Rank CLUs
Study Area
HUC (12) Watersheds

Sources: Subwatersheds & Site Visit
Locations: Stone Environmental; HUC 12
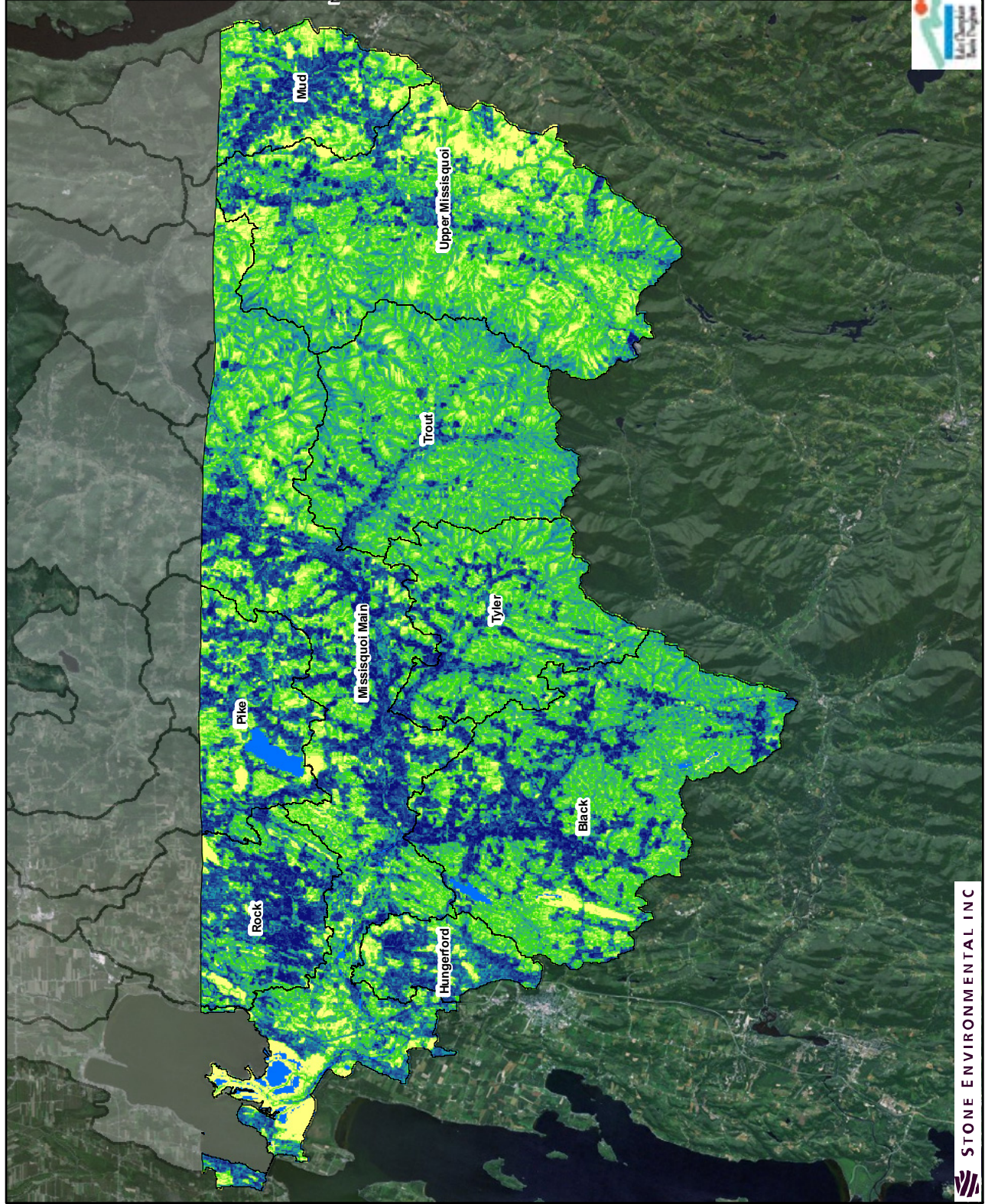Watersheds: USGS; Imagery (2009): esri.

Locations of Field
Verification of
CSA Rankings

Full Watershed

Identification of Critical Source
Areas of Phosphorus Pollution
within the Vermont Sector of
the Missisquoi Bay Basin

Map 3.26

N

Miles
0   2.5   5

STONE ENVIRONMENTAL INC

O:\Proj09\LNM2156-G_LCBP_Phosphorus_Critical_Source_Areas\Data\MapDocuments\Presentations AndReports\PresentinMap3.26_SiteVisitLocations.mxd

240

GIS-Based CSA Ranking
by Percentile

GIS-Based CSA Ranking
by Percentile

- < 0.1
- 0.1 - 0.2
- 0.2 - 0.3
- 0.3 - 0.4
- 0.4 - 0.5
- 0.5 - 0.6
- 0.6 - 0.7
- 0.7 - 0.8
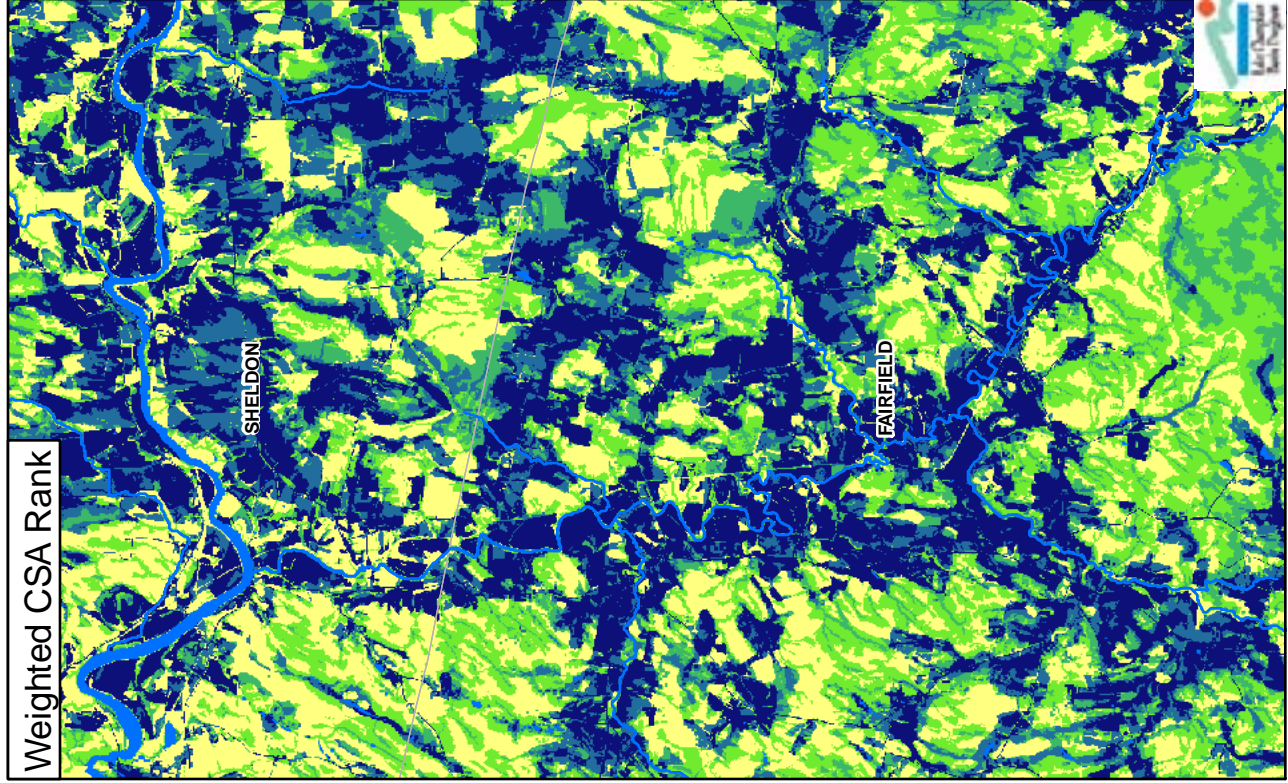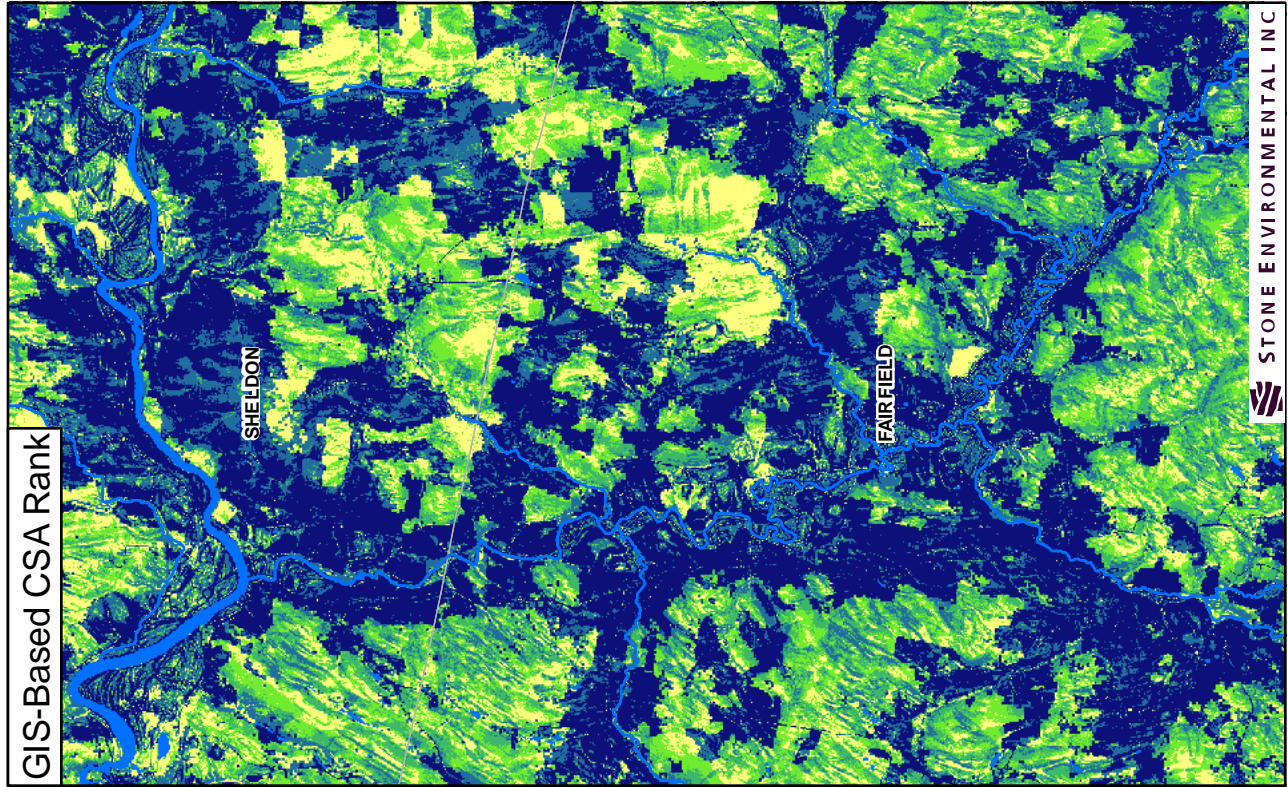- 0.8 - 0.9
- 0.9 - 1
- HUC (12) Watersheds
- Water

Map 3.27

GIS-Based CSA Ranking
by Percentile

Full Watershed

Identification of Critical Source
Areas of Phosphorus Pollution
within the Vermont Sector of
the Missisquoi Bay Basin

Miles
0   2.5   5

N

STONE ENVIRONMENTAL INC

Mud

Upper Missisquoi

Trout

Tyler

Missisquoi Main

Pike

Black

Rock

Hungerford

GIS-Based CSA Rank

Weighted CSA Rank

SHELDON

FAIRFIELD

SHELDON

FAIRFIELD

STONE ENVIRONMENTAL INC

GIS-Based and Weighted
CSA Rank, by Percentile

0 - 0.2
0.2 - 0.4
0.4 - 0.6
0.6 - 0.8
0.8 - 1

Rivers and Streams

Water

Sources: Rivers and Streams, GIS-Based &
Weighted CSA Rank: Stone Environmental;
Town Boundaries: VCGI; Imagery (2009): esri.

Map 3.28

GIS-Based CSA Rank
and Weighted CSA
Rank Comparison

Full Watershed

Identification of Critical Source
Areas of Phosphorus Pollution
within the Vermont Sector of
the Missisquoi Bay Basin

0 0.5 1 Miles

N